Université du Québec
INRS-Institut Armand-Frappier

Characterization of the receptors involved in adrenomedullin clearance in the lungs

Par
Yan Fu

Thèse présentée pour l'obtention du grade
Docteur ès sciences (PhD)
Biologie

Jury d'évaluation

Évaluateur interne (président du jury) :	Dr Patrick J. Devine INRS-Institut Armand-Frappier
Évaluateur externe :	Dr Gaétan Guillemette Université de Sherbrooke
Évaluateur externe :	Dr János G. Filep Université de Montréal
Directeur de recherche	Dr Alain Fournier INRS-Institut Armand-Frappier
Codirecteur de recherche	Dr Jocelyn Dupuis Université de Montréal

Octobre 2008

Summary

Adrenomedullin (AM), a 52-amino acid peptide, is mostly produced in adrenal, lung, kidney, and heart tissues. The main physiological action of AM appears to be as a potent vasodilator. So far, AM was shown to bind to two different receptor subtypes, AM_1, produced by the association of the calcitonin-receptor-like receptor (CLR) and the receptor-activity-modifying protein 2 (RAMP2) and AM_2, obtained by linking CLR to RAMP3. No significant physiological differences upon activation of the AM_1 and AM_2 receptors were identified, thus the functional significance of this receptor redundancy remains unclear. Receptor binding studies revealed that the greatest density of AM binding sites in a variety of rat tissues was in the heart and lungs. Hence, this peptide is well designed to be a lead compound for the development of imaging radiopharmaceuticals of these organs.

Currently, only one agent is used in clinical imaging of the pulmonary circulation: ^{99m}Tc-macroaggregated albumin (MAA). However, this agent is larger than most small pulmonary vessels. As a result, the central problem about MAA in the clinical imaging application is its limited sensitivity to investigate small vascular defects. To provide a more powerful tool for diagnostic purposes and for monitoring the treatment responses in the lung system, we proposed a ^{99m}Tc delivery system with lung specific targeting ligands. The proposed system maximizes the uptake of the ^{99m}Tc-complex by the pulmonary system and enhances the influx as well as retention of the complex in the lung. This delivery system includes three main components: 99m-technetium, a carrier of the ^{99m}Tc, and a targeting moiety. Thus, we have designed a series of AM derivatives and the results of our evaluations showed that ^{99m}Tc-linear AM, a system that utilizes ^{99m}Tc as the radiation source and AM as a carrier and a targeting moiety (ligand), displayed a clear image of the pulmonary circulation through AM receptors that appear to be acting as clearance receptors.

To pursue our study, we have performed binding assays to characterize AM binding sites in dog lung homogenates. First, we observed that the non selective agonist AM bound

with high affinity, displaying two binding sites. Moreover, competition binding assays using ^{125}I-AM and some unlabeled ligands showed the following ranking for displacement: AM > AM(13-52) > CGRP ≈ AM2 ≥ AM(22-52) ≥ AM2(16-47) > CGRP(8-37) > AMY. Thus, these results strongly suggest that the AM binding site found in the dog lungs is mainly the AM_1 receptor subtype.

Receptor specific imaging provides a powerful asset for clinical applications and biological research. Since AM is a long peptide with 52 amino acids, further studies are pursued using AM fragments of various lengths. By determining the amino acids, the minimal peptide fragment, and some relative secondary structures of AM retaining good affinity for the AM receptors in the dog lung, it will facilitate the identification of the pharmacophores underlying AM_1 binding affinity and specificity. Those information are essential for the discovery of a selective probe for AM_1 receptors. Furthermore, they will help in the development of better and smaller lung-specific diagnostic and/or therapeutic molecules after radiopharmaceutical optimization.

Yan Fu
Student

Alain Fournier
Director of research

Acknowledgement

In the autumn of 2003, I sowed a seed called PhD. Here I look back on my research and writing to obtain it. The road went through enormous challenges and frustration, great excitement and depression. I have grown with this PhD. Today I am filled with pleasure with great appreciation to reap the professional knowledge, self-confidence, kindness and friendship along the road. With the deepest gratitude I wish to thank every person who has walked the road with me and inspired, touched, and illuminated me through his or her presence.

The first person I would like to thank is my research director, Dr. Alain Fournier. I have been working on his project since autumn 2004. During these years his encouragement, support and guidance have accompanied with my PhD study and research. He could not even know how much I have learned from him. Herein, I would like to express especially my gratitude for his belief in me. The belief is the very power and force of my study in the project. I am really glad that I have come to know Dr. Alain Fournier and greatly appreciated his involvement and insight.

I would also like to acknowledge and express my gratitude to the following people for their magnificent support and contributions to my research on technetium labeling and *in vivo* experiments. They are Dr. Jocelyn Dupuis, my co-director, Dr. François Harel and the staff in the research center of the Montreal Heart Institute, University of Montreal.

Myriam Létourneau, a great research assistant I have seen, has been as close as a relative and a good friend to me in the laboratory. She provided me with generous assistance at all aspects from ordering reagents to experiments in my PhD research. She is the kind of person one can share all experiences and stories about my successes and failures, happiness and sadness.

Dr. Richard Villemur and Ms. Anne Philippon, respectively the program director for the PhD program in biology and the secretary of the program who provided me with much

assistance. I would not be involved in such an exciting project without them. I am very grateful to all people who helped me both known or behind the scenes for providing me with the opportunity to complete my PhD study.

I would like to thank the members of the committee who monitored my work and took effort in reading and providing me with valuable comments on earlier versions of this thesis: Dr. János G. Filep at University of Montreal, Dr. Gaétan Guillemette at University of Sherbrook, and Dr. Patrick J. Devine at INRS-IAF. Thanks to you all.

My precious friends and colleagues for their love and support: Dr. Steven Holden, Dr. Yi Pan, Dr. Chantal Langlois, Dr. Stéphane Boivin, Steve Bourgault, Martin Viau, Jacinthe Aubin, Kathy Turcotte.

I wish to thank my parents for giving me health and a happy life in China. I also wish to thank my sisters for taking care of my mother and father as well as my son when I was absent. And finally to my families, my husband and my son, Yi Guo and Xiaotong Guo, thank you for your love and unshakable support. I will never forget you were always supporting and watching me from the back each time I made a presentation.

This research has been supported and funded by the Fondation Armand-Frappier and PulmoScience.

Content

List of Figures

List of Tables

List of Abbreviations

ACN	Acetonitrile
AM	Adrenomedullin
AMBP-1	Adrenomedullin-binding protein-1
AMY	Amylin
APM	Aminopeptidase M
BAPE	butanol:acetic acid:pyridine:water/30:6:24:20
BCA	Bifunctional chelate agent
Boc	t-Butyloxycarbonyl
BOP	Benzotriazol-1-yl-oxy-tris(dimethylamino)-phosphonium Hexafluorophosphate
BSA	Bovine serum albumin
CAT	Chloramine-T
CPAE	Cow pulmonary artery endothelial cells
CCl_4	Tetrachloromethane
CGRP	Calcitonin gene-related peptides
CLR/CRLR	Calcitonin receptor-like receptor
CNBr	Cyanogen bromide
CPY	Carboxypeptidase Y
CRF	Corticotrophin-releasing factor
CRSPs	Calcitonin receptor-stimulating peptides
CT	Calcitonin
CTR	Calcitonin receptor
DADS	Diamidedithiols
DADT	N_2S_2 diaminedithiols

DCC	1,3-Dicyclohexylcarbodiimide
DCM	Dichloromethane
DHDTPA	Diethlenetriaminepentaacetic dianhydride
DIEA	Diisopropylethylamine
DMF	Dimethylformamide
DMS	Dimethylsulfide
DMSO	Dimethylsulfoxide
DOTA	1,4,7,10-Tetraazacyclododecane-1,4,7,10-tetraacetic acid
DTNB	5,5'-Dithiobis(2-nitrobenzoic acid)
DTPA	Diethylenetriaminepentaacetic acid
DTT	Dithiothreitol
EDT	Ethanedithiol
EDTA	Ethylenediaminetetraacetic acid
FCS	Fetal calf serum
Fmoc	9-Fluorenylmethyloxycarbonyl
Fmoc-Rink Amide-AM resin	(4-(2',4'-Dimethoxyphenyl-Fmoc-aminomethyl)-phenoxyacetamidonorleucylaminomethyl resin
GHRH	Growth hormone-releasing hormone
GIP	Glucose-dependent insulinotropic peptide
GLP	Glucagon-like peptide
GPCRs	Guanine nucleotide-binding protein-coupled receptors
HBTU	2-(H-benzotriazole-1-yl)-1, 1, 3, 3-tetromethyluronium hexafluorophosphate
RP-HPLC	Reverse-phase high performance liquid chromatography
hAM	Human adrenomedullin
HYNIC	6-Hydrazinonicotinamide
IBS	Irritable bowel syndrome

ID	Injected dose
IMD	Intermedin
ITLC-SG	Instant thin layer chromatography on Silica-Gel-impregnated glass-fiber paper
MAG_3	Mercaptoacetylglycylglycylglycine
MALDI-TOF	Matrix-assisted laser desorption ionization time-of-flight
MAMA	Monoamidemonoaminedithiols
MRI	Magnetic resonance imaging
MW	Molecular weight
MS	Mass spectrometry
NMP	1-Methyl-2-pyrrolidone
PAC	Pituitary adenylate cyclase
PACAP	Pituitary adenylate cyclase-activating polypeptide
PAMP	Proadrenomedullin N-terminal peptide
PBS	Phosphate buffer solution
PET	Positron emission tomography
PnAO	propylene amine oxime
PTH	Parathyroid hormone
PTHrP	Parathyroid hormonone-related protein
RAMPs	Receptor activity-modifying proteins
RCP	Radiochemical purity
RP-HPLC	Reverse-phase high performance liquid chromatography
SG	Silica-Gel-impregnated glass-fiber paper
SPECT	Single photon computed tomography
SPPS	Solid-phase peptide synthesis
TFA	Trifluoroacetic acid
TIP39	Tuberoinfundibular peptide of 39 residues
TLC	Thin Layer Chromatography

TMP	2, 4, 6-Collidine or 2, 4, 6-trimethylpyridine
t_R	Retention time
UCN	Urocortin
USP	United States Pharmacopeia
VIP	Vasoactive intestinal peptide
VPAC	Vasoactive intestinal peptide receptor

Chapter 1 : The development of radiopharmaceuticals

In the pharmaceutical science and biological studies, the radiopharmaceutical-based molecular imaging is a useful tool for drug development and biological research. X-ray, computed tomography, Magnetic Resonance Imaging (MRI), ultrasound, gamma camera, Positron Emission Tomography (PET), and Single Photon Computed Tomography (SPECT) are technologies currently used to help physicians to diagnose and treat diseases. Some of these advanced technologies also drive the growth of demand for imaging agents required by the technologies. For example, the increased demand for MRI contrast agents drives the development of new contrast agents forward and the demand for PET agents prevails in the development of radiopharmaceuticals. So far, molecular imaging has been attracting more and more interest since it represents a potential avenue for specific targeting diagnosis and therapy of disease in the future.

1.1. Definition of a radiopharmaceutical

Radiopharmaceuticals are usually small organic or inorganic compounds containing a radionuclide that are used routinely in nuclear medicine for the diagnosis or therapy of various diseases. They were also known as radiotracers or biological markers. Nuclear imaging was pioneered by using inhaled xenon-133 to image lungs in 1955. After that, technetium-99m prevailed as a medical imaging radioisotope. Presently, nearly 85% of clinical imaging agents are labeled with technetium-99m.

1.2. Classes of radiopharmaceutical

Radiopharmaceuticals can be divided into two generations. The first generation radiopharmaceuticals were made from a radionuclide and a metal chelator, also called non-specific radiotracers according to the uptake model based on the concentration mechanism of the agent in the target organ. This generation is usually applied in the study of some physiological functions, and its biodistribution is determined by their chemical and physical properties. The second generation of radiopharmaceuticals, also called specific radiotracers, were prompted by the growing demands for even more specific agents. A biomolecule, i.e. protein, or peptide, or steroid hormone, is covalently linked to

the radionuclide complex. Thus, the ultimate distribution of the second generation radiopharmaceuticals resides in the biomolecule and is determined by their receptor binding properties or other biological interactions. The distribution of a specific radiopharmaceutical is determined by the action of a protein, peptide or steroid hormones binding to a specific site. It serves as a vehicle that carries the radionuclide to the target organ or tissue. Therefore, the radiopharmaceutical bound to a specific site is often called a target-specific radiopharmaceutical.

1.3. Target-specific radiopharmaceuticals

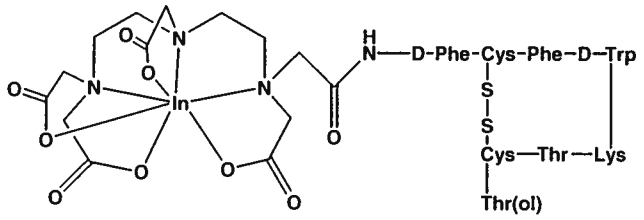

Figure 1: ^{111}In-DTPA-Octreotide.

The field of target-specific radiopharmaceuticals was pioneered by the use of radiolabeled monoclonal antibodies. Radiolabeled monoclonal antibodies were among the first receptor radiopharmaceuticals used for diagnostic purposes. They are often referred to as "magic bullets" because antibodies have a high binding affinity and specificity. In the last two decades, monoclonal antibodies (~150kDa) have been studied for their potential applications in both diagnostic and therapeutic nuclear medicine. Generally, after injection i.v. of radiolabeled monoclonal antibodies, imaging diagnosis is delayed until 1 - 3 days later for the clearance of blood-pool radioactivity. Some technologies were developed to improve the circulation clearance in the past. For example, antibody Fab-fragments that can bind with their Fab regions to targets (Klibanov *et al.*, 1988; Fritzberg *et al.*, 1988). However, their unfavorable target-to-background ratios and their slow blood clearance urged the need for new radiolabeled molecules free from these drawbacks. The successful use of ^{111}In-DTPA-Octreotide (OctreoScan, Figure 1) in diagnosis of somatostatin receptor-positive tumors has intensified the search for new target-specific

radiopharmaceuticals based on small biomolecules. So far, many small biomolecules have been already synthesized, radiolabeled, and studied for their potential use as new diagnostic imaging agents for various diseases.

1.4. Target-specific radiopharmaceuticals produced with peptide

Peptides are a unique class of biomolecules containing less than 100 amino acids. Because of their inherent flexibility, they are less susceptible to a loss of integrity upon labeling. Additionally, they are generally weak antigens, in comparison to antibodies. In humans, many body functions are efficiently regulated by peptides through interaction with specific receptors. Because of their high receptor specificity and short biological plasma half-life, peptides are therefore obvious targets. Solid Phase Peptide Synthesis (SPPS) provides the rapid and almost limitless preparation of small peptides. Furthermore, the advanced modification strategies resist effectively *in vivo* peptide degradation by endogenous peptidases (Werle and Bernkop-Schnürch, 2006). Those strategies permit the development of target-specific radiopharmaceuticals produced with peptide (Shapiro, 1996). Some of the peptide-radiopharmaceuticals used in diagnostic research are shown in Table 1.

Table 1: Peptide-radiopharmaceuticals in diagnostic research.

Receptor Ligand	Radiolabeled Compound	Receptor	Targeted Disease
RGD	RP419/DMP444	platelet/GPIIb/IIIa	thrombosis
CYT-379	^{99m}Tc-CYT-379	platelet/fibrinogen	thrombosis
RGD-peptidomimetic	^{99m}Tc-P280/Thromboscan	GPIIb/IIIa/Platelet	thrombosis
VIP	^{99m}Tc-HMPAO	liposome/VIP-R	breast cancer
TKPR	^{99m}Tc-RP128	tuftsin	inflammation
chemotactic peptides	^{99m}Tc fMLFK-HYNIC	leukocytes	inflammation
folate antagonists	^{111}In-DTPA-folate	folate	tumor
octreotide	^{111}In-DTPA-Octreotide	somatostatin	tumor(neuroendocrine)
bombesin analogs	^{99m}Tc-Lys^3(DADT)-Bombesin	bombesin/GRP	tumor
bombesin	^{99m}Tc-MAG3-Bombesin	bombesin/GRP	tumor
bombesin analogs	^{111}In-DOTA-X-BBN(7-14)NH_2	bombesin/GRP	tumor

Chelator: HYNIC: 6-hydrazinonicotinamide; DTPA: diethyenetriaminepentaacetic acid; MAG_3: mercaptoacetylglycylglycylglycine; DOTA: 1,4,7,10-tetraazacyclododecane-1,4,7,10-tetraacetic acid; DADT: N_2S_2 diaminedithiols.
(Behr *et al.*, 2002; Dagar *et al.*, 2003; Okarvi and al-Jammaz, 2003)

1.5. Peptide-radiopharmaceuticals in lung imaging

More and more radiopharmaceuticals designed from peptides are being used for the diagnosis of various diseases or are in their late stages of development. A new term of 'molecular medicine' was considered and introduced in clinical diagnosis and treatment along with the availability of receptor-specific radiopharmaceuticals. This is especially true for lung diseases, where a number of new radiopharmaceuticals are being applied for diagnosis.

1.5.1. Diagnosis of lung cancer

Lung cancer is the leading cause of cancer mortality worldwide. The routine chest radiographs are limited in their ability to detect small lung tumors. This drive the study of lung cancer and led to identification of peptide growth factors that can generate signals and control tumor growth by activating G protein-coupled receptors (GPCRs) or tyrosine kinase receptors on the cell-surface, either in a paracrine or autocrine manner. The role of growth factors and their receptors in lung cancer has extensively been studied, and successfully applied to the design and development of new, less toxic and more specific anticancer drugs, such as ^{111}In-DTPA-octreotide (Figure 1). This peptide-radiopharmaceutical was prepared by using a radiolabeled analog of somatostatin, and selectively targets somatostatin receptors. It has efficiencies higher than 85% (the PIOPED investigators, 1990) in detecting small cell lung cancer tumors and metastases.

1.5.2. Diagnosis of pulmonary embolism

Pulmonary embolism is a blockage of a pulmonary artery. The embolus could be a blood clot, fat, air, amniotic fluid, injected talc or clumped tumor cells. Pulmonary arteriography is the standard for the accurate diagnosis of a pulmonary embolism (the PIOPED investigators, 1990). Although the pulmonary arteriography allows physician to investigate pulmonary emboli, a large proportion of cases are still undetermined or undetected after a lung scan. In these cases, both spiral and electron beam computed

tomography, as well as Duplex ultrasonography have been recommended for the diagnosis, which allows identifying the source of the thromboembolus. In fact, the reliability of these technologies in the diagnosis of embolism needs further confirmation in large prospective trials. Additionally, Duplex (Doppler) effect ultrasonography exhibits poor sensitivity for asymptomatic lower-extremity thrombosis. In the past years, thrombus imaging has been improved by means of radiolabeled peptides that are directed against the fibrinogen receptor glycoprotein IIb/IIIa. The integrin is found on platelets and required for normal platelet aggregation. The molecular studies on biology and platelet aggregation mechanism benefit in the development of emboli-targeting imaging agents (Calvete, 1995). For instance, the synthetic peptide-radiopharmaceutical, ^{99m}Tc-P280 (also called ^{99m}Tc-apcitide), could bind to the glycoprotein IIb/IIIa receptors with high affinity and be used to visualize thrombi in acute thrombosis (Taillefer *et al.*, 2000). As a leading compound, this complex already showed higher sensitivity, specificity and reliability when compared with the well-known contrast venography technology.

1.5.3 Inflammatory or infectious diagnosis

In the view of pathologies, inflammatory or infectious conditions induced by bacteria are a normal immune response, and cause anatomical and structural changes in the lungs. The changes can be detected and located by radiological techniques, such as x-ray, computed tomography and magnetic resonance. However, these techniques lack accuracy in an early phase of infection, when anatomical structures have not yet been altered, and also in immunocompromised patients in whom inflammatory and repair mechanisms are impaired because of immunodeficiency. In this case, nuclear medicine techniques may provide assistance for diagnosis and for monitoring treatment efficacy. The inflammatory response is characterized by a series of biochemical changes. The three major events in the affected tissue and surrounding structures are increased local blood perfusion, increased vascular permeability and leukocyte infiltration. Accordingly, a non-specific radiopharmaceutical can accumulate and be retained at the site of inflammation through extravasal leakage. However, accumulation may also occur through specific binding to cell-associated receptors. So far, only a limited number of peptide receptor-targeting

molecules have reached the clinical stage, including mainly radiolabeled polyclonal antibodies and ^{111}In-pentetreotide. In medicine, granulomas often appear in the lungs as small inflammatory nodules. ^{111}In-pentetreotide, a radiolabeled somatostatin analog, could visualize granulomatous diseases in patients with sarcoidosis (Kwekkeboom *et al.*, 1998).

For the reasons stated above, peptide-radiopharmaceuticals targeted to cell-surface receptors are emerging as an important class of diagnostic tools in lung diseases. Their binding to specific cell membrane receptors allows for selective and non-invasive administration of local receptor distribution *in vivo* by means of nuclear medicine imaging. Information thus obtained can be used for diagnostic purposes and for predicting and monitoring response to treatment in lung cancer, pulmonary thromboembolism and lung inflammation/infection.

Chapter 2 : Calcitonin peptide family and adrenomedullin

2.1. The calcitonin peptide family

Peptides contribute to most life processes and there can be no doubt that they are among the most fascinating molecules. Being relatively efficacies, biodegradable and easily excreted, they represent a class of compound with appealing properties compatible with, for instance, antibody *in vivo* diagnostic and/or therapeutic applications. As such, it was recently described that the 52-amino acid peptide, adrenomedullin (AM), exhibits an unusual lung uptake. Consequently, related AM analogs became attractive targets for the development of pharmaceuticals useful for pulmonary imaging. AM shares sequence homologies with peptides belonging to the calcitonin peptide family (Figure 2). Members of this family can thus be depicted as potential lead compounds and therefore, we will first review their structural and biological characteristics.

```
hCT                      CGNLSTCMLGTYTQDFNKFHTF PQTAIGVGAP   32
                                 7
h CGRPα                   ACDTATCVTHRLAGLLSRSGGVVKNNFVPTNVGSKAF  37
                            2    7
h CGRPβ                   ACNTATCVTHRLAGLLSRSGGMVKSNFVPTNVGSKAF  37
                            2    7
hAMY                      KCNTATCATQRLANFLVHSSNNFGAILSSTNVGSNTY   37
                            2    7
hAM     YRQSMNNFQGLRSFGCRFGTCTVQKLAHQIYQFTDKDKDNVAPRNKISPQGY   52
                               16   21
hAM2          TQAQLLRVGCVLGTCQVQNLSHRLWQLMGPAGRQDSAPVDPSSPHSY   47
                               10   15
hIDM          TQAQLLRVGCVLGTCQVQNLSHRLWQLMGPAGRQDSAPVDPSSPHSYG  48
                               10   15
```

Figure 2: Structures of peptides for the calcitonin family.

2.1.1. Calcitonin

The first peptide of this family, which was isolated in 1961, is calcitonin (CT). It was extracted from the human thyroid gland, and its sequence and structure were determined in 1968 (Neher *et al.*, 1968). CT is a single-chain peptide hormone consisting of 32 amino acids, and is secreted in humans by the parafollicular cells of the thyroid (Foster, MacIntyre and Pearse, 1964). This peptide is implicated in calcium homeostasis and bone resorption (Copp, 1969).

2.1.2. Calcitonin gene-related peptides

In 1982, while studying molecular cloning of DNA complementary to rat CT mRNA, it was revealed that the CT gene could generate a second distinct transcript coding for a 37-amino acid peptide. The second peptide named calcitonin gene-related peptide (CGRP) has a disulfide bridge between positions 2 and 7, an amphiphilic α-helix conformation between residues 8-18, two β-turn structures between residues 17-21 and 29-34, as well as a random-coil segment formed by residues 23-29, and a C-terminal phenylalanylamide (Rosenfeld *et al.*, 1983). CGRP shares 25% sequence homology with CT (Wimalawansa *et al.*, 1990). By screening libraries, the possible existence of other gene products related to CGRP was investigated. This led to identification of a polypeptide coded by a novel rat mRNA which differed by only one amino acid from the primary sequence of CGRP (Amara *et al.*, 1985). To distinguish the two peptides, they were termed as CGRPα for the former peptide and CGRPβ for the latter, respectively (Poyner *et al.*, 2002). In humans, two isoforms of CGRP were also isolated. hCGRPβ differs by three amino acids from the homologous peptide hCGRPα.

2.1.3. Amylin

Amylin (AMY), characterized in 1987, is another peptide showing structural homologies with CT and CGRP. AMY was first isolated from amyloid deposits in human insulinoma. It is a 37-amino acid peptide, sharing a 46% sequence homology with the sequence of human CGRP, and a 15% sequence similarity with that of human CT. It is synthesized by and secreted primarily from pancreatic β-cells together with insulin. AMY exhibits a CT-like activity on bone metabolism and a CGRP-like activity on the vasculature (Poyner *et al.*, 2002; Westermark *et al.*, 1986).

2.1.4. Adrenomedullin

In 1993, Japanese scientists (Kitamura *et al.*, 1993) isolated a new peptide from human pheochromocytoma. The peptide stimulates cAMP production in human platelets and evokes potent and long-lasting hypotension in the rat. Since the peptide was produced by the adrenal medulla, it was named "adrenomedullin". The human AM was sequenced as a 52-amino acid polypeptide. It shares approximately 25% homology with CGRP and belongs to the CT peptide family. The discovery of AM opened a new research field to scientists in all over the world. Thousands of publications that involved in all aspects of AM studies have followed this initial discovery. It is well established that AM functions as a circulating hormone as well as a paracrine mediator with multiple biological activities (Hinson, Kapas and Smith, 2000). Sequence analysis of cloned human AM cDNA showed that its precursor is 185 amino acids in length. Interestingly, in addition to this precursor, the gene also encodes a unique 20-amino acid sequence, designated proadrenomedullin N-terminal peptide (PAMP). Based on its structure, PAMP does not belong to the CT peptide family. However, both AM and PAMP elicit potent hypotensive activity in anesthetized rats (Kitamura *et al.*, 1993; Sakata *et al.*, 1993). PAMP binding sites have been found in various tissues and organs. Recently, it was reported that PAMP specifically bound to and activated by Mas-related gene toxin 2 (MrgX2), a GPCR for cortistatin. The receptor was considered a potential PAMP receptor (Kamohara *et al.*, 2005).

2.1.5. Adrenomedullin 2/intermedin

In 2003, a new member of the AM family was identified in humans. It is a 47-amino acid peptide with an intermolecular ring of six amino acids formed by a disulfide bond between the positions 10 and 15, and an amidated C-terminus. Although the peptide was named adrenomedullin 2 (AM2), its sequence identity with AM is low. Moreover, intravenous injection of synthetic AM2 exhibited more potent and long-lasting hypotensive actions than AM in anesthetized mice (Takei *et al.*, 2004). Almost at the same time, intermedin (IMD) was cloned and reported by another research group (Roh *et al.*, 2004). Human IMD is a 48-amino acid peptide and its sequence is almost identical to that of human AM2, differing only by an extra glycine at position 48. At present, AM2

and IMD are treated as identical peptides since they all derived from the same precursor and display the properties of the CT peptide family. By immunohistochemistry AM2/IMD located in human hypothalamus, heart and kidney (Takahashi *et al.*, 2006). Recently, by radioimmunoassy and immunocytochemistry AM2/IMD was also detected in human brains, neurons of paraventricular, supraoptic nuclei, paraventricular nucleus, and neural fibers in the neurohypophysis (Morimoto *et al.*, 2007). AM2/IMD shares ~28% sequence homology with AM and less than 20% with CGRP. It causes hypotension in normal and spontaneously hypertensive rats through calcitonin receptor-like receptor (CLR)/ receptor activity-modifying proteins (RAMP)-like receptors. Its structure and bioactivity pattern suggest that it could be involved in cardiovascular regulation and central nervous system, and of course be a new member of the CT peptide family.

2.1.6. Calcitonin receptor-stimulating peptide

In 2003, three newly biological active peptides involved in Ca^{2+} homeostasis were cloned from porcine brain, the CT receptor-stimulating peptides (CRSPs). CRSPs seemed to act via the CT receptor (CTR) complex (Katafuchi *et al.*, 2003). Following studies on CRSP-1, a 38-amino acid peptide that has sequence similarity with CGRP, has been identified in cow, pig, dog, and horse; CRSP-2 in pig and dog; and CRSP-3 in pig. Like CT, CRSP-1 has shown to inhibit osteoclastogenesis (Notoya *et al.*, 2007). Based on structural similarities and the receptor binding characteristics, these peptides have been included in the CT peptide family.

2.2. Distribution of peptides in the CT family and their binding sites

The distribution of the members of the CT peptide family, as well as that of their binding sites, reflects their differences in biological properties and functions. The peptides from the CT peptide family are widely distributed in various peripheral tissues and in the central and peripheral nervous systems in rats and humans. While, CT is predominantly expressed in the thyroid gland, CGRP is produced by the peripheral projections of spinal afferent fibers, dilates arterioles, and AMY is released from the pancreatic β-cells. Table

2 displays the distribution of these peptides in rat (Table 2a) and human (Table 2c), as well as their binding sites (Table 2b). It is worth to mention that the bioactivities of the CT family peptides exhibit species differences.

Table 2a: Distribution of the peptides belonging to the CT family and their binding sites in rat (van Rossum, Hanish and Quirion, 1997; Rink *et al.*, 1993; Kitamura *et al.*, 1993; Owji *et al.*, 1995; Takei *et al.*, 2004).

	CGRP	AMY	AM	AM2
Tissue distribution (Decreasing order)	Endocrine Nervous system Spinal cord	Stomach Colon Lung Dorsal root Ganglia	Pheochromocytoma Adrenal medulla Lung Kidney Brain cortex Intestine Ventricle	Kidney Stomach Mesentery Pituitary Lung Pancreas Intestine Spleen Thymus
The distribution of their binding sites (Decreasing order)	Brain Cerebellum Heart Liver Spleen Skeletal muscle Lung Lymphocytes	Lung Stomach Spleen Liver Brain	Lung Heart Spleen Whole brain Liver Thyroid Stomach Adrenal Kidney	Not determined

Table 2c: Distribution of the peptides belonging to the CT family in human (Brain and Grant, 2004; Marutsuka *et al.*, 2003; Wookey, Lutz and Andrikopoulos, 2006; Morimoto *et al.*, 2007).

	CGRP	AMY	AM	AM2
Tissue distribution (Decreasing order)	Nerves Coronary artery Vein	Islets Brain Bone Kidney	Adrenal gland Heart Lung Kidney Liver Gallbladder Spleen Stomach Urinary bladder ...	Pituitary Kidney Frontal cortex Cerebellum Hypothalamus Heart

Table 2b: Distribution of CTR, CLR and RAMPs in rat and human tissues and cells (Wookey, Lutz and Andrikopoulos, 2006; Cottrell *et al.*, 2005; Hagner *et al.*, 2002).

	CTR	CLR	RAMP1	RAMP2/3
Tissue distribution of binding sites (Decreasing order)	Area postrema	Nerve fibers of the myenteric and submucosal plexuses	Enteric and dorsal root ganglia neurons	Gastrointestinal tract
	Kidney	Muscularis externa and lamina propria of the gastrointestinal tract	Dorsal horn	Dorsal root ganglia
	Brain	Dorsal horn of the spinal cord		Dorsal horn
	Bone	Soma of enteric and dorsal root ganglia		Smooth muscle cells
		Spinal neurons		
	Human tissues and cells			
	Prostate	Arteriolar smooth muscle		Cultured macrovascular endothelial cells
	Medulla oblongata	Venular endothelium		Dermal microvascular endothelial cells
		Lung, heart ventricle and kidney		

2.3. Bioactivities of the members of the CT peptide family

Table 3: Bioactivities of the members of the CT peptide family (Doods, 2001; Powell *et al.*, 2000; Beltowski and Jamroz, 2004; Roh *et al.*, 2004).

Peptide	Purported physiological role	Potential therapeutic target
CT	Bone resorption regulator	Inhibitor of bone resorption; Pagets' bone disease; Osteoporosis
CGRP	Vasodilator; Osmoregulation	Hypertension; Migraine; Pain
AMY	Food intake regulator	Body weight control; Type 2 diabetes
AM	Vasodilator; Diuretic and bronchodilatory effects; Aldosterone hormone	Hypertension; Renal failure; Heart failure; Pregnancy loss; Septic shock
AM2/ IMD	Gastrointestinal regulator; Cardiovascular	Diverse pathological conditions in cardiovascular, pulmonary, gastrointestinal and neuroendocrine systems

CT is involved in Ca^{2+} homeostasis whereas CGRP, AMY, AM and AM2/IMD induce a broad variety of biological effects including potent vasodilatatory actions, control of food

and water intake, facilitation of learning and memory processes, as well as modulation of various sensory (pain and others) and neuroendocrine functions (Joint international symposium in Zurich, 2004; Table 3).

2.4. The receptors of the CT peptide family-Class B GPCRs

Table 4: Human Class B GPCRs and their peptide ligand.

Receptor	Receptor subtypes	Peptide ligand
CRF	CRF_1	CRF, UCN1
	CRF_2	UCN1, UCN2, UCN3
GHRH	-	GHRH
GIP	-	GIP
Glucagon	-	Glucagon
GLP	GLP_1	GLP-1
	GLP_2	GLP-2
PTH	PTH_1	PTH, PTHrP
	PTH_2	TIP39
Secretin	-	Secretin
VPAC	$VPAC_1$	VIP, PACAP
	$VPAC_2$	
PAC_1	-	PACAP
CTR	-	CT
CTR/RAMPs	CTR/RAMP1	AMY
	CTR/RAMP2	
	CTR/RAMP3	
CLR/RAMPs	CLR/RAMP1	CGRP, AM
	CLR/RAMP2	
	CLR/RAMP3	

To understand the function of living cells at the molecular level is one of the greatest challenges in modern biological science. Despite unprecedented information available today, there are still large gaps of knowledge in the field. Generally, the functions of a living cell depend on various receptor-mediated signalling. In the human genome, one of

the largest protein super families is the Guanine nucleotide-binding Protein-Coupled Receptors (GPCRs). So far, more than 70% of the drugs on the market are targeted to GPCRs. GPCR proteins have at least six classes (Class A to Class E and others) that show no sequence similarity. Of these families, less is known for the Class B family, which comprises only 15 peptide-binding receptors in human and involves in regulating endocrine and neuroendocrine functions (Table 4). The receptors of the CT peptide family belong to Class B GPCR's.

Class B CGRPs is small. However, it is becoming attractive because as targets some efficient drugs are on market and more in clinical trial for the treatment of diseases. Table 5 shows the state of development of drugs that are targeted to Class B GPCRs (Hoare, 2005; Table 5). Without question, the use of GPCRs as effective therapeutic targets will continue to play a key role in the development of drugs in the future.

Table 5: Drug development status of peptide and nonpeptide ligand-targeting Class B GPCRs.

Peptide	Receptor	Agonist/antagonist	Indication	Status
Salmon CT	CTR	Agonist	Osteoporosis, Hypercalcemia	On market
			Paget's disease	On market
PTH(1-34)	PTH	Agonist	Osteoporosis	On market
PTH(1-84)				Phase III
Exendin-1	GLP_1	Agonist	Type II diabetes	Phase III
GLP-1 analog				Phase I/II/III
Porcine secretin	Secretin	Agonist	Autism	Unknown
Nonpeptide ligands				
BIBN4096BS	CLR/RAMP1	Antagonist	Migraine	Phase II
Numerous	CRF_1	Antagonist	Depression, anxiety	Phase I/II
Numerous	Glucagon	Antagonist	Type II diabetes	Unknown

2.4.1. The ligand binding and activation model of Class B GPCRs

At present, most studies of the mechanisms and principles of GPCRs activation focus on the GPCRs in Class A that directly activate G protein through a heptahelical domain. Recently, a study on Class C GPCRs revealed that they share a common activation model with Class A (Binet *et al.*, 2007). Could the heptahelical domain activation model in Class A GPCRs be a general model for all GPCR families? It is noticeable that the GPCRs in Class B have no sequence homology with GPCRs in Class A, although both families share a similar morphology. So far, there are at least two models describing the ligand binding and activation of Class B GPCRs derived from complementary mutagenesis, photoaffinity cross-linking and structural modelling approaches.

The consensus model is a two-step model involving the whole molecule of peptide ligand, i.e. N-terminus and C-terminus, as well as the body of receptor. In this model the C-terminal sequence of the peptide ligand firstly binds to the extracellular N-terminal domain of Class B GPCRs. Then, the free N-terminal region of the peptide ligand interacts with GPCR transmembrane helix domains (TM) and activates its intercellular signal pathway. It was reported that GLP-1 (Al-Sabah and Donnelly, 2003), secretin (Dong, *et al.*, 2003), CT (Dong, *et al.*, 2004), PTH (Castro *et al.*, 2005), and VIP (Tan *et al.*, 2006) bound to the N-terminal domain of their receptors. The binding affinity of the peptide-receptor interaction had no significant loss by using peptide fragments truncated from or modified at their N-terminus. However, no significant intracellular cAMP elevation were found with the fragments or analogs, whereas peptides with full of N-terminal region can activate their receptor and act as agonists.

The alternative model is a new model originating from studies of the secretin-receptor. The study on the interaction of the secretin-receptor initially followed the consensus pattern. The two-step model was confirmed in the early studies of the peptide by photoaffinity labeling technique. However, the following study showed secretin analogs modified in the N-terminus, directly bound at the N-terminus of receptor without being cross-linked on the receptor TM and acted as full agonists (Dong, Pinon and Miller,

2005). In this model, the whole peptide molecule does not act as a functional activator of its receptor anymore. According to this new model, an agonist epitope resides in the N-terminal region of Class B GPCRs, which is exposed by a "ligand-induced comformational change" (Beinborn, 2006). The designed oligopeptide epitope found in the N-terminal region of secretin receptor showed lower receptor binding affinity but full agonist activity. The similar region was also found in the N-terminal domain of other Class B GPCRs, such as CTR and $VPAC_1$ (Dong, *et al.*, 2006).

2.4.2. The receptors of the CT peptide family

Table 3 shows that CGRP, AMY, AM and AM2/IMD share some biological effects. This led to the hypothesis that these peptides might act via a common receptor. On the other hand, each peptide in the CT peptide family demonstrates particular biological actions and this was considered as evidence for the existence of distinct CGRP, AMY, AM and CT receptors. This apparent contradiction was solved when it was established that the effects of these peptides are mediated through their interaction with receptor complexes found by a combination of two seven transmembrane domain proteins, known as the CTR (Lin *et al.*, 1991) and the CLR (Flühmann *et al.*, 1995), three single transmembrane domain proteins termed RAMP1, RAMP2 and RAMP3 (McLatchie *et al.*, 1998) and an intracellular protein called the receptor-component-protein (RCP) (Evans *et al.*, 2000).

Table 6: Receptors for the members of the CT peptide family.

Peptides	Receptor Complex	Receptor subtype	Potency order of agonists	Potency order of antagonists
CT	CTR	CTa, CTb	sCT≥hCT>>CGRP≥AM≥AM(13–52)≥AMY	sCT(8–32)
AMY	+RAMP1	AMY_1	sCT, AMY≥CGRP>hCT	sCT(8–32), AC187
	+RAMP2	AMY_2	AMY	
	+RAMP3	AMY_3	AMY, sCT>CGRP>hCT	sCT(8–32), AC187
	CLR	Not functional		
CGRP	+RAMP1/RCP	$CGRP_1$	CGRP >AM≥AM(13–52)≥AMY>sCT≥hCT	CGRP(8–37)>AM(22–52)
AM	+RAMP2	AM_1	AM≥AM(13–52)>CGRP≥AMY>sCT≥hCT	AM(22–52)>CGRP(8–37)
	+RAMP3	AM_2		CGRP(8–37)>AM(22–52)
AM2/IMD	+RAMP1		CGRP> IMD=AM	IMD(17-47)> CGRP(8–37)> AM(22–52)
	+RAMP2		AM>IMD=CGRP	
	+RAMP3		AM>IMD>CGRP	

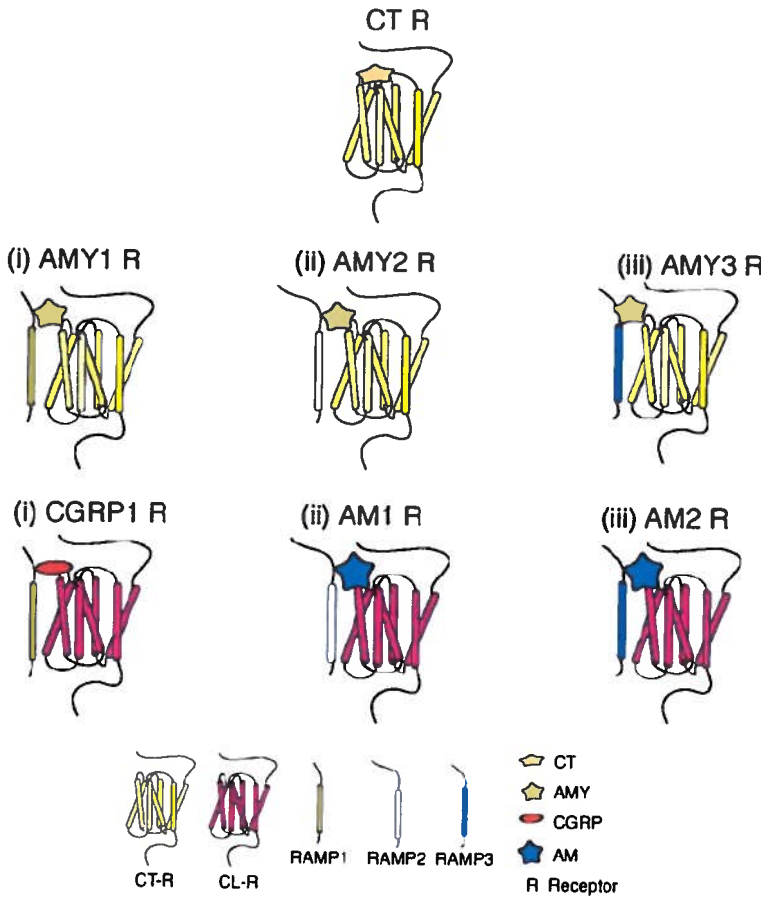

Figure 3: Binding of the CT family peptide to the dimer of CTR or CLR and RAMPs (Parameswaran and Spielman, 2006). The interaction positions of peptide and proteins do not represent the binding sites.

The two GPCRs for the CT peptide family, CTR and CLR, CTR were cloned in 1991, which is translated alone to the plasma membrane and activated by CT. CLR was cloned in 1996 as an orphan Class B GPCR, $CGRP_1$. The problem of CLR expression on the cell surface, except HEK-293 cells, promoted the study on a co-factor of CLR. In 1998, RAMPs were discovered as accessory proteins of CLR and CTR, whilst the interaction of RAMP1 with CLR forms CGRP receptors; the interaction of RAMP2 and RAMP3 with CLR forms AM receptors; the interaction of RAMP1, RAMP2 and RAMP3 with CTR forms AMY receptors (Table 6). Interestingly, as shown in Table 6, depending on the complex issued from the association of the two type GPCRs and the three RAMPs, different ligand selectivity profiles can be obtained, thus giving rise to receptor-like

subtypes such as AM_1 (CLR/RAMP2), AM_2 (CLR/RAMP3), AMY_1 (CTR/RAMP1), AMY_2 (CTR/RAMP2) and AMY_3 (CTR/RAMP3) (Udawela, Hey and Hexton, 2004; Figure 3). Regarding the newly isolated peptide AM2/IMD, it exhibits similar affinity but no selectivity for the CLR and the three RAMPs (Roh *et al.*, 2004), while the CRSPs apparently bind to the CTR without showing any affinity for the CLR/RAMP complexes (Katafuchi *et al.*, 2003). Additionally, RAMPs also interact with some other Class B GPCRs and Class C GPCRs, such as glucagon, parathyroid hormone and VIP/PACAP receptor, as well as a calcium-sensing receptor (Parameswaran and Spielman, 2006).

For the CGRP receptors, their classification, namely $CGRP_1$ and $CGRP_2$, made by our laboratories (Dennis *et al.*, 1990; Mimeault *et al.*, 1991; Mimeault *et al.*, 1992), was based on functional studies using various analogs and fragments. Nevertheless, even after many years, the molecular identity of the $CGRP_2$ subtype remains unsolved, although cells and tissues exhibiting a $CGRP_2$ pharmacological profile express CLR and RAMP1 (Chakravarty *et al.*, 2000; Rorabaugh *et al.*, 2001). Other CGRP receptor subtypes might even be present in the same tissues. As a matter of fact, in some but not all tissues in which both α and β isoforms of CGRP are active, the fragment CGRP (8-37) was found to be able to antagonize the effect of hCGRPα but not that of hCGRPβ (Wisskirchen, Gray and Marshall, 1999). Recently, it was clarified that $CGRP_2$ might be AMY_1or AMY_3 or AM_2 in past pharmacological studies because CGRP had broad actions on other receptors of the CT peptide family (Hay, Poyner and Quirion, 2008). Thus, it was clarified that $CGRP_1$ is the CGRP receptor, the interaction of RAMP1 with CLR.

Similarly, little information is currently available on the effect of AM on its receptors. Pharmacological studies revealed the existence of at least two AM receptors: one that recognizes CGRP, and the other is activated by AM and antagonized by AM(22-52) (Zimmermann *et al.*, 1996). Another study on AM receptor using transiently transfected cells revealed that AM_1 had a high specificity and selectivity for AM compared to other peptides in the CT family. AM (22-52) was an unselective antagonist to AM receptor subtypes, AM_1 and AM_2. However, AM_1 proved to be more sensitive to AM (22-52) than AM_2 when compared to antagonist CGRP (8-37) (Hay et al., 2003). Studies on the

structure-activity profile of the CLR/RAMPs and CTR/RAMPs complexes may help to clarify this issue. Nevertheless, the differences of species exist in the study of AM ligands and receptors interaction. Recently, a GPCR for AM was found in pancreatic cancer cell lines, named adrenomedullin receptor (ADMR, also called L1-R). Western blotting showed that AM binding sites expressed on the surface of pancreatic cancer cells was ADMR rather than CLR. The AM receptor, a potentially new therapeutic target of cancer, is selective for AM but not CGRP, and also expressed in primary human pancreatic stellate and endothelial cells (Ramachandran *et al.*, 2007). As mentioned in Section 2.1.5, AM2/IMD exhibited binding affinity to the CLR/RAMPs dimers. A recent study on rat hypothalamic oxytocin-secreting neurons indicated the possible presence of an AM2-specific receptor in the central nervous system (Hashimoto *et al.*, 2007).

2.5. AM sequence and structure in different species

Human	**H_2N-YRQSMNNFQGLRSFGCRFGTCTVQKLAHQIYQFTDKDKDNVAPRSKISPQGY-$CONH_2$**
Porcine	**H_2N-YRQSMNNFQGLRSFGCRFGTCTVQKLAHQIYQFTDKDKDGVAPRSKISPQGY-$CONH_2$**
Bovine	**H_2N-YRQSLNNFQGLRSFGCRFGTCTVQKLAHQIYHFTDKDKDGSAPRSKISPQGY-$CONH_2$**
Dog	**H_2N-YRQSMNNFQGPRSFGCRFGTCTVQKLAHQIYQFTDKDKDGVAPRSKISPQGY-$CONH_2$**
Rat	**H_2N-YRQSMN - -QGSRSTGCRFGTCTMQKLAHQIYQFTDKDKDGMAPRNKISPQGY-$CONH_2$**
Mouse	**H_2N-YRQSMN - -QGSRSNGCRFGTCTFQKLAHQIYQLTDKDKDGMAPRNKISPQGY-$CONH_2$**
Horse	**H_2N-YRQSMNNFQGLRSFGCRFGTCTVQKLAH(...)-$CONH_2$**
Zebra fish	**H_2N- - - - SKNSINQSRRSGCSLGTCTVHDLAHRLHDLNNKLKIGNAPVDKINPYGY-$CONH_2$**
Takifugu	**H_2N-TKRSKNLVNQSRKNGCSLGTCTVHDLAFRLHQLGFQYKIDIAPVDKISPQGY-$CONH_2$**

Figure 4: AM sequence comparisons across species. The red indicates the amino acid(s) in species different from human AM.

Human AM is a long peptide with 52 amino acids. The identical features comparable to other peptides from the CT family are one intermolecular disulfide bridge formation and a C-terminal amidated Tyr; while the most obvious difference in its structure is a long N-terminal loop with 15 amino acids. The amino acid differences in peptide sequence are

low if compared across human, porcine, bovine, and dog (Figure 4). Comparing to human AM, porcine AM has only one different amino acid at position 40 (G); dog AM displays two different amino acids at position 11 (P) and 40 (G) respectively; bovine AM exhibits 4 differences in peptide sequence, they are the number 5 (L), 32 (H), 40 (G), and 41 (S) residues. The rat and mouse AM are shorter than human AM, totalling 50 amino acids with 6 and 7 different amino acids in their sequence respectively compared to human AM. More differences in AM sequence can be found in non-mammalian species, such as zebra fish and takifugu.

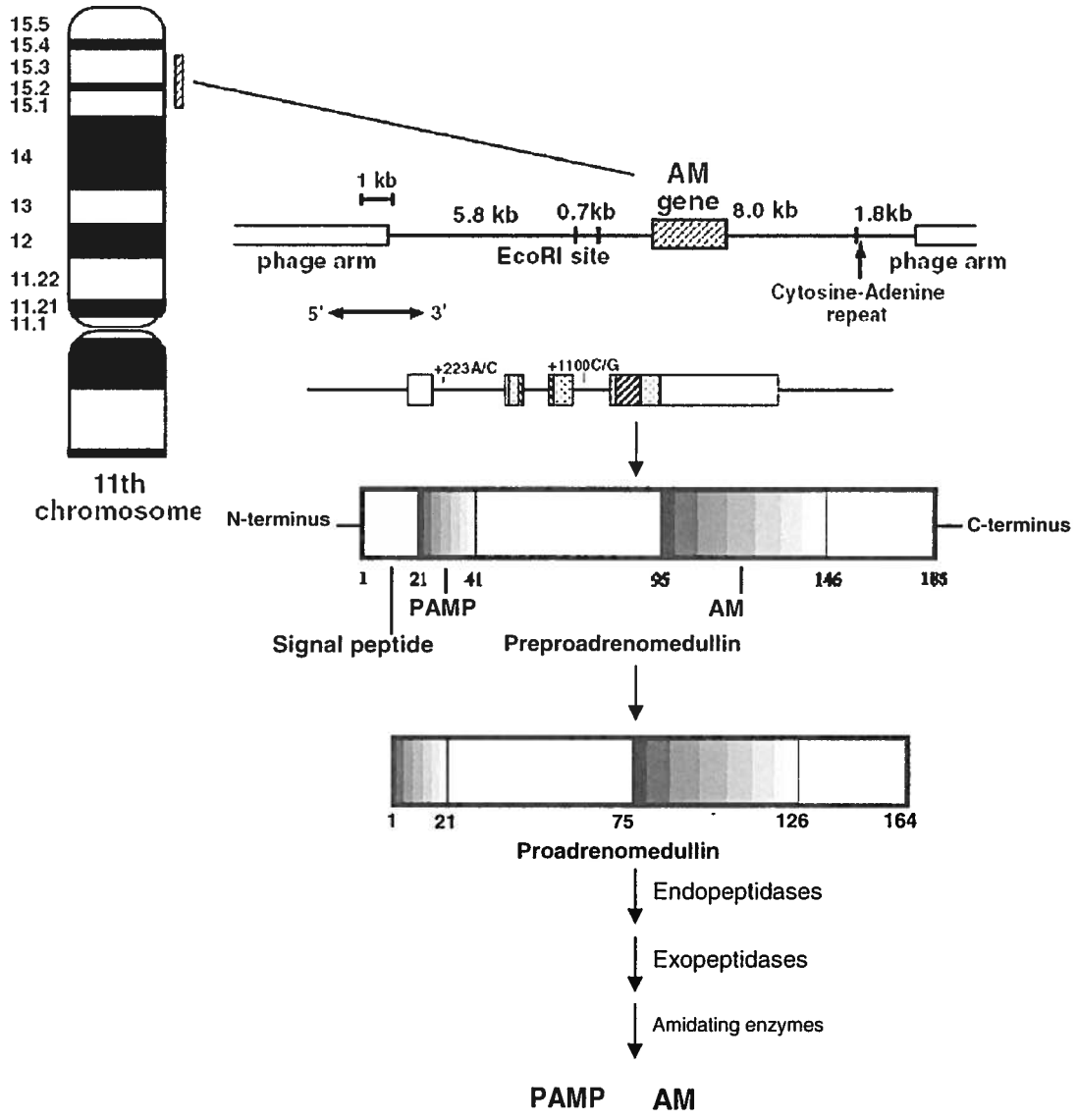

Figure 5: Human AM biosynthesis (Julián *et al.*, 2005; Ishimitsu *et al.*, 2006).

2.6. Human AM biosynthesis

The human AM gene has been located to chromosome 11, and is composed of 4 exons and 3 short introns, as well as TATA, CAAT, and GC boxes in the distal end of the short arm. AM gene expression is found in various cell types, with high expression in vascular endothelial cells and smooth muscle cells. Preproadrenomedullin, a 185-amino acid molecule, which consists of a signal peptide at N-terminus, PAMP, a 20-amino acid peptide, and AM (Figure 5). The precursor is cleaved within the endoplasmic reticulum and gives rise to proadrenomedullin, a 164-amino acid molecule. It is then modified by peptidases and enzymes to yield PAMP and AM.

2.7. AM receptor-mediated endocytosis

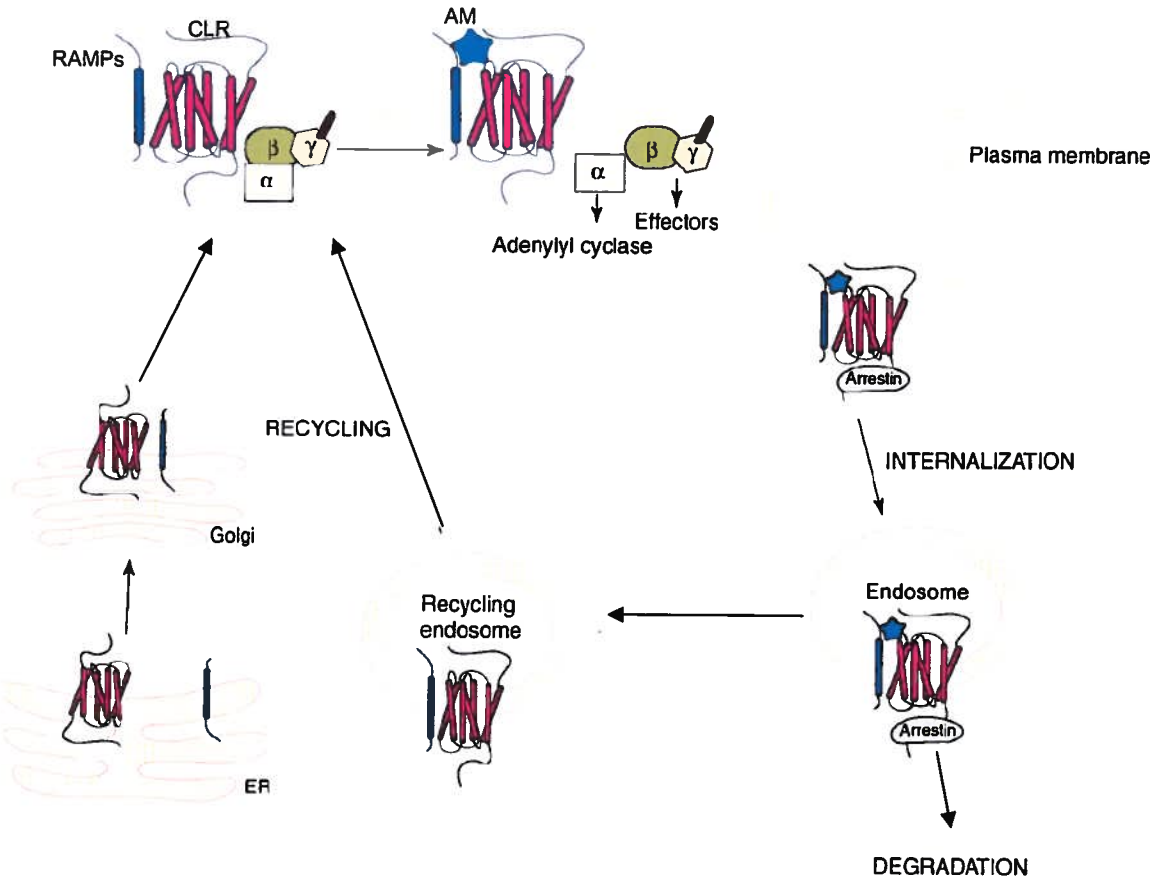

Figure 6: The regulation and intracellular trafficking of AM and its receptor (Parameswaran and Spielman, 2006).

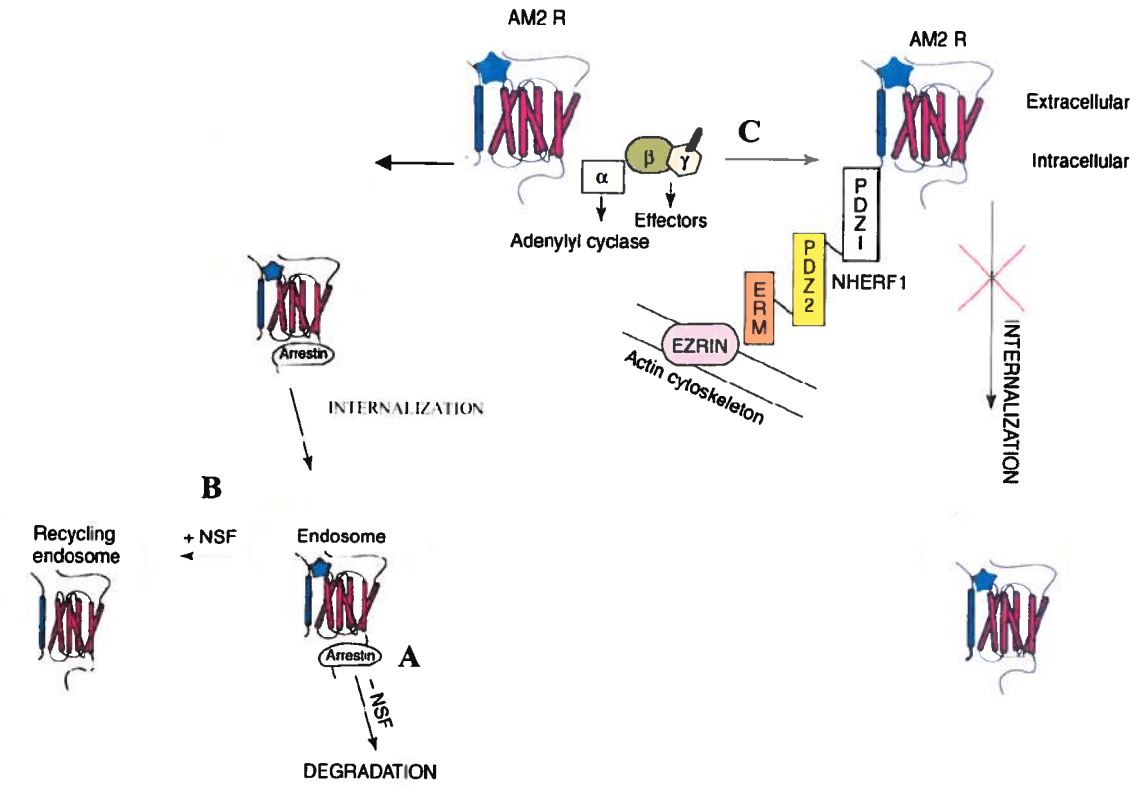

Figure 7: The regulation and intracellular trafficking of AM_2 receptor (Parameswaran and Spielman, 2006). In HEK293 cells internalized AM_2 undergoes degradation pathway (A), however, when co-expression with NSF, the internalized receptor undergoes a fast recycling (B). Co-overexpression of NHERF in HEK293 cells inhibits the internalization of AM_2 (C).

Many macromolecules enter the cell by the process of receptor-mediated endocytosis. CLR and RAMP2/3 located in the endoplasmic reticulum interact with each other within the Golgi to form a stable heterodimer. The heterodimer is then expressed on the plasma membrane as an AM receptor (AM_1 and/or AM_2) (Mclatchie *et al.*, 1998; Steiner *et al.*, 2002). When the ligand, AM binds to the extracellular domain (N-terminus) of the AM receptor, the agonist-activated receptor is phosphorylated by GPCR kinase (GRKs). Phosphorylation of GPCRs inhibits receptor coupling to interotrimeric G proteins at the plasma membrane (desensitization). A phosphorylated receptor binds arrestins, which prevents receptor interaction with G protein and mediates the interaction of the receptor with a clathrin-coated pit. The ligand-receptor complexes that are formed on the cell

surface can be selectively recruited into clathrin-coated pits - small areas of the plasma membrane that can invaginate inward and pinch off vesicles into the cytoplasm. Endocytic vesicles that are formed by invagination and pinching of clathrin-coated pits become uncoated in the cytoplasm and fuse with specialized membrane organelles known as endosomes. From the endosomes, receptors and their ligands are sorted to various intracellular destinations. Internalized molecules can be directed to lysosomes for degradation or be recycled back from recycling endosomes to the plasma membrane (Figure 6; Parameswaran and Spielman, 2006). It has been reported that the heterodimer of CLR and RAMPs maintains stablility during its expression, activation, internalization, and degradation or recycling (Hay, Poyner and Sexton, 2006).

In the AM receptor-mediated endocytosis, the C-terminal tails of RAMPs are required for the intracellular trafficking of ligand-receptor complexes. In the presence of the N-ethylmaleimide-sensitive factor (NSF), AM_2 exhibits a faster recycling pathway (Figure 7 B) in HEK293 cells, otherwise, it undergoes degradation with a slow recycling (Figure 7 A; Bomberger *et al.*, 2005). There is a PSD95/Discs-large/ZO-1 (PDZ) domain residing in the C-terminal tail of RAMP3, and not present in RAMP1 and RAMP2. The overexpression of Na^+/H^+ exchanger regulatory factor-1 (NHERF-1), a physiologically relevant ezrin binding protein, interacts with the CLR/RAMP3 complex and the ezrin-radixin-moesin complex (ERM) in HEK293 cells. Membrane–cytoskeletal linking proteins have NH_2- and COOH-terminal domains that associate with the plasma membrane and the actin cytoskeleton, by two PDZ domains. The PDZ-mediated interactions resulted in the inhibition of AM_2 internalization. In human kidneys, NHERF-1 was detected in proximal tubules. The expression of NHERF protein was also found in the kidney, small intestine and other organs (Weinman *et al.*, 2006).

2.8. Intracellular signalization of AM

Attempts have been made to explain the signalization of AM on smooth muscle cells, endothelial cells, and cardiac myocytes. So far, it is clear that AM_1 and AM_2 exhibit different intracellular signalling pathway. However, it remains unclear as to the

pharmacological differences of two AM receptor subtypes. The intracellular signalization of AM is affected by two types of AM receptor and correlated mainly with cyclic adenosine 3',5'-monophosphate-protein kinase A (cAMP-PKA) and calcium, mitogen-activated protein kinase (MAPK; it is also called extracellular signal-regulated protein kinase, ERK) in smooth muscle cells, nitric oxide (NO), endothelial nitric oxide synthase (eNOS) and cyclic guanosine 3',5'-monophosphate (cGMP), as well as phosphatidylinositol-3-kinase (PI3K)/Protein kinase B (Akt) in endothelial cells (Figure 8).

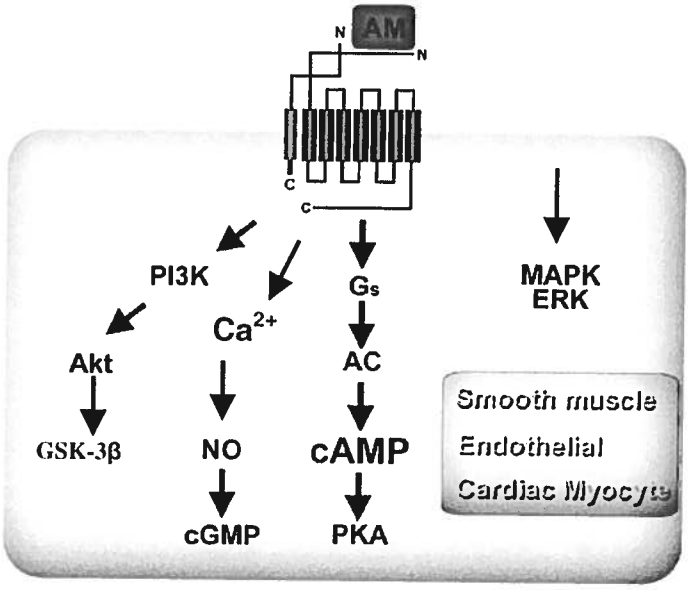

Figure 8: The intracellular signalization of AM (Gibbons *et al.*, 2007).

2.8.1. Intracellular signal pathway of AM related vasodilation

cAMP-PKA pathway: In smooth muscle cells, AM binds to the extracellular loops of the receptors and activates Gs. The activated protein then interacts with an effector called adenylyl cyclase (AC), and induces increases in intracellular cAMP. PKA is a cAMP-dependent enzyme, which is activated by the increased cAMP level. Both cAMP accumulation and PKA activation mediates AM vasodilation (Ishizaka *et al.*, 1994).

Calcium-NO-cGMP pathway: AM-induced intracellular Ca^{2+} increase and cGMP occurred in cultured bovine carotid and aortic endothelial cells. In endothelial cells, the

increase of intracellular Ca^{2+} and cGMP was observed (Shimekake *et al.*, 1995). Another study has revealed that the NO-cGMP pathway plays a role in AM-induced vasodilation (Hayakawa *et al.*, 1999). Because the site for phosphorylation by cAMP-dependent protein kinase on endothelia NOS has been reported (Lamas *et al.*, 1992), the increase in Ca^{2+} might be induced by endothelial constitutive NOS activated by cAMP directly. The increased NO release from vascular endothelium remained unclear. The elevation of intracellular calcium concentration might activated endothelia NOS and resulted in the release of NO in the cell. NO is the activator of cGMP synthetic enzymes and stimulated the produce of cGMP in neighbor cells. cGMP acts as a second messenger, and leads to vasodilation in blood vessels.

2.8.2. Intracellular signal pathway of AM related cell apoptosis

PI3K-Akt-GSK pathway: The mechanisms of AM via cAMP and intracellular Ca^{2+} mediated by CLR/RAMPs complexes have been well characterized. Recently, AM in apoptosis was investigated by using endothelial cells. PI3Ks are a family of enzymes related to inositol phosphorylation, and linked to various cellular functions. The activated PI3K by receptor tyrosine kinase phosphorylates PIP_2 to phosphatidylinositol-3,4,5-triphosphate (PIP_3). The activated Akt is one result of PI3K activity because Akt requires the formation of PIP_3 in order to be translocated to the cell membrane. Akt family involves in cellular survival pathway and insulin signalling pathway, and regulates cell growth by inducing protein synthesis pathway, and inhibiting apoptotic processes. AM showed an antiapoptotic function via a PI3K-Akt pathway (Kim *et al.*, 2002). The mechanism was then verified by using the gene transfer in hypertensive rats, and that glycogen synthase kinase (GSK-3β), a down-stream signal protein kinase, was responsible for the AM protection from apoptosis in cells (Yin, L. Chao and J. Chao, 2004).

MAPK/ERK pathway: MAPK are serine/threonine-specific protein kinases. They regulate gene expression, mitosis, differentiation, and cell survival/apoptosis. Since AM could be a protector in mannitol-induced apoptosis, the effects of AM on the MAPK/ERK

signal-transduction were explored. In vascular smooth cells, AM was found to stimulate cell proliferation as a growth factor via the MAPK/ERK pathway, however, it has been shown that the AM stimulation was not mediated by CLR/RAMP complexes on plasma membrane (Shichiri *et al.*, 2003).

2.9. AM transport and clearance in circulation

AM is a native peptide. As mentioned in Section 2.6, the gene encoding AM has been located to chromosome 11 in humans. The name of AM derives from adrenal medulla where the peptide is produced at a high level. However, subsequent reports have shown that high expression of AM gene is to be found in endothelial and vascular smooth muscle cells as well as in the myocardium. Presently, it is believed that AM is released from vascular endothelial cells into plasma (AM concentration in plasma is about 2-10 pM) (Beltowski and Jamroz, 2004). As a result, a higher biodistribution of AM can be found in vascularised organs or tissues, such as the lung, heart, and kidney.

2.9.1. Transport

In the circulatory system, there are two forms of AM, termed as immature AM (glycine-extented 53-amino acid peptide) and mature AM (*i.e.* AM). The inactive immature AM can be converted to the active mature AM by enzymatic amidation (Kitamura *et al.*, 1998). The $t_{1/2}$ of AM in the circulation is very short, about 20 min. However, AM circulates in the blood as a complex composed of AM and AM-binding protein-1 (AMBP-1, also called complement factor H) (Beltowski and Jamroz, 2003). The complexed AM is stable in the blood and able to liberate AM into the circulation when the concentration of AMBP-1 is lowered. It was reported that the AMBP-1 bound to AM has no effect on AM receptor-mediated bioactivities, whereas it plays an important role in the direction of AM to its receptor binding sites (Gibbons *et al.*, 2007).

2.9.2. Clearance

Peptides are mainly cleared through binding to the peptide clearance receptors and proteolysis by peptidase (Wilkins, Redondo and Brown, 1997). To date, two pathways for AM clearance have been reported: receptor binding in the lungs and protease hydrolysis in the kidney (Jiang *et al.*, 2004; Figure 9).

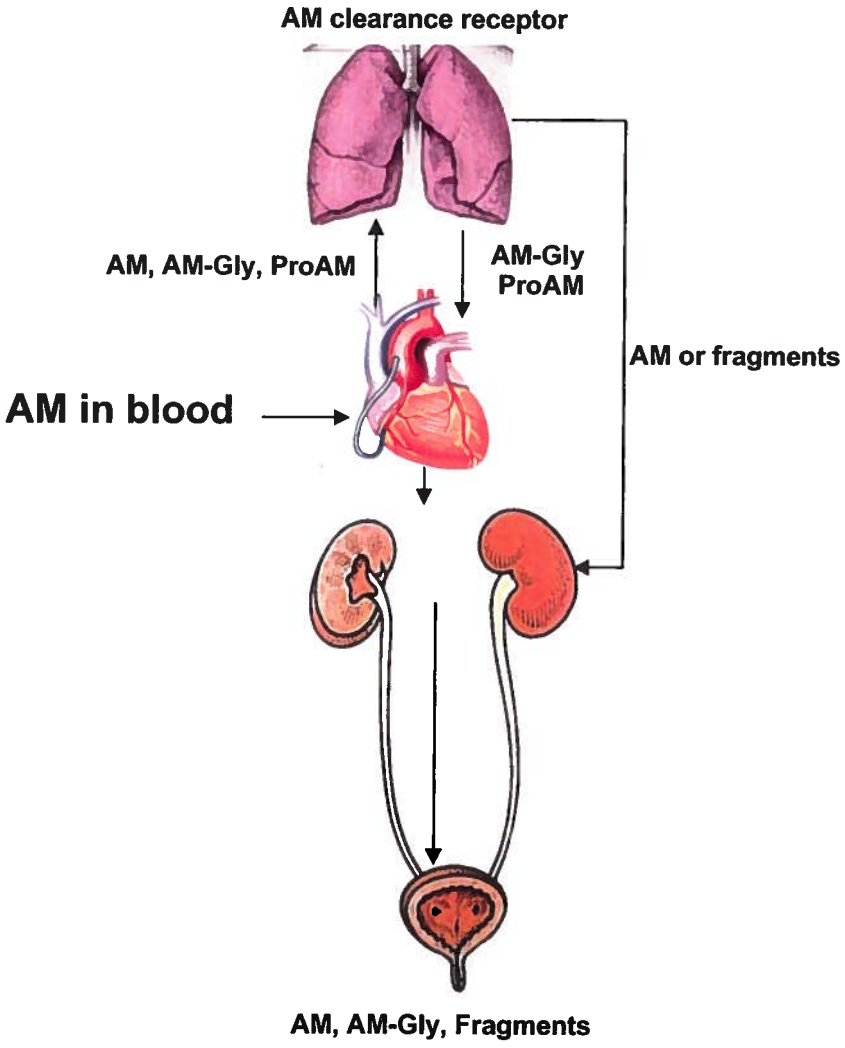

Figure 9: AM clearance in circulation system.

2.9.2.1. Pulmonary clearance

In a study on the tissues concentration and gene expression of AM, reduced AM concentration was first detected in the lungs (Shimokubo *et al.*, 1995). The supposition

that indicated the clearance receptor of AM is in the lungs was born. Meanwhile, abundant binding sites of AM were found in rat lung and heart, and the receptors in the lungs displayed different specific binding properties compared with the receptors in the heart (Owji *et al.*, 1995). Administration of human AM into the left atrium but not through the right atrium of piglets could induce systemic pressure reduction (Sabates *et al.*, 1996). Additionally, when the two forms of AM passed through the pulmonary artery, the concentration of the mature form of AM was observed to be significantly lower than the constant AM-Gly concentration (Nishikimi *et al.*, 2000). A significantly lower AM concentration in pulmonary artery supported by radioimmunoassays (RIAs), especially in the pulmonary capillary, also assayed that the location of AM clearance was in the lungs (Hirayama *et al.*, 1999). Recently, AM metabolism was evaluated in rats and dogs *in vivo* by using ^{125}I-labeled AM. The data of AM distribution and pharmacokinetics as well as its clearance furthermore proved that the specific AM receptor responsible for AM clearance is in the lungs (Dupuis, Caron and Ruël, 2005). As a result, the AM bound to an AM clearance receptor might internalize through clathrin-coated pits, and then be sent to an endosomal compartment. The low pH in an acidic endosomal compartment would release AM receptor-bound, eventually leading to its degradation by intracellular peptidases. The free receptor can then be directed to the lysosome for degradation or back to the plasma membrane.

2.9.2.2. Endopeptidase clearance in kidney

Generally, the level of AM in blood and tissues depends on the balance of AM production and clearance. Although AM can be degraded through binding to its clearance receptors in the lungs, both AM-glycine and the mature form of AM found in human plasma and urine with different ratios (Nishikimi, 2007). The higher level of AM found in the urine (comparable to AM in plasma) suggested that the existence of another AM clearance pathway in the kidney. It was reported that the pro-AM was cleaved from N-terminal region by neutral endopeptidase (NEP), and then converted to AM. Later, inhibition experiments in dogs have also displayed that AM might be the substrate of NEP, and that AM degradation in the kidney could be catalyzed by NEP to yield smaller inactive

peptide fragments (Lisy *et al.*, 1998). However, this does not occur in humans (Petrie *et al.*, 2001). NEP is a membrane-bound Zn-metalloproteas that is abundant in the kidney. Besides AM, the peptides that have been reported to be degraded by NEP include opioid-peptides, bradykinin, bombesin-like peptide and endothelin-1 (Sansoè *et al.*, 2005). Consequently, NEP in kidney might be involved in the clearance of AM.

2.10. Structure-activity relationship studies of the CT peptide family

In an attempt to gain information about the structural prerequisites for biological activity and in order to establish the functional significance of each receptor of the CT peptide family, agonists and partial agonists, as well as peptide or non-peptide antagonists were developed (Table 7). All of the information gathered from the structure-activity relationship studies on the members of the CT peptide family can be summarized below:

Table 7: The reported agonists and antagonists as well as non-peptide antagonists of the CT peptide family.

Receptor subtypes	Agonists	Antagonists
CTR	CT	
CTR/RAMPs	AMY(1-37)	AMY(8-37), sCT(8-32), AC187, AC253, AC413, AC512
CLR/RAMP1	CGRP(1-37)	CGRP(8-37), CGRP(12-37), CGRP(27-37),), BIBP4096BS, [Tyr^{27},Pro^{34},Phe^{35}]-CGRP(27–37), [Asp^{31},Pro^{34},Phe^{35}]-CGRP(27–37), [Tyr^{27},Asp^{31},Pro^{34},Phe^{35}]-CGRP(27–37)
CLR/RAMP2 or RAMP3	AM(1-52),AM(13-52), AM(15-52),AM(16-52)	AM(22-52), AM(26-50), AM(27-52), AM(34-52), AM(40-52)

BIBN4096BS: [1-piperidinecarboxamide, *N*-[2-[[5-amino-1-[[4-(4-pyridinyl)-1-piperazinyl]-carbonyl]pentyl]amino]-1-[(3,5-dibromo-4-hydroxyphenyl)methyl]-2-oxoethyl]-4-(1,4-dihydro-2-oxo-3(2*H*)-quinazolinyl)-, [*R*-(*R**,*S**)]]

2.10.1. N-terminal loop region

The extra long N-terminal loop of AM is a structural element distinct from other members of the CT peptide family. The region may principally be involved in triggering the ensuing signal transduction process. The amino acids (position 1 to 15) in the region

located before the ring structure of AM appear not to be necessary for full expression of its bioactivity. Human AM (13-52) (Hao *et al.*, 1994) and AM(15-52) (Santiago *et al.*, 1995) were shown *in vivo* to possess vasodilator activity similar to that of human AM, in the pulmonary vascular bed of the rat and the mesenteric vascular bed of cat. The receptor-binding affinity and cAMP activity of the AM fragments with a shorter or absent N-terminal loop, i.e. human AM(13-52) and AM(16-52), are the same as to that of AM in vascular smooth muscle cells from rat aorta (Eguchi *et al.*, 1994). Meanwhile, human AM(1-10) has no effect on the receptor-binding and cAMP release. The other members of CT peptide family, CT, AMY and CGRP, are the native and active peptides without an N-terminal loop. However, it was reported that the N-terminus of CGRPα interact with the transmembrane of $CGRP_1$ where it might be involved in receptor activation (Conner *et al.*, 2007).

2.10.2. Disulfide bridge formation

In the CT peptide family, the disulfide bridge between the two cysteines (position 16 and 21), as well as the amino acid residues between them (six amino acids in total) play an important role in the stabilization of the α-helical conformation and in the expression of bioactivity. Removal of the six-membered ring structure in CGRP, AMY and AM resulted in losses of activity. Some peptide fragments, such as CT(8-32) (Silvestre *et al.*, 1996), CGRP (8-37), AMY(8-37) and AM(22-52) (Champion *et al.*, 1997) that do not possess the ring structure, lack agonistic activity, but show antagonistic actions. Poor potency was detected when using linear human AM derivative, (carbamoylmethyl-$Cys^{16,21}$)AM-NH_2, comparing to human AM in vascular smooth muscle cells from rat aorta (Eguchi *et al.*, 1994).

2.10.3. The amphiphilic α-helix conformation

The α-helix secondary structure following disulfide bridge formation plays a role in maintaining the 3D-structure required for the peptide receptor interaction leading to vasodilation. AM fragments, such as human AM(1-25), AM(11-26), AM(15-22), AM(16-

21), AM(16-31) and AM(16-36) (Watanabe *et al.*, 1996; Kitamura *et al.*, 2001; Champion *et al.*, 1996; Champion *et al.*, 1997), all α-helix truncated analogs, were shown to possess vasopressor activity *in vitro* and *in vivo*, while the native peptide generates vasodilation. The vasopressor activity of the AM fragments was mediated by catecholamine released from the adrenal medulla through the activation of α-adrenergic receptors in rat (Champion *et al.*, 1996; Champion *et al.*, 1997). CGRP antagonists, CGRP(19-37) and CGRP(28-37), had decreased binding affinity to the CGRP receptor and cAMP respond since they lost the amphipathic nature compared to antagonist CGRP(8-37) and native peptides (Howitt and Poyner, 1997).

2.10.4. C-terminal region

The C-terminal region is required for the peptide receptor interaction. Generally, C-terminal fragments are devoid of bioactivity but not of binding affinity because significant antagonism is observed with fragments, such as CT(9-32) (Rennert, Neundorf and Beck-Sickinger, 2008), CGRP (8-37) (Conner *et al.*, 2002), AMY(8-37), AM(22-52), AM2(16-47) or AM2(17-47). The CT(9-32) was reported as a CT-derived targeting peptide, and the C-terminus of CGRPα could interact with the extracellular N-termini of $CGRP_1$ where it might be involved in ligand-receptor binding activity (Conner *et al.*, 2007). The receptor-binding and cAMP activity of human AM(1-51), the fragment of AM without the 52^{nd} Tyr at C-terminus, exhibited very low activity compared to the native AM in vascular smooth muscle cells of rat (Eguchi *et al.*, 1994). Whereas, no receptor-binding and induction of cAMP was found with human AM(33-52), either.

2.10.5. Non-peptide antagonist

Notably, besides peptide agonists and antagonists, some non-peptide small molecules acting as selective antagonists of native internal CGRP (William et al., 2006), such as BIBN4096BS, are very useful tools in the study of CT peptide family. In the past, non-peptide BIBN4096BS have shown selectivity to $CGRP_1$ (Doods *et al.*, 2000), low affinity for AMY_1 and non-affinity for AM_1 and AM_2 (Hay, Poyner and Quirion, 2008). To date,

no selective agonists or antagonists have been reported for AM receptor subtypes. Likewise, little information is available on the effect of AM2 on its receptors. The development of non-peptide antagonists might be an effective solution in the peptide study of AM and AM2.

2.10.6. Species differences

The species difference is an inevitable problem in the study of structure-activity relationship of peptides. On one hand, a peptide could display different potency in various species. In the study of the vasodilator effect of human AM and CGPR by using the pulmonary vascular bed of cats and rats, the effect of AM is 10-fold higher in cats than in rats, whereas CGRP exhibits the same potency in cats and in rats (Nossaman, et al., 1995). On the other hand, the potential range of peptides in species is different. The vasodilation activity of AM is higher in cats but lower in rats compared to CGRP. The AM(15-52), an agonist of AM, displays a similarity to AM in cats but difference in rats. In receptor-binding studies, the binding affinity of AM, AM(22-52) and CGRP has no significant difference in porcine. The order of AM and its analogs for inhibiting ^{125}I-rAM binding to porcine lung are rAM≥hAM≥hAM(22-52)>hαCGRP≥hαCGRP(8-37) >>>> sCT (Dang K, *et al.*, 1999). The displacement in rat lung is AM>>hAM(13-52)>>hAM(22-52)>> hαCGRP≥hαCGRP(8-37) by using ^{125}I-hAM(13–52) as radioligand. The binding affinity of AM was 1000-fold and 3000-fold higher than AM(13–52) and AM(22–52), respectively (Juaneda *et al.*, 2003). The considerable species variation in the study of CT peptide family depends quite on the peptide, radiolabled peptide and animal or cells or membrane used under experimental conditions. The AM sequences difference in species has been shown in Section 2.5, the CLR and RAMPs differences in species remain unclear. Thus, species difference is an important issue in the study of the CT peptide family.

Hypotheses and specific objectives

Known for their numerous stimulating, inhibiting, or regulating functions, peptides have been considered as potential agents for therapeutic applications. Meanwhile, the nuclear medicine researchers have been keeping their eyes on these new targeting molecules with high specificity in organs or tissues. Currently, there is only one agent used for the clinical imaging of the pulmonary circulation, i.e. ^{99m}Tc-macroaggregated albumin (MAA) derived from human albumin. This agent is exclusively used for the diagnosis of pulmonary embolus. These particles are irregular in shape, and have jagged edges in a size distribution of 10 to 90 microns. It is large enough to be trapped in small pulmonary vessels, thus enabling external detection. The important limitations of MAA include the inability to perform imaging of small pulmonary vessels beyond the point of obstruction, which limit its sensitivity to detect small vascular defects and emboli. Furthermore, this technique could increase the potential risks of infection since the albumin was made from human blood, and the blood might be contaminated by virus.

Adrenomedullin (AM), a 52-amino acid peptide, displayed a dense population of binding sites particularly acting as clearance receptors in pulmonary vessels. These findings thus suggested that AM-derived compounds could be well suited for the development of radiopharmaceuticals for useful lung-specific imaging. It has been observed previously by Dupuis (Dupuis, Caron and Ruel, 2005) that ^{125}I-labeled AM had a high binding selectivity for the lungs when injected intravenously. This data suggested that labeled AM could be used as a target-specific lung imaging tool. In the beginning of the present study, we hypothesized that labeled AM could penetrate deeply in the pulmonary vasculature and give a sharp imaging of the very small pulmonary circulation. Such a compound could potentially replace MAA for the diagnosis of pulmonary circulation, especially in small vessels, and other indications as well. The proposed AM analogs should hypothetically show good lung imaging properties in the dog.

Herein, an AM delivery system was then designed as a receptor targeting radiopharmaceutical for pulmonary imaging. Nevertheless, ^{125}I-labeled human AM is not well suited for imaging because of ^{125}I, a γ-emitting radionuclide with a long physical half-life of 60 days. In clinical application, ^{131}I, a β and γ-emitting radionuclide with a

half-life of 8 days, is usually used in treatment of diseases. However, the drawbacks when using iodine as a radionuclide involve its thyroid concentration, multiple iodinated by-products, low labeling yield (less than 30%), and the emission of a potentially cytotoxic dose of radiation. Therefore, iodine was replaced with ^{99m}Tc in our designed system, a radionuclide with ideal nuclear properties and a physical half-life of 6 h. The designed system is composed of 99m-technetium, the carrier of the radionuclide, and the targeting biomolecule as receptor ligand (Figure 10: A). The techniques to prepare the new tracer included the chemical modification of a biomolecule, the conjugation of carrier and the biomolecule and the attachment of a radionuclide. We also considered inserting a spacer as a linker between the biomolecule and the carrier to maximize the ligand-receptor binding, especially as the biomolecule is a small peptide.

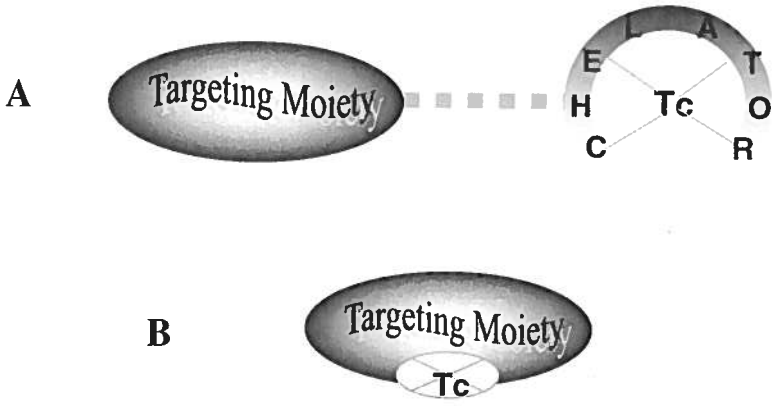

Figure 10: 99m-technetium delivery system.

Objective 1: The development of an AM-based target-specific radiopharmaceutical for imaging human pulmonary circulation. In the present study, by using AM, a direct labeling of linear AM with ^{99m}Tc was achieved without the need of a chelating agent as a carrier (Figure 10: B), while maintaining excellent binding affinity for pulmonary circulation system in the dog. To evaluate the effectiveness of the potential imaging agent in clinical applications, the pharmacokinetics and pharmacodynamics of the AM analogs was performed in dogs and rats. The data collected from the lung images, as well as the distribution and kinetics of the radiotracer in the dog strongly supports the pulmonary specificity and clearance of AM. The lung perfusion after surgery further confirmed the

application of the new tracer in pulmonary diagnosis, including pulmonary embolus and possibly infection.

Objective 2: Characterization of the specific binding sites found in dog lungs by using ^{99m}Tc-linear AM, and the specific sites involved in the AM clearance in the lungs. As a member of the CT peptide family, AM binds to and activates at least two types of such GPCRs named AM_1 and AM_2. A German research group suggested that the receptor found in isolated rat lungs and endothelial cells (Dschietzig *et al.*, 2002) is of the AM type. Therefore, in the following study, we then hypothesized that the specific binding sites found in dog lungs by using ^{99m}Tc-linear are AM receptor, and the receptor responsible for the AM clearance in the lungs is AM_1. The discovering pharmacologically AM binding sites *in vivo* by using ^{99m}Tc-linear AM encouraged us to characterize the specific binding sites in dog lungs by means of known agonists and antagonists of the CT peptide family, and AM labeled with ^{99m}Tc or ^{125}I used as receptor imaging probes *in vitro*.

Objective 3: Characterization of the sequence and structure in AM required by the receptor-binding activity. By using a receptor-radioligand binding assay, the dominance of the AM_1 receptor subtype in the clearance of AM in dog lungs was then characterized. The receptor occupancy was confirmed *in vivo* and *in vitro* in the present study. Since AM is a long peptide with 52 amino acids, the smaller AM fragments, the key structures and peptide sequences, as well as some key amino acid residues of AM required by the AM receptors in the dog lung were pursued. We hypothesized that the binding site of AM required by the receptors found in dog lungs is at C-terminal region of AM. In this case, it is possible to find a smaller peptide that could keep a high specificity for the lung target, while exhibiting a low bioactivity in the circulation system.The purpose of the study is to compare the receptor-binding activity of AM in dog lungs to portions of the AM molecule. By the screening of a selective probe for AM_1 receptors in dog lungs, a new delivery system derived from AM is expected to support eventually clinical decision, as well as to reduce the cost of diagnosis. That information is essential for the development

of better and smaller lung-specific diagnostic and/or therapeutic molecules after radiopharmaceutical optimization.

Altogether, in clinical applications, receptor imaging provides a powerful tool for diagnostic purposes and for monitoring the responses to treatments. By further characterizing the receptor population found in lung tissues, especially that receptor subtype AM_1 is responsible for AM clearance, highly selective lung imaging molecules like ^{99m}Tc-linear AM could then be designed and used for diagnostic purposes after radiopharmaceutical optimization. The present study in pharmaceutical research may continue to provide critical thresholds for adverse events, and clinical testing requires GMP-like production.

Chapter 3 : Materials and methods

3. Preparation of human AM and its analogs

Solid-phase peptide synthesis (SPPS) is based on the sequential addition of α-amino and side-chain protected amino acid residues to an insoluble polymeric support. The synthetic method was developed by Dr. Bruce Merrifield (Nobel Prize in Chemistry 1986). In SPPS, according to the N-α-protection scheme two strategies were used, the t-butyloxycarbonyl (Boc)-strategy and the 9-fluorenylmethyloxy-carbonyl (Fmoc)-strategy. In the present study, all peptides and their analogs were prepared by a solid phase procedure using standard Fmoc/benzotriazol-1-yl-oxy-tris(dimethylamino)-phosphonium hexafluorophosphate (BOP) methodology (Castro *et al.*, 1975; Fournier, Wang and Felix, 1998; Figure 11).

3.1. The apparatus preparation for peptide synthesis

The syntheses of all peptides or their analogs were carried out on a custom-designed semi-automatic multireactor synthesizer. The coupling reaction takes place in a glass funnel reactor. The funnel reactor was pre-treated by washing with hydrogen chloride (HCl; Sigma-Aldrich, St-Louis, MO), rinsed with distilled water, and methanol (MeOH; Fisher Scientific, Ottawa, ON) three times, then dried under a stream of nitrogen. The vessels were filled with 10% w/v dichlorodimethylsilane ($Si(CH_3)Cl_2$; Sigma-Aldrich) in toluene (Fisher Scientific), after 2 h, the solution was drained and the reactors were washed with MeOH then dried in an oven.

3.2. Fmoc solid-phase peptide synthesis

Before the synthesis, a 4-(2',4'-dimethoxyphenyl-Fmoc-aminomethyl)-phenoxyacetamidonorleucylaminomethyl resin (Fmoc-Rink amide resin, ~ 0.5 mmol/g, 200-400 mesh, Chem-Impex International, Wood Dale, IL) as solid support was added and swollen in dimethylformamide (DMF; Fisher Scientific) with constant shaking for 50 min using N_2 bubbling.

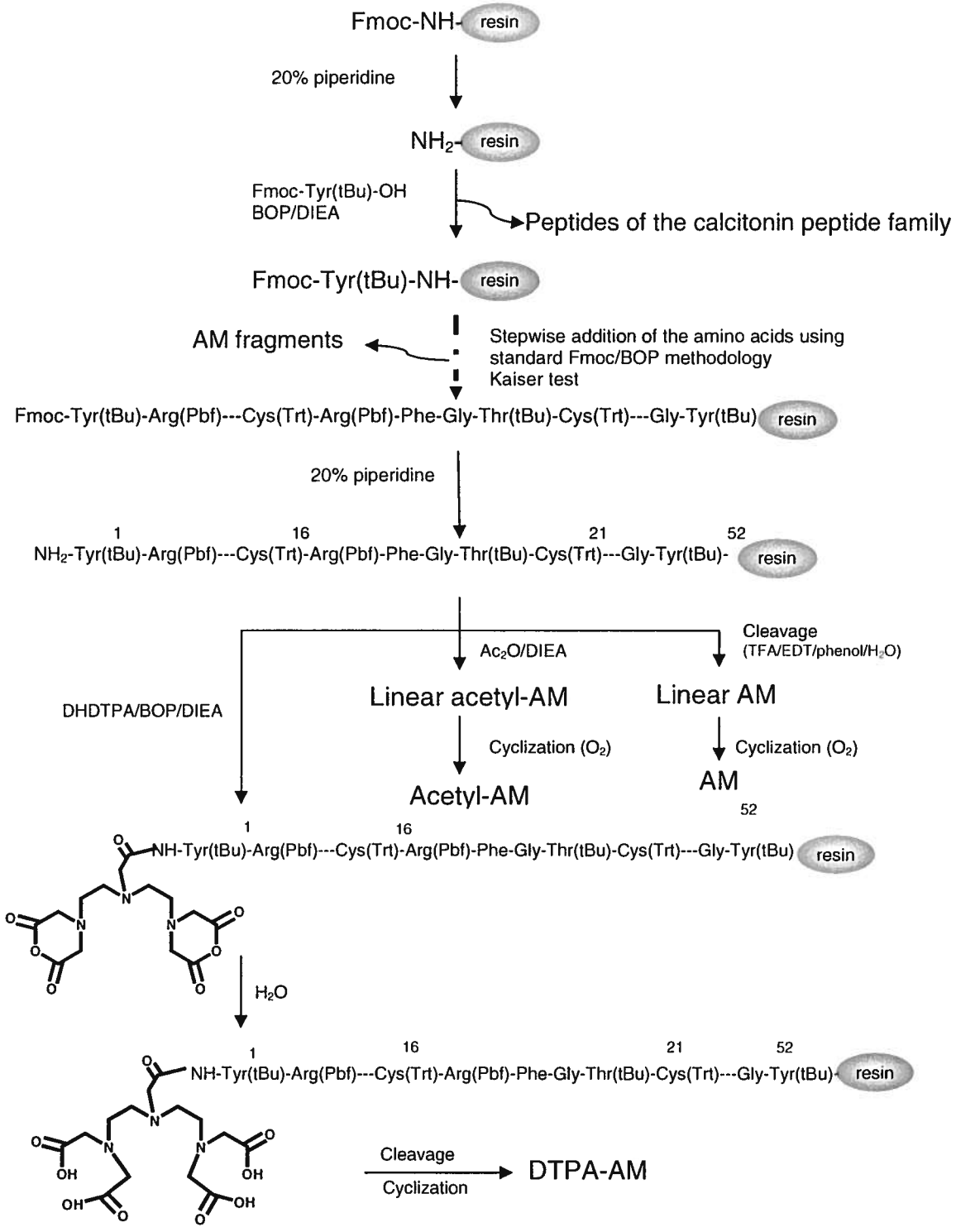

Figure11: Peptide synthesis by Fmoc strategy.

3.2.1. Removal of N-terminal Fmoc group

The Fmoc group on the N-terminus of resin or amino acid was removed with a 20% piperidine (twice: 1×2 min, 1×15 min; A&C American Chemicals Ltd, Saint-Laurent, QC)/ DMF mixture, except for Fmoc-glutamic acid (Glu, E) or glutamine (Gln, Q) which was removed by one treatment with 50% piperidine/DMF for 10 min. After the reaction, the N-protecting moiety was removed to leave a free amine anchor on the solid support or amino acid.

3.2.2. Coupling reaction : General protocol

After washing with DMF (2 ×2 min), dichloromethane (DCM; 2 ×2 min) (Fisher Scientific), DMF (2 ×2 min), the first amino acid of the synthesis, corresponding to the last residue of the peptide sequence, was coupled to the resin with BOP reagent (Matrix-Innovation, Montreal, QC) in presence of diisopropylethylamine (DIEA; Aldrich). In function of the resin substitution with the "Rink moiety", a ratio of 3 eq of Fmoc-amino acid (Table 8), 3 eq of BOP and 3 eq of DIEA was used for each coupling step and its completion was monitored with a ninhydrin test. The coupling time was usually about 30 min with a gentle stream of N_2 bubbling. For some amino acids that were difficult to couple to the growing peptide chain, a prolonged reaction time and/or an extra 1 mL-2 mL 1-methyl-2-pyrrolidone (NMP; Sigma) was added. After the assembling of the peptide chain, a final Fmoc deprotection step was carried out. The peptide resins were washed with DMF (2 ×2 min), DCM (2 ×2 min), and methanol. Then the beads were dried in open atmosphere and stored at -20°C.

3.2.2.1. The coupling protocol for proline-containing peptide

The amino acid after proline (Pro, P) was double coupled with general protocol. Then, the Kaiser-test (Kaiser *et al.*, 1970) of Fmoc-deprotection was performed in addition to the routine test after coupling. The double coupling procedure was carried out until the deprotective Kaiser test gave a positive result (dark blue color).

Table 8: Fmoc amino acids in peptide solid phase synthesis.

Fmoc-Ala-OH	N-α-(9-Fluorenyl-methoxycarbonyl)-L-Alanine	Albatross Chem, Montreal, QC
Fmoc-Arg(Pbf)-OH	N-α-(9-Fluorenyl-methoxycarbonyl)-N-ω-(2,2,4,6,7-penta-methyldihydro-benzofuran-5-sulfonyl)-L-Arginine	Matrix Innovations Montreal, QC
Fmoc-Asn(Trt)-OH	N-α-(9-Fluorenyl-methoxycarbonyl)-N-γ-trityl-L-Asparagine	Chem-Impex International, Wood Dale, IL
Fmoc-Asp(OtBu)-OH	N-α-(9-Fluorenyl-methoxycarbonyl)-L-Aspartic acid-β-t-butylester	Albatross Chem, Montreal, QC
Fmoc-Cys(Trt)-OH	N-α-(9-Fluorenyl-methoxycarbonyl)-S-trityl-L-Cysteine	Chem-Impex, International, Wood Dale, IL
Fmoc-Gln(Trt)-OH	N-α-(9-Fluorenyl-methoxycarbonyl)-N-δ-trityl-L-Glutamine	Matrix Innovations, Montreal, QC
Fmoc-Gly-OH	N-α-(9-Fluorenyl-methoxycarbonyl)-Glycine	Albatross Chem, Montreal, QC
Fmoc-His(Trt)-OH	N-α-(9-Fluorenyl-methoxycarbonyl)-N-im-trityl-L-Histidine	Chem-Impex, International, Wood Dale, IL
Fmoc-Ile-OH	N-α-(9-Fluorenyl-methoxycarbonyl)-L-Isoleucine	Albatross Chem, Montreal, QC
Fmoc-Leu-OH	N-α-(9-Fluorenyl-methoxycarbonyl)-L-Leucine	Albatross Chem, Montreal, QC
Fmoc-Lys(Boc)-OH	N-α-(9-Fluorenyl-methoxycarbonyl)-N-ε-(t-butyloxycarbonyl)-L-Lysine	Matrix Innovations, Montreal, QC
Fmoc-Met-OH	N-α-(9-Fluorenyl-methoxycarbonyl)-L-methionine	Chem-Impex, International, Wood Dale, IL
Fmoc-Phe-OH	N-α-(9-Fluorenyl-methoxycarbonyl)-L-phenylalanine	Albatross Chem, Montreal, QC
Fmoc-Pro-OH	N-α-(9-Fluorenyl-methoxycarbonyl)-L-proline	Chem-Impex, International, Wood Dale, IL
Fmoc-Ser(tBu)-OH	N-α-(9-Fluorenyl-methoxycarbonyl)-O-(t-butyl)-L-serine	Albatross Chem, Montreal, QC
Fmoc-Thr(tBu)-OH	N-α-(9-Fluorenyl-methoxycarbonyl)-O-(t-butyl)-L-threonine	Albatross Chem, Montreal, QC
Fmoc-Trp(Boc)-OH	N-α-(9-Fluorenyl-methoxycarbonyl)-N-(t-butyloxycarbonyl)-L-tryptophan	Chem-Impex, International, Wood Dale, IL
Fmoc-Tyr(tBu)-OH	N-α-(9-Fluorenyl-methoxycarbonyl)-O-(t-butyl)-L-tyrosine	Albatross Chem, Montreal, QC
Fmoc-Val-OH	N-α-(9-Fluorenyl-methoxycarbonyl)-L-valine	Albatross Chem, Montreal, QC
pGlu	Pyroglutamic acid	Richelieu biotechnologies Inc., Montreal, CA

3.2.2.2. The coupling protocols for cysteine

DCC protocol: A ratio of 6 eq of Fmoc-Cys(Trt)-OH in DMF/DCM (1:3) and 2 eq of 1,3-dicyclohexylcarbodiimide (DCC; Sigma) in a few DCM was stirred and reacted in an ice-bath for 5 min under N_2 atmosphere. Then the solid was filtered out and the filtrate was poured in the vessel containing peptide-resin reactants. The coupling time was 45 min with a gentle steam of N_2 bubbling. After coupling, the non-reactants were removed by washing with DMF and DCM.

HBTU/TMP protocol: The protocol was as same as the general protocol except a ratio of 3 eq of Fmoc-Cys(Trt)-OH, 3 eq of 2-(H-benzotriazole-1-yl)-1, 1, 3, 3-tetramethyluronium hexafluorophosphate (HBTU; Quantum Biotechnologies, Laval, QC) and 3 eq of 2, 4, 6-collidine (2, 4, 6-trimethylpyridine, TMP; Aldrich) was used for the coupling step.

3.3. Preparation of AM and metal chelator conjugant: DTPA-AM

300 mg hAM-resin was stirred in 20 mL of DMF for 1 h, then added dropwise to a solution of diethylenetriaminepentaacetic dianhydride (DHDTPA; 160 mg, 0.15 mmol) (Aldrich) and DMF (20 mL) in 10 min under a N_2 atmosphere. A few beads were taken out from the reactive vessel then, a Kaiser test was performed. The reactants were washed in turn with DMF (2 ×2 min), 10% DMF/H_2O (1×2 min), DMF (2 ×2 min), DCM (2 ×2 min), diethylether (Fisher Scientific) and air dried.

3.4. Kaiser test

The Kaiser test is used for the detection of free amino groups and for the determination of coupling efficiency in SPPS (Kaiser *et al.*, 1970; Figure 12). A positive test, which indicates incomplete coupling reaction, leaves the resin beads dark blue. The following 3 reagents are needed for the test: 2% (v/v) KCN aq. of 1mM aqueous potassium cyanide

(KCN; J. T. Baker Inc., Phillipsburg, NJ) in pyridine (Aldrich); 4:1 (w/v) of phenol (Fisher Scientific) in denatured ethanol (Commercial Alcohols Inc., Bramton, ON); and 5% (w/v) of ninhydrin (Sigma) in denatured ethanol. Three drops of each reagent were added in a small glass tube with 1-2 mg resin. The mixture was heated at 110°C for 5 min. When the resin colour remains unchanged (yellow), the test is a negative and it confirms the completion of the coupling.

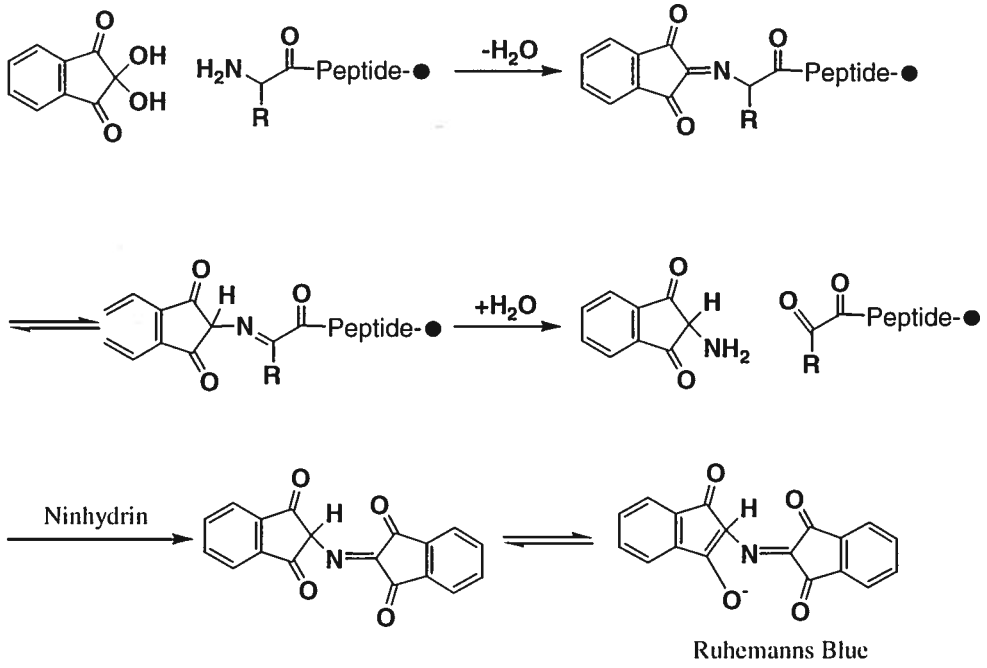

Figure 12: The ninhydrin reaction of Kaiser test.

3.5. Cleavage of peptides and analogs from resin

The peptide was then cleaved from the resin at room temperature, with a mixture of trifluoroacetic acid (TFA; Halocarbon Products Corporation, River Edge, NJ)/ethanedithiol (EDT; Aldrich)/phenol/H_2O (9.5 mL/0.25 mL/0.3 g/0.25 mL; 10 mL/g of resin) for 2-3 h while agitating with a magnetic stirring-bar. After evaporation under vacuum, the crude material was precipitated in ether to remove phenol and other scavengers, filtered and washed thoroughly using anhydrous diethylether. The peptide material was solubilized in water from Ultra-pure water system (Millipore, Montreal,

QC), and frozen in liquid nitrogen, then lyophilized using a corrosion resistant Freeze-dryer (Flex-Dry, New York, NY). The crude peptide was kept at -20°C until cyclization and purification.

3.6. Cyclization of peptide and analogs : Disulfide bridge formation using oxygen

The crude peptide containing free sulfhydryl group (-SH) (characterized by matrix-assisted laser desorption ionization time-of-flight (MALDI-TOF) mass spectrometry and Ellman's test) was dissolved in 10% to 20% acetonitrile (ACN)/H_2O, and the peptide concentration was established at about 0.5 mg/mL by dilution. The pH of the solution was adjusted to 8.4 by adding NH_4OH (aq.) dropwise using a pH meter (PHM61, Hach-Simpson Limited, London, ON). The solution was left to open atmosphere during the reaction. The reaction was monitored and judged to be complete by analytical C_{18} reverse-phase high performance liquid chromatography (RP-HPLC) or by the Ellman's test.

3.6.1. HPLC analysis

Analytical RP-HPLC analyses were performed on a Jupiter C_{18} (5 mm, 300 Å, 250mm×4.6 mm) column (Phenomenex, Torrance, CA) connected to a Beckman 128 pump module coupled to a Beckman 168 PDA detector. The flow rate was maintained at 1 mL/min and the elution was carried out with a linear gradient of ACN (OPTIMA, Fisher Scientific) in TFA/H_2O (0.06%, v/v) from 0 to 60% in 30 min. The sample (50 or 100 μL) was taken by micropipettes (Fisherbrand, Fisher Scientific) at 0 min, 15 min, 30 min, 60 min, 180 min, and 12 h from the reaction mixture of peptide cyclization. The volume of injection was 30 or 50 μL.

3.6.2. Ellman's test

This reaction test is for the free –SH of cysteine. A deep, yellow colour is a positive test and indicates the presence of free –SH groups (Figure 13). On an UV plate (Costar 96 well flat bottom, Hercules, Fisher Scientific), 10 µL of sample from the reaction mixture of Section 3.6.1 was taken and diluted with 290 µL phosphate buffer (0.1 M, pH 8). To the diluted sample 10 µL of Ellman reagent - prepared by dissolving 40 mg 5,5'-dithiobis(2-nitrobenzoic acid) (DTNB, Aldrich) in phosphate buffer – was added, and let the mixture stand for 15 min. The control solution was prepared by adding DTNB reagent in the mixture of 10% ACN/H_2O (10 µL, pH 8.4) and 290 µL phosphate buffer (Ellman, 1959).

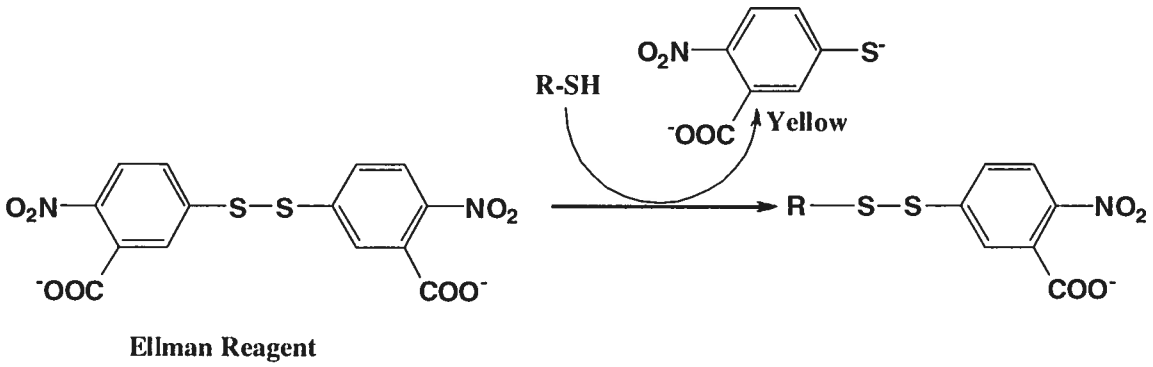

Figure 13: Ellman test.

3.7. Purification and characterization of peptides and analogs

Peptides in 0.06% TFA/H_2O v/v or the solution after a disulfide bridge formation was injected onto a preparative RP-HPLC (Varian ProStar) connected to a Jupiter C_{18} (15 µm; 300 Å) column (250 × 21.20 mm) (Phenomenex, Torrance, CA) or a Waters PrepLC500A system equipped with an absorbance detector model 441 adjusted at 229 nm (no photolysis occurred). The flow rate was fixed at 20 mL/min and the peptide was eluted with a linear gradient of ACN (Fisher Scientific) in 0.06% TFA/H_2O. The homogeneity of the various fractions corresponding to the right mass, as established by MALDI-TOF mass spectrometry (Voyager DE spectrometer-Applied Biosystem, Foster City, CA) were pooled and evaporated. MALDI-TOF analysis were performed with a

nitrogen laser (337 nm) using α-cyano-4-hydroxycinnamic acid (10 mg in 500 µL ACN, 100 µL 3% of TFA/H_2O and 400 µL H_2O; MW > 2000 Da) or 2,5-dihydroxybenzoic acid (10 mg in 1 mL H_2O for smaller peptides, MW < 2000 Da) as a matrix for peptide inclusion and ionization, and each mass spectrum was recorded in linear mode at an accelerating voltage of 25 kV. Semi-preparative and analytical RP-HPLC analyses were performed on a Vydac Semi-Prep C_{18} (cat: 218tp510, USA) and a Jupiter C_{18} (5 mm, 300 Å, 250 mm×4.6 mm) column (Phenomenex, Torrance, CA), respectively, connected to a Beckman 128 pump module coupled to a Beckman 168 PDA detector. The flow rate was maintained at 3 mL/min for semi-preparative HPLC or 1 mL/min for analytical HPLC, and the elution was carried out with a linear gradient of ACN (OPTIMA, Fisher Scientific) in 0.06% TFA/H_2O v/v.

3.8. Methionine sulfoxide test and its isolation

Methionine sulfoxide test: Peptides with methionine can be oxidized during the coupling reaction, cleavage, cyclization or prolonged storage. The methionine sulfoxide can be reduced without destruction of the existing disulfide bridge (Figure 14). The purified sample was dissolved in TFA to give rise to a 10 mg/mL peptide solution in an ice-bath, 20 eq. of ammonium iodide (NH_4I; Baker Chemical Inc, Phillipsburg, NJ) and dimethylsulfide (DMS; Sigma) was added, and the mixture was left to stand for 30 min in the ice-bath. The mixture was poured in a 4-times excess of water, and then the aqueous layer was washed with carbontetrachloride (CCl_4) about 3 times. The water layer was lyophilized and analyzed by HPLC.

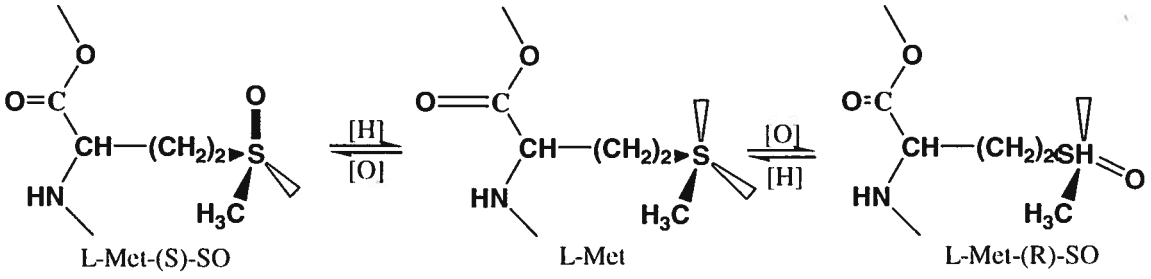

Figure 14: The methionine sulfoxide reduction.

Methionine sulfoxide isolation: The methionine sulfoxide of human AM was isolated using semi-preparative and analytical RP-HPLC analyses that were performed on a Vydac Semi-Prep C_{18} (cat: 218tp510, USA) column, connected to a Beckman 128 pump module coupled to a Beckman 168 PDA detector. The flow rate was maintained at 3 mL/min, and the elution was carried out with a linear gradient of ACN (OPTIMA, Fisher Scientific) in 0.06% TFA/H_2O v/v from 20% to 60% in 60 min and characterized by MALDI-TOF mass spectrometry (MS).

3.9. Reduction of disulfide bridge with DTT

$$\text{R-S-S-R} + \text{HS-CH}_2(\text{CHOH})_2\text{CH}_2\text{-SH} \rightarrow \text{R-SH} + \overline{\text{S-CH}_2(\text{CHOH})_2\text{CH}_2\text{-S}}$$

Peptides with cysteines could be oxidized to give rise to disulfide bridges partially during their storage. Traditionally, two reagents are used in the reduction of disulfide bridge, dithiothreitol (DTT) and 1,3-propanedithiol. The latter is particularly useful for peptides that have limited solubility in water. DTT is the standard reagent for the reduction of cystinyl peptide, and reduces disulfide bridges quantitatively in aqueous media at pH 8. To confirm the linear formation, peptides were dissolved in water (1 mg/mL), adjusted to pH 8 by using NH_4OH (aq.) then, 5 eq. of DTT (Sigma) was added. The solution was then left to stand overnight under a N_2 atmosphere. The solution was acidified with TFA to pH 2.5 - 3.0, and purified by HPLC, the column was first eluted with 0.06% TFA/H_2O v/v to remove DTT, then followed by washing with 50% ACN in 0.06% TFA/H_2O v/v to collect the reduced peptides. The reduction was monitored by HPLC and MALDI-TOF MS. After evaporation under reduced pressure, the peptide product was lyophilized and applied in different experiments.

4. Preparation of technetium-99m-labeled peptide

At present, ^{99m}Tc is the most important radionuclide in clinical applications. The isotope widely exploited since the 70's is used diagnostically as a radioactive imaging agent.

4.1. Peptides, buffers and solution preparation

All chemicals and reagents are from pharmacopoeial-quality raw materials (Sigma-Aldrich), except for ethanol (SAQ, Montreal, QC) and stannous chloride dihydrate ($SnCl_2 \cdot 2H_2O$) which was purchased in analytic grade with purity of 99.99%.

Peptides: A sample of peptide or its analog was dissolved in pure sterile water at a concentration of 1 mg/mL. Then, aliquots (2.89 nmol) of this solution were placed into sterile 2 mL polypropylene vials, lyophilized and kept at -20°C until radiolabeling was performed.

$SnCl_2$ solution: Under sterile laminar flow hood, 1 mg of $SnCl_2 \cdot 2H_2O$ was added to 5.0 mL of autoclaved nanopure water in an empty sterile, apyrogenic 10-mL glass vial. 4.0 mL of the $SnCl_2$ solution was withdrawn by using a sterile needle and syringe. A sterile apyrogenic 0.20 µm filter was connected to the syringe after removing the needle, and a sterile needle was affixed to the end of the filter. The content of the syringe was filtered into another empty sterile apyrogenic 10-mL glass vial.

Buffer: The autoclaved acetate buffer (1 M, pH 5.5) and phosphate buffered saline (1 M, pH 7.4) were prepared using autoclaved nanopure water. The desired pH value was adjusted by using sterile 1 M HCl or 1 M sodium hydroxide (NaOH). Similarly, these buffers were aseptically filtered (0.20 µm) into empty sterile apyrogenic 10-mL glass vials.

Others: In addition, autoclaved 1 mM hydrochloric acid in nanopure water and either 50% or 95% of ethanol in a 0.9% sodium chloride injection United States pharmacopeia (USP) solution were also filtered (0.20 µm) into empty sterile 30-mL glass vials, respectively.

4.2. Radiolabeling reaction

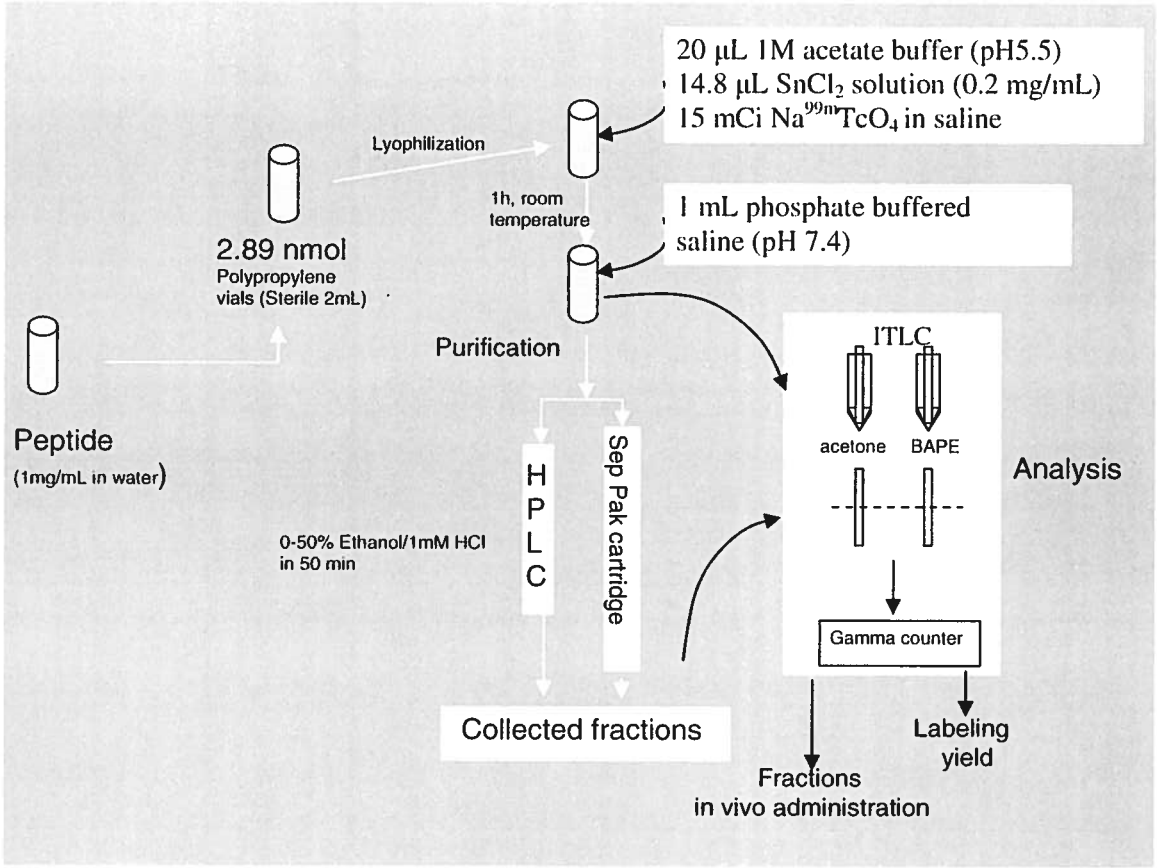

$$Na^{99m}TcO_4 + SnCl_2 + \text{Linear AM} \rightarrow {}^{99m}\text{Tc-linear AM} + SnCl_3$$

Figure 15: Radiolabeling with ^{99m}Tc.

The labeling procedure (Figure 15) was performed using sterile techniques under a laminar flow hood. In a sample vial of the peptide substance, 20 µL of acetate buffer 1 M (pH 5.5) and 14.8 µL of freshly prepared $SnCl_2$ solution (0.2 mg/mL, 13 nmol) were added. After dissolution, a sterile and fresh daily prepared 15 mCi of sodium technetium tetraoxide ($Na^{99m}TcO_4$, 28.9 pmol, $^{99}Mo/^{99m}Tc$ chromatographic generator) in a sodium chloride injection USP solution was immediately added to the mixture. The mixture was adjusted to a final volume of 200 µL with sterile nanopure water and left to stand at room temperature for 1 h. The radiolabeling reaction was stopped by adding 1 mL of sterile phosphate buffered saline (pH 7.4).

4.3. Purification of technetium-99m-labeled complex

HPLC: Analytical RP-HPLC analyses were performed on a Jupiter C_{18} (10 μm, 300 Å, 250mm×4.6 mm) column (Phenomenex, Torrance, CA) connected to a Millipore Waters 501 pump module coupled to a diode array detector (Perkin Elmer 235C). The flow rate was maintained at 1 mL/min and the elution was carried out with a linear gradient of ethanol in 1 mM HCl from 0 to 100% in 50 min. The radiolabeling mixture (see Section 4.2.) was injected through a Waters 715 Ultra Wisp sample processor (Millipore). The fractions (500 μL per tube) were collected by an automatic collector and determined by Wallac 1272 Clinigamma counter (LKB-Wallac, Markham, ON).

Sep Pak cartridge: The radiolabeling reaction mixture was separated by using a C_{18} Sep Pak cartridges Vacc 1cc (100mg) (Waters, Lachine, QC). The Sep Pak cartridge was pre-treated with 10 mL of a 95% ethanol solution, and followed by 10 mL of 1 mM hydrochloric acid. Then, the reaction mixture was loaded to the top of the pre-treated column, and washed with 10 mL of 1 mM hydrochloric acid to remove free 99m-technetiun, and collected into sterile polypropylene tubes as fractions of 1 mL. The reaction mixture was then eluted with 10 ml of a 50% ethanol solution and collected into sterile polypropylene tubes (0.5 mL/per tube), the three tubes with the highest radioactivity were pooled as final product. After purification, the Sep Pak cartridge was also counted to determine the colloids. The final purified product was diluted by using 200 μL of 10X sterile phosphate buffered saline (pH 7.4) and evaluated for pH, total radioactivity and radiochemical purity. Before administration, the final product was passed through a 0.2 μm filter into an empty sterile apyrogenic 10-mL glass vial. Filters were assessed by a bubble point test for membrane integrity after the filtration procedure.

4.4. Characterization of radiochemical purity

To evaluate the amount of ^{99m}Tc-linear AM, colloids and free ^{99m}Tc, instant thin layer chromatography on Silica-Gel-impregnated glass-fiber paper (ITLC-SG, Pall

Corporation P/N 61886) was performed on samples of the radiolabeling reaction mixture and after the HPLC and Sep Pak cartridge purification process. ITLC SG solvents were acetone for dosage of free ^{99m}Tc and butanol:acetic acid:pyridine:nanopure water = 30:6:24:20 (BAPE). Samples (2-3 μL) were spotted 1 cm from the bottom of an ITLC-SG paper (1 cm x 10 cm) and air-dried. Papers were then placed into conical 15 mL polypropylene tubes containing 1.5 mL of an ITLC solvent. The chromatography process was stopped by removing the paper from the tube when the solvent was within 1 cm of reaching the top of the paper. Once the paper was completely air-dried it was cut into two equal parts perpendicular to the direction of solvent flow and ^{99m}Tc activity of one each part was assessed using Wallac 1272 Clinigamma counter. Two papers, and each paper was cut into 2 parts. Acetone was used for the assessment of the free ^{99m}Tc (#2, $R_f = 0.9$) which was at the top part of the paper by the chromatography and the colloids along with the ^{99m}Tc-peptide complex remained at the point of application (#1), whereas the BAPE could separate the ^{99m}Tc-peptide and the free ^{99m}Tc (#4, at the top part of the paper) from the colloids (#3, at bottom part). The formulae used to calculate the labeling yield are shown below:

$$\text{The \% of free pertechnetate (A)} = \frac{\text{Total count of \#2}}{\text{Total count of \#1 and \#2}} \times 100$$

$$\text{The \% of free pertechnetate and } ^{99m}\text{Tc-peptide (B)} = \frac{\text{Total count of \#4}}{\text{Total count of \#3 and \#4}} \times 100$$

$$\text{The \% of colloids} = \frac{\text{Total count of \#3}}{\text{Total count of \#3 and \#4}} \times 100$$

The % of ^{99m}Tc-peptide = B-A

5. Peptide synthesis for structural analysis of technetium-99m-labeled complex

The samples of AM(13-52), AM(16-52), AM(17-52), AM(18-52), AM(19-52), AM(20-52), and AM(21-52) were dissolved in pure sterile water at a concentration of 1 mg/mL. A sample containing 2.89 nmol of peptide was taken from each of these solutions and placed into sterile 2 mL polypropylene vials, lyophilized and kept at -20°C until radiolabeling was performed. The labeling procedure and the calculation of labeling yield were performed according to methods described in Section 4.2. and 4.4.

6. Preparation and isolation of iodine-125-labeled AM

Lactoperoxidase method: 20 μL of AM (1.66×10^{-4} M) in 0.2 M acetic acid solution, 40 μL phosphate buffer (50 mM, pH7.4), 40 μL lactoperoxidase (1→100 diluted by phosphate buffer; Sigma), and 10 μL of either sodium iodide (NaI, 6.7×10^{-4} M in 0.1 M NaOH solution, Fisher Scientific) or $Na^{125}I$ (102 mCi/mL, Amersham Biosciences, Montreal, QC) were mixed. After adding 40 μL hydrogen peroxide (H_2O_2, 0.03% diluted by phosphate buffer from 30% H_2O_2; Sigma) and briefly stirring the mixture was left to stand for 10 min at room temperature, then an extra 40 μL H_2O_2 was added in the mixture and reacted for another 10 min. The reaction was stopped by lyophilization or by immediate purification using HPLC (0-25% ACN/H_2O (0.06% TFA/H_2O v/v) in 10 min; 25-35% ACN/H_2O (0.06% TFA/H_2O v/v) in 90 min). The fractions were collected in 1.5 mL polypropylene tubes, 0.5 mL per tube, and characterized by MALDI-TOF MS analysis or counted by an auto-gamma counter (Packard Instrument Co., Meriden, CT).

Chloramine-T (CAT) method: AM (1.66×10^{-4} M, 20 μL) in 60% ACN/H_2O (1% TFA/H_2O v/v) solution, 40 μL phosphate buffer (500 mM, pH7.4), and either 10 μL NaI (6.7×10^{-4} M in 0.1 M NaOH solution, Fisher Scientific) or $Na^{125}I$ (102 mCi/mL, Amersham Biosciences) were mixed for 30 sec. Then 4.3 μL CAT (1 mg/mL in phosphate buffer) were added, mixed for 1 min at room temperature. The reaction was stopped by lyophilization or isolation by HPLC as for the lactoperoxidase method described above.

7. Investigation of iodinated tyrosine on AM

Since there are three Tyr groups located at the N-terminus, mid-position and C-terminus of AM respectively, each individual AM might have 1, 2, 3, or more I's. The radio-ligands of iodine-125-labeling AM can thus be a mixture of mono-iodinated and di-iodinated as well as multi-iodinated AM. The structure of the I-AM prepared by lactoperoxidase method was investigated by exopeptidases (Carboxypeptidase Y, CPY; Aminopeptidase M, APM) and cyanogen bromide (CNBr).

7.1. Exopeptidase method

Exopeptidases can remove amino acids from the end of a peptide chain one by one. The removal number of amino acids depends on the concentration of exopeptidases and digestive time. APM can cleave a single amino acid from the N-terminal, whereas CPY will cleave a single amino acid from the C-terminal.

Table 9: Preparation of exopeptidase dilutions.

Dilution Number	Combine the following:
Dilution 1	The stock concentrates exopeptidase
Dilution 2	0.5 μL Dilution 1 + 0.5 μL buffer
Dilution 3	0.5 μL Dilution 2 + 0.5 μL buffer
Dilution 4	0.5 μL Dilution 3 + 0.5 μL buffer
Dilution 5	0.5 μL Dilution 4 + 0.5 μL buffer

Note: Buffer for CPY: 30 mM ammonium citrate, pH 6.1.
Buffer for APM: 3.2 M ammonium sulphate, 10 mM magnesium chloride, pH 5.9.

Digestion of AM: The exopeptidase dilutions were prepared from the stock concentrates of CPY (1 g/L; Sigma) or APM (1 g/L; Pierce, Rockford, IL) with buffers (Table 9). A peptide sample was prepared by weighing 1 mg of the pure AM and dissolving it in 1 mL

of 0.06% TFA/H_2O v/v. The peptide sample was digested by CPY or APM in 0.5 mL micro tubes (Sarstedt, St Leonard, QC) for 30 min at room temperature. The digestion was stopped by adding 24 µL of matrix solution of α-cyano-4-hydroxycinnamic acid. Then, 1 µL of the mixture in each of the consecutive tubes (Table 10) was spotted on a sample plate and allowed to dry. Each spot was then analyzed by MALDI-TOF MS.

Table 10: Digestion of peptide samples.

To tube	Add	Use a clean pipette tip for each and add
1	0.5 µL sample	0.5 µL exopeptidase Dilution 1
2	0.5 µL sample	0.5 µL exopeptidase Dilution 2
3	0.5 µL sample	0.5 µL exopeptidase Dilution 3
4	0.5 µL sample	0.5 µL exopeptidase Dilution 4
5	0.5 µL sample	0.5 µL exopeptidase Dilution 5
6	0.5 µL sample	-

Digestion of iodinated AM: The crude iodinated AM from the lastoperoxidase method in Section 6 was purified by analytical HPLC (Beckman), the elution was carried out with a linear gradient of ACN (OPTIMA, Fisher Scientific) in 0.06% TFA/H_2O v/v from 10-50% in 50 min at 1 mL/min of flow rate. The fractions with AM and I-AM were characterized by MALDI-TOF MS and pooled to give rise to a testing sample that mainly contained a mixture of AM and I-AM, called "Sample 1", after lyophilisation. The testing sample was dissolved in 20 µL of 0.06% TFA/H_2O v/v as testing solution ($<1.66\times10^{-4}$ M of peptide). 0.5 µL of the solution was digested with 0.5 µL Dilution 2 of exopeptidase and characterized according to the protocol above.

7.2. CNBr method

CNBr (Sigma) is a reagent that can selectively react with Met in peptide chain, and break the polypeptide chain from the C-terminal of the Met (Figure 16). The crude iodinated AM from the lastoperoxidase method in Section 6 was purified by an analytical HPLC (Beckman, method see the Section 7.1). The fractions with I-AM and I,I-AM were characterized by MALDI-TOF MS and pooled to yield the mixture of AM, I-AM and I,I-AM as another testing sample, called Sample 2, after lyophilisation. Sample 1 from the Section 7.1 was lyophilized to remove solvent. Sample 1 and 2 were dissolved in 20 μL of 50% TFA/H_2O v/v to be testing solutions. 5 μL of the iodinated AM solution were mixed with CNBr/ACN solution (2.36 M, 5 μL) in 1.5 mL microtubes covered by aluminium foil and left to stand about 16 h at room temperature. The reaction was stopped by adding 6 volumes water (pH 7 adjusted with NH_4OH aq.) to the reactive mixture, lyophilized and characterized by MALDI-TOF mass analysis described as described in the Section 7.1.

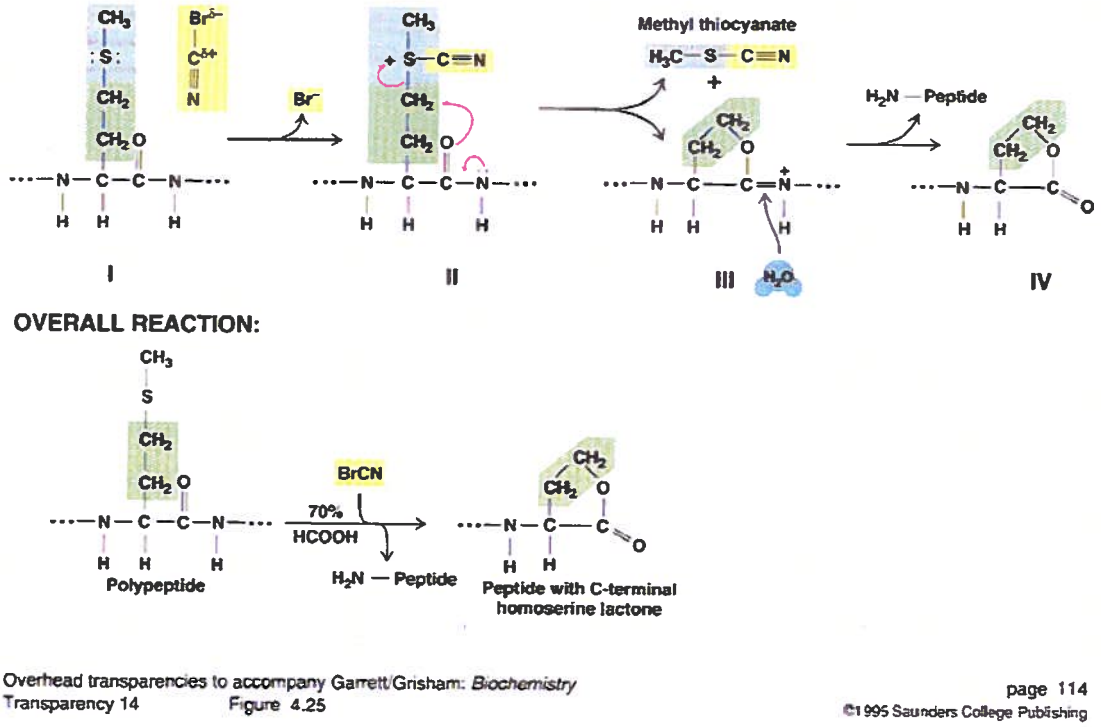

Figure 16: Mechanism of cyanogen bromide cleavage.

8. Evaluation in vitro: Receptor-radioligand assay

Receptor binding assay was first developed in the 70's. Since the advent of radioreceptor methods, it is now possible to measure receptor-ligand interactions directly. There are three commonly used experimental protocols to measure the rate and extent of binding and provide information on the number of binding sites, and their affinity and biological characteristics, i.e. saturation binding experiments, kinetic experiments and competitive binding experiments.

8.1. Cell culture

Pulmonary artery endothelial cells (CPAE, No.CCL-209; American Type Culture Collection (ATCC), Manassas, VA), an endothelial cell line derived from the main stem pulmonary artery of a young cow (Bos taurus), were frozen in a solution containing 95% medium (Minimum Essential Medium) and 5% DMSO v/v. After defrosting in a water bath at 37°C, the cells were poured in a 15 mL tube with 9 mL of fresh Minimum Essential Medium (Sigma) supplemented with 2 mM L-Glu (Sigma), 1 mM sodium pyruvate (Sigma), 100 U/mL penicillin (Sigma), 100 µg/mL streptomycin (Sigma), and 20% fetal calf serum (FCS, Sigma). The tube was centrifuged at 1, 000xg at 4 °C for 7 min, and transferred to a 25 mL tissue culture flask (Sarstedt) with 25 mL medium. Then, the cells in medium were grown in a humidified 5% CO_2 atmosphere (Forma Scientific, Marietta, OH) as the first passage. Each following passage was rinsed with sterile phosphate buffer solution (PBS), detached and dispersed with Trypsin-EDTA (Sigma) at 37 °C for 5 min, and separated in 175 mL tissue culture flasks with 38 ml medium. Cell culture was performed in sterigard hood.

8.2. Preparation of cell membrane

Membranes were prepared by differential centrifugation as described by Dschietzig (Dschietzig *et al.*, 2002). After counting (166×10^4 Cell/mL, 81 mL) and centrifuging, cells (passage 6) were lysed in ice-cold 50 mM Tris/HCl buffer, pH 7.4, containing 0.25

M sucrose, and a cocktail of protease inhibitors (Sigma). Cell lysates were centrifuged (IEC Centra GP8R, Milford, MA) at 1, 500 × g for 20 min, and supernatants were centrifuged (Beckman L8-M ultracentrifuge, Mississauga, ON) at 100, 000 × g for 1 h at 4°C. Pellets were resuspended in 10 volumes of the above buffer without sucrose and centrifuged at 100, 000 × g for 1 h at 4°C. Pellets were resuspended as above to a final protein concentration of 2.5 mg/mL, aliquoted, and stored at -80°C. The protein concentration was measured by using bovine serum albumin (BSA, Sigma) as standard.

8.3. Preparation of lung homogenates

A male Mongrel's dog of 31 kg (approval by the animal ethics and research committee of the Montreal Heart Institute) was anesthetized with sodium pentobarbital. Then the lung was directly removed after the heart excision, washed and placed in cold PBS (137 mM NaCl, 2.6 mM KCl, 8.1 nM Na_2HPO_4, and 1.4 mM KH_2PO_4). The lung homogenates were prepared according to the method of Juaneda *et al* (Juaneda *et al.*, 2003) with some minor modifications as described below. The dissected tissues in 200 mL (15 volumes based on tissue weight) of 25 mM Tris, 50 mM NaCl and 2 mM $MgCl_2$ at pH 7.4 containing 1 mL protease inhibitors (Sigma) without trachea were homogenized using Brinkmann polytron (20 s, setting 6; Westbury, NY) twice, and centrifuged at 49, 000×g for 20 min. Pellets were washed, resuspended in the original volume of Tris buffer and centrifuged. The last step was repeated twice. The pellets were combined, suspended in 500 mL of 50 mM Tris, 100 mM NaCl and 4 mM $MgCl_2$ at pH 7.4 and centrifuged at 1, 000×g for 3 min to remove cellular debris. Finally, the supernatants were divided into equal aliquots and frozen at -80°C. All steps were performed at 4°C. Protein concentration (2.4 mg/mL) was measured by using BSA as standard.

8.4. The protein measurement of membrane

5 dilutions of a BSA standard (400 µg/mL) containing from 50 to 400 µg/mL protein were prepared by using Tris buffer (50 mM, pH 7.4). On a UV plate (Costar 96-well flat bottom), 20 µL of each standard, 10 µL of Reagent A and 80 µL Reagent B (Bio-rad,

Hercules, CA) were added in each well. The blank control and sample were prepared by using 20 μL Tris buffer and 2 μL of sample in 18 μL buffer instead of protein standard solution. Each well was duplicated. After gently agitating the plate to mix the reagents and leaving to stand 15 min, the plate was placed in microplate reader (Bio-Tek instrument, Palo Alto, CA) to read the absorbance at 750 nm. The protein concentration of sample was calculated according to the equation of standard linear curve.

8.5. Binding experiments

Saturation binding experiment: The total binding of ^{125}I-labeled AM was performed by the addition of 20 μL membrane (0.24 mg/mL for dog lung homogenates) to polypropylene tubes (0.5 mL) containing the labeled AM from 0.01 nM to 1 nM in the binding buffer (0.5 mM Tris, 100 mM NaCl and 4 mM $MgCl_2$ at pH 7.4 containing 0.15% protease inhibitors). The final volume was 100 μL and incubated 90 min at room temperature. Non-specific binding was determined in the presence of 1 μM of the unlabeled AM. The binding incubation of the samples were stopped by filtration under vacuum through glass fibre filter papers (previously soaked in 0.3% polyethyleneimine) using a compact cell harvester (Millipore 1225 sampling Vacuum Manifold, Milford, MA). Filter papers were rinsed twice with 3 mL of buffer composed of 50 mM Tris, 100 mM NaCl and 4 mM $MgCl_2$ at pH 7.4 and the radioactivity retained by the filter papers was measured using a γ-counter (Packard Instrument Co., Meriden, CT).

Time course: 12 polypropylene tubes (1.5 mL) contained ^{125}I-AM (0.1 nM) and dog lung homogenates (100 μL, 0.24 mg/mL) in the binding buffer, the final volume was 0.5 mL. The incubation time was 5 min, 10 min, 15 min, 20 min, 30 min, 50 min, 70 min 90 min 110 min, 130 min, 150 min, and 180 min. The measurement of radioactivity remaining on the membranes was made as the protocol described for the saturation binding experiment.

Competitive binding experiments: ^{125}I-labeled AM or ^{99m}Tc-linear AM (10^{-10} M), various competitors (at concentrations ranging from 10^{-15} M to 10^{-6} M), and 100 μL

membrane (0.24 mg/mL for dog lungs; 0.25 mg/mL or 2.5 mg/mL for CPAE membrane) were combined in a binding buffer (0.5 mM Tris, 100 mM NaCl, 4 mM $MgCl_2$ and 0.1% BSA at pH 7.4 containing 0.15% protease inhibitor cocktail). The final volume was 0.5 mL. The competitive ligands were prepared from the stocks solutions (1 mg/mL in water) with binding buffer. After 90 min of incubation the radioactivity retained by the filter papers was measured as described in the saturation binding experiment.

9. Evaluation in vivo: Lung imaging assay

Any new candidate molecules for imaging must be tested *in vivo*. These *in vivo* studies, carried out at the Montreal Heart Institute, were completed in a species having a lung size close to that of human, *i.e.* dogs.

9.1. Stability of ^{99m}Tc-linear AM in PBS

To determine the stability of ^{99m}Tc-linear AM, the purified labeled peptide was incubated with and without PBS 10X buffer (200mL) at room temperature and the quality control by ITLC was assessed after 24 h or 48 h of labeling.

9.2. Plasma kinetics of ^{99m}Tc-linear AM in dogs

Purified ^{99m}Tc-linear AM was injected into the right saphenous vein of mongrel dogs weighing 20-30 kg (n = 5). Serial 2 mL blood samples were collected via the left saphenous vein every 1 min for a 10-min period, then every 5 min for the following 50-min period. An equal amount of physiological saline was injected into the animal to maintain stable blood volume. The collected blood samples were assayed in a gamma counter to determine ^{99m}Tc activity. Results were expressed as a percentage of total activity injected. During the assay the blood pressure and heart rhythm were continuously monitored.

9.3. Molecular imaging of lungs and biodistribution in dogs

Biodistribution was evaluated with a dual-head camera (Siemens, Malvern, PA). The gamma camera was equipped with high-resolution collimators. After confirmation of radiochemical purity of products by ITLC, 2-4 mCi of >95% purity of ^{99m}Tc-linear AM per dog (n = 7) was administered. Upon injection of the radiopharmaceutical, a dynamic study of the thorax was started, lasting 30 min. Subsequently, whole-body scans were performed with a scan speed of 10 cm/min. The whole body acquisitions were performed at 30, 60, 120 and 240 min after initial injection. Results were expressed as a percentage of the total radioactivity injected.

9.4. Molecular imaging of lung perfusion defects

Dogs were anaesthetized. After medial thoracotomy the selective surgical ligation of a lobar pulmonary artery was performed, and 2 to 4 mCi of purified ^{99m}Tc-linear AM was injected. An image was collected with a planar camera to detect the perfusion defect corresponding to a ligated middle lobe of the right lung in anterior (left) and oblique views (right).

9.5. Biodistribution and plasma kinetics of ^{99m}Tc-linear AM in rats

The lung imaging studies were performed by using Male Sprague-Dawley rats weighing between 200-225 g. The injected dose of ^{99m}Tc-linear AM was in a volume of 200 µL (0.3 pmol, 0.5 mCi) into the right jugular vein. Two approaches, imaging *in vivo* with a gamma camera system (Siemens) and surgically removing and counting organ in a gamma counter, were used in the evaluation of body biodistribution of ^{99m}Tc-linear AM. Data was collected by the research group of Dr. Jocelyn Dupuis in Montreal Heart Institute.

In vivo biodistribution A planar camera fitted with a low-energy parallel-hole collimator was used for static acquisitions recorded for whole individual organs, including lungs, kidneys, liver, heart, bladder, at 30 and 60 min after initial injection.

Ex-vivo Biodistribution At the end of the *in vivo* biodistribution experiments, the rats were sacrificed at 30 or at 60 min after administration, and the lungs, liver, kidneys, heart, spleen, stomach, thyroid, duodenum and gut were removed and gravity-drained. The organs were then placed in a gamma-counter to determine the ^{99m}Tc radioactivity.

Plasma kinetics Similar to the study of plasma kinetics in dog, the radiolabeled ^{99m}Tc-linear AM, approximately 700 μCi per rat, was injected in a volume of 200-300 μL into the right heart chambers (via a right jugular vein catheter) of male Sprague-Dawley rat, weighing 400-450 g (n=19). 200 μL blood samples were collected at 1 min after the initial injection and every 5 min for a 30-min period.

10. Data analysis and statistics

Plasma kinetic was fitted using a 2-phase exponential decay equation with GraphPad Prism version 4.0 software. Differences between AM(22-52) and CGRPα(8-37) were evaluated by two-tailed t-tests. A P value of <0.05 was considered significant. Specific binding *in vitro* was determined by the difference between total binding and non-specific binding. The receptor-binding data were analyzed by nonlinear regression using the Graphpad Prism 4.0 with models using one or two binding sites and compared by using the nonlinear least-squares curve-fitting which is based upon a statistical F-test. The best fit binding model (one-binding model or two-binding model) was determined by a P value of <0.05. Data were collected from at least three independent experiments, each experiment in duplicate, and reported as mean ± SEM.

Chapter 4 : Results

10. Synthesis, radiolabeling and characterization of ^{99m}Tc-linear AM as a lung imaging agent in vivo

Generally, peptides containing cysteine can chelate metal ion, such as radionuclides. The linear peptide analogs were prepared to investigate the possibilities that AM itself could act as a radionuclide carrier without losing their specificity in organs or tissues. Since the modification of N-acetylation protects the native peptide from degradation, acetyl-AM analogs were designed in the initial experiment. Although there are various bifunctional chelate agent (BCA) used in the construction of 99m-technetium conjugation, in this study, DTPA was chosen first and conjugated at the N-terminus of AM as a metal chelator because ^{99m}Tc-DTPA has been used as a radiopharmaceutical in clinical application. According to the designed delivery system of radionuclide, human AM and its four analogs, linear AM, acetyl-AM, linear acetyl-AM and DTPA-AM, were in the initial screening list. Their sequences and structures are shown in Figure 17.

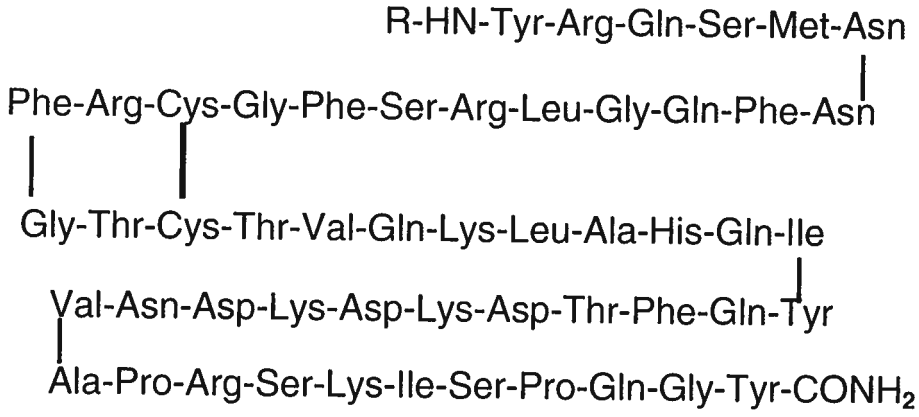

R=-H, AM (1-52, human); Linear AM without link between Cys
R=-$OCCH_3$, acetyl-AM (1-52, human); Linear acetyl-AM without link between Cys
R=-DTPA, DTPA-AM (1-52, human)

Figure 17: Primary structures of AM and its analogs.

10.1. Peptide and analog synthesis

The synthetic pathway by Fmoc SPPS was outlined in Figure 11. AM, a 52-amino-acid peptide, was prepared in a 17% yield by the standard Fmoc/BOP methodology. Rink amide AM resin was used to construct the C-terminal amide. The acetyl-AM analog was prepared by using acetic anhydride (A&C American Chemicals Ltd) to modify the N-terminus of AM in the presence of 3 eq. of DIEA. All crude products were purified by preparative or semi-preparative RP-HPLC with a linear gradient of 0-40% ACN in 0.06% TFA/H_2O v/v for 1 h. Among the pure products DTPA-AM was obtained in poor yield with a lower purity (Table 11).

$$\text{Yield of peptide} = \frac{\text{The weight of pure peptide (>90\%)}}{\text{The weight of crude peptide}} \times 100\%$$

Table 11: The parameters of synthetic peptides and analogs.

Name	MW (Da)	Measured MW (Da)	t_R (min)	Purity (%)	Yield (%)
AM	6028	6028.50	31.37	97.20	17
Linear AM	6030	6030.96	33.77	95.90	27
Acetyl-AM	6070	6069.45	18.93	96.49	18
Linear acetyl-AM	6072	6074.64	19.67	92.34	31
DTPA-AM	6404	6407.15	18.80	82.32	2
Linear AM(13-52)	4534	4535.14	19.60	96.80	18
Linear AM(16-52)	4244	4243.18	44.58	95.42	18
AM(17-52)	4141	4141.90	31.70	93.06	38
AM(18-52)	3985	3985.22	46.00	95.81	30
AM(19-52)	3837	3838.02	31.57	96.27	29
AM(20-52)	3780	3779.43	31.63	93.84	28
AM(21-52)	3679	3678.80	41.73	92.64	41

10.2. Peptide and analogs cyclization

The purified products with two cysteines were dissolved in ACN/H_2O solution and cyclized at open air for disulfide bridge formation. The retention time (t_R) of cyclic peptide with one disulfide bridge is approximately 1 min less than the its linear precursor with a linear gradient of 0-60% ACN in 0.06% TFA/H_2O v/v for 30 min elution. After cyclization, the t_R of AM was changed from 19.45 min (Linear AM) to 18.50 min (Figure 18). The t_R of acetyl AM was changed from 19.67 min to 18.93 min. The t_R of DTPA-AM was changed from 19.90 min to 18.90 min. The oxidation was monitored by analytical HPLC, and the end point of reaction was determined by the presence of a sole peak with the shorter t_R. After purification and lyophilization, an Ellman test of the final product gave a negative indication comparing to blank.

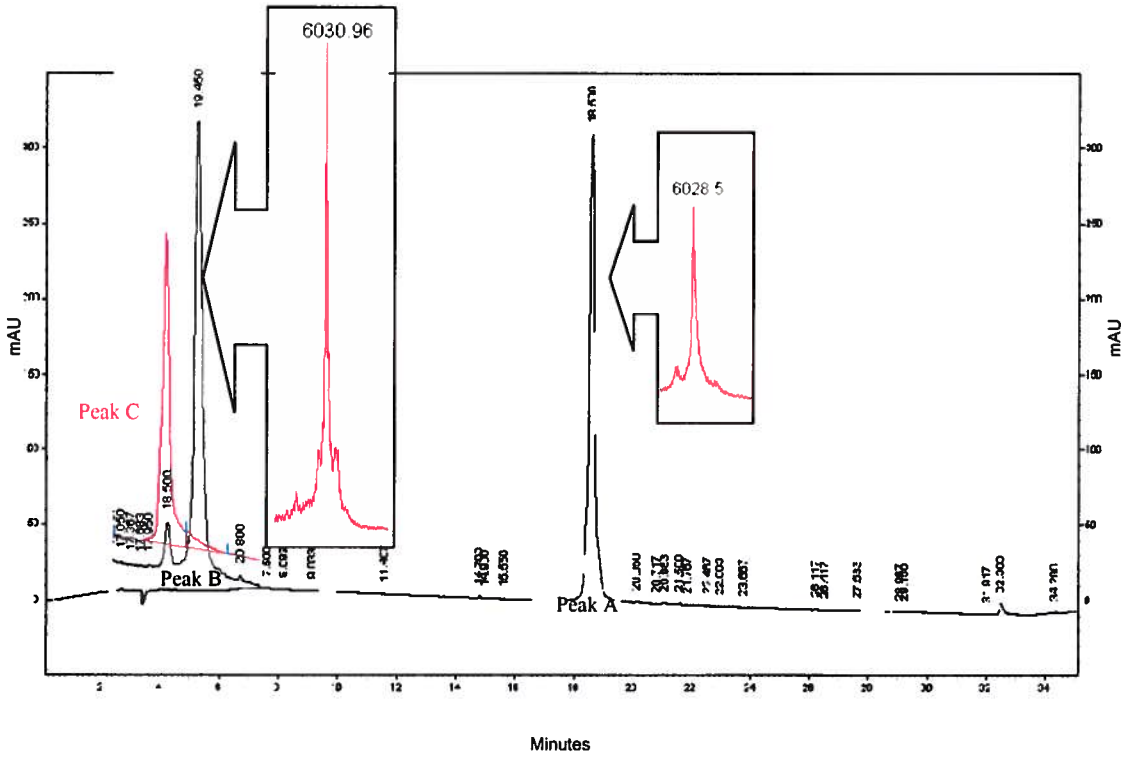

Figure 18: The cyclization and characterization of AM. The final product of AM with the right MW (in black frame) was analyzed by HPLC with a linear gradient of 0-60% ACN in 0.06% TFA/H_2O v/v for 30 min elution. It showed a sole peak (Peak A). On the left of the figure, HPLC analysis before cyclization (black) and after cyclization (red) showed that linear AM (Peak B) with the right MW was completely converted to Peak C, as shown in red. The Peak C was then characterized by MS as AM.

10.3. Characterization of peptides and analogs

A 1 mg test sample was dissolved in 1 mL water. The purity of AM analogs was characterized by analytical HPLC with a linear gradient of 0-60% ACN in 0.06% TFA/H_2O v/v for 30 min; the purity of AM and its smaller fragments were characterized by analytical HPLC with a linear gradient of 0-60% ACN in 0.06% TFA/H_2O v/v for 60 min. The identities (i.e. molecular weight, MW) of products were confirmed by mass spectrometry. The relative parameters were outlined in Table 11.

10.4. Separation of methionine sulfoxide AM

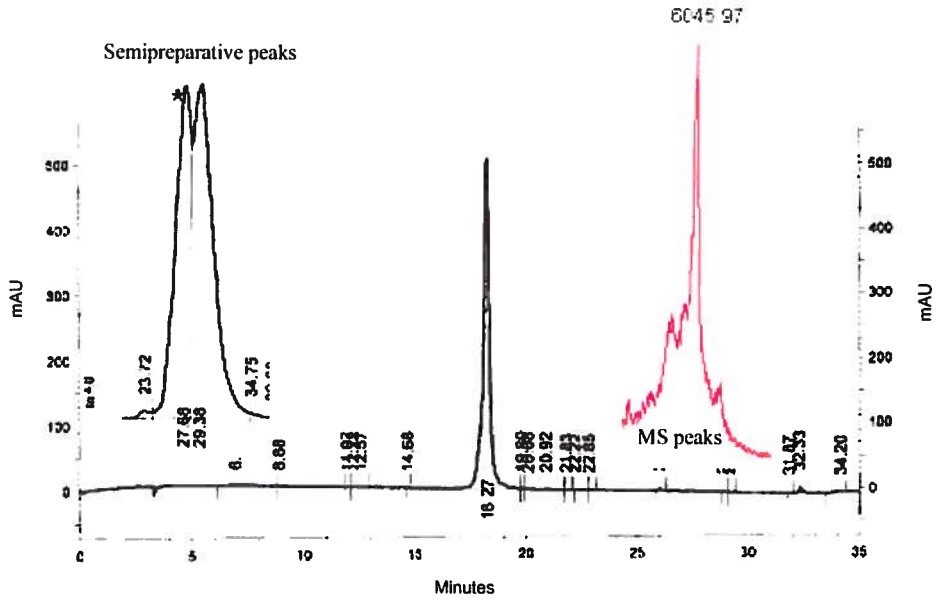

Figure 19: Separation and characterization of methionine sulfoxide AM. On the left of the figure, semi-preparative HPLC analysis showed the separation of AM oxide (indicated by *) from AM with a linear gradient of ACN in 0.06% TFA/H_2O v/v from 20% to 60% in 60 min. The collected AM oxide fraction (from 24 min to 27 min) was analyzed by HPLC with a linear gradient of 0-60% ACN in 0.06% TFA/H_2O v/v for 30 min elution. It showed a sole peak (t_R = 18.27 min) with the right MW in red.

Because there are no study on the methionine sulfoxide AM, the effect of the oxide product in receptor-binding activity and lung imaging *in vivo* remains unclear. The trace of AM oxide found in the final AM product was separated by semi-preparative HPLC. AM oxide and its analogs can be monitored by MALDI-TOF mass analysis. Small amounts of oxidized AM could be detected in the synthesis, purification and cyclization of AM. In the present study, large amounts of methionine sulfoxidation only occurred during the cyclization and iodination of AM.

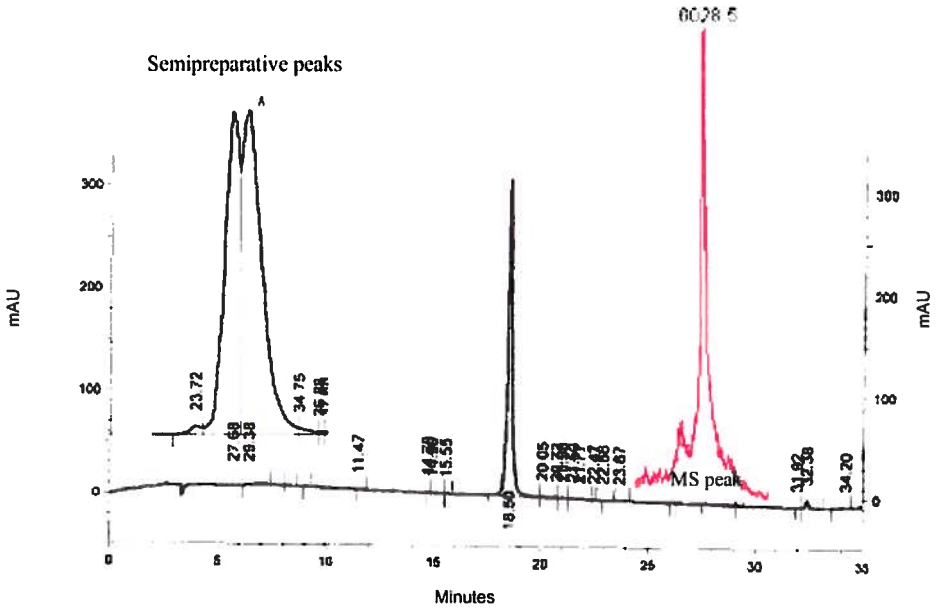

Figure 20: Separation and characterization of AM. On the left of the figure, semi-preparative HPLC analysis showed the separation of AM (indicated by *) from AM oxide with a linear gradient of ACN in 0.06% TFA/H_2O v/v from 20% to 60% in 60 min. The collected AM fraction (from 29 min to 32 min) was analyzed by HPLC with a linear gradient of 0-60% ACN in 0.06% TFA/H_2O v/v for 30 min elution. It showed a sole peak (t_R = 18.50 min) with the right MW in red.

The mixture with traces of oxidized peptide can be separated by semi-preparative HPLC during purification with a linear gradient of ACN in 0.06% TFA/H_2O v/v from 20% to 60% in 60 min and characterized by MALDI-TOF. The separation of methionine sulfoxide AM was shown in Figure 19 and Figure 20. AM oxide had a t_R of 27.68 min with MW6045.97 Da, compared to the native AM which exhibited a t_R of 29.38 min with MW6028.5 Da. The purity and identity of fractions was determined by analytical HPLC with a linear gradient of ACN in 0.06% TFA/H_2O v/v from 0 to 60% in 30 min and MALDI-TOF mass analysis. Although the methionine sulfoxide peptides can be reduced by NH_4I and DMS, and monitored by MS analysis, traces of the AM oxide were found in the purification of synthetic AM by preparative HPLC.

10.5. ^{99m}Tc-radiolabeling of linear acetyl-AM

The initial ^{99m}Tc labeling experiment was performed on AM, linear AM, acetyl-AM, linear acetyl-AM, and DTPA-AM. The ITLC analysis indicated that the higher labeling yields were attributable to linear AM and linear acetyl-AM (Table 12). Although the labeling yield of DTPA-AM was higher than one of AM and acetyl-AM, it is too low to use as a radiopharmaceutical. After reaction, free technetium was <1% and most of side products were ^{99m}Tc-microcolloids that remained at the original spots in ITLC. The labeling linear acetyl-AM was purified by analytic HPLC and monitored by γ-counting. The results suggested that linear AM and its analogs could chelate with ^{99m}Tc in good yield. Therefore, AM with an open disulfide bridge could be a radionuclide carrier in the designed delivery system and exhibited a better property as a chelating agent comparable to DTPA-AM.

Table 12: The radiolabeling yields of AM and its analogs.

Peptide Derivatives	AM	Linear AM	Acetyl-AM	Linear acetyl-AM	DTPA-AM
Labeling Yield (%)	2	47	2	65	10

10.6. Lung imaging with ^{99m}Tc-linear acetyl-AM

Linear acetyl-AM was used in the initial dog lung imaging experiment to investigate the organ target specificity as a potential tracer. After administration, it produced a good lung image (Figure 21). The images showed that ^{99m}Tc-linear acetyl-AM was substantially uptaken in the dog lungs.

The total radioactive density of injection was determined by the gamma camera system before administration. A quantitative analysis on the ratio of radioactive density in the dog organs after 30 min indicated that about 21% of ^{99m}Tc-linear acetyl-AM activity in the lungs, 23% in the kidneys, 14% in the urinary bladder, only 4% in the heart and liver, and minimal (about 1%) in the gallbladder and snout. The biodistribution studies are shown in Figure 22. The initial data indicated that the potential radiotracer had a high specificity in the lungs compared to other organs and tissues. It is noteworthy that ^{99m}Tc-

linear acetyl-AM exhibited a low uptake and retention by heart, liver and brain (the snout indicated the retention in the brain because the snout of dog was over its brain during the lung imaging. The results implied that linear acetyl-AM could not only carry ^{99m}Tc acting as a metal chelate, but also selectively target to the lung as a biomolecule. It could be a new potential radiopharmaceutical.

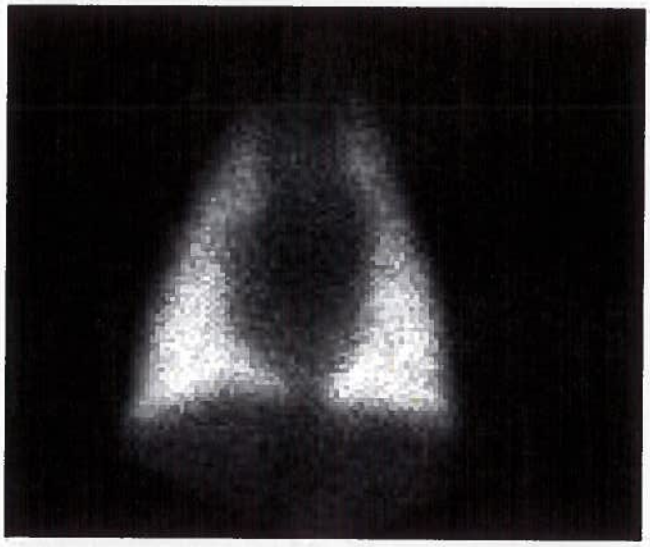

Figure 21: Dog lung imaging by using ^{99m}Tc-linear acetyl-AM.

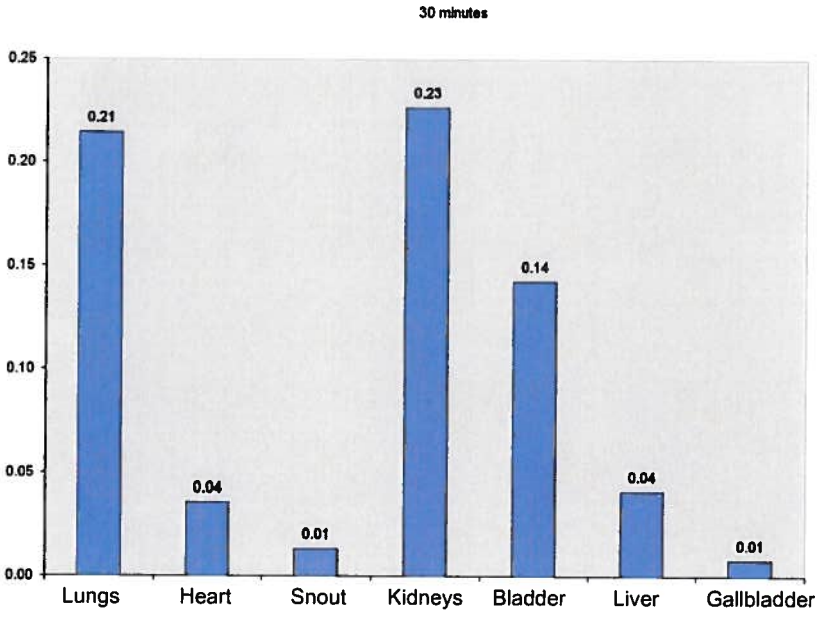

Figure 22: Biodistribution of ^{99m}Tc-linear acetyl-AM in dog.

10.7. The selection of the optimal potential radiopharmaceutical

Although the linear acetyl-AM shows both a high radiolabeling rate and good lung imaging properties in the dog, it is a small chemical modification at N-terminal of linear AM, and has almost the same chemical properties as linear AM. On the basis of the advanced data, we hypothesized that linear AM could be a carrier as well as a targeting moiety by itself. It is obvious that if this new hypothesis was true it would extremely simplify the preparation and modification of a new lung-imaging compound.

10.7.1. Competitive binding experiments

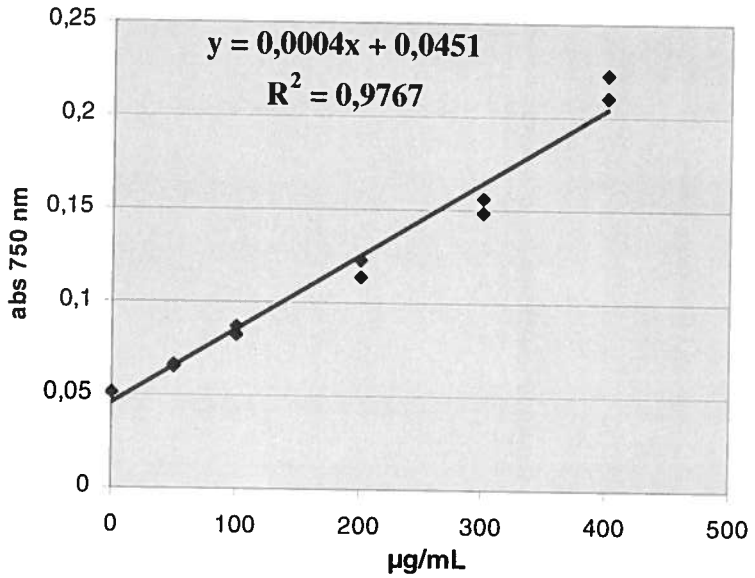

Figure 23: Protein measurement of dog lung homogenates.

To verify the difference of lung specificity between linear AM and linear acetyl-AM, the competitive binding experiments were performed on dog lung homogenates using ^{125}I-AM as radioligand; unlabeled linear AM and linear acetyl-AM as competitors. The protein concentration of homogenates prepared from dog lungs was 2.4 mg/mL, which was calculated according to the equation of standard curve (Figure 23). The IC_{50} values are calculated from Figure 24. For AM, the IC_{50} value was 89 pM (95% confidence interval ranges from 27 to 291 pM). For linear AM, the IC_{50} value was 7 nM (95%

confidence interval range 4 to 11 nM). For linear acetyl-AM, the IC_{50} value was 16 nM (95% confidence interval range 6 to 58 nM). The order of displacement according to IC_{50} values is AM> linear AM > linear acetyl-AM. The binding sites found in dog lungs had high binding affinity to linear AM. Each point represents the mean ± s.e.m. of data obtained from three independent experiments in duplicate, and expressed as percentage of specific binding.

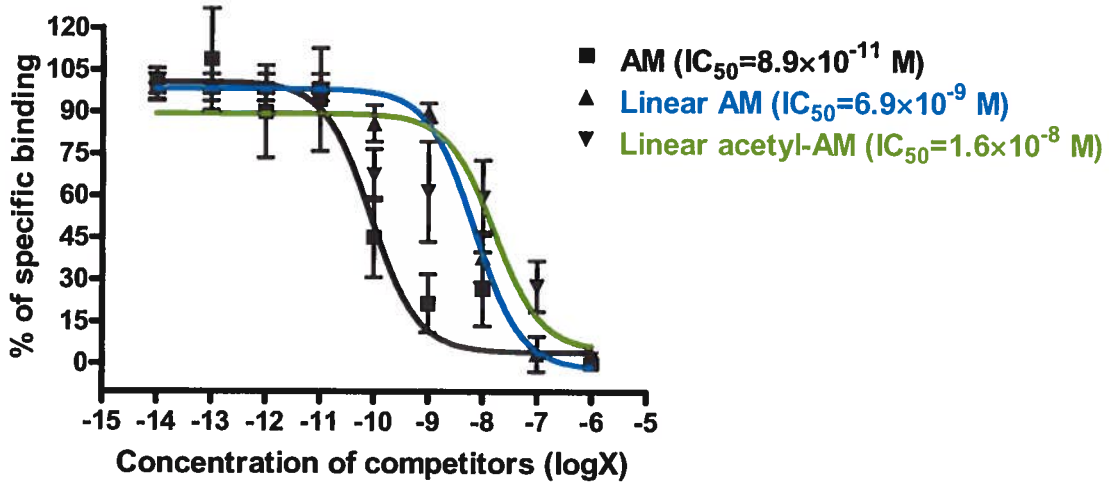

Figure 24: The competitive binding experiment of AM and its analogs. Data points are the mean ± S.E.M. (standard error of the mean) of three independent experiments performed in duplicate.

10.7.2. Comparison of radiolabeling experiment

Table 13: Comparison of radiolabeling yield for linear AM and linear acetyl-AM.

	The labeling yield of linear acetyl-AM(%)			The labeling yield of linear AM(%)		
1	21	27	25	37	37	36
2	45	48	48	61	66	69
3	32	33	54	65	64	65

The following ^{99m}Tc labeling experiment was performed on linear AM and linear acetyl-AM. The ITLC analysis indicated that the higher labeling yields were obtained in the radiolabeling of linear AM (average 56%, Table 13). The formation of mainly a single radioactive species of ^{99m}Tc-linear AM or ^{99m}Tc-linear acetyl-AM was obtained by analytic HPLC purification. After purification, the radiochemical purity was >92 ± 2% by

ITLC analysis. The results were collected from three independent experiments, each performed in triplicate and expressed as percentage of radiolabeling.

10.8. Preparation and purification of ^{99m}Tc-linear AM as an optimal radiopharmaceutical

Table 14: Labeling efficiency by ITLC of ^{99m}Tc-linear AM before and after Sep-Pak purification.

	Before purification	After purification
Tc-free	11	1
Colloids	35	2
Labeled AM	55	97
Tc-free	4	0.8
Colloids	43	3
Labeled AM	53	97
Tc-free	3	0.4
Colloids	43	4
Labeled AM	54	96
Tc-free	6	1
Colloids	34	4
Labeled AM	60	94
Tc-free	16	1
Colloids	27	3
Labeled AM	57	96

Multiple experiments were performed in order to optimize the conditions of the labeling reaction and confirm the protocol of ^{99m}Tc-linear AM preparation. The reaction and purification procedures were monitored by ITLC, HPLC and radioactivity analysis. The present protocol could give rise to a labeling yield about 55%. To simplify the purification procedure and shorten time cost before administration, the reaction mixture was purified by Sep-Pak instead of analytical HPLC. The t_R of ^{99m}Tc-linear AM detected by UV were around 20 min at 215 nm and 255 nm respectively. The collected fractions by Sep-Pak with the higher radioactivity corresponded well to the results of HPLC

analysis. The data supported strongly the simplified protocol and the high purity of final product. The pooled fraction was analyzed by ITLC and the purity of final product, ^{99m}Tc-linear AM, was over 95% (Table 14). The data in the table represented the mean of each independent experiment performed in triplicate.

10.9. Stability of ^{99m}Tc-linear AM in PBS

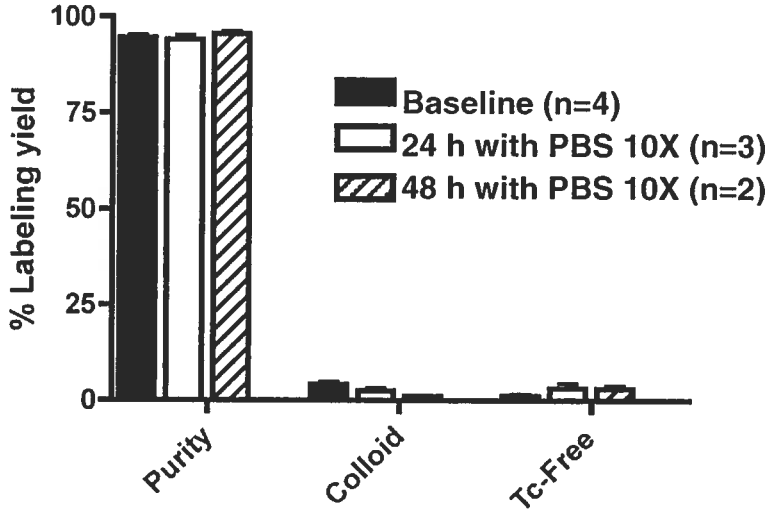

Figure 25: Stability of ^{99m}Tc-linear AM in PBS.

As shown in Figure 25, the labeled peptide was stable up to 48 h in PBS 10X buffer.

10.10. Molecular imaging with ^{99m}Tc-linear AM

Shortly after injection i.v., the radio-labeled ^{99m}Tc-linear AM was clearly seen in the inferior vena cava and the right heart chamber. The tracer could be seen to be retained by the lungs after only 20 seconds. However, there was still mild activity of the tracer over the heart. Only 5 min, this radiotracer was retained by lungs. The lung activity persists for after 30 min, and then, after 1 h the tracer becomes evident in the gallbladder. After 2 h the density of radiotracer in the lungs was decreasing slightly while increasing obviously in the gallbladder (Figure 26). The specific uptake of ^{99m}Tc-linear AM by the lungs persists from 5 min to 60 min after administration. A stable, specific and good quality

imaging of the lungs could therefore be obtained rapidly, and maintained for more than 1 h. This is a clinically desirable quality for an imaging agent.

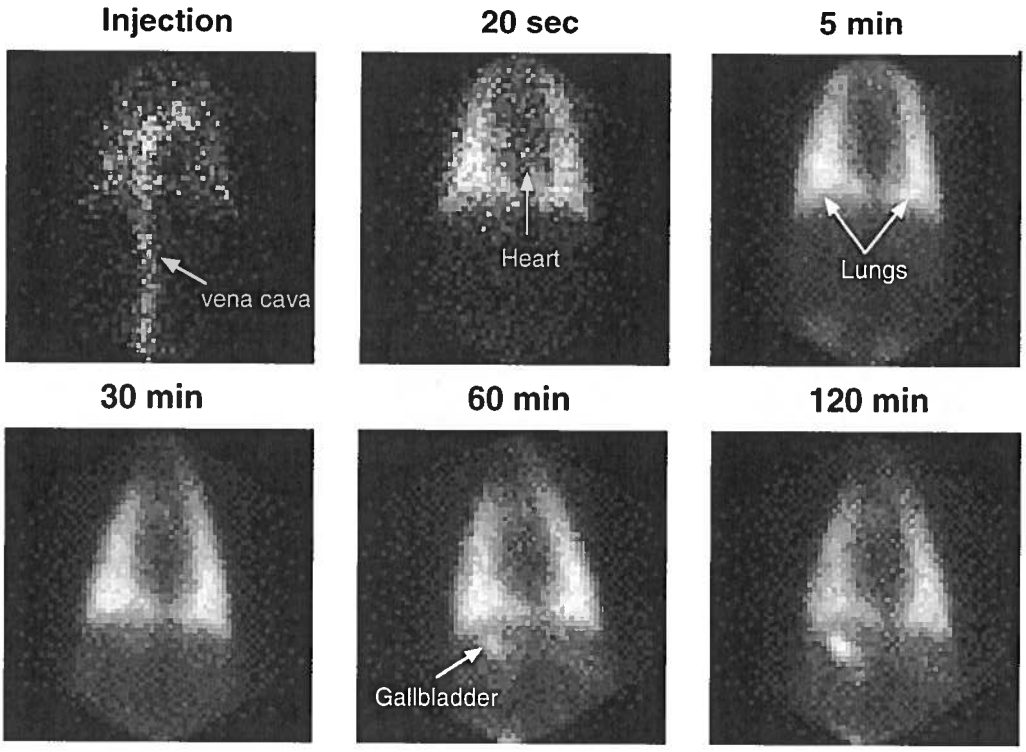

Figure 26: Molecular imaging trace of ^{99m}Tc-linear AM.

10.11. Clearance of ^{99m}Tc-linear AM in dog lungs

After administration, during 30 min to 240 min, representative gamma camera images (anterior and posterior view) of ^{99m}Tc-linear AM of the whole body were presented. The radiotracer uptake in the lungs was seen clearly after 30 min, also seen were kidneys. Then, it reduced after 1 h and became unclear after 4 h in the lungs. However, during 30 min to 240 min the retention of the radiotracer in the kidneys displayed a lasting identical activity from both side of view. The tracer was held in the bladder after the uptake in the lungs and kidneys, and exhibited a continuous accumulation along with time by anterior and posterior views. A significant retention demonstrated in gallbladder was seen after the bladder uptake from anterior view, and accumulated along with the retention in the bladder. The typical experiment was shown in Figure 27. As a result, after the high and

specific lung uptake, the radiotracer appeared to be cleared from lungs and eliminated by the kidneys and liver.

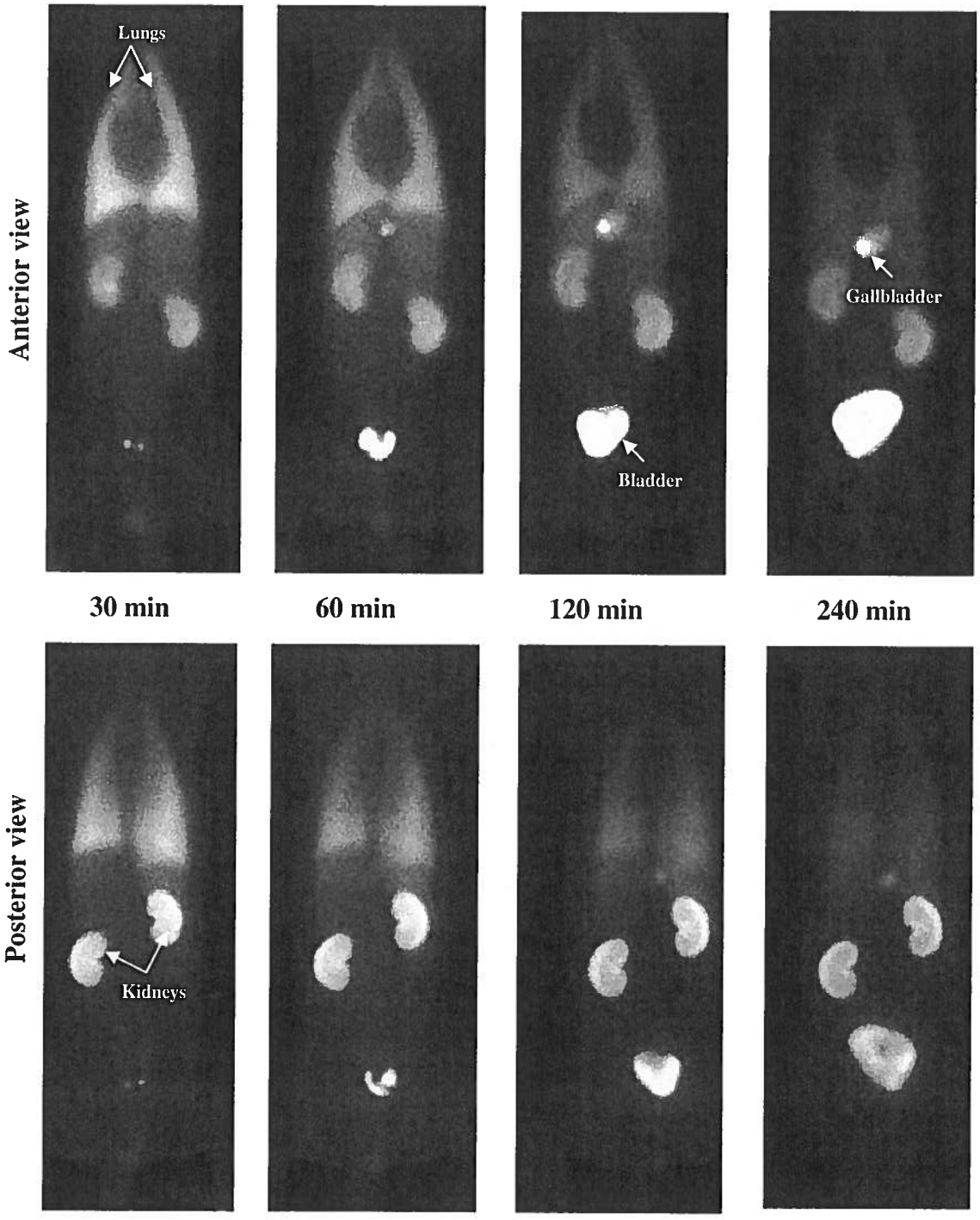

Figure 27: The clearance of ^{99m}Tc-linear AM in the lungs. The gamma camera images (anterior and posterior view) were collected by the whole-body scans of a dog after administering ^{99m}Tc-linear AM at 30 min, 60 min, 120 min, and 240 min.

10.12. Biodistribution of ^{99m}Tc-linear AM in dog

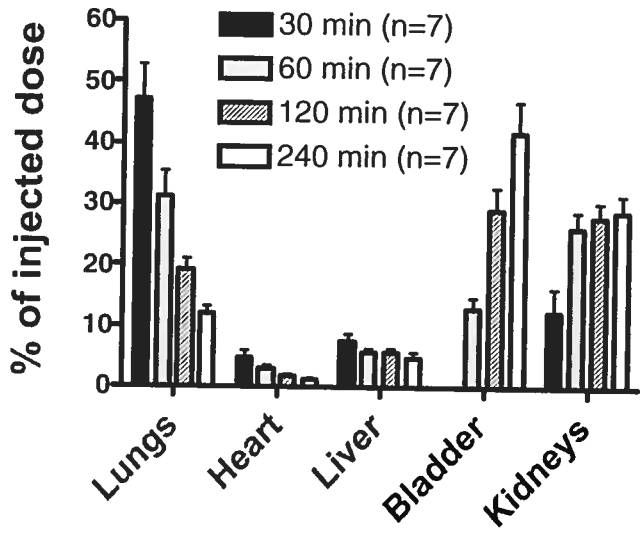

Figure 28: Biodistribution of ^{99m}Tc-linear AM in the dog.

As shown in Figure 28, the lungs predominantly retained the radiopharmaceutical 30 min after the injection. A quantitative analysis of the images after 30 min indicated that 47% of ^{99m}Tc-linear AM was in the lungs, as compared to 5 % in the heart, 8% in the liver, 12% in the kidneys, none in the gallbladder. After 60 min, ^{99m}Tc-linear AM was reduced in the lungs (31%), heart (2%) and liver (6%), obviously increased in the bladder (13%) and kidneys (26%). At 120 min, only 19% in the lungs and 2% in the heart remained, and the retention of tracer in the liver (6%) remained similar. Meanwhile, they were increasing continually in the bladder (29%) and kidneys (28%). At 240 min, only 12% of ^{99m}Tc-linear AM was left in the lungs and 2% in the heart, 5% in the liver, as most was retained in the bladder (42%) and kidney (29%). The lung retention of the radiotracer was maintained over 4 h. The rapid and initially predominant activity in the lung suggested the importance of the lung as a target organ of this radiotracer. There was proportionally only minor retention by the liver and heart. At late time points (60-240 min), the high kidney and bladder radioactivity were attributable to the main elimination route of the radiolabeled peptide. The data was obtained from seven independent animals.

10.13. Plasma kinetics of ^{99m}Tc-linear AM in dog

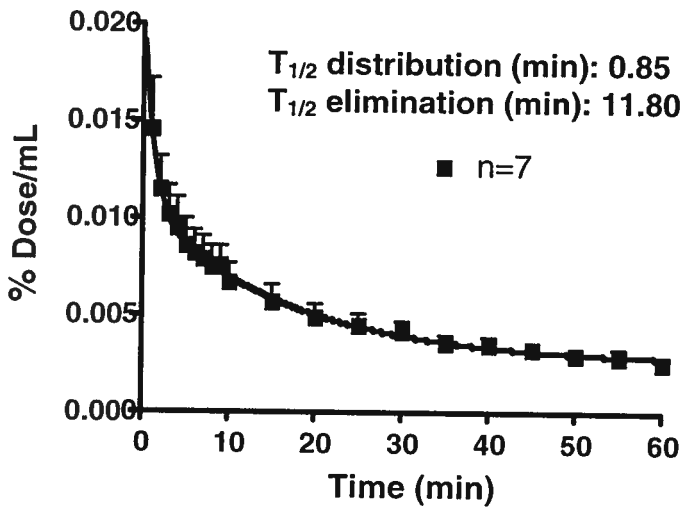

Figure 29: Plasma kinetics of ^{99m}Tc-linear AM in dogs. 2 mL blood samples were collected at every 1 min for 10-min period and then 5 min for the following 50-min period. Results are expressed as a percentage of total radioactivity injected dose per mL (% Dose/mL).

^{99m}Tc-linear AM was derived from the linear form of human AM. The main action of this native peptide is to cause vasodilation. The quantity of the radiotracer injected in dogs (2.9 to 5.8 nmol) was a trace amount devoid of any biological activity that could result in modifications of heart rate or blood pressure. The measured quantity in 1 mL of dog plasma 1 min after injection was about 0.01% of the injected amount. Plasma clearance rate was rapid as shown in Figure 29. The circulating level of radioactivity decreased to < 0.01% ID/mL (injected dose) by 5 min after administration. The plasma kinetic curve was drawn beginning with a blood sample 1 min after injection; levels of ^{99m}Tc-linear AM in whole blood followed a bi-exponential pattern. The half-life of distribution and elimination were 0.85 min and 11.80 min respectively.

10.14. Pulmonary perfusion defect detected with ^{99m}Tc-linear AM

Images of pulmonary perfusion defect detected with ^{99m}Tc-linear AM are shown in Figure 30. The dotted red lines outlined the non-perfused region in the anterior view (A) and

oblique view (B). In the marked regions, an obviously lower activity can be seen. They correspond well to the region of ligation of the pulmonary lobar artery of the right lung, which is indicated with the arrows.

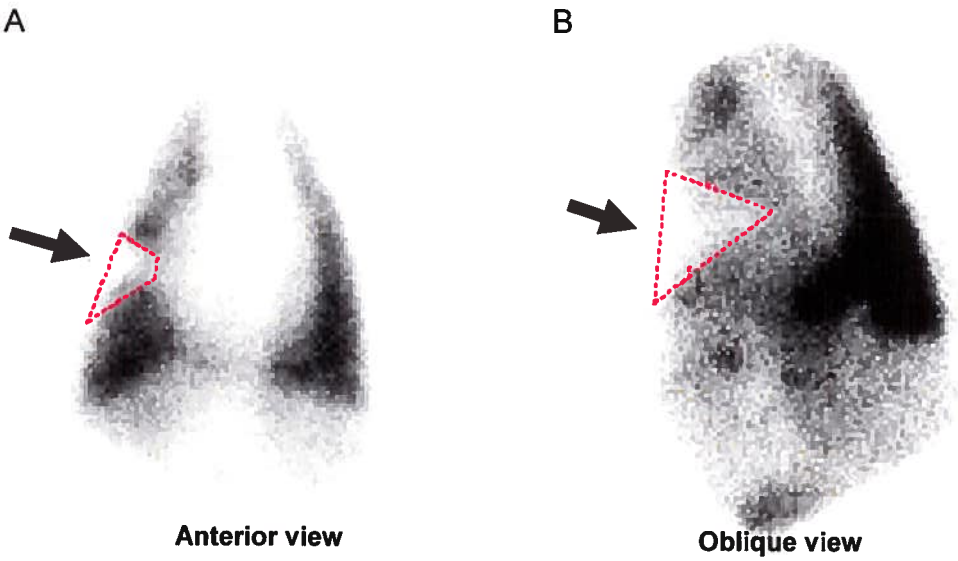

Figure 30: Detection of pulmonary perfusion defect after artery ligation in dogs.

10.15. Proposed structure of ^{99m}Tc-linear AM complex

Table 15: Radiolabeling of AM fragments with ^{99m}Tc.

	^{99m}Tc free (%)	Colloid (%)	Labeling (%)
Linear AM(13-52)	11	39	50
Linear AM(16-52)	32	38	30
AM(17-52)	1	94	6
AM(18-52)	2	80	18
AM(19-52)	1	83	16
AM(20-52)	4	93	4
AM(21-52)	44	53	3
AM(22-52)	1	98	2

The radiolabeling results using smaller AM fragments are outlined in Table 15. Linear AM(13-52) had the highest labeling yield. Linear AM(16-52) exhibited a lower labeling yield and the higher ^{99m}Tc free, but the colloids similar to linear AM(13-52). AM(18-52) and AM(19-52) could labeled by ^{99m}Tc in an even lower yield with a high colloids. The labeling yield of AM(21-52) was also very low, but the free ^{99m}Tc was remarkably higher than the others. Nevertheless, AM(17-52), AM(20-52) and AM(22-52) produced the highest colloid and very low labeling yields. Therefore, they were not well suited to the radiolabeling protocol.

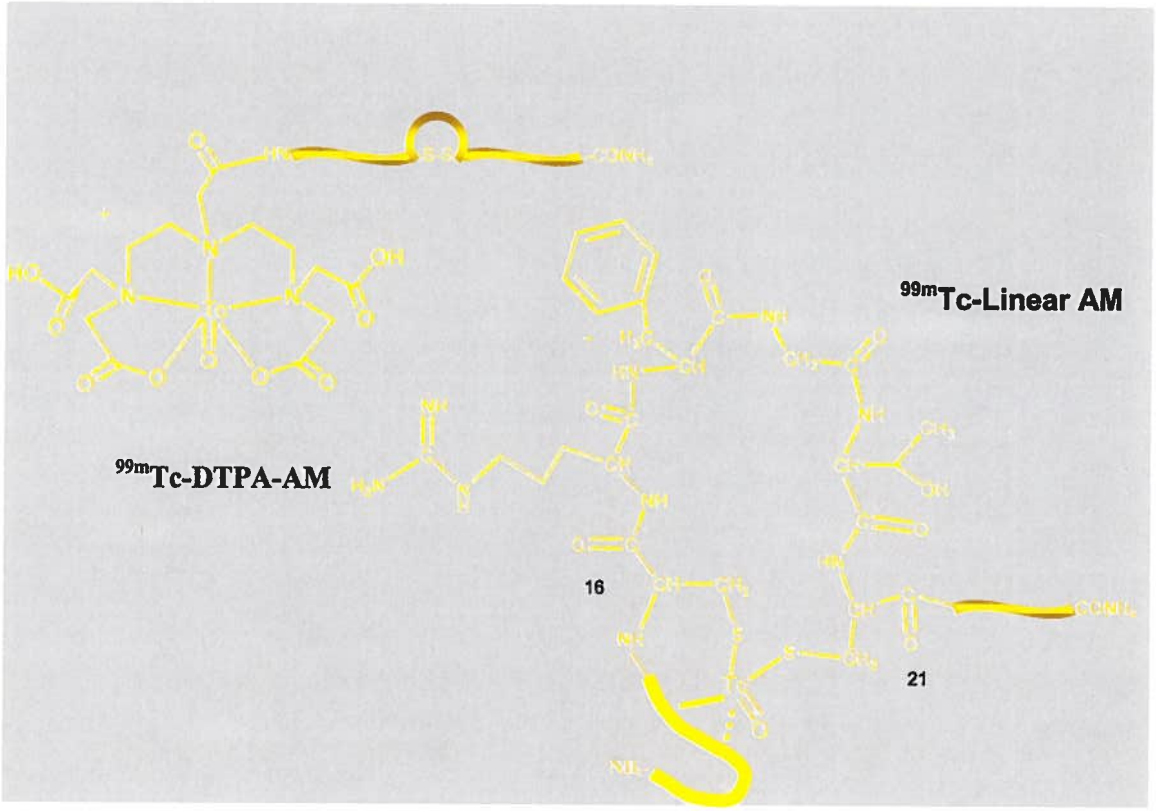

Figure 31: Proposed ^{99m}Tc-labeled complexes.

The results indicate that the 21st sulfhydryl group in linear AM or its fragments could trap the free ^{99m}Tc oxide to give rise to unstable labeled complexes. In this case, the free pertechnetium was inhibited to convert to colloids in the existence of free Sn^{2+} ions. The extra 16th sulfhydryl group could contribute to the stability of the intermediate complex and increase labeling yield. In addition, some groups (electron donors) in the N-terminal region also contributed to the chemical stabilization of ^{99m}Tc labeled AM. As a result, the

proposed chemical structure of ^{99m}Tc-linear AM was shown in Figure 31. The proposed structure of ^{99m}Tc-DTPA-AM was drawn according to publication (Dilworth and Parrott, 1998).

10.16. Biodistribution of ^{99m}Tc-linear AM in rats

The rat was not suitable for lung imaging because the low lung uptake and the high liver uptake of human AM. However, the study of plasma kinetics and biodistribution by using ^{99m}Tc-linear AM were performed in rats. The whole body biodistribution of radiolabeled linear AM was evaluated by *in vivo* imaging with a gamma camera. Rats were injected as described in Section 9.5. Results are expressed as a percentage of total radioactivity injected dose per organ (ID/organ). ^{99m}Tc-linear AM was retained by the lungs (7 ± 1% ID/organ) 30 min after injection and predominantly excreted by the kidney (37 ± 1% ID/organ; Figure 32).

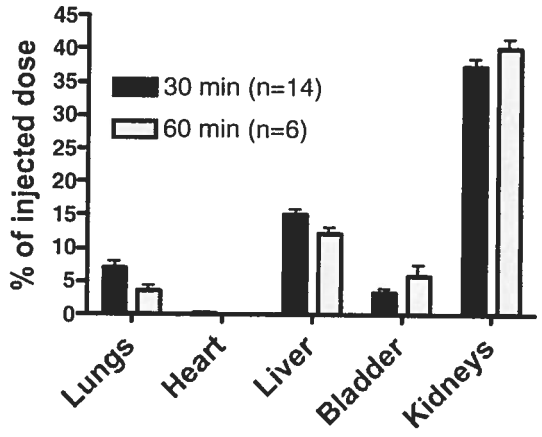

Figure 32: In vivo biodistribution in rats. These recordings were performed both in ventral and dorsal positions. Results were expressed as a percentage of the total radioactivity injected (ID/organ).

The whole body biodistribution of radiolabeled linear AM was then evaluated by removing and counting organs in a gamma counter. These biodistribution studies demonstrated a moderate uptake in the lung (7±1% ID/organ) at 30 min which was

decreased to 3±0.5% ID/organ at 60 min, less then 1% of the total activity was present in the heart, spleen, colon, intestine and duodenum. There was no evidence of thyroid uptake (Figure 33). It suggested a lung clearance pathway of the radiolabeled peptide. Furthermore, these biodistribution data demonstrate that ^{99m}Tc-linear AM is mainly excreted via the kidney with moderate uptake by the hepatobilary system.

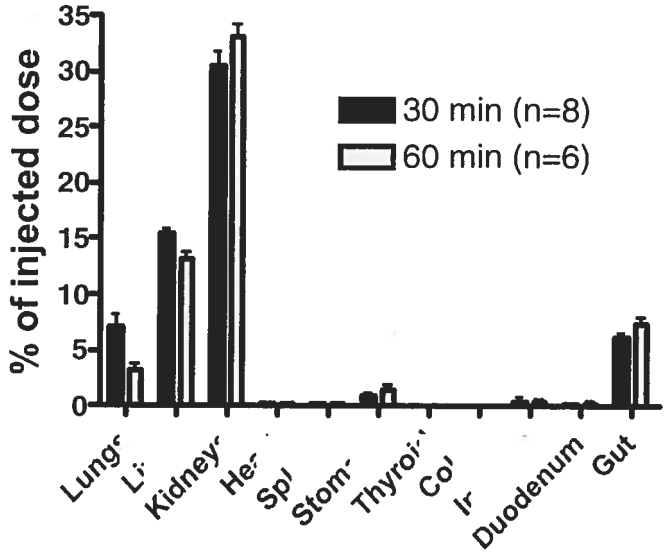

Figure 33: Ex-vivo biodistribution in rats. Results are expressed as a percentage of total radioactivity injected dose per organ (ID/organ)

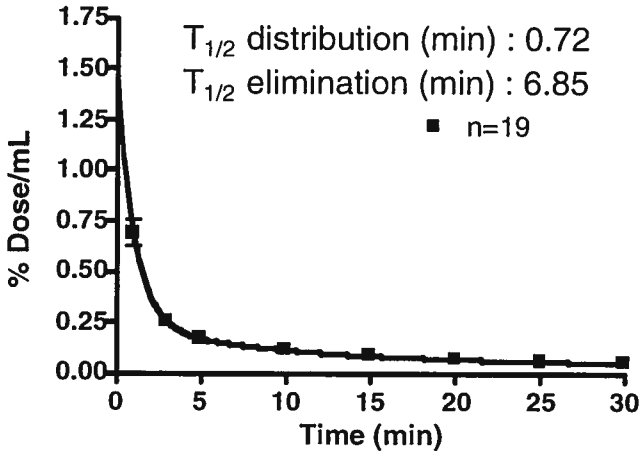

Figure 34: Plasma kinetics of ^{99m}Tc-linear AM in rats. Results are expressed as a percentage of the total radioactivity of the injected dose per mL (% Dose/mL).

10.17. Plasma kinetics of ^{99m}Tc-linear AM in rats

As shown in Figure 34, after intravenous administration of ^{99m}Tc-linear AM, the plasma activity of the radiotracer rapidly decreased following a two-compartment model with a very rapid distribution half-life of 0.72 min and an elimination half-life of 6.85 min.

11. Characterization of the ^{99m}Tc-linear AM binding sites as AM_1 receptor responsible for the AM clearance in vitro

AM is an unselective native agonist of AM receptors. In the molecular imaging study, lung tissues retained ^{99m}Tc-linear AM about 10-fold higher than in the dog heart, the data demonstrated that specific AM receptors are present in the lungs. At present, most of publications (in Table 2b) focus on the AM receptor found in the human and rat. The magnitude of differences in species between the AM receptors subtypes results in the large difficulties encountered when studying the AM receptors. The ^{99m}Tc-linear AM as a radiotracer was administrated i.v., however, only minor retention was found in the heart. Since there are no publications about the AM binding sites in dogs until now, the specific binding sites in the dog lungs might display some differences of physiological and functional significance from those in the heart. In the course of the present study, the binding assays were performed to characterize the ^{99m}Tc-linear AM binding sites in dog lungs by radioligand binding techniques.

11.1. Peptide synthesis

At present, without selective agonists or antagonists of AM receptors, specific AM receptor is usually characterized by AM with high binding affinity and the other members of the calcitonin peptide family with more than 100-fold lower binding affinity (Coppock *et al.*, 1999). In this study, the human peptides and their antagonists, which receptors are composed of CLR and RAMPs complexes were synthesized by standard Fmoc/BOP methodology. The sequences are shown in the Figure 35, and relative parameters

displayed in the Table 16. Because the antagonist of AM2, AM2(16-47), has a glutamine at the N-terminus and that N-terminal Gln of peptide undergoes a spontaneous transformation into a pyroglutamic residue during synthesis and purification (Figure 36), a pyroGlu-peptide was prepared to determine the composition of AM2(16-47) in the total material.

h CGRPα	ACDTATCVTHRLAGLLSRSGGVVKNNFVPTNVGSKAF	37
	8	
hAMY	KCNTATCATQRLANFLVHSSNNFGAILSSTNVGSNTY	37
hAM	YRQSMNNFQGLRSFGCRFGTCTVQKLAHQIYQFTDKDKDNVAPRSKISPQGY	52
	13 22	
hAM2	TQAQLLRVGCVLGTCQVQNLSHRLWQLMGPAGRQDSAPVDPSSPHSY	47
	16	
PAMP	ARLDVASEFRKKWNKWALSR	20

Figure 35: The human peptides of the calcitonin peptide family and PAMP.

11.2. Peptide cyclization

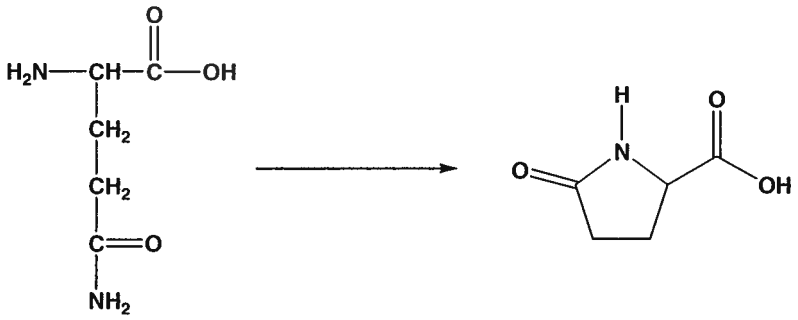

Figure 36: Gln to pyroglutamic acid structures.

After purification by preparative HPLC, the fractions with pure products were pooled. The peptides without cysteines were lyophilized directly and stored at -20°C. Meanwhile, the peptides with two cysteines were adjusted pH to 8.4 and cyclized at open air in their pooled ACN/H_2O solution. The duration of peptide cyclization was monitored by analytical HPLC. The initial peptide cyclization was performed by using synthetic linear AM(15-25) (Figure 37). After cyclization, the t_R of AM2 was changed from 21.53 min (Linear formation) to 21.30 min for the cyclic form in 4 h (Figure 38). The t_R of AMY was changed from 22.85 min to 21.52 min overnight. The t_R of peptide with one disulfide

bridge is about 0.5 -1 min shorter than its linear precursor when analyzing by HPLC with a linear gradient of 0-60% ACN in 0.06% TFA/H_2O v/v for 30 min elution.

Table 16: The parameters of synthetic peptides.

Name	MW (Da)	Measured MW (Da)	t_R (min)	Purity (%)	Yield (%)
AM(13-52)	4532	4531.26	18.20	91.00	-
AM(22-52)	3576	3574.88	17.07	95.58	10
CGRPα	3789	3790.63	20.08	92.93	-
CGRPα(8-37)	3125	3126.79	18.12	93.68	-
AM2	5102	5100.20	21.53	95.63	9
AM2(16-47)	3560	3559.27	17.48	69.63	33
AM2(pGlu-17-47)	3542	3548.27	18.83	77.48	34
AMY	3903	3905.94	22.85	76.37	8
PAMP	2462	2461.52	17.04	94.34	61

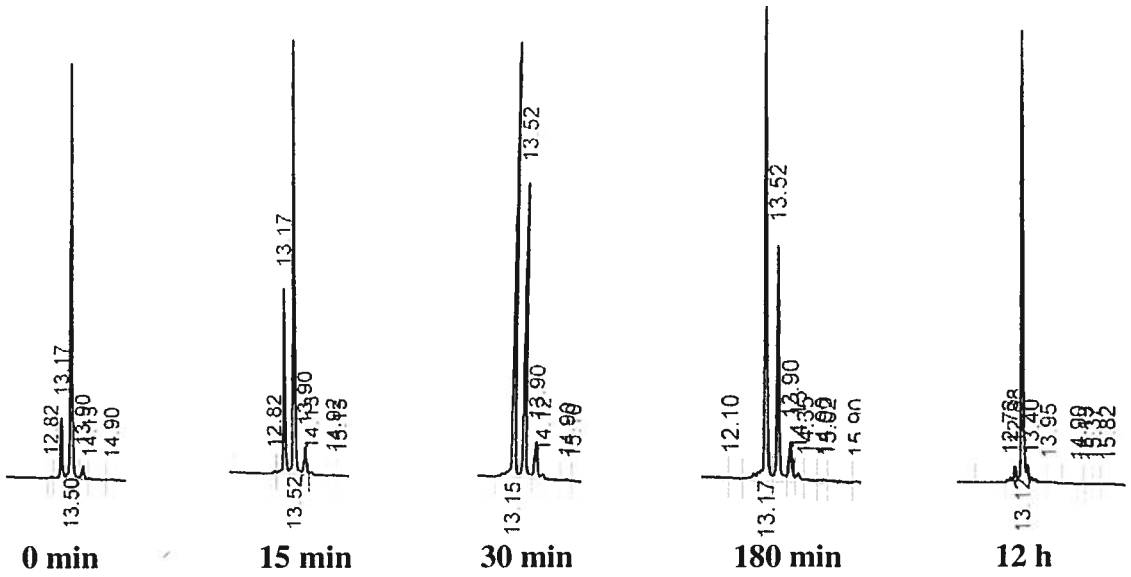

Figure 37: Cycliaztion of AM(15-25) with air. The peptide cyclization was monitored by HPLC analysis with a linear gradient of 0-60% ACN in 0.06% TFA/H_2O v/v for 30 min elution. Before cyclization (0 min), the main peak was linear peptide with a t_R of 13.5 min, by prolongation of reactive time the peak became lower than before, and a new peak with a t_R of 13.1 min appeared on the left. After cyclization, it showed a solo peak with a short t_R.

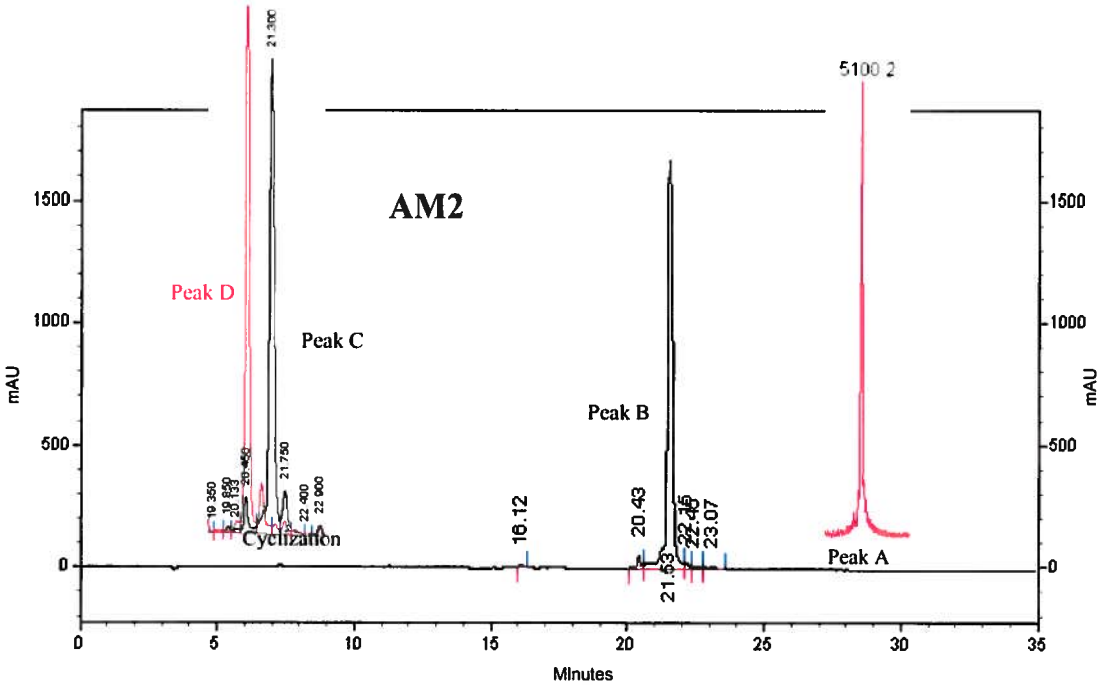

Figure 38: Characterization of AM2. The final product of synthetic AM2 with the right MW (Peak A in red) was analyzed by HPLC with a linear gradient of 0-60% ACN in 0.06% TFA/H_2O v/v for 30 min elution. It showed a sole peak (Peak B in black). On the left of the figure, HPLC analysis before cyclization (black) and after cyclization (red) showed that linear AM2 (Peak C in black) was completely converted to AM2 (Peak D in red) with a linear gradient of 0-60% ACN in 0.06% TFA/H_2O v/v for 30 min elution.

11.3. Characterization of peptides

The identity of products was confirmed by HPLC and mass spectrometry, as shown with AM2 (Figure 38). The relative parameters of other synthetic peptides are outlined in Table 16. Among of them, AMY was prepared at a lower yield with a poorer purity. The pyroglutamic residue in the total material of synthetic AM2(16-47) was 24% with a t_R = 18.83 min (Figure 39) characterized according to the parameters of synthetic pyroglutamic acid.

11.4. Investigation of competitive binding time course

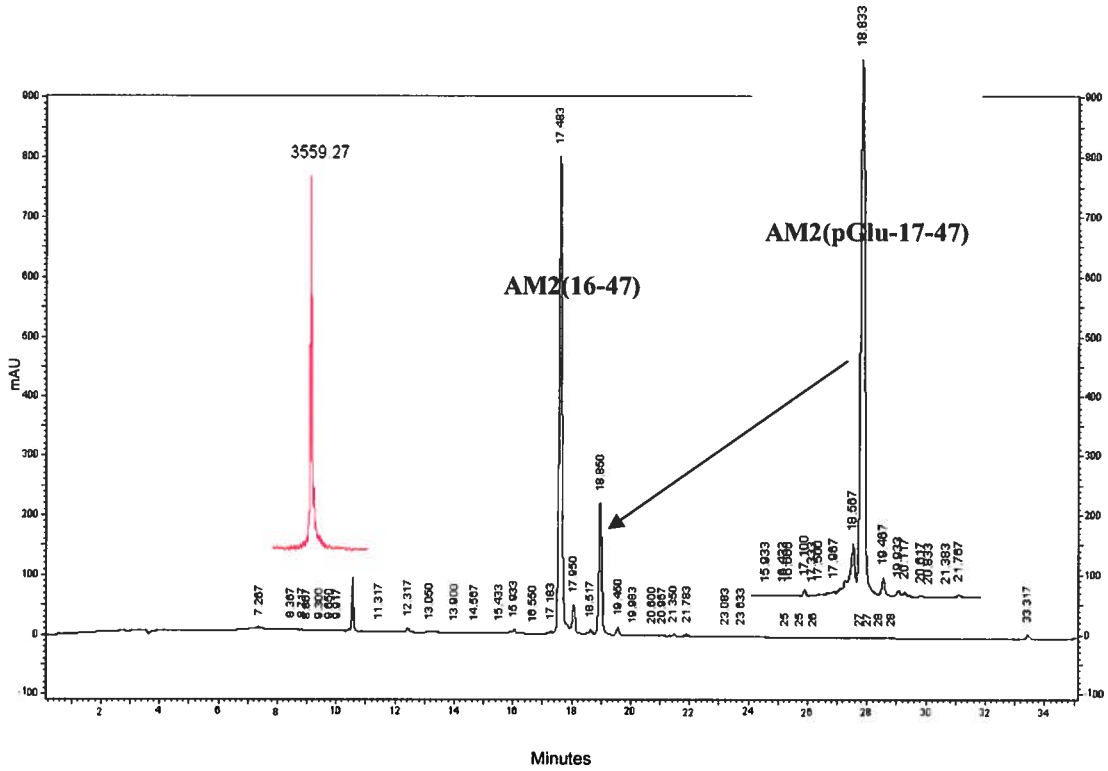

Figure 39: Characterization of AM2(16-47). The synthetic AM2(16-47) was analyzed by HPLC with a linear gradient of 0-60% ACN in 0.06% TFA/H_2O v/v for 30 min elution. The main peak with a t_R of 17.48 min was characterized as AM2(16-47) with the right MW (Peak in red), a small peak on the right with a t_R of 18.83 min was characterized as AM2(pGlu-17-47) by using synthetic AM2(pGlu-17-47).

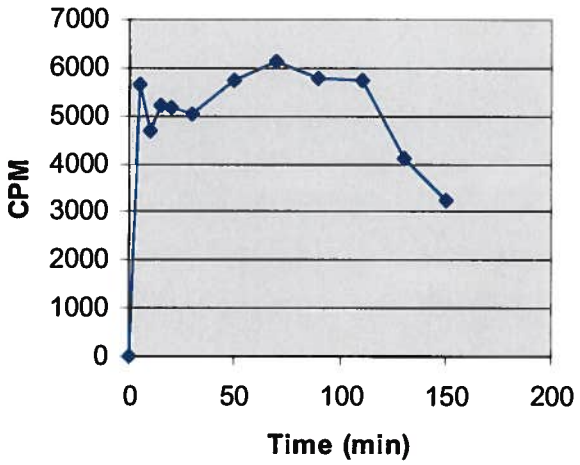

Figure 40: Competitive binding time course of ^{125}I-AM (0.1 nM) with dog lung homogenates.

The time course experiment was performed using the same concentration of ^{125}I-AM as in the binding experiments. The radioactivity retained by the filter paper was detected after the incubation at different time course. The measurement was made at a range of incubation times from 5 min to 3 h. The result showed that the specific binding of radioligand on the lung homogenates happened in a very short time and reduced after 2 h at room temperature. The data represents the mean of two independent experiments. The differences in radioactivity measured on filter paper were least between 50 min to 110 min (Figure 40). The binding assay supported that a stable binding data could be obtained in 90 min incubation time.

11.5. Competitive binding experiment with ^{125}I-AM vs. AM

Competitive binding experiments using ^{125}I-AM as the radioligand and AM as the competitor displayed that non-selective agonist AM bound the binding sites in the dog lung homogenates with high affinity (Figure 41), the experimental data fits better to a two binding model (blue) by statistics (F value = 4.337 and P = 0.0167), displaying one high-affinity site with IC_{50} = 23 pM (95% confidence interval 7 pM to 71 nM) and one low-affinity site with IC_{50} = 28 nM (95% confidence interval 1 nM to 606 nM).

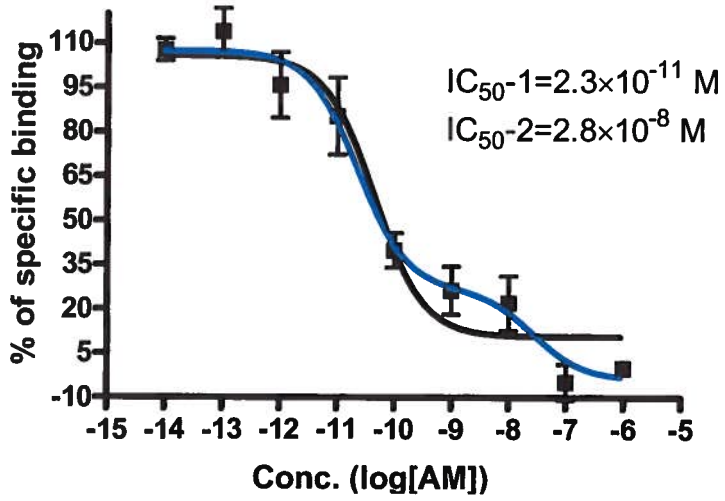

Figure 41: Competitive binding study of ^{125}I-AM bound to dog lung homogenates. One binding model is in black, and two binding model is in blue. Data points are the mean ± S.E.M. (standard error of the mean) of five independent experiments performed in duplicate.

11.6. Competitive binding experiment with ^{99m}Tc-linear AM vs. AM

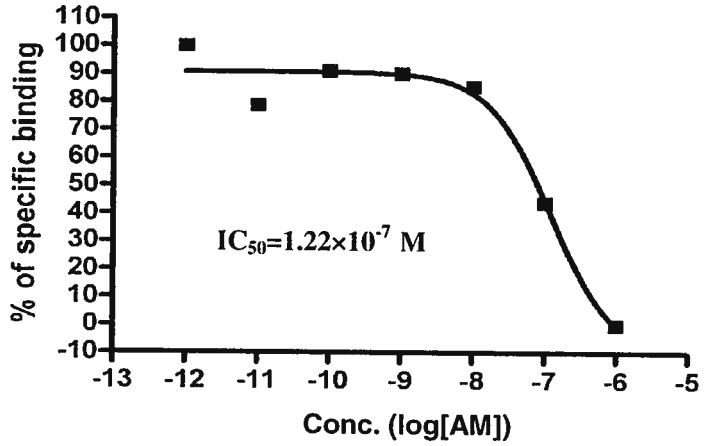

Figure 42: Competitive binding study of ^{99m}Tc-linear AM bound to dog lung homogenates. Data points are at the mean of three independent experiments.

Although ^{99m}Tc has a short half-life, 6 hours, the initial competitive binding experiment using ^{99m}Tc-linear AM as the radioligand and AM as the competitor was carried out. The data showed that the specific binding of the radiotracer in the dog lung homogenates was able to be inhibited by AM with an IC_{50} value 122 nM (the data was collected from three independent experiments; Figure 42). In the Section 11.5, when ^{125}I-AM was used as a radioligand, the IC_{50} of cold AM was very low (about 0.02 nM). The two distinct IC_{50} values of cold AM in the competitive binding experiments by using different tracers implied that both radioligands might bind to different sites. However, the amounts of linear AM (2.89 nmol) in labeling reaction was over the dose of $Na^{99m}TcO_4$ (28.9 pmol, the maximum dose from ^{99}Mo/^{99m}Tc chromatographic generator; Section 4.2) whereas the labeling yield was about 55% (Section 10.8). In this case, most of linear AM (about 2.87 nmol calculated by the amounts of linear AM and labeling yield in the reaction) were not labeled. By the purification of Sep-Pak, the cold linear AM (unlabeled linear AM) could not isolated completely from the final product (^{99m}Tc-linea AM), and the amounts of the cold peptide can not be determined. The linear AM as a weak ligand of AM receptor might cause a right shift in binding curve. We are considering the interference of cold linear AM in the competitive binding experiment by using ^{99m}Tc-linear AM as a

radioligand, and data did show the displacement of ^{99m}Tc-linear AM bound to dog lung homogenates by AM. As a result, it indicated that the radiotracer had identified the correct AM binding sites in the lungs, and ^{125}I-AM could be used as the radioligand instead of ^{99m}Tc-linear AM to characterize the receptor found in the dog lungs.

11.7. Competitive binding experiment with ^{125}I-AM vs agonist and antagonist of AM

In order to characterize the binding sites found in the dog lungs, the competitive binding was performed using the known agonist AM(13-52) and antagonist AM(22-52) of AM as competitors. The data shows that the binding sites of ^{125}I-AM in dog lung homogenates can be displaced by AM agonist and antagonist with different IC_{50} values (Figure 43). The related IC_{50} values and their 95% confidence interval are shown in Table 17. The order of displacement according to IC_{50} values is AM>Linear AM>AM(13-52)>AM(22-52). Although the binding sites found in dog lungs had lower binding affinity to AM analogs, they could be identified by AM, AM agonist AM(13-52) and antagonist AM(22-52). The result suggested that the binding sites of ^{99m}Tc-linear AM found in the dog lungs might be AM receptors.

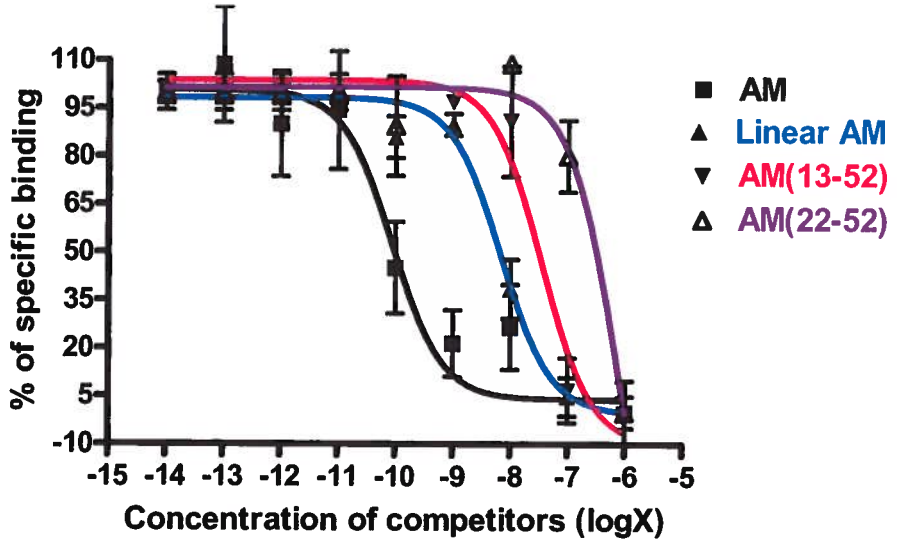

Figure 43: Displacement of ^{125}I-AM bound to dog lung homogenates by AM, linear AM, AM(13-52) and AM(22-52). Data points are the mean ± S.E.M. of at least three independent experiments performed in duplicate.

11.8. Competitive binding experiment with ^{125}I-AM vs. agonists of the calcitonin peptide family

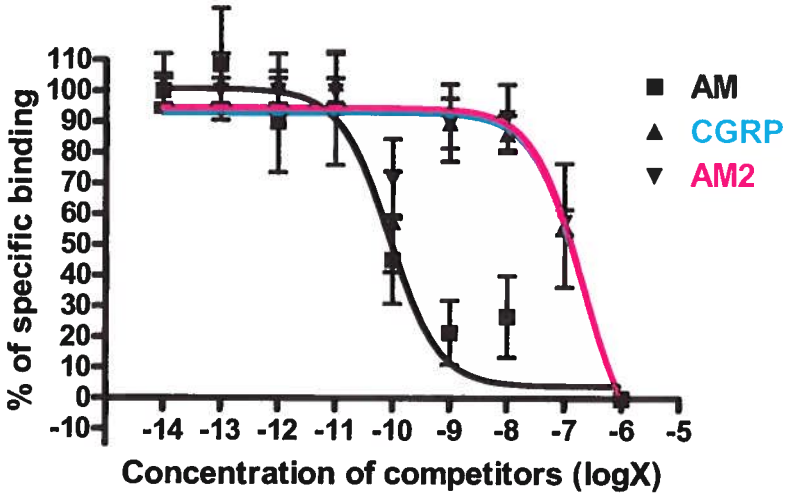

Figure 44: Displacement of ^{125}I-AM bound to dog lung homogenates by AM, CGRP$_\alpha$ and AM2. Data points are the mean ± S.E.M. of at least three independent experiments performed in duplicate.

Table 17: Data for binding sites of dog lung homogenates obtained from competitive binding assays using ^{125}I-AM.

Ligand	IC_{50} (M)	95% confidence interval (M)
AM	8.9×10^{-11}	2.7×10^{-11} to 2.9×10^{-10}
Linear AM	6.9×10^{-9}	4.3×10^{-9} to 1.1×10^{-8}
AM(13-52)	3.5×10^{-8}	1.3×10^{-8} to 9.4×10^{-8}
AM(22-52)	8.4×10^{-7}	1.0×10^{-7} to 6.8×10^{-6}
CGRPα	2.0×10^{-7}	4.4×10^{-8} to 9.3×10^{-7}
AM2	2.1×10^{-7}	9.1×10^{-8} to 4.9×10^{-7}
AMY	N.E.	-
PAMP	N.E	-
CGRPα(8-37)	$\geq10^{-6}$	-
AM2(16-47)	2.9×10^{-7}	1.0×10^{-7} to 8.2×10^{-7}

* IC_{50} from one site competition mode.
* N.E.: No effect; no displacement was observed.

According to publications (Zimmermann *et al.*, 1996; Poyner *et al.*, 2002; Roh *et al.*, 2004), there are at least three different receptors that could bind to AM. They are AMY receptor, CGRP receptor and AM2 receptor. To verify the presence of a specific AM receptor in the dog lungs, the following competitive binding experiments were carried out with other members of the calcitonin peptide family. The binding sites were characterized by the high affinity for AM and >1000-fold lower affinity for the CGRPα and AM2 (Figure 44 and Table 17), no displacement was found when using AMY and PAMP as competitors. The result strongly supports that the AM binding sites in dog lungs are related to CGRPα and AM2 receptors, i.e. CLR/RAMPs complexes, rather than AMY and PAMP. The order of displacement (IC_{50} values) is AM>>AM2≈CGRPα>>AMY and PAMP.

11.9. Competitive binding experiments with ^{125}I-AM vs. antagonists of the calcitonin peptide family

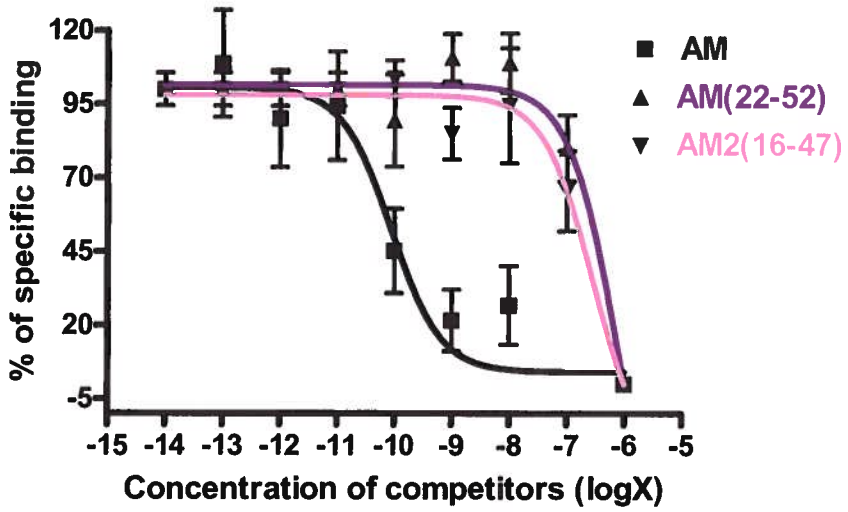

Figure 45: Displacement of ^{125}I-AM bound to dog lung homogenates by AM, AM(22-52) and AM2(16-52). Data points are the mean ± S.E.M. of at least three independent experiments performed in duplicate.

Two AM receptor subtypes have been defined in molecular terms. In order to further characterize the AM receptor in the dog lung, the competitive binding assays were also performed using the antagonists of the CT peptide family as competitors. The binding

sites found in the dog lungs exhibited a higher selectivity to AM(22-52) than CGRPα(8-37) (Figure 45 and Table 17). It suggests that the AM binding sites with high binding-affinity appear to have AM_1 characteristics. The order of displacement (IC_{50} values) is AM>> AM2(16-47) > AM(22-52) >CGRPα(8-37).

12. Characterization of the sequences and secondary structures of AM required by the AM receptor in the dog lungs

AM is a long peptide with 52 amino acids and non-selective binding capability for AM receptors. According to publication (Yu and Hsu, 2005), the peptide is composed of N-terminal loop (1-15th amino acid), disulfide bridge (16-21st amino acid), followed by a α-helix secondary structure and a disordered structure (after the 22nd amino acid), and ends in a C-terminal amidated Tyr (the 52nd). Study of its sequence and secondary structure required by the binding sites found in the dog lungs could contribute to the peptide structure-activity relationship and the development of smaller peptide or other derived compounds that appear to have specificity to lungs as target molecules instead of AM. The assumed substitute, would be much easier to synthesize and less prone to side-reactions and therefore potentially a great improvement. For this reason, in part of the present study, the amino acids, minimal peptide fragment, and some related secondary structures in the AM molecule that retain higher binding affinity for the AM receptor in dog lungs were studied.

12.1. Synthesis and characterization of peptides

Table 18: The parameters of synthetic peptides.

Name	MW (Da)	Measured MW (Da)	T_R (min)	Purity (%)	Yield (%)
AM(26-52)	3120	3119.43	15.48	91.51	8
AM(40-52)	1416	1415.29	13.82	90.86	4
AM(1-25)	2927	2927.29	18.02	95.21	6
AM(1-40)	4744	4744.76	25.25	91.56	20

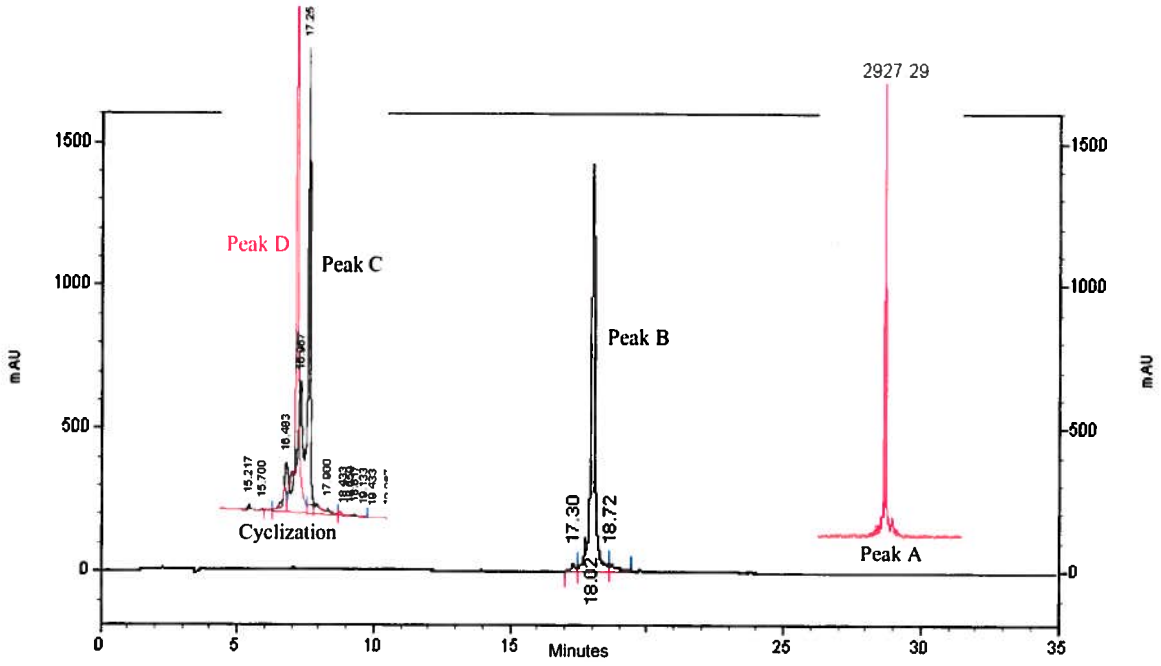

Figure 46: Cyclization and characterization of AM(1-25). The final product of synthetic AM(1-25) with the right MW (Peak A in red) was analyzed by HPLC with a linear gradient of 0-60% ACN in 0.06% TFA/H_2O v/v for 30 min elution. It showed a sole peak (Peak B in black). On the left of the figure, HPLC analysis before cyclization (black) and after cyclization (red) showed that linear AM(1-25) (Peak C in black) was completely converted to AM(1-25) (Peak D in red) with a linear gradient of 0-60% ACN in 0.06% TFA/H_2O v/v for 30 min elution.

To investigate the required sequences and structure of AM, a set of AM fragments was designed and synthesized according to the predicted mature region. Linear AM has the full amino acid sequence of AM without disulfide bridge structure. AM(13-52) is a AM agonist lacking the N-terminal loop. AM antagonist, AM(22-52), lacks both the N-terminal loop and disulfide bridge secondary structure. The fragments, AM(1-25), contains the full N-terminal region of AM and disulfide bridge; while AM(26-52) keeps the rest of the entire C-terminal region. AM(1-40) retains almost all of the sequence and structure except the C-terminus; conversely, AM(40-52) only retains a small C-terminal region with an amidated Tyr. These peptides were prepared, cyclized and characterized by methods identical to those described previously. The t_R of peptide with one disulfide bridge is about 1 min less than its linear form when analysed by HPLC with a linear gradient of 0-60% ACN in 0.06% TFA/H_2O v/v for 30 min elution. For instance, with cyclization, the t_R of AM(1-25) decreased from 17.25 min for the linear form to 16.97

min for the cyclized form (Figure 46). Similarly, the t_R of AM(1-40) was reduced from 26.12 min to 25.25 min after overnight cyclization. The identities of peptides were shown in the Table 18.

12.2. Competitive binding experiment with ^{125}I-AM vs. N- and C-terminal AM fragments

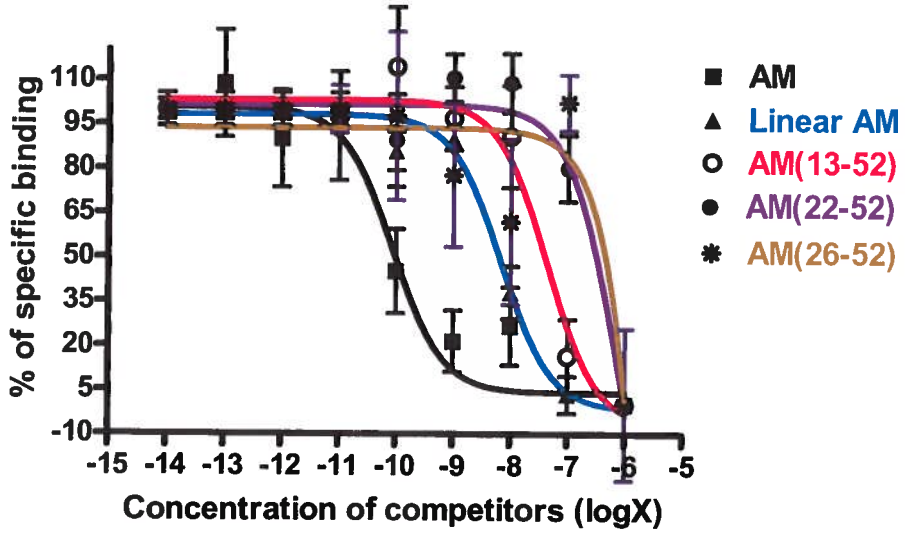

Figure 47: Displacement of ^{125}I-AM bound to dog lung homogenates by AM and its fragments. Data points are the mean ± S.E.M. of at least three independent experiments performed in duplicate.

To help the characterization of AM binding sites in the lung, the rank of displacement among the AM fragments was investigated by competitive binding experiments (Figure 47). The order of displacement (IC_{50} values, Table 19) is AM>>linear AM>AM(13-52)>AM(22-52)>AM(26-52)>AM(1-25), AM(40-52) and AM(1-40). The displacement of ^{125}I-AM bound to dog lung homogenates is less effective where there is a lack of disulfide bridge structure and N-terminal loop, as well as the impairment of the α-helix. It suggests that these geometrial elements are necessary and contribute to the binding affinity of AM to the receptors in dog lungs. Nevertheless, an AM fragment without the C-terminus, even if exhibiting all sequence and structure properties mentioned above, such as AM(1-40), has no displacement found in the competitive binding assay. The study results indicate that the location required by binding sites found in dog lungs was around the C-terminal tail of AM.

Table 19: Affinity data for binding site of ligands in dog lung homogenates obtained from competitive binding experiments using ^{125}I-AM.

Ligand	IC_{50} (M)	95% confidence interval
AM (one binding model)	8.9×10^{-11}	2.7×10^{-11} to 2.9×10^{-10}
AM(26-52)	$> 10^{-6}$	-
AM(40-52)	N.E.	-
AM(1-25)	N.E.	-
AM(1-40)	N.E.	-

*Values represent means ± S.E.M. from three experiments performed in duplicate.
*N.E.: No effect; not displacement was observed.

12.3. Iodination of AM by lactoperoxidase method

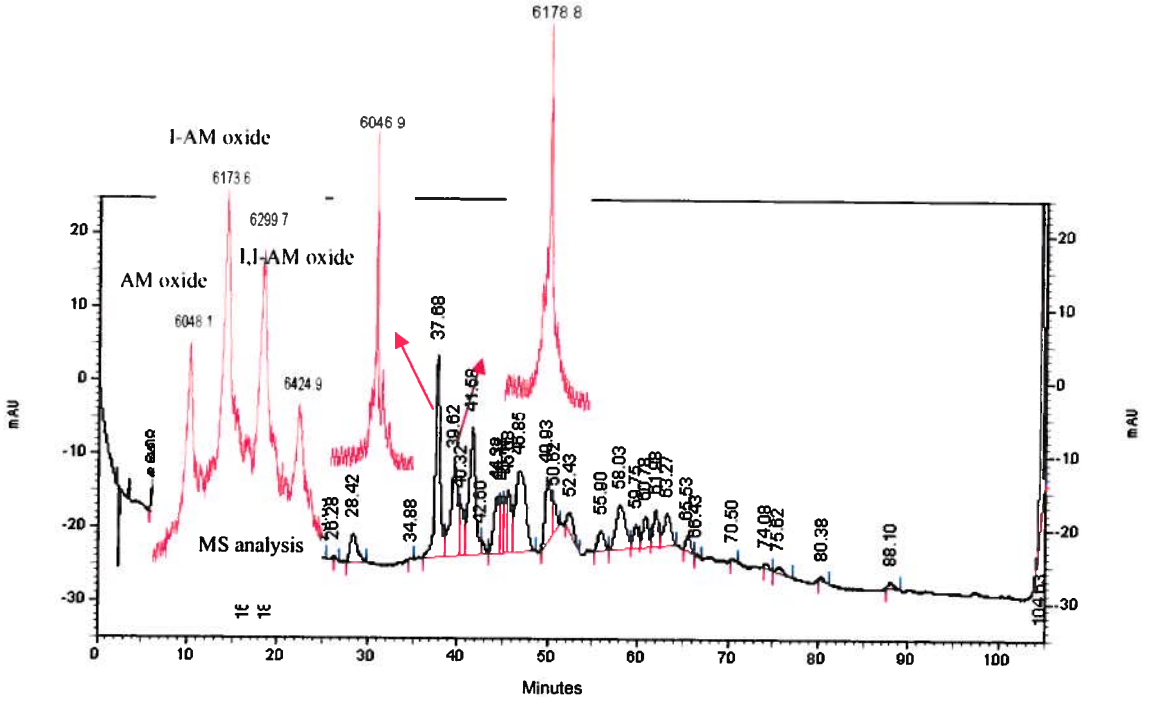

Figure 48: Separation and characterization of iodinated AM prepared by lactoperoxidase method. After iodination, AM was oxidized and iodinated to yield AM products contained AM oxide, I-AM oxide and I,I-AM oxide by MS analysis. The reactive mixture was analyzed. They were separated by HPLC with a linear gradient of 0-25% ACN/H_2O (0.06% TFA/H_2O v/v) in 10 min; 25-35% ACN/H_2O (0.06% TFA/H_2O v/v) in 90 min elution, as shown in black. The fraction collected around with a t_R of 37.68 min is characterized as AM oxide (MW6046 Da); the following fraction collected around with a t_R of 39.62 min is I-AM oxide, as shown in red.

After iodination, the AM and iodinated AM products in the mixture were determined by mass analysis. The mixture was then separated by HPLC, and all collected fractions were analyzed by MALDI-TOF MS analysis. The mono-iodinated AM was found in the fractions collected around 39.62 min. The method by HPLC can separate well AM oxide (MW = 6046 Da, t_R = 37.68 min), mono-iodinated AM oxide (I-AM oxide; MW = 6178 Da, t_R = 39.62 min) and di-iodinated AM oxide (I,I-AM oxide; MW = 6304 Da, t_R = 41.68 min) from the mixture iodinated with lactoperoxidase method. The molecular weight of the components was obtained by MALDI-TOF mass analysis (Figure 48).

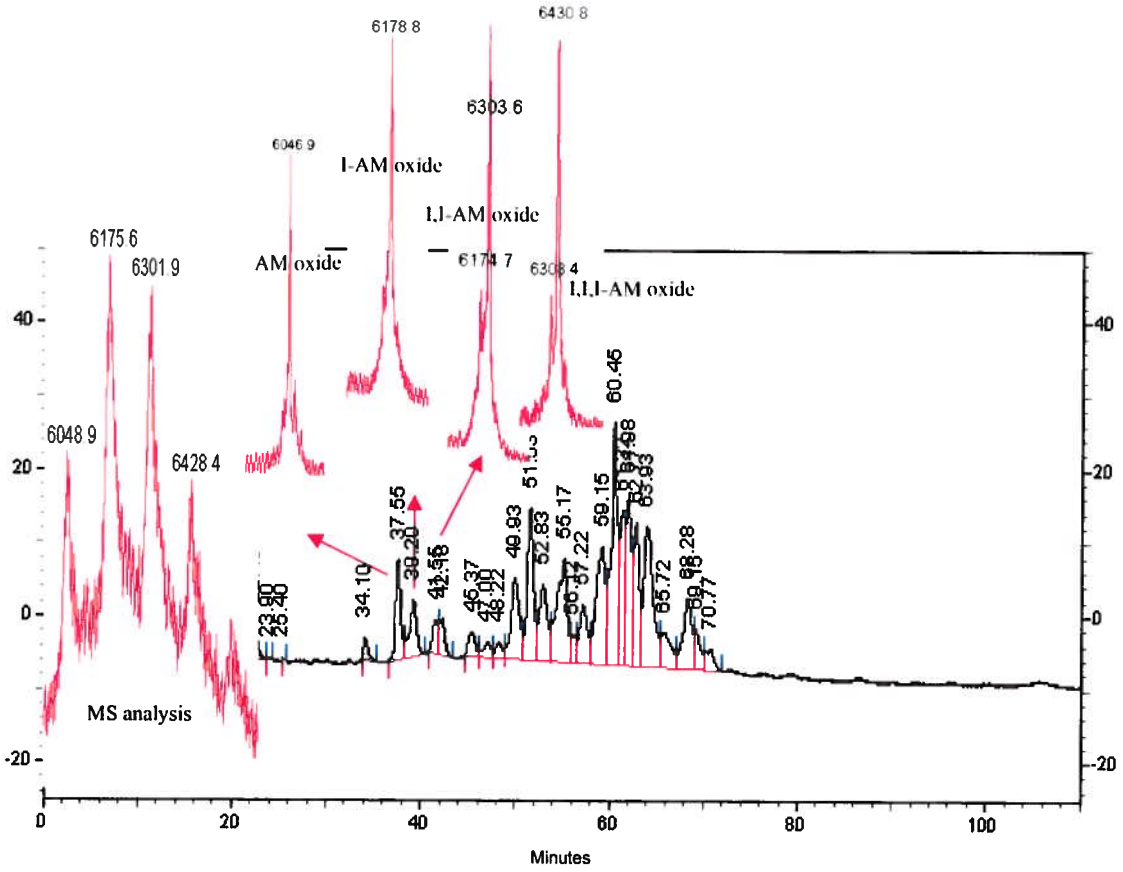

Figure 49: HPLC and MALDI-TOF mass analysis of AM iodination by the Chloramine-T method. After iodination, AM was oxidized and iodinated to yield AM oxide, I-AM oxide, I,I-AM oxide and I,I,I-AM oxide by MS analysis. The reactive mixture was analyzed by HPLC with a linear gradient of 0-25% ACN/H_2O (0.06% TFA/H_2O v/v) in 10 min; 25-35% ACN/H_2O (0.06% TFA/H_2O v/v) in 90 min elution. The fraction collected around 37.55 min is characterized as AM oxide; the fraction collected around 39.20 min is I-AM oxide; the fractions collected from 41.55 to 42.18 min are a mixture of I-AM oxide, I,I-AM oxide and I,I,I-AM oxide.

12.4. Iodination of AM by chloramine-T

In comparable experiments, the AM iodination was also carried out with the Chloramine-T method. Figure 49 showed that there are AM oxide (MW = 6046 Da, t_R = 37.55 min), I-AM oxide (MW = 6178 Da, t_R = 39.20 min) and I,I-AM oxide (MW = 6304 Da, t_R = 41.55 min), as well as multiple iodinated peptides. The result indicated a lower labeling yield and more side-products than with the method utilizing the lactoperoxidase.

12.5. Preparation of ^{125}I-Tyr^1-AM by lactoperoxidase

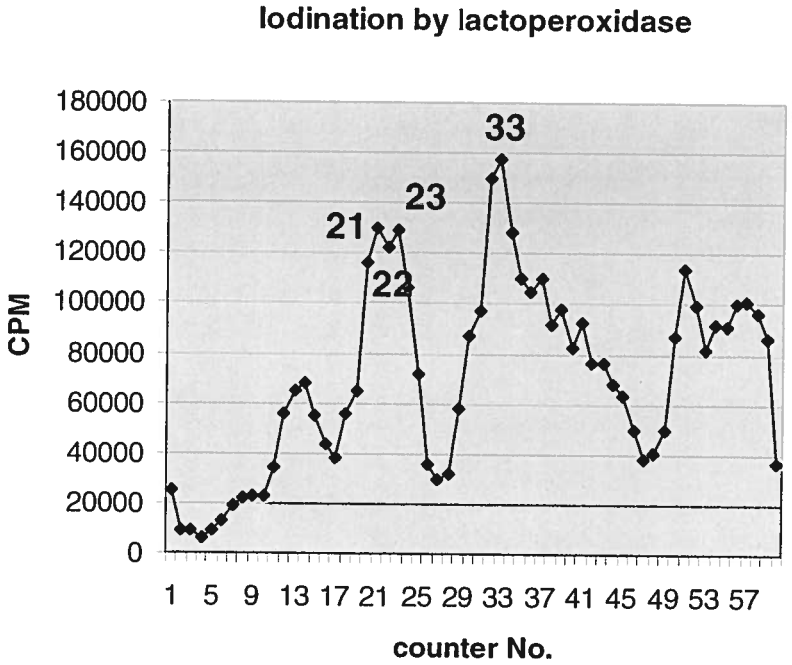

Figure 50: Isolation and identification of ^{125}I-Tyr^1-AM. The ^{125}I-labeling reaction was stopped by immediate purification using HPLC with a linear gradient of 0-25% ACN/H_2O (0.06% TFA/H_2O v/v) in 10 min; 25-35% ACN/H_2O (0.06% TFA/H_2O v/v) in 90 min elution. The eluent in the first 10-min was collected in a 15 mL tube; then fractions were collected in 1.5 mL polypropylene tubes, 0.5 mL per tube. The fractions collected from 29 min (counter No. 1) to 57 min were counted by an auto-gamma counter.

After iodination by lactoperoxidase, the reaction mixture was isolated by analytical HPLC. The fractions collected at 30 min to 90 min in the polypropylene tubes were counted. The radioactivity of these fractions is shown in Figure 50. The proposed ^{125}I-Tyr^1-AM and its oxide (No.21-23), as well as bi-iodinated AM (No.33) were further verified by competitive binding experiments. The competitive binding experiments were performed by using Fractions No.21, No.22, No.23 and No.33 as the radioligand and AM as the competitor. Fraction No.21, 22 and 23 (10^{-10} M) displayed the specific binding in

the dog lung homogenates, which was able to be inhibited by AM with the IC_{50} value 14 nM (95% confidence interval 1 nM to 155 nM), 71 nM (95% confidence interval 10 nM to 498 nM), 67 nM (95% confidence interval 16 nM to 281 nM) and >1 μM (no displacement was observed) respectively. The data was collected from at least two independent experiments in duplicate (Figure 51).

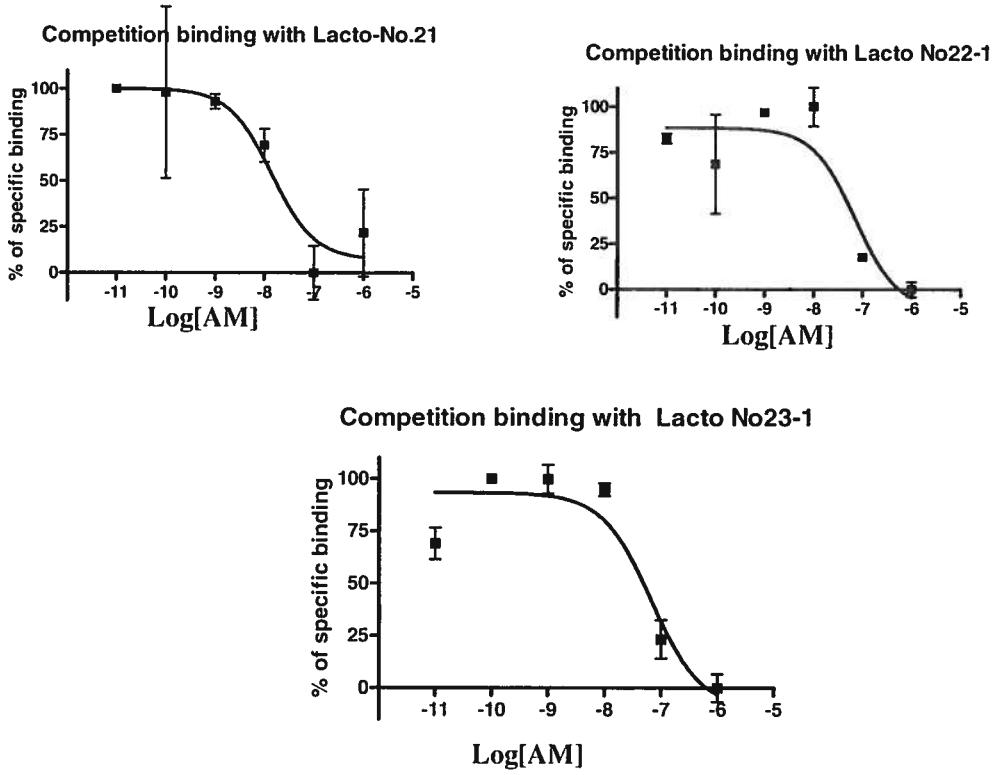

Figure 51: The screening of ^{125}I-Tyr^{1}-AM by binding assay.

12.6. Investigation of the iodinated tyrosine on AM by lactoperoxidase method

CPY and APM, the exopeptidase, digested single amino acid from C-terminal and N-terminal respectively. Both of them are usually used in the investigation of peptide iodination. The initial tests were performed with AM(13-52) and displayed well cleavage at both C- and N-terminus of the peptide. The initial method was then carried out in AM digestion.

12.6.1. The investigation on AM by exopeptidase and CNBr

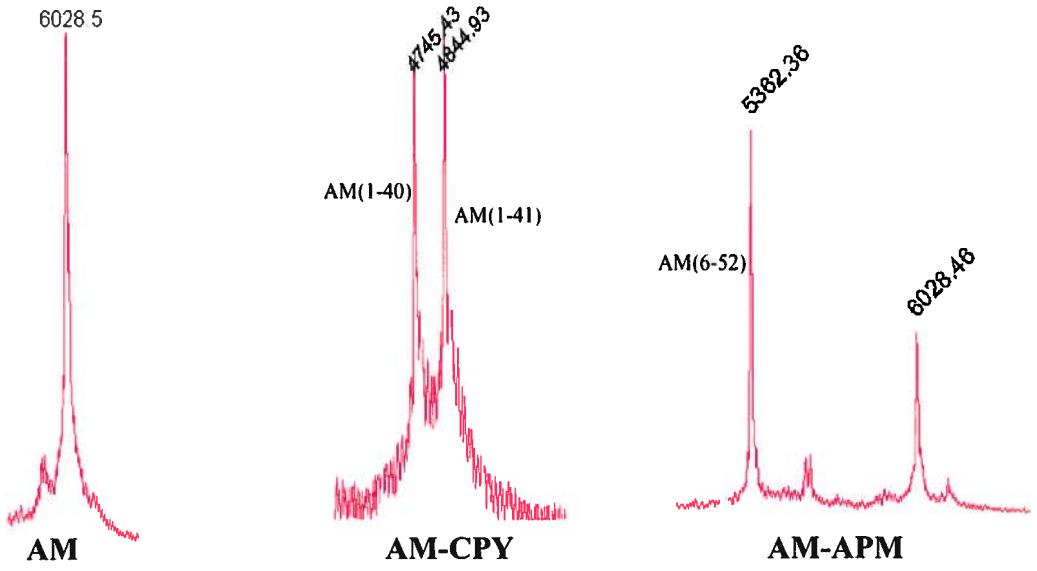

1YRQSMNNFQGLRSFGCRFGTCTVQKLAHQIYQFTDKDKDNVAPRSKISPQGY 52

↑→5361 Da
APM

4744 Da←↑↑
4844 Da←↑
CPY

Figure 52: MALDI-TOF mass analysis of AM after CPY and APM treatments.

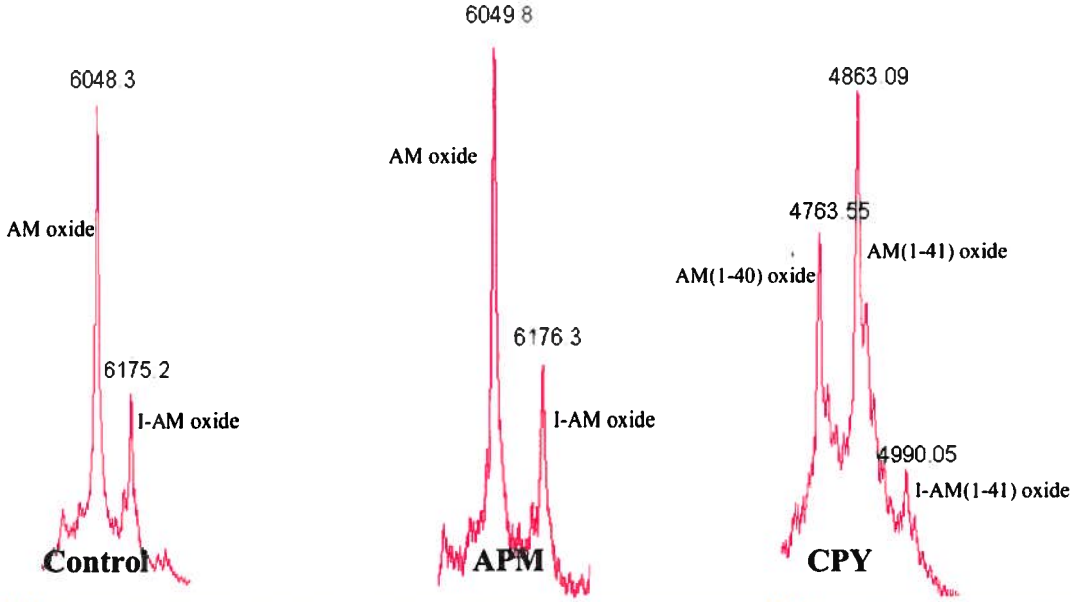

I-YRQSMNNFQGLRSFGCRFGTCTVQKLAHQIYQFTDKDKDNVAPRSKISPQGY52

~~APM~~

4760 Da←↑↑
4860 Da←↑
CPY

Figure 53: MALDI-TOF mass analysis of the iodinated species of AM after CPY and APM treatments.

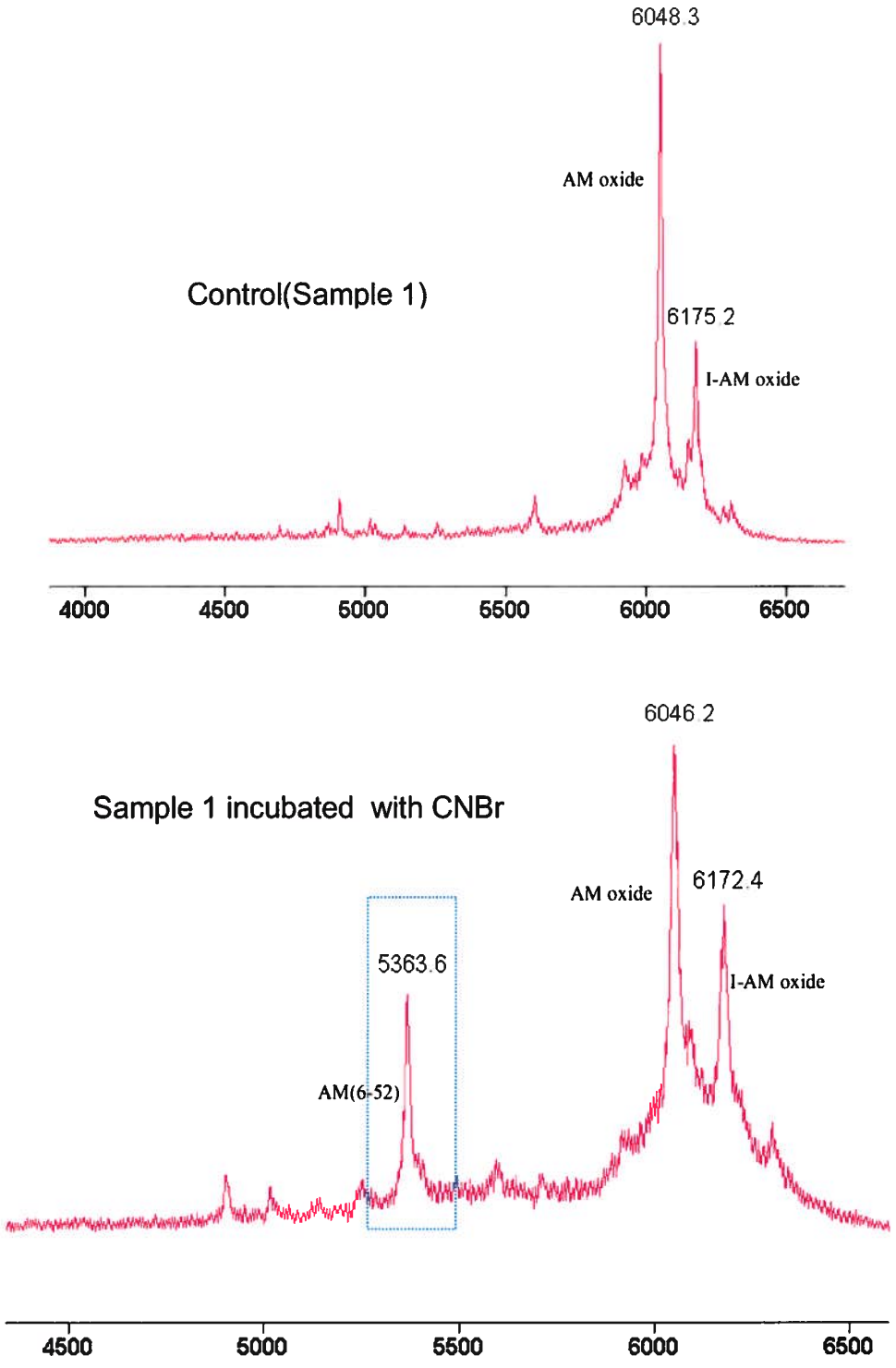

1YRQSMNNFQGLRSFGCRFGTCTVQKLAHQIYQFTDKDKDNVAPRSKISPQGY 52

↑→5361 Da

CNBr

Figure 54-1: MALDI-TOF mass analysis of iodinated AM after CNBr cleavage.

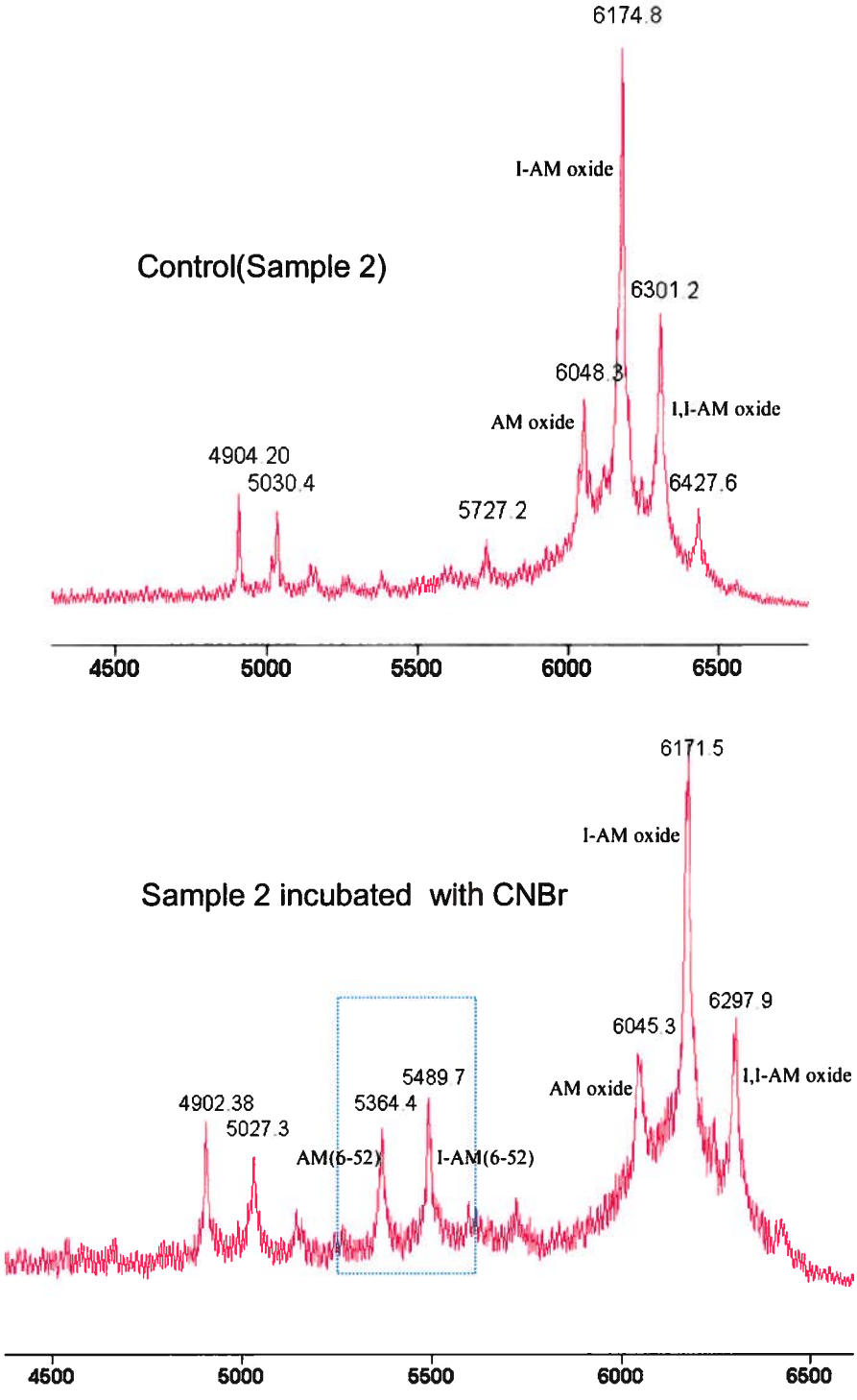

1YRQSMNNFQGLRSFGCRFGTCTVQKLAHQIYQFTDKDKDNVAPRSKISPQGY 52

↑→5361 Da or 5488 Da (+I)

CNBr

Figure 54-2: MALDI-TOF mass analysis of iodinated AM after CNBr cleavage.

AM was digested by CPY from C-terminal tail to give rise to two smaller fragments, AM(1-40) (MW = 4744 Da) and AM(1-41) (MW = 4844 Da). APM digested AM from N-terminus and yielded a smaller fragment, AM(6-52) (MW = 5361 Da). CNBr could selectively react with Met of the AM sequence and break the peptide chain from the C-terminus of Met to produce an AM fragment as same as APM, AM(6-52) (MW = 5361 Da). The measured MW of these AM fragments is shown in Figure 52.

12.6.2. The investigation on iodinated AM by exopeptidases

The crude mixture of AM and iodinated AM obtained with lactoperoxidase method was digested with CPY into the two smaller mono-oxide fragments (MW: 4763.55 Da and 4863.09 Da) and their monoiodinated analogs (MW: 4990.05 Da, Figure 53 and Table 20). The iodine atom still resided in the digested AM fragment. The result suggested that the iodination could not happen at the C-terminal tyrosine, and the presumed iodinated position might be N-terminal (1^{st}) or the internal (31^{st}) tyrosine. However, the digestion of the iodinated AM by using APM failed, and no new small fragments were found in mass analysis.

Table 20: Molecular weight of peptides after iodination step.

Peptide	MW (Da)	Measured MW (Da)
AM	6028	6028.50
AM oxide	6044	6047±2
AM(1-40)	4744	4745.43
AM(1-40) oxide	4760	4763.55
AM(1-41)	4844	4844.93
AM(1-41) oxide	4860	4863.09
AM(6-52)	5361	5363.4±1

Peptide	MW (Da)	Measured MW (Da)
I-AM	6155	-
I-AM oxide	6171	6173.9±2.4
I-AM(1-40)	4871	-
I-AM(1-40) oxide	4887	-
I-AM(1-41)	4971	-
I-AM(1-41) oxide	4887	4990.05
I-AM(6-52)	5488	5489.7

12.6.3. The investigation of iodinated AM after CNBr cleavage

Because there is only one methionine in the AM sequence and it is situated close to the N-terminal region, CNBr can be used to investigate the iodination at N-terminal tyrosine instead of APM. After reacting a mixture of AM and monoiodinated AM as Sample 1, one new smaller fragment was detected, MALDI-TOF mass analysis shows the MW5363.6 of AM(6-52) (Figure 54-1). In addition, there are no iodinated fragments with it. The data indicated that mono-iodination by lactoperoxidase method located at the N-terminal tyrosine of AM had occurred. To verify whether the second iodine was reacting with the same tyrosine or not, the Sample 2 with AM, I-AM and I,I-AM mixture was investigated by using CNBr reagent. Following the reaction, two new fragments were found in the mixture, the fragment AM(6-52) (MW5364.4 Da) and monoiodinated AM(6-52) (MW5364+I) (Figure 54-2). The result proved that the second iodine was not located in the N-terminal Tyr, and therefore the ^{125}I-labeled AM at the N-terminal tyrosine can be prepared by lactoperoxidase method and separated from iodinated mixture by HPLC.

12.7. Saturation binding experiments

It was interesting that ^{99m}Tc-linear-AM and ^{125}I-Tyr^{1}-AM displayed a stronger binding affinity or more binding sites in the dog lungs compared to that of ^{125}I-AM since the specific binding of these radioligands was inhibited by AM with higher IC_{50} values in their competitive binding assay. So far, the radiolabeled ^{125}I-AM in various publications was made by the chloramine-T, Iodo-beads and Iodo-gen method. The iodinated AM on the C-terminal and middle tyrosine was confirmed by exopeptidases (Lewis *et al.*, 1998). Our previous studies showed that the AM sequence required by the AM receptors found in the dog lungs is localized in the C-terminal tail. When AM lost C-terminal sequence 41-52, i.e. AM(1-40), no displacement happened in the competitive binding assay. Both the iodination of ^{125}I-Tyr^{1}-AM and the conjugation of ^{99m}Tc-linear-AM occurred in N-terminal region of AM. Did the modification at the C-terminal Tyr affect the peptide affinity and/or specificity in the dog lungs? To verify this hypothesis, saturation binding experiments by using ^{125}I-AM and ^{125}I-Tyr^{1}-AM were carried out to obtain to their K_D (ligand affinity) and B_{max} (the number of binding sites).

12.7.1. Saturation binding experiments with ^{125}I-AM

The results of saturation binding experiments using ^{125}I-AM (10 μCi; Phoenix Pharmaceuticals, Burlingame, CA) as the radioligand showed high specific and nearly saturable binding for ^{125}I-AM with K_D = 554 pM (95% confidence interval range 66 to 1042 pM) and B_{max} = 444 fmol/mg (95% confidence interval range 254 to 635 fmol/mg) protein on dog lung homogenates in the one site model (Figure 55). There was no significant difference (F value = 1.979 and P>0.05) between the one site binding and two site binding models by statistics (F-test) in the comparison of fits, and the preferred model is one site model.

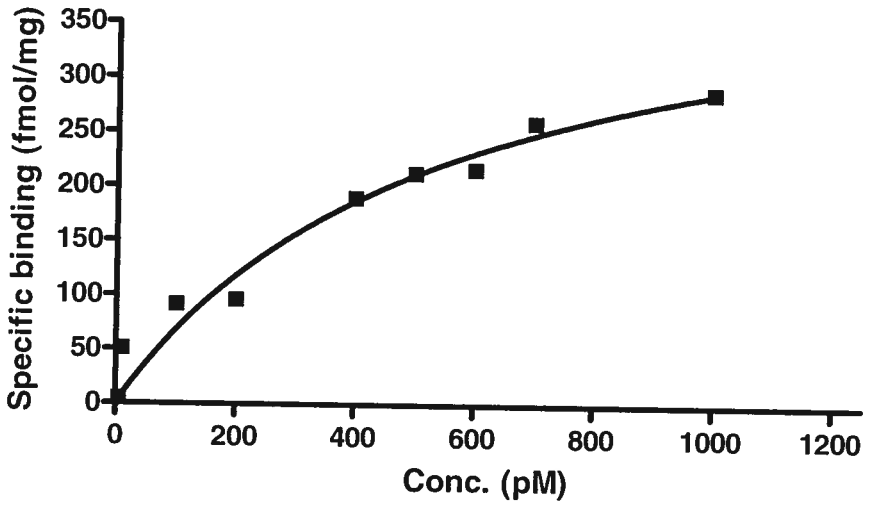

Figure 55: Saturation binding analysis of ^{125}I-AM in dog lung homogenates. Each data point represents the mean of three independent experiments in duplicate.

12.7.2. Saturation binding experiments with ^{125}I-Tyr^1-AM

The saturation binding experiments using ^{125}I-Tyr^1-AM as the radioligand also showed high specific and saturable binding with K_D = 171 pM (95% confidence interval range 20 to 322 pM) and a B_{max} = 1194 fmol/mg protein (95% confidence interval range 882 to 1507 fmol/mg) protein on dog lung homogenates (Figure 56). In the comparison of fits, there was no significant difference (F value = 1.6047×10^{-6}, P>0.05) between the one site

binding and two site binding model. The data suggested that the radioligand, ^{125}I-Tyr^{1}-AM, had more binding sites and higher binding affinity to the AM receptors in dog lung homogenates than that of ^{125}I-AM.

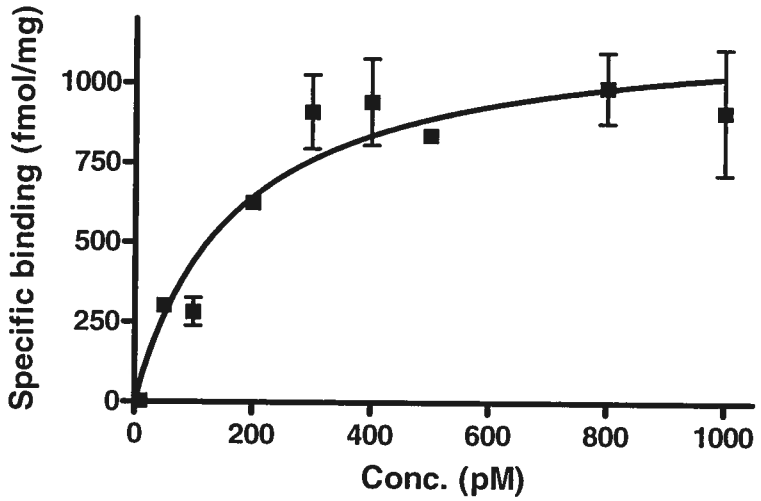

Figure 56: Saturation binding analysis of ^{125}I-Tyr^{1}-AM in dog lung homogenates. Each data point represents the mean of two independent experiments. The data of each experiment represents the mean of three independent experiments in duplicate. Vertical lines indicate S.E.M. (standard error of the mean) from two independent experiments.

12.8. Competitive binding experiment of ^{125}I-Tyr^{1}-AM in dog lung homogenates and CPAE membrane

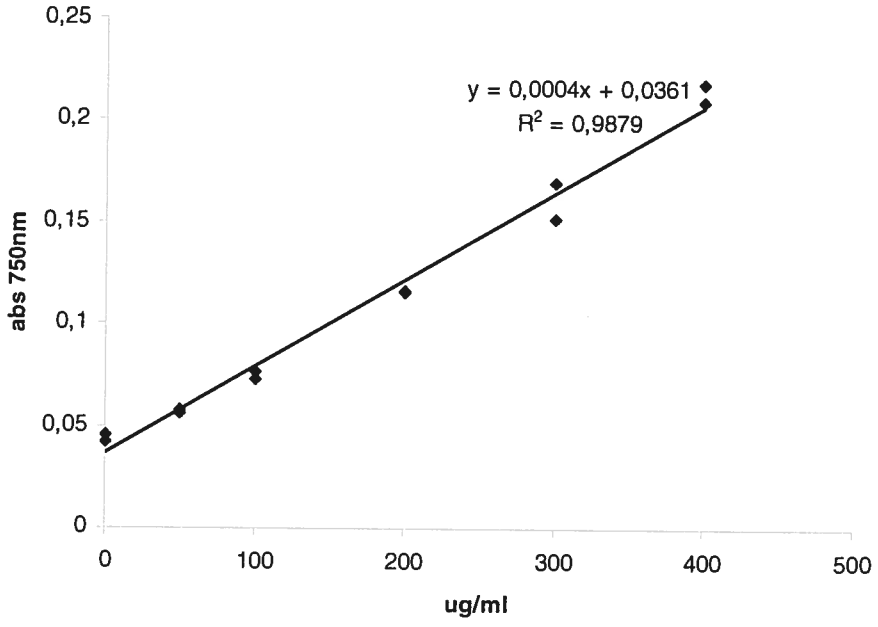

Figure 57: Protein measurement in CPAE membrane.

Additionally, competitive binding experiments were performed using ^{125}I-Tyr^{1}-AM as the radioligand and AM as the competitor on dog lung homogenates and the CPAE membrane. The protein concentration of CPAE membrane was 2.5 mg/mL, which was calculated according to the equation of standard curve (Figure 57). ^{125}I-Tyr^{1}-AM was displaced with the non selective agonist AM with an IC_{50} = 11 nM (95% confidence interval range 3 nM to 35 nM) on dog lung homogenates, the experimental data fit better to a one site binding model (Figure 58). No displacement was found when using CPAE membrane in the protocol. The data indicated that the radioligand, ^{125}I-Tyr^{1}-AM, could be used as a new radioactive marker in the pharmacological study. The biodistribution of AM receptors has evident differences between different species.

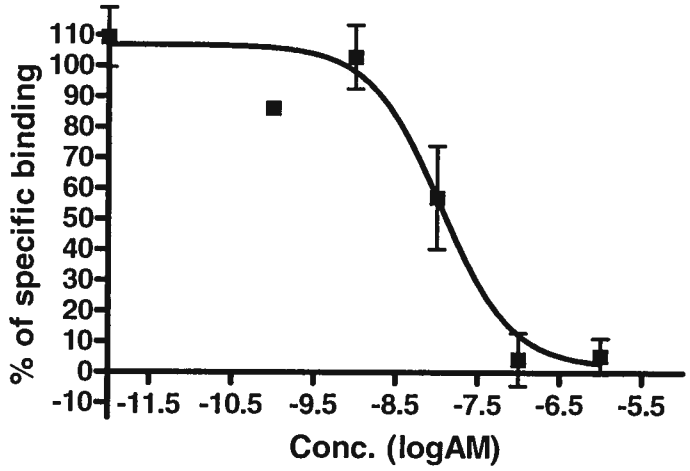

Figure 58: Competitive binding study of ^{125}I-Tyr^{1}-AM bound to dog lung homogenates. Data points are the mean ± S.E.M. (standard error of the mean) of four independent experiments performed in duplicate.

Chapter 5 : Discussion

13. Characterization of AM receptor in dog lungs by competitive binding assay

Specific AM binding sites have been demonstrated in rat tissue, endothelial cells, rat vascular smooth muscle cells (Coppock *et al.*, 1996), and cat pulmonary vascular bed (Nossaman *et al.*, 1995). In the present study, the dog lung specificity of AM was vividly verified for the first time by molecular imaging by using ^{99m}Tc-linear AM. The receptor responsible for the AM specific binding in the lungs then becomes the key to further study. Although at least two receptor subtypes of AM were confirmed, the functional importance of these receptor subtypes, especially in the cardiovascular biology, is unclear, and most relevant reports were concerned on molecular and cellular studies. The two receptor subtypes were first considered as pharmacologically indistinguishable because they were usually co-expressed in the same tissue (Kuwasako *et al.*, 2002). Later, their functional differences were confirmed by studies using dimers of CLR and RAMPs in cells (Hay *et al.*, 2003). So far, little is known of AM influence in vivo by using dog.

The distribution and function of AM receptor subtypes respectively are the concerned points in the AM study. According to previous reports, the high binding sites of AM are located in rat lung and heart. However, the radiotracer of AM in the present study displayed the specificity only in the lungs *in vivo*, and no specific retention found in heart. AM is a non-selective ligand, and sensitive to all AM receptors. In this case, the AM receptors in the heart might be different from the receptors in the lungs. Therefore, the extra AM in circulation went through the right atrium and ventricle, and then spread over dog lungs and not the heart by some unknown process. To determine whether specific AM receptor subtypes are present in dog lung, the binding of ^{125}I-AM was examined in dog lung homogenates.

To identify the AM receptor in dog lungs, the known pharmacological profiles for the AM receptor were referred at first. Since no selective agonists or antagonists specific to AM receptors or their subtypes exist today, the competitive binding assay is one useful method to investigate and analyze the specific binding sites found in the dog lungs. Thus,

to help the characterization of the binding sites in dog lungs, the members of the CT peptide family were used as agonists or antagonists in competition studies. These peptides have similar structures and share some bioactivities and receptor binding sites. As such, CGRP interacts with a similar receptor complex to that of AM and AMY also has lung binding sites that could be the same as AM. Furthermore, AM2 and PAMP are two peptides that belong to the AM family in accordance to their structure and origin, respectively. The binding sites was then identified as AM receptors with the agonist AM and AM(13-52), as well as the antagonist AM(22-52). AMY, $CGRP_{\alpha}$ and AM2, as well as their antagonists were poor inhibitors with low binding-affinity, which suggested that the binding sites were specific AM receptors.

Subtypes of receptors can be distinguished pharmacologically by their rank of affinity for a series of ligands. Although two AM receptor subtypes have been defined in molecular terms, the AM_1 and AM_2 have never been thoroughly characterized. One of the reasons is the lack of selective agonists or antagonists for these subtypes as research tools. Another is the interspecies differences between receptor and ligand used in designed experiments. In the present study, the human AM(22-52) and $CGRP_{\alpha}$(8-37) were both poor inhibitors in dog lung homogenates. However, by the difference selectivity of AM(22-52) (more selective to AM_1) and CGRP(8-37) (more selective to CGRP receptor and AM_2) to the AM receptor found in dog lungs, the binding site with high binding-affinity was characterized as AM_1. Although there is still no precise report involving the AM study in the dog, the AM_1 found in the lungs is also supported by other reports. It is known that antagonist AM(22-52) has a high selectivity to AM_1 over the AM_2 compared to antagonist $CGRP_{\alpha}$(8-37) in AM_1 receptor cell line (Wunder *et al.*, 2008), human, porcine, bovine CLR complexes with RAMPs (Aiyar N, 2001; 2002). The same results from a combination of rat or human CLR, RAMP2 or RAMP3 also supports the pharmacological difference of the two antagonists to AM receptor subtypes (Hay, *et al.*, 2003). The study of molecular biology on the amino acid sequence structure of RAMPs elucidated that RAMP1 and RAMP3 had similar peptide sequences, and compose of CGRP receptor and AM_2 with CLR/RAMP1/3 complexes (Weinman *et al.*, 2006). However, the peptide sequence of RAMP2 is different, and displays in AM_1 with CLR/RAMP2 complex but

not $CGRP_1$ and AM_2. The selective difference of AM(22-52) and CGRP(8-37) to AM receptor subtypes might be based on the different sequences among RAMPs.

The competitive binding results by ^{125}I-AM and AM fit better to a two-site binding model in the present study. The two site binding usually occurs in a competitive binding experiment when using an agonist as competitor (unlabeled ligand, e.g. AM; Motulsky, 1995-2001). The two sites could represent the high and low affinity states of one receptor (e.g. AM_1), or two different subtypes of one receptor (e.g. AM_1 and AM_2), or more than one receptor displaying different affinities (e.g. AM_1 and $CGRP_1$). Otherwise, the binding site with low affinity was not characterized because there is no selective antagonist available to separate the receptor subtype in the present study. Although some peptides do not bind to specific AM binding sites with equipotent displacement of AM, the peptides from the CT family are helpful for the characterization of AM receptor. Along with the characterization of the receptor, the present study evaluated the possibility of the members of this peptide family as potential candidates for lung imaging. To confirm the AM_1 in dog lungs, Western Blot by using human CLR and RAMP2 antibody (Santa Cruz Biotechnology Inc., Santa Cruz, CA) was performed. Considering species difference between dog receptor and human antibodies, a human breast adenocarcinoma cell line (MCF-7) was evaluated as a control. These cells express approximately 50,000 AM receptors per cell (Miller, *et al.*, 1996). Unfortunately, the CLR and RAMP2 in human cell membrane were probed by using human antibodies, but not detected in the dog lung homogenates.

The high AM_1 was found not only in the present study, but also in other species or their cells. The higher mRNA expression of RAMP2 in the rat lung was also reported by comparing the RAMP1/3 expression (Nagae *et al.*, 2000). Administration of AM can increase the vascular relaxation in transgenic mice overexpressing RAMP2 in smooth muscle through AM_1 comparing with wild type mice (Tam, *et al.*, 2006). In immortalized human microvascular endothelial cells, backwards AM elicited upregulation of both CLR and RAMP2, while one of RAMP3 did not show significant change with the same treatment (Schwarz, *et al.*, 2006). In human, AM receptor was first determined in situ

hybridization in normal and malignant lungs (Martínez, *et al.*, 1997). The distribution of human CLR was studied by using tissue microarray technology, and the receptor was widely expressed in normal human tissues, including lung and kidney (Nikitenko, *et al.*, 2006). So far, the expression of AM_1 subtype in human lungs remains to be determined. For CT peptide family, most of studies on receptor sensitization or desensitization focused on the CGRP receptor. Recently, the ligand-induce internalization (in 5-15 min) of AM receptors were observed by exposing the receptors to 10 nM to 1 μM AM in endothelial cells. The desensitization (loss of the ability to induce Akt phosphorylation) of AM receptors was examined by using AM (100 nM) within 15 min (Nikitenko, *et al.*, 2006). Thus, the dose of linear AM in ^{99m}Tc-linear AM used in the study is low and appears to be safe for repeated administrations of the tracer in clinical applications because the maximum amounts of the ligand are 2.89 nmol each injection in circulation system.

14. Characterization of AM receptor in dog lungs responsible for AM clearance

The pulmonary clearance of AM has been reported in various research studies, which is reviewed in Section 2.9.2.1. However, the visible AM clearance from blood to kidney was demonstrated for the first time *in vivo* by using ^{99m}Tc-linear AM in the present study. To verify the radiotracer clearance pathway, the plasma kinetic and biodistribution of the tracer were also monitored when ^{99m}Tc-linear AM was administrated i.v. in dog. The lung imaging molecules then trace vividly the transport of administrated ^{99m}Tc-linear AM by i.v. and simplify the study of the tracer excretion by kidneys and the liver. Study on the plasma kinetics of the radiotracer displayed a rapid elimination and clearance in circulation. However, its biodistribution demonstrated the retention of tracers was more than 1 h in the lungs. Comparing to the rapid elimination of radioactivity in plasma, the long retention in the lungs indicates that AM as a targeting molecule may involve in trapping ^{99m}Tc in the receptor binding.

In present study, the receptor found in dog lungs was characterized as AM_1 by competitive binding assay. The data corresponds very well to the study on the fast recycling pathway of AM_1, i.e. AM_1 bound with AM could internalize within the cell, and then the released AM was degraded by intracellular peptidase (Bomberger *et al.*, 2005). While AM_2 internalization was inhibited by PDZ domain residing in the RAMP3 C-terminal region but not in RAMP1/2. So, AM_2 cannot help AM in pulmonary circulation to clear (Weinman *et al.*, 2006). In this case, the characterization of ^{99m}Tc-linear AM clearance from blood to kidney then acts as the confirmation that AM_1 is the receptor responsible for the administrated AM pulmonary clearance from blood to kidney. The present study will be a major finding for the further characterization of physiological and pathological states, and the development of more accurate and simple lung imaging molecules. Nevertheless, the species difference also exists in the clearance pathway of the radiolabeled peptide. The biodistribution data in rat demonstrates that ^{99m}Tc-linear AM is mainly excreted via the kidneys with moderate uptake by the hepatobilary system. While, in dog a lower retention of the tracer was present in the liver, the tracer undergoes a single-pass pulmonary extraction. Thus, the species difference in the clearance pathway of AM necessitates a study in humans.

15. The search for peptides as substitutes for AM

There are some problems inherent to the synthesis and applications of this type of imaging agent. It was reported that the concentration of AM in circulation was generally too low (<10 pM) to play a key role in the regulation of blood pressure. However, administration of AM (5.2 nmol/kg in conscious, 12 nmol/kg in anesthetized mice) i.v. can cause vasodilation *in vivo* (Tam, *et al.*, 2006). In the present study, the dose of linear AM in administration was 2.89 nmol for 20–30 kg dog. Although the dose of linear AM is too low to cause vasodilation activity in the lung imaging, the amounts of ^{99m}Tc-linear AM in the administration was less than 16 pmol. Thus, there is still the need to obtain a highly specific preparation, which allows administration of low doses of peptide and thus, minimize the biological effects. To overcome this problem, a high level of isotope incorporation must be obtained. Also, separation of the radiolabeled peptide from its

unlabeled counterpart must be performed, in such a way that not much agonist or antagonist is needed to obtain an imaging useful for clinical diagnoses. To attain these objectives, it is necessary to design optimized chelating conditions to ultimately achieve the development of a lung imaging kit. Finally, a long peptide chain, such as AM, represents a tremendous synthesis challenge as well as a large investment in time and amino acid derivatives. The development of smaller peptide compounds, much easier to synthesize and less prone to side-reactions during the harsh chemical conditions encountered during the synthesis or the radiolabeling steps, would be a great improvement. Moreover, small peptides are usually low immunogenic, and can have rapid blood clearance. All those factors make small peptides excellent candidates for the development of target-specific radiopharmaceuticals. However, the agonistic or antagonistic properties of peptides, as well as the introduction of a chelating compound into the chain, are possible source of drawbacks when using labeled peptides as imaging drugs. Therefore, it is crucial to design new tools in accordance to SAR studies performed on well characterized peptide receptor preparations.

The assay on cell lines could be used for a drug selective bioassay because of its low cost and high quality. However, untransfected natural cell lines often have low or undetectable levels of target gene expression make it difficult to identify suitable immortalized cells that can provide the necessary signal for a high-quality assay. In this case, high expression cells through transfection of target cDNA into cell lines are becoming increasingly useful for drug screening. Nevertheless, transfected cell lines may not provide meaningful pharmacological data, as the target protein may not be expressed to physiologically relevant levels, forms and locations, causing misleading pharmacological behaviour due to overexpression. In the present study, the dog lung tissue was used in the screening of promising candidates.

Competitive binding assays can compare the affinity of different peptides for a common binding site. In fact, it is a simple and exact method to evaluate peptide analogs as new targeting molecules and various BCAs as targeting chelators, respectively. The experiment is used to validate an assay; investigate the interaction of low affinity drugs

with receptors; determine receptor number and affinity by using the same compound as the labeled and unlabeled ligand; and determine whether a peptide binds to the receptor. It allows the screening of thousands of fragments or derivatives to find new peptides that bind to the receptor. This can be faster and easier than any other screening methods. In the course of this project, competitive binding assays were performed against [^{125}I]-AM. The results from the binding experiments with peptide fragments could be used to facilitate the design of the best imaging agent.

15.1. The investigation of peptides in CT and AM family

CGRPα and AM2 two peptides with less amino acids than AM are peptides from the CT/AM family. The action of CGRPα and AM2 was reported to be through the activation of the receptor complexes of CLR/RAMPs. According to publications (van Rossum *et al.*, 1997; Brain and Grant, 2004), the distribution of CGRPα binding sites spreads widely in various organs and tissues, while AM2 has binding properties similar to CGRPα and AM. The competitive binding experiments in the present study showed that CGRPα, AM2 and AM2(16-47) (AM2 antagonist) could inhibit the AM specific binding with really higher values of IC_{50} (lower affinity). Among these, the specificity of CGRPα and AM2 in dog lungs was clearly lower than AM, linear AM and AM(13-52), but lightly higher than AM(22-52), AM antagonist. Although CGRPα(8-37) showed no displacement in dog lung, AM2(16-47) displayed a similar binding property to AM(22-52) in the competitive binding assay. As a result, *in vivo* lung imaging with CGRPα/β, AM2 and AM2(16-47) will be considered in the experiment follow-up. PAMP has similarities to AM on their biological origin and activities. However, it does not act on the same receptor complex. PAMP could not inhibit AM specific binding in dog lung homogenates in the study. Thus, the small peptide with 20-amino acid cannot be a potential substitute of AM.

15.2. The investigation of AM fragments with less amino acids in the sequence

In this peptide family, AM is the longest ones (52-amino acid). Generally, a peptide with less than 15 residues can be easily synthesized in terms of time, yield and purity. When the length of a peptide increases, the purity of the crude product will decrease and result in a lower yield. Once the biologically interesting sequences in a native peptide are known, smaller peptides can be designed. However, it is not that easy to determine the amino acids that are essential or non-essential residues. Generally, changes of relative unimportant residues are the key for the design of smaller peptide substitutes design.

In the present study, all C-terminal truncated fragments lost receptor-binding activity in dog lung homogenates. AM segments truncated at the N-terminal region, i.e. AM(13-52), AM(22-52) and AM(26-52), showed lower receptor-binding activity than AM, whereas the C-terminal fragment AM(40-52) as competitors had no displacement. With the exception of linear AM, AM(13-52) and AM(22-52), no other AM segments showed significant receptor-binding activity in dog lung homogenates. It is corroborated with other data obtained with shorter AM peptides in AM_1 receptor cell line (Wunder *et al.*, 2008). So far, most studies in rat and cat reported that AM(13-52) have very low (almost equal) differences on the cAMP responses and receptor binding affinity studies from AM. In this present study, ^{99m}Tc-labeling reaction with linear AM(13-52) gave rise to a radiolabeling yield of 50%, while the radiolabeling yields of other smaller fragments, i.e. AM(16-52), AM(17-52), AM(18-52), AM(19-52), AM(20-52) and AM(21-52), were under 30%. Thus, linear AM(13-52), a partial agonist of AM, can be a substitute of linear AM directly. Among other smaller AM segments, AM(22-52) might be a potential candidate when conjugated with an appropriate BCA. It was reported when establishing the binding characteristics of AM with the membranes of porcine tissues that human AM(22-52) had less potency than AM in the lung, whereas, in spleen, atrium, renal cortex and renal medulla hAM (22-52) showed distinct low potency compared with AM (Dang K, *et al.*, 1999). Thus, hAM (22-52) could be a candidate with certain specificity in the lung while exhibiting a low imaging in the kidney. Meanwhile, the lung specificity of AM(22-52) conjugate has to be investigated in following studies.

Collectively, the whole molecule of AM might be required by the binding sites found in the dog lungs. Is it possible to select a potential substitute with high affinity similar to AM itself from AM sequence? Follow-up competition binding experiments using human cell lines (MCF-7, the data excluded in the thesis) showed that there were no significant difference between AM and linear AM by statistic analysis. The receptor was verified by Western blot and recognized by CLR and RAMP2 antibody. Considering the differences of AM and its receptor between species, it may be possible to find smaller peptide substitutes with high specificity in the human lungs.

15.3. The investigation of bioactivity

Using AM knockout mice (Shindo *et al.*, 2001) and AM transgenics (Shimosawa *et al.*, 2002) AM has been shown to be important in vascular relexation and protection in cardiovascular damage. According to the structure-activity relationship (in Section 2.10) and receptor-binding activity studies of AM in the present study, the disulfide bridge of AM is crucial to receptor-binding activity and cAMP responses. The modification of Cys^{16} and/or Cys^{21} could be the best solution to reach the goal that a target molecule retains sufficient receptor-binding activity in functions loss, such as cAMP responses.

Although ^{99m}Tc-linear AM did not show any interference in blood pressure and heart rate (monitored continuously over 4 h) at the doses used in the present study, its bioactivities may appear when increasing the dose. So far, it has been confirmed that the increase dose of linear AM (>2-fold administration dose of linear AM) reduced the blood pressure in rats (data from the research group in Montreal Heart Institute and excluded in the thesis). Thus, do we need to design a new lung targeting peptide in the experiments follow-up?

In fact, in the present study, the two Cys in AM are crucial for the ^{99m}Tc labeling. ^{99m}Tc-linear AM is the modification of AM around the N-terminal region and disulfide bridge formation. Even if the linear AM retains sufficient receptor-binding activity and cAMP responses, one cannot simply extend the same properties onto ^{99m}Tc-linear AM. The safety of the tracer has to be determined by the conjugation of technetium and linear

peptide but not the peptide itself. ^{99m}Tc-linear AM has shown sufficient receptor-binding activity in dog lungs *in vivo* and *in vitro* in the present study, whereas its structure-activity relationship will be explored in following studies.

Further works are also pursued using AM fragments for the development of new imaging probes. The challenge is to identify the minimal peptide sequence of AM that retains high affinity for the receptors in the lungs, while being adequate for ^{99m}Tc-labeling. So far, we focus now on a new set of analogs using AM(13-52) as a template. The main advantage coming from the use of this fragment is that the sulhydryl functions, allowing a direct chelation with ^{99m}Tc, are present in the peptide compound. This strategy avoids the derivatization of the material with chelating moieties.

16. Characterization of the receptor-binding activities relationship in dog lungs

Although AM2 and CGRPα could bind to the receptor with higher values of IC_{50}, the receptor shows strong specificity to AM and its analogs, which exhibits an AM receptor property. The present study demonstrated for the first time the receptor-binding activities of human AM in dog lungs by using a variety of synthetic CT family peptides and AM analogs. The receptor binding activity was stronger with AM, linear AM, and the agonist AM(13-52), whereas, the binding affinity of the peptide-receptor interaction was significantly reduced by using the antagonist AM(22-52) and some peptides of the CT family, including, CGRPα, AM2 and its antagonist. No displacement was found by using antagonist CGRPα(8-37) or AMY or PAMP as a competitor. The range of displacement for the AM receptors in dog lungs are AM>linearAM>AM(13-52)>AM(22-52)>AM2≈CGRPα>AM2(16-47)>CGRPα(8-37), AMY, PAMP.

To investigate the proposed smaller peptide substitutes derived from AM in dog lungs, competitive binding assays were also performed by using AM segments designed according to previous reports of bioactivities and structures. In the present study, all N-terminal fragments AM(1-25), AM(1-31), and AM(1-40) had no displacement in

receptor-binding assay. It suggested that N-terminal residues were not essential for the interaction with the receptor found in the dog lungs. In contrast, some C-terminal fragments AM(13-52), AM(16-52), AM(17-52), AM(18-52), AM(19-52), AM(20-52), AM(21-52), AM(22-52) and AM(26-52) were capable of receptor binding with reduced affinity. It suggested that the essential peptide segment for receptor binding was located in the C-terminal tail.

However, it should be noted that the shorter C-terminal fragments AM(31-52), AM(40-52) resulted in the functional loss of receptor binding activity. Collectively, the present study suggests that the binding affinity depends mostly on the C-terminal tail, and to a lower extent on the N-terminal loop, the disulfide bridge formation, and the α-helix secondary structures of AM. Nevertheless, it suggests that they were required to obtain a higher specificity by the binding sites found in the dog lungs. Hence, the competitive data indicated for the fist time that the whole molecule of human AM might be needed for the binding sites in the dog lungs.

17. Strategy and results of human AM iodination

Radioligands are useful tools in biological study and drug screening. So far, there are 4 methods that have been used in the iodination of AM or its fragments, the Bolton and Hunter method (Bhogal, Smith, and Bloom, 1992), the iodo-beads and iodogen method (Chakravarty *et al.*, 2000), the lactoperoxidase method (Eguchi *et al.*, 1994) and the chloramine-T method (Lewis *et al.*, 1998). All these methods were usually used in the iodination of peptides. Among of them, the Bolton and Hunter method is used to iodinate the peptides lacking the tyrosine or histidine residues in their sequence. The chloramine-T method is not new but effective in the iodination of AM. However, the iodo-beads and iodogen iodination reagents are more convenient, gentle and effective method for iodinating soluble and membrane bound proteins, and become the most common reagent available, i.e. ^{125}I-labeled AM at C-terminal region, in commercial products. The lactoperoxidase method appears to be good at selective mono-iodination on the peptides that have more than one tyrosine residues, like AM (with 3 tyrosines). In fact, the iodo-

beads and iodogen iodination reagents undergoes the same chemical reaction mechanism with chloramine-T since the reagents are made by anchoring chloramine-T molecules.

Because the radiolabeled ^{125}I-AM in various publications (Zimmermann *et al*, 1996; Lewis *et al.*, 1998; Coppock *et al*, 1999; Chakravarty *et al.*, 2000) was made by the chloramine-T and Iodo-beads and Iodo-gen methods, in order to compare experiments, both chloramine-T and lactoperoxidase methods were performed in the present study. It was reported that the iodination products with chloramine-T contained a monoiodotyrosine at the C-terminus and at least another labeled tyrosine (Lewis *et al.*, 1998). The N-terminal tyrosine of the iodination products was not iodinated by analysis of carboxypeptidase-digested iodination products. In the present study, data indicated that a lower labeled yield and more side-products by chloramine-T method than with the lactoperoxidase method. So far, there are no publications about the investigation of AM iodination with the lactoperoxidase method.

17.1. The investigation of iodinated AM structures

By competitive binding assay, without its disulfide bridge, linear AM exhibited a low affinity to AM receptor in dog lungs. However, the high specificity of ^{99m}Tc-linear AM in dog lungs was verified *in vivo*. According to SAR studies in Section 2.10.2., the disulfide bridge is important to stabilize α-helix conformation, and α-helix of AM is crucial to AM receptor binding. Our proposed structure of ^{99m}Tc-linear AM suggests that its labeled segments include Cys^{16}-Cys^{21} and N-terminal region of AM. In the case, after linear AM was labeled by technetium, the α-helix conformation required by AM receptor could be restored. However, the value of IC_{50} by using ^{99m}Tc-linear AM as radioligand is much higher than that obtained when using ^{125}I-AM (about 20 pM) in competitive binding experiments. So far, the amounts of cold linear AM in the tracer were unclear, however, the specific dog lungs imaging was obtained by using less than 16 pmol (calculated by the amounts of $Na^{99m}TcO_4$ and labeling yield in reaction) of ^{99m}Tc-linear AM within the interaction of cold linear AM. Analysis on our results of ^{99m}Tc-linear AM and relative publication of ^{125}I-AM (Lewis *et al.*, 1998), showed that of the labeled peptide segments

or positions of the two AM radioligands are different. The proposed structure of ^{99m}Tc-linear AM suggests that its labeled segments are around the N-terminal region of AM where are far from the binding site required by AM receptor in dog lungs. However, the labeled peptide segments of ^{125}I-AM reside in the C-terminal Tyr^{52} and/or the mid-segment Tyr^{31}. According to the studies of AM SARs, the iodinated Tyr of ^{125}I-AM are located at the C-terminal region that is involved in the receptor binding of AM. By the structural analysis of the two kind of labeled AM, it indicates that the labeling position of radionuclide might involve in the receptor-binding properties of AM.

The review of reports on receptor-ligand binding assay shows that ^{125}I-AM was used as the radioligand in most studies. In fact, most of these reports and commercial products did not investigate the position of iodination. Interestingly, in the present study, a high value of IC_{50} also appeared in the competitive binding experiment using a radioligand that was prepared with lactoperoxidase method in the present study. Therefore, the investigation of the iodinated AM by using peptidase and CNBr was performed. Using exopeptidases and CNBr, the present study investigated for the first time the iodinated AM prepared by the lactoperoxidase method. The results revealed a selective iodination at the N-terminal Tyr (Tyr^1) of AM. Thus, although ^{99m}Tc-linear AM with a short $t_{1/2}$ is not suitable for the study on the binding properties of labeled AM to receptors, the ^{125}I-Tyr^1-AM made by lactoperoxidase method could be a tool for bringing to light the differences of IC_{50} by using different AM radioligands modified in the positions of distinct peptide segments or residues.

17.2. Saturation binding experiments by using ^{125}I-AM and ^{125}I-Tyr^1-AM

The study on human AM receptor-binding activity and cAMP response in rat vascular smooth muscle cells (Coppock *et al.*, 1996) demonstrated that the C-terminal amidated residue was more important than the Tyr^{52} residue itself. Although AM(1-51)-NH_2 displayed a lower potency than AM, the response of AM(1-52)-OH was reduced significantly compared to AM(1-51)-NH_2. In this case, the iodination of Tyr^{52} should not

influence in rat vascular smooth muscle cells the AM receptor-binding activity if the C-terminal residue retains amidation. However, in the present study, ^{125}I-AM and ^{125}I-Tyr^{1}-AM displayed different receptor-binding affinities in dog lung homogenates. Thus, comparison of the receptor-binding activity of different radioligands is essential to verify the role of Tyr^{52} in receptor-binding affinity in dog lungs.

Saturation binding experiments can measure specific radioligand binding at equilibrium at various concentrations. The measurement is used to determine the receptor number and its affinity. The data measured on the same receptor by using different radioligands can then be analyzed as the properties of radioligand on receptor-binding activity. In the experiment, K_d is the dissociation constant, the lower K_d indicates the higher receptor binding affinity of radioligand. B_{max} is the maximal receptor binding sites of radioligand, the higher B_{max} indicates larger amounts of receptors in tissues or cells. As a result, the approximately 3-fold difference between the K_d of two radioligands, and almost paralleled difference of their B_{max} suggested that the difference of receptor-binding affinity might exist between two iodinated AM, i.e. ^{125}I-AM (K_d=554 pM; B_{max}=444 fmol/mg) and ^{125}I-Tyr^{1}-AM (K_d=171 pM; B_{max}=1194 fmol/mg), in dog lungs. Thus, the increased value of IC_{50} with ^{125}I-Tyr^{1}-AM is due to their higher receptor-binding affinity and more binding sites in dog lungs.

17.3. Competition binding experiments by using ^{125}I-AM and ^{125}I-Tyr^{1}-AM

A radioligand is a radioactive labeled compound that can associate with a receptor, transporter, enzyme, or any protein of interest. Measuring the rate and extent of binding provides information on the number of binding sites, and their affinity and accessibility for various drugs. Radioligand binding experiments are easy to perform, and provide useful data in many fields. Competitive binding assays measure the binding of a single concentration of labeled ligand in the presence of various concentrations of unlabeled ligand. One of the most common applications of receptor-ligand competition studies is to identify the pharmacological receptor of native peptide in a particular tissue or cells. So

far, according to publications (Juaneda *et al*, 2003; Owji *et al*, 1995; Owji *et al*, 1996), the AM receptor-binding activity has been done well for the rat. In the present study, by using labeled ligands, e.g. ^{125}I-AM and ^{125}I-Tyr^{1}-AM, the competitive binding experiments were performed in the lungs of rat and dog, as well as CAPE cells. The pharmacological receptor of AM was confirmed in the rat and dog lungs by competitive binding experiments, no specific receptor binding was found in the CAPE cells in the present study.

18. Lung imaging *in vivo*

The availability of high-quality and high-throughput bioassays is playing a key role in the current drug discovery because it could guide researchers in promising compound selection and the following evolution of these leads into clinical application by assignment of the pharmacological parameters. One of the most important factors for an ideal drug discovery bioassay is a high signal-to-noise ratios and indistinguishable activity from those performed in fresh human tissue. However, for the purpose of development a new medicine, an economic, safe technique that is amenable to high-throughput screening is of equal importance in an ideal bioassay.

18.1. Lung imaging in rat and dog

The rat could be a useful species for the development of imaging methods because of its size and low cost. Indeed, the distribution of an imaging agent can be monitored easily in the whole body using standard imaging equipments. Unfortunately, the rat was not found to be a suitable testing model for lung imaging because the lung uptake of human AM was proportionality lower in rats. Additionally, a rat liver is larger than other organs, such as lungs, heart, and is partly covered by the lungs in the anterior view. Consequently, the lung anatomical resolution was reduced by overlapping liver activity. Conversely, the liver activity contaminated lung imaging in the posterior view. Meanwhile, imaging by means of ^{99m}Tc labeled AM was carried out in the lungs of the dog in a similar way to rat imaging experiments because of the similar size of dog lungs to a human. Thus, more

accurate imaging results and lung structural information can be obtained with the dog since the final goal of the potential lung imaging agent study is for diagnosis and treatment of human diseases. Despite these limitations to the use of rats as a lung imaging model, it does not represent an obstacle for the study of plasma kinetics and biodistribution of potential radiotracers. The reduced lung uptake of AM derivatives in rats suggests the importance of interspecies differences in AM binding to its specific receptors.

18.2. Species differences between rat and dog *in vivo* study

Study *in vivo* showed ^{99m}Tc-linear AM had some differences in biodistribution and plasma kinetics between rat and dog. The radiotracer exhibited the highest biodistribution in kidneys after 30 min, and the specificity was high in rat liver and less in lungs, and displayed a two-compartment model in plasma kinetics. Whereas, the highest biodistribution of the tracer underwent only in the lungs of dog with very few tracer in liver, and demonstrated a high specificity and selectivity in dog lungs with a single-compartment model on plasma kinetics, i.e. lung clearance pathway. The observed difference in lung retention between rats and dogs must be attributed to inter-species difference of adrenomedullin. In fact, AM here is the linear form of the human peptide that has 52 amino acids. The rat AM has 2 deletions and 4 substitutions (50 amino acids), and the dog AM has 52 amino acids with 2 substitutions. This data therefore suggests interspecies difference in AM specificity and clearance. Since dog AM is more closely related to human AM, it represents a more suitable model for plasma kinetics, biodistribution and dosimetry analysis. Thus, for the purpose of the clinical application of the potential radiotracer, these *in vivo* studies in the rat were then completed in a species closer to that of human i.e. dogs. Finally, tests will be performed in human to verify the usefulness of the most promising ^{99m}Tc-labeled peptide analogs. Those studies will be carried out at the Montreal Heart Institute.

18.3. Comparison of MAA and ^{99m}Tc-linear AM in pulmonary imaging

Generally, the capability of a new compound as a radiopharmaceutical depends on its diagnostic potential in clinical applications. Thus, the application of MAA and potential application of ^{99m}Tc-linear AM were outlined in Table 21. It suggested that ^{99m}Tc-linear AM can reduce the potential risk of infection, increase the selectivity of organs and tissues, and enlarge the range of diagnosis. Therefore, ^{99m}Tc-linear AM, a potential new lung imaging agent designed by using AM as target molecule, has sufficient merits in its chemical, physical and immunological properties compared to MAA.

Table 21: Diagnostic application of MAA and ^{99m}Tc-linear AM.

Applications	MAA	^{99m}Tc-linear AM
Diagnosis of anatomical perfusion defects (e.g. pulmonary embolus)	Yes	Yes
Potential for diagnosis of functional defects (molecular imaging)	No	Yes
Blocks >300,000 small arteries per exam	Yes	No
Binds to specific receptors without perturbation of lung flow	No	Yes
Potential infectious risk (derived from human blood product)	Yes	No

19. Strategy and results of radiolabeling with 99m-Tc

Target-specific radiopharmaceuticals are of particular interest in the development of new imaging and treatment strategies. The ligand molecule serves as the vehicle that carries the radionuclide to the receptor sites at the target tissues. The location of a receptor determines the radiopharmaceutical design. If the receptors are intracellular, the radiolabeled receptor ligand has to cross the cell membrane to reach the receptor site. In this case, the receptor ligand is usually small and shows little tolerance for chemical modifications. However, if the receptor is extracellular, the radiolabeled receptor ligand will not have to cross the cell membrane to interact with the receptor and in this situation, there is usually a higher degree of tolerance toward chemical modifications (Hom and Katzenellenbogen, 1997). For the CT peptide family, the receptors are extracellular and consequently, a molecule such as AM could be chosen and chemically designed to avoid

or minimize the interference in the secondary structure of peptide, and the affinity of binding to the receptors according to the requirements of an imaging ligand.

19.1. The choice of radionuclide

The radionuclide is the radiation source. The choice of the radionuclide depends largely on the physical and nuclear properties, i.e. half-life and γ-energy, availability, and cost. More than 80% of all radiopharmaceuticals used in nuclear medicine are ^{99m}Tc-labeled compounds. Its 6 h half-life is long enough to allow the radiochemist to carry out the radiopharmaceutical synthesis and the nuclear medicine practitioner to collect useful images. At the same time, it is short enough to permit the administration of millicurie amounts of radioactivity without giving a significant radiation dose to the patient. The monochromatic 140 keV photons are readily collimated to give images of superior spatial resolution. Furthermore, ^{99m}Tc is available from commercial ^{99}Mo-^{99m}Tc generators at low cost (Hom and Katzenellenbogen, 1997).

19.2. The choice of a BCA

Between the targeting molecule and the radionuclide is the BCA, which traps metal ion through strong coordinate bonds. An ideal BCA covalently attached to the targeting molecule either directly or through a linker is able to form a stable metal ion complex in high yield, at a very low concentration of the BCA-peptide conjugate. The selection of a BCA is largely determined by the nature and oxidation state of the metallic radionuclide. For technetium, the binding unit must selectively stabilize an intermediate of a lower oxidation state so that the ^{99m}Tc complex is not subjected to redox reactions. Thus, the BCA has to form a ^{99m}Tc complex that shows thermodynamic stability and kinetic inertness, with respect to dissociation rate. Also, the conjugation group needs to be easily attached to the peptide, such as a carboxyl group. Finally, a chiral centre must be avoided in a radionuclide chelate. For instance, if a technetium complex contains two or more chiral centres, diastereomers are formed and they might require to be separated with appropriate HPLC methods, before being used.

The coordination chemistry of metallic radionuclide will also determine the geometry of the metal chelator and influence the solution stability of the radiopharmaceuticals. The use of metallic radionuclides offers many opportunities for designing new radiopharmaceuticals by modifying the coordination environment around the metal with a variety of chelators. The BCAs usually used in ^{99m}Tc- labeling peptides are shown in Figure 59 (Lever *et al.*, 1994; del Rosario *et al.*, 1994; Edwards *et al.*, 1997). According to chemical structure, a BCA can be divided into three parts: a binding unit, a conjugation group, and a spacer (if necessary). Metallic radionuclides have their own coordination chemistries and require BCAs with different donor atoms and ligand frameworks. Although DTPA was not been successfully used to radiolabel AM, the other BCAs that were not tested in the present study might be useful in the following studies, especially for smaller fragments without Cys in their sequences.

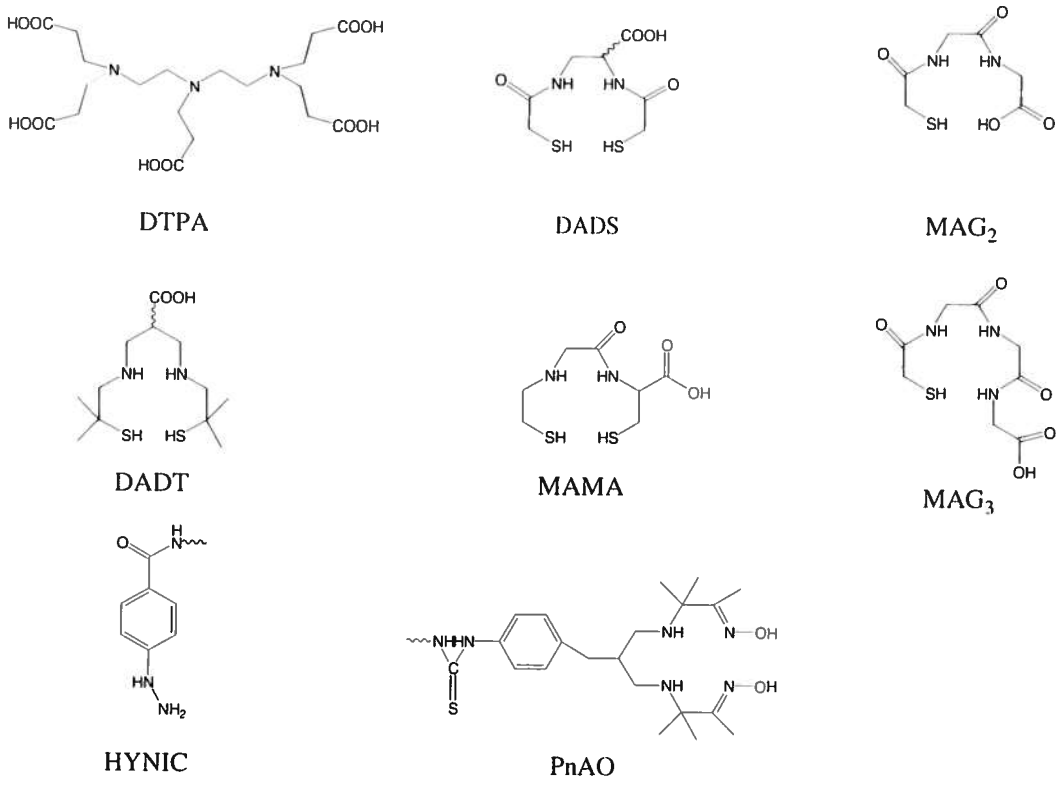

Figure 59: BCAs useful for ^{99m}Tc-labeling peptides.

19.3. The choice of radiolabeling methods

The choice of radiolabel approach depends on the type of biomolecules to be labeled and the purpose of the study. So far, the method used for radiolabeling includes the prelabeling approach, the postlabeling approach, and the direct labeling approach.

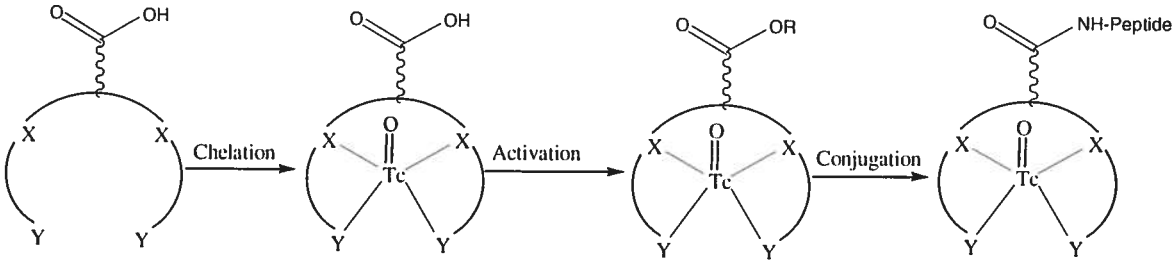

Figure 60: The prelabeling approach.

The prelabeling approach (Figure 60) has three separate steps, i.e. the formation of the ^{99m}Tc complex with a BCA, the activation of the ^{99m}Tc-BCA complex, and the conjugation of the activated complex to a protein or peptide. For research purposes, this approach is very useful to demonstrate the proof of concept in a short period of time, before making extensive efforts in preparing a peptide-BCA conjugate. However, it is too complicated and time-consuming for routine clinical use, such as lung imaging. In fact, the multiple-step synthesis prolongs preparation time, and consequently, shortens the operation time for imaging in the $t_{1/2}$ of ^{99m}Tc (Edwards *et al.*, 1997).

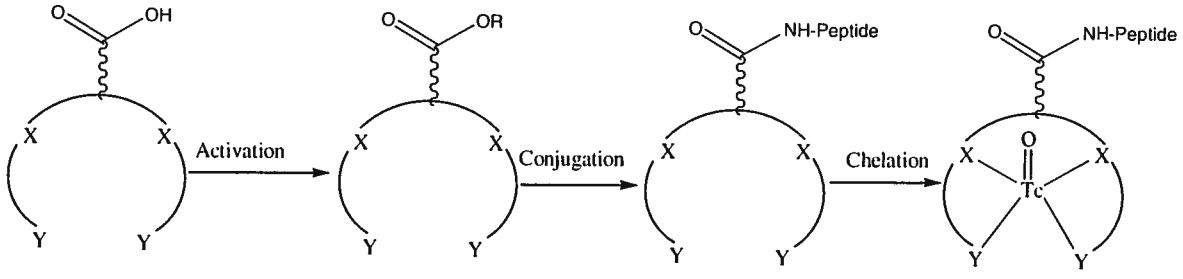

Figure 61: The postlabeling approach.

The postlabeling approach (Figure 61) implies that a BCA is first attached to the peptide to form a BCA-peptide conjugate. BCA is attached frequently to the C- or N-terminus of the peptide chain. Nevertheless, it can also be attached to the side chain of the peptide or incorporated in the peptide backbone, as long as that incorporation of the BCA does not significantly affect the receptor binding affinity. Thus, this approach involves a multiple-step organic synthesis. However, the radiolabeling can be accomplished by direct reduction of $^{99m}TcO_4^-$ in the presence of a BCA-peptide conjugate or by ligand exchange with an intermediate ^{99m}Tc complex. Presently, it is the most practical approach for the development of commercial peptide-based target-specific radiopharmaceuticals. The conjugate of DTPA-AM was then prepared and labeled according to the postlabeling approach.

The direct approach is like a simplified prelabeling and postlabeling approach, in this approach the peptide acts as a target molecule and a BCA. The method usually uses a reducing agent (e.g. Sn^{2+}) to convert a disulfide linkage into free thiols that are able to bind ^{99m}Tc. A limitation of the method in application to peptides is that the disulfide bond of peptide is too critical in most cases for maintaining their biological properties. The difference of AM sequence from its family members is a long N-terminal loop, its disulfide bond is following the loop and exhibits bioactivities. The related studies (Zimmermann *et al.*, 1996; Champion *et al.*, 1997; Hay et al., 2003; Wunder *et al.*, 2008) encourage us to investigate the possibility of AM itself being used as a metal ion carrier and receptor specific targeting molecule. In fact, the ^{99m}Tc-linear AM shows good and specific properties for dog lung imaging in the present study. However, the approach is limited in the development of smaller peptides of AM, especially the peptide lacking a Cys residue.

19.4. The site-specific conjugation of DTPA

As for DTPA, the –COOH group is the general conjugation group for the attachment of the radiopharmaceutical to the peptide or protein. There are at least two factors to be considered when DTPA is conjugated to a peptide. At first, the location of conjugation in

peptide sequence should be away from the peptide segment that is crucial to the targets. In the case of AM, conjugation should occur at the N-terminal region of AM, rather than its C-terminal tail. Secondly, to search for a reasonable conjugation chemistry according to peptide sequence analysis. For example, some sensitive amino acid residues like Asp, Glu, Lys, and Cys with reactive groups at their side chain terminus. If a peptide has all sensitive residues mentioned above, there is no way to get a single site of conjugation at one end. What is more, multiple conjugates could induce an immune response. AM has 52 amino acid residues and it contains N-terminal amino function and δ-amino groups from 4 Lys side chains, as well as Asp and Cys are present in the molecule. Thus, a site-specific conjugation of DTPA was required in the present study.

19.4.1. Conjugation chemistry of DTPA

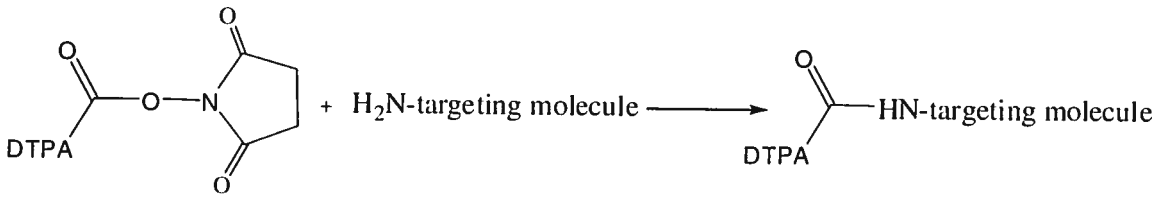

NHS esters

Figure 62: The conjugation of DTPA-NHS.

Since DTPA has the functional group, -COOH, the direct coupling reaction with DTPA and peptidyl resin was performed by Fmoc/BOP methodology at the beginning of the study. The reaction failed to yield the right products because of the poor solubility of DTPA in all organic solvents that were used in routine Fmoc-SPPS. The general conjugation of DTPA was developed in the 70's. The first method was the mixed carboxycarbonic anhydride approach (Krejcarek and Tucker, 1977), and then the cyclic DTPA anhydride method (Hnatowich, Layne and Childs, 1982) became the most widely used method for radiopharmaceuticals because of its simplicity and commercial availability of cyclic DTPA anhydride. Finally, it was reported that N-hydroxysuccinimide (NHS)-activated esters can be attached to any primary amine group

of a peptide. Virtually any molecule that contains a carboxylic group can be converted into its NHS ester, such as DTPA (Figure 62; Paxton, *et al.*, 1985). The method could reduce the intermolecular coupling of biomolecules. All three methods produce conjugates with identical structures.

19.4.2. The site-specific conjugation of DTPA

It is possible to undergo site-specific conjugation through Lys side-chain with a protecting group that is stable to the normal deprotection and cleavage procedures in Fmoc SPPS, but that can be removed selectively before or after peptide cleavage. Herein, before peptidyl-resin cleavage, all amino acid residues with reactive groups were protected during the SPPS. Consequently, after the incorporation of the last amino acid and deprotection of the Fmoc protecting group, only one amino group is exposed on the peptidyl-resin, i.e. the N-terminal amino group. In this case, the site-specific conjugation of DTPA on the N-terminal tail of AM can be carried out by the SPPS technique. This method involves activation of the conjugation group of DTPA to produce an anhydride or an NHS-activated ester, followed by a coupling reaction with the peptidyl-resin containing a free terminal amino group. The site-specific covalent attachment of a chelating group to the N-terminus of a peptide, which is then present only in the N-terminal region and, therefore, distal to the receptor binding site identified in the C-terminal region, can avoid the use of special side chain protector and an extra deprotection procedure, and also maintain the organ specificity. In the present study, DTPA-AM was accomplished by coupling DTPA anhydride (DHDTPA) by SPPS with the formation of imides between DTPA and side chain protected peptidyl resin of AM. However, more than one of the carboxyl groups of the DTPA can react with the N-terminus of AM. The intermolecular cross linking raised more by-products and difficulties in purification. No efforts were made further on the reaction because DTPA did not show any good chelating properties in the ^{99m}Tc-labeling test.

19.5. Purification, quality and quantity control of ^{99m}Tc-labeled peptide

HPLC has been used as routine analysis in labs and industry. The analytical technique is also applied in clinical laboratory tests because of its good reproducibility and automatization. In the present study, the technique was the first method used to separate un-reactive materials and by-products, i.e. free technetium, colloids from labeling reaction, and enriched labeling sample. It is worth mentioning that HPLC is not available in all clinical applications since the technique requires some demands on the instrument and technology. It is necessary to find a simplified and rapid approach in the preparation of labeled peptide, so the method could be suitable to clinical applications such as lung imaging.

Nowadays, another technique called solid-phase extraction also plays an important role in sample preparation (also called column solid-phase extraction). The mechanism of this technique is the same as the HPLC. So far, the applications of the technique are covering various fields requiring trace enrichment and sample clean-up. It is a technique that suits different sample preparation needs and is versatile with positive-pressure or vacuum-assisted flow in manual or automated applications. Sep-Pak cartridges with hydrophobic, non-polar bonded silica phase are usually applied for the isolation of hydrophobic species from aqueous solutions, such as trace organics, drugs or peptides. In the present study, the application of Sep-Pak cartridge instead of HPLC not only simplifies the method for the purification of labeling peptide, but also gives a rapid enrichment of labeled peptide. The technique is advantageous to concentrate trace radiopharmaceuticals in a buffer, and more convenient to make the sample size smaller for the sake of clinical treatments. The facilitation and feasibility was verified by chromatographic techniques and a γ-counter in the present study.

Thin Layer Chromatography (TLC) is the most frequently used procedure for the quality control of small ^{99m}Tc-labeled peptides. The method gives the radiolabeling yield, which includes all ^{99m}Tc species containing the peptide. However, it is not suitable for the separation of different isomeric forms. In the present study, an ITLC-SG was used as quality and quantity control. It is simple and quick, usually taking less than 30 min to complete the whole procedure. The radiochemical purity (RCP) of the ^{99m}Tc-BCA-

peptide complex can be estimated by ITLC-SG after appropriate calculation. The different chromatographic technique, i.e. HPLC and TLC, as well as conditions is useful to confirm that no radioimpurities or isomeric forms were coeluted with the ^{99m}Tc-BCA-peptide complex or ^{99m}Tc- linear peptide.

19.6. The investigation of ^{99m}Tc-labeling reaction and relative by-products

Table 22: The results of ITLC for labeling reaction with EDTA and DTPA.

ITLC-EDTA				
ITLC-SG solvent	Position and count (%)		Yield (%)	
Acetone	Bottom	7		
	Top	20	Free ^{99m}Tc	74
BAPE	Bottom	1	Colloid	6
	Top	16	Labeled	20
Acetone	Bottom	4		
	Top	13	Free ^{99m}Tc	76
BAPE	Bottom	1	Colloid	6
	Top	16	Labeled	18

ITLC-DTPA				
ITLC-SG solvent	Position and count (%)		Yield (%)	
Acetone	Bottom	26		
	Top	7	Free ^{99m}Tc	21
BAPE	Bottom	17	Colloid	71
	Top	7	labeled	8
Acetone	Bottom	25		
	Top	5	Free ^{99m}Tc	17
BAPE	Bottom	19	Colloid	73
	Top	7	labeled	10

Historically, two methods are usually applied in radiolabeling reaction. The labeling protocol in the present study is one of the traditional methods, called direct radiolabeling

protocol. In this method stannous chloride as a reducing agent plays an important role in converting the pertechnetate to technetium oxide so that radiolabeling formation is induced. Meanwhile, the excess amounts of stannous ion in reactive mixture can accelerate the formation of colloids, the main by-product in the present labeling protocol. In the present study, the techniques of ITLC, γ-counter and HPLC, were used to investigate the radiolabeling reaction and determine the by-products in the reaction. In the ^{99m}Tc-labeling reaction, the yield of labeled peptide was more than 50%, other products less than 50% were mainly colloids.

Besides the direct radiolabeling protocol, an exchange radiolabeling method can be usually applied to reduce the yield of colloids. In the exchange radiolabeling method, the key reagent is a second metal chelate agent which can form coordination compounds with Sn^{2+} to reduce the amounts of the free ion in reactive mixture but do not interfere in the normal redox reaction. In a parallel test, EDTA and DTPA were investigated as the second chelating agents for tin ion in the ^{99m}Tc radiolabeling of linear AM (the reaction time was 15 min). As a result, DTPA protocol exhibited a very low level of free Tc and labeled peptide, but a high level of colloids (Table 22: ITLC-DTPA). Although EDTA did not give a good labeling yield, it demonstrated very low level of colloids (Table 22: ITLC-EDTA). As a result, it is possible to improve the labeling yield by changing the reaction conditions, such as to prolong the reaction time and raise the reaction temperature. However, the two reagents have poor solubility in water and acidic solution, and stannous chloride tends to hydrolyze when the pH (>2.6) of the reactive solution is raised. This might be the reason why both methods gave rise to lower labeling yields.

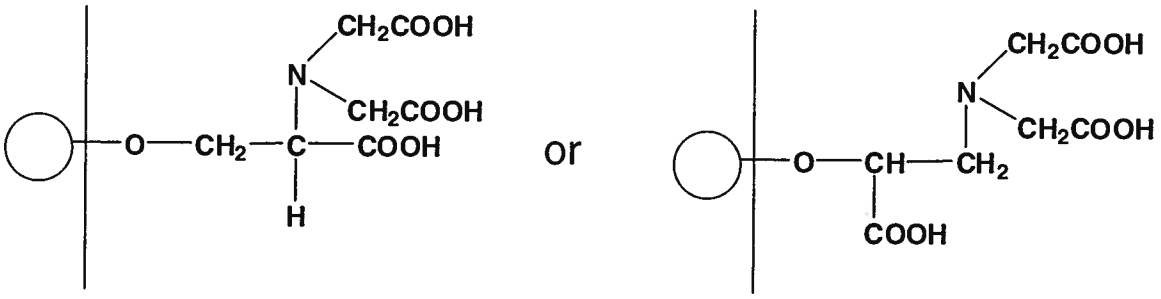

Figure 63: The structure of redox polymers.

Free Tc and colloids can be removed easily by chromatographic methodology. However, the unlabeled linear peptide is difficult to separate totally from its labeled forms. To increase the ratio of labeled products and reduce the amounts of unlabeled peptide could therefore be a successful approach. According to the literature (Kleisner, *et al.*, 2000), some polymer chelating reagents have been used in radiolabeling reaction instead of traditional methods. It is reported that redox polymers are effective reducing reagents and give rise to pure radiolabeled products with a high yield (>95%). Thus, efforts were made for the preparation of redox polymers by anchoring functional groups as tin carrier on Sephadex G-10 (medium and fine, Figure 63). In the study, quantitative and qualitative determination was established, and then the amounts of bifunctional groups on Sephadex were determined by titrimetric analysis and malachite green test, respectively. The coordination of bifunctional groups and Sn^{2+} was indicated by a tin indicator. Unfortunately, the redox polymers can trap AM during the mixing procedure, and only release it at very low pH (i.e. by 1M HCl). In the present study no further efforts were made on the radiolabeling reaction because the purified labeled linear AM demonstrated a sharp lung image in dog, and at the dose used in the study there were no detectable detrimental effect on blood pressure and heart rate.

20. Strategy and results of peptide synthesis

The choice of a synthesis technique depends mainly on the need for synthetic versatility and the required yields. The current synthetic procedures for peptide were composed of the hydrolysis of proteins and the chemical synthesis. Among the synthetic methods that have been widely applied in biological science stands solution phase peptide synthesis and SPPS. SPPS is particularly useful when a large number of analogs are required and a rapid screening of peptides is planned. SPPS is based on the sequential addition of α-amino and side-chain protected amino acid residues to an insoluble polymeric support. Generally, two strategies can be used in SPPS, according to the N-α-protection scheme: utilisation of the acid-labile Boc-group as a protecting group or the base-labile Fmoc-group. In Fmoc synthesis, the growing peptide is submitted to mild base treatments using

piperidine for Fmoc-group deprotection and TFA is required only for the final cleavage step and the deprotection of the peptidyl-resin. In contrast, cleavage and deprotections in the Boc strategy require the use of rather strong acids, such as hydrogen fluoride (HF) and TFA. These acid treatments are rather harsh and therefore, the repetitive acid treatments result in premature cleavage of uncompleted peptide-chain and to various side reactions. Because most of the peptides that were proposed as synthetic targets in the present study exhibit a long sequence, the Fmoc strategy that gives rise to lower levels of side reactions was favored.

20.1. Resin

Table 23: Resins for Fmoc SPPS and preparation of peptide carboxamide.

Name	Acid sensitive	By-products	The attached group
Rink Amide resin	high	high	Fmoc protected
Rink Amide MBHA	low	low	Fmoc protected
Rink Amide AM resin	low	low	Fmoc protected
Rink Amide PEGA resin	low	low	Free amino group
Rink Amide NovaGel™	low	low	Free amino group

AM is a carboxamide peptide, and its amidated C-terminus are important to the bioactivity of AM according to a study on structure-activity relationship (Eguchi, *et al.*, 1994). In this case, the resin used in the Fmoc SPPS of AM and its fragments were selected from resins with Rink Amide linker (Table 23). In the table Rink Amide resin was the first to be used in the synthesis of C-terminal amidated peptides. Without an electron-withdrawing acetamido spacer in the linker formation, Rink Amide resin is more acid sensitive and is easily broken during cleavage reaction to yield coloured by-products that are not easy to remove from the product by washing. Other resins in Table 23 are devoid of these drawbacks. Among of them, both Rink Amide AM and Rink Amide MBHA resin are the resins incorporating with stable Rink linker, derivatized sequentially with norleucine and the Fmoc protected modified Rink Amide linker. An acetic acid

spacer protects the modified linker from degradation by TFA, and therefore the resins shows compatibility to TFA cleavage and is less prone to by-products. In the present study, most peptides were synthesized by using Rink Amide AM resin as solid support. In the latter part of the study, the resin was replaced by PAL resin (Matrix Innovation) which was used in the following synthesis of AM and its fragments. The new resin was reported to be the best resin on the market for preparing peptide amide, and it did exhibit superior results, comparable to conventional polystyrene-based Rink Amide AM resin in the synthesis of long linear peptides with a high purity and yield for the final products.

20.2. The special amino acid coupling reaction

The synthesis of peptides in the present study was carried out by standard Fmoc/BOP methodology except for the coupling of some amino acids with specific chemical properties. The end of coupling reaction was indicated by the Kaiser test (yellow).

20.2.1. Pro-containing peptides

The Kaiser test is widely used in SPPS. The test is especially applied in monitoring the presence of free amino group after deprotection (dark blue colour) and successful coupling reaction (yellow colour). Although the Kaiser test is one of the most popular qualitative tests in organic chemistry, it is well known that in some cases it can give rise to false indication. According to publications (Fontenot *et al.*, 1991; Vazquez, Qushair and Albericio, 2003), the test does not lead to the typical dark blue colour with the coupling of Pro, Asp, Asn, Arg, and Cys after Fmoc-deprotection. In these cases, the synthesis of these amino acids and the following amino acids in the present study were then performed by double coupling reactions at first. However, the analysis of HPLC and MS showed more by-products and low yield during peptide chains assembly.

It was reported that the coupling of Asp, Asn, His, and possibly Trp or Ser as the first or even the second amino acid following to Pro can indicate a false result after Fmoc-deprotection by using the Kaiser test (brown colour; Zikos and Papasarantos, 2006). In

present study the synthetic peptides, especially AM and AM2, have these amino acids mentioned above and more than one Pro as well as Asp or Ser followed to Pro in their sequences. In the present study, by introducing the deprotective Kaiser test in addition to the routine test after coupling reaction, the following peptide syntheses exhibited less by-products and better yields than before.

20.2.2. Gly in the N-terminal tail

Sometimes, a Gly in a peptide can cause position-dependent diketopiperazine formation, and the by-product can be accelerated by the Pro or Gly in the N-terminus of a peptide. Diketopiperazine formation will result in the cleavage of the first two amino acids (Gly and the amino acid after Gly). It occurs by nucleophilic attack of the nitrogen atom on the carbonylamide between the 2nd and 3rd amino acid (Figure 64). There is a Gly^3 in the N-terminus of AM(17-52), and the second and third amino acid are Thr and Cys, respectively. In the acidic purification procedure of AM(17-52), no diketopiperazine by-product (i.e. a peptide devoid of the first two residues, i.e. Gly and Thr, MW3679 Da) was detected by MALDI-TOF mass analysis.

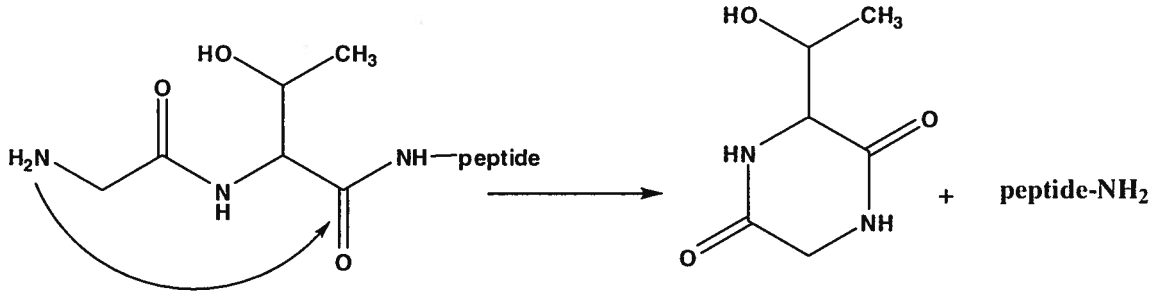

Figure 64: The proposed diketopiperazine formation of AM(17-52).

20.2.3. Gln in the N-terminus

In previous reports, AM2(17-47) was used as the antagonist of AM2 instead of AM2(16-47). However, the peptide does not act as a full functional antagonist in the central nervous system or pituitary (White and Samson, 2007). In the present study, AM2(16-47) was prepared as the antagonist of AM2, and the solution of AM2(16-47) was not stable

and the concentration of pGlu was seen to increase on storage - even if kept at -20°C. Conversely, AM2(16-47) concentrated to dryness was more stable than in solution. Therefore, the sample of AM2(16-47) used in the study was prepared fresh from a solid powder that was kept at -20°C. In this way, the amount of pGlu in a sample was controlled to under 20% by HPLC. AM2(16-47) also showed specific binding in dog lung homogenates, and could inhibit the binding of AM with a similar IC_{50} value to AM(22-52) (i.e. AM antagonist).

20.2.4. Cys-containing peptide

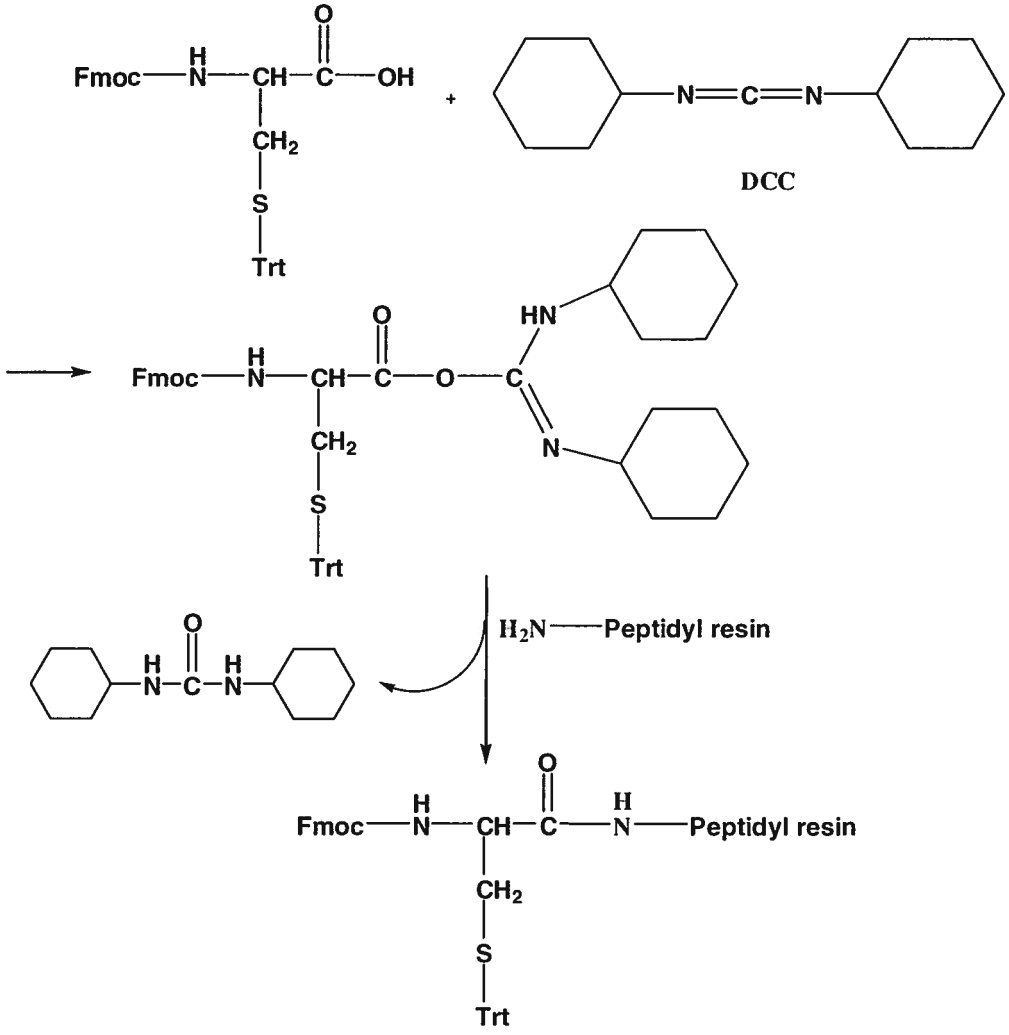

Figure 65: Mechanism of DCC-promoted peptide coupling.

One of the most common structural characteristics of peptides in the CT family is an intermolecular disulfide bridge. Thus, the native peptides have at least two Cys in their peptide sequences. Generally, Trt-protected Fmoc-Cys is recommended in routine synthesis because the protecting group is routinely removed by TFA. However, racemization is more of a concern during the introduction of Fmoc-Cys(Trt)-OH in SPPS because the transformation is very hard to detect and difficult to control. The racemization converts L-form enantiomer of Cys to a 1:1 mixture of L- and D-enantiomers under base-catalyzed conditions, e.g. piperidine in Fmoc-group deprotection.

To avoid the chiral transformation of Cys, the DCC and HBTU/TMP protocol are used instead of the standard Fmoc/BOP methodology in Fmoc-coupling. The DCC protocol (Figure 65) was introduced in the 50's as a peptide coupling reagent without racemization. The drawback of the protocol is the formation of insoluble dicyclohexylurea. As a result, the activation and acylation of Fmoc-Cys(Trt)-OH have to be performed in another vessel in an ice-bath, and the filtrate poured into a reaction vessel containing SPPS to start the coupling reaction. At the beginning of the study, DCC protocol was used in the coupling of Cys. However, in 2002, HBTU/TMP protocol (Figure 66) was reported as a 'safe' method to incorporate Cys (Angell *et al*, 2002) without Cys racemization. The new method, used in the last part of the present study, simplifies Cys coupling operation because it could be carried out by routine procedure of SPPS.

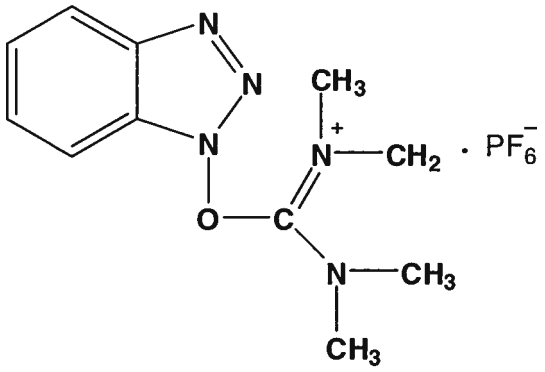

HBTU

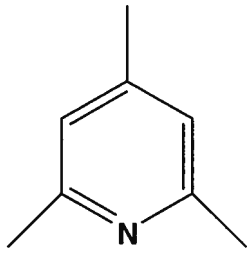

TMP (Collidine)

Figure 66: Chemical structure of HBTU and TMP.

20.3. The cleavage of peptidyl-resin

After the desired protected peptidyl-resin is synthesized by Fmoc/BOP standard methodology, the following step requires the removal of all side-chain protecting groups and the detachment of the peptides from the solid support. In Fmoc-SPPS, both peptide and protecting group can be cleaved by TFA. Although some new methods have been used in TFA-cleavage based on appropriate protected amino acid derivatives and resins, the method by using a cleavage mixture is still the most popular in SPPS.

Generally, the choice of the cleavage method depends mostly on the sequence of peptide. In the process of TFA-cleavage, a nucleophilic reaction can occur between some sensitive amino acids of the peptide and free reactive cations. The sensitive amino acids include Trp, Met, Tyr and Cys, which contain nucleophilic functional groups, and cations can be generated easily from peptide protecting groups and the handles on the resin. A cleavage mixture was prepared by TFA and the scavengers that are more reactive nucleophilic reagents, and quench the reactive cationic species released from peptidyl resin, therefore suppress side reactions in TFA cleavage.

There are at least four aspects that have to be considered in finding an optimum cleavage conditions, the linker to the resin used, side-chain protecting groups of Fmoc-amino acid, the nature of the amino acid residues, their number, and as well as the sequence. Most synthetic peptides in the study have Cys, Tyr residues, and some of them also have Trp residues. In these cases, phenol became one component of the cleavage mixture since the reagent was considered as a good protector for the residues i.e. Tyr and Trp with aromatic ring moieties. For the sequence with Cys and t-butyl protected residues, a cleavage mixture with EDT is usually the best choice because EDT can quench t-butyl cation as a scavenger, prevent some sensitive amino acids from acid catalyzed oxidation (especially Trp), and promote the side chain protecting group (trityl) to leave from Cys(Trt), considered as a difficult protecting group to liberate. Additionally, nitrogen was used in the present study to provide a non-oxygen atmosphere, and minimize oxidation (for example, methionine sulfoxide formation).

A high efficiency of TFA-cleavage also correlates with the size of a peptide. In the study, the size of synthetic peptides are various from 1400 Da to 6000 Da. The TFA-cleavage mixture and conditions employed in the present study can yield the desired peptide with MW<4000 Da using small amounts of peptidyl-resin sample as preliminary cleavage for a routine reaction time of 2 h. However, for peptides with MW>4000 Da, a peptide with some side-chain protecting groups can be detected by HPLC and MALDI-TOF MS analysis. Since some bulky, hydrophobic and more acid-labile side chain protecting groups, such as Trt and Pbf, as well as some residues with sluggish deprotection (like Asn(Trt) residue) are on those long peptidyl-resins. The problem was overcome by simply extending the cleavage reactive time to 3 or 4 h depending on which peptide.

20.4. Cyclization of peptide

Disulfide bridges frequently play a key-role in the maintenance of biological activity and conformational stability of peptides. Consequently, various strategies were developed to produce the S-S bond by means of oxidation. Among the oxidants that were investigated for this purpose, the most utilized are oxygen, potassium ferricyanide ($K_3Fe(CN)_6$), iodine, DMSO (dimethylsulfoxide), as well as mixtures of oxidized and reduced glutathione, and Ellman's reagent coupled to a solid matrix (Annis, Chen, and Barany, 1998). Of these methods developed for the formation of disulfide bonds, air oxidation in an aqueous medium is the most commonly used procedure. However, air oxidation usually requires a long reaction time in alkaline or neutral pH for the disulfide bond formation, and a high dilution of peptide to be effective. However, its benefit comes from the fact that it produces a harmless by-product i.e. H_2O. Also, stronger oxidizing agents, such as I_2 and $K_3Fe(CN)_6$ are often used for simple peptides containing only a single disulfide bridge because of their efficacy and production of kinetic-controlled products. Care must be taken because these S-S-forming agents are rather potent and they can lead to over oxidation. Although they have the advantage of being applicable in acidic media, they suffer from the limitation that the by-products will require a purification step. Furthermore, several nucleophilic amino acids such as Met, Tyr, Trp, and His are

particularly sensitive to these oxidation conditions. Therefore, an appropriate analysis of the oxidizing conditions must be carried out to evaluate the "benefits: drawbacks" ratio encountered with the selected techniques.

20.4.1. The method of peptide cyclization

Because many of the peptides and their fragments planned in the project are molecules containing a single disulfide bond, the oxidizing agents, including I_2, $K_3Fe(CN)_6$, DMSO and oxygen oxidation, were considered as candidates for disulfide bridge formation. Meanwhile, nucleophilic amino acids mentioned above for their sensitivity to oxidation also resides in the peptide sequences in the present study especially in AM. In these cases, I_2, $K_3Fe(CN)_6$ as strong oxidizing agents may not be suitable to the disulfide bridge formation in the study.

20.4.1.1. Disulfide bridge formation using potassium ferricyanide

$K_3Fe(CN)_6$ oxidation (Mccurdy, 1989) is the routine method used for the formation of disulfide bridge within endothelin peptide in our laboratory. The general procedure involved preparation of purified linear peptide solution (0.5 mg/mL in water at pH 9.0 by adding diluted ammonium hydroxide), and oxidation with 20 eq of $K_3Fe(CN)_6$ for 30 min. In the present study, after purification by semi-prep HPLC and lyophilization, the proposed AM presented itself as a blue powder. The colour could be removed by repeated treatment with EDTA to yield a colourless material that, according to MALDI-TOF MS analysis, was a mixture of the reported peptide and its oxide.

Although $K_3Fe(CN)_6$ oxidation typically has a very short reaction time as a routine method, it did not show any benefits in the disulfide bridge formation of AM in the present study. On the contrary, the procedure was prolonged by exchange chelating reaction. Because AM showed the property of a chelator which can trap a metal ion by coordinate bonds, the proposed AM-metal-chelate (blue powder) was difficult to dissolve in water, and had a low solubility in TFA. As a result, the product increased the difficulty

of purification and could not be applied in the bioassay follow-up before the treatment by using EDTA which is also metal chelator and could capture metal ions from AM. Furthermore, it did increase the risk of oxide by-products due to the detection of AM oxide, and lowered the yield of AM with extra multiple procedures. Thus, $K_3Fe(CN)_6$ oxidation was not considered as an appropriate condition in the cyclization of AM since it did not come with a good ratio of "benefits: drawbacks" (at least >1) to be the selected technique for disulfide bridge formation in the present study.

20.4.1.2. Disulfide bridge formation using DMSO

Among the so-called "mild" conditions, the DMSO procedure (Tam *et al.*, 1991) is very useful for S-S bond production. It produces H_2O and dimethyl sulfide, two harmless by-products, and the method is miscible with H_2O at all concentrations and thus, a high concentration of DMSO can be used to obtain an adequate rate of reaction. Moreover, an advantage of oxidation with DMSO is that the reaction can be performed at acidic to neutral pH. The acidic condition can protect sensitive residues from oxidation. Generally, a linear peptide is dissolved in a solution of 20% to 50% DMSO/ H_2O, in order to generate the disulfide bridge between two Cys side-chains. The reaction is usually completed within 1h to 4 h.

In the present study, the DMSO oxidation reaction was performed by using purified linear AM, and the whole progress of the DMSO oxidation was monitored by analytical C_{18} reverse-phase HPLC and MALDI-TOF MS analysis. Unfortunately, the yield of disulfide bond formation in the present study is lower than 50%. Even when efforts were made to increase DMSO concentration and reaction time, the maximum ratio of cyclic peptide could only reach over 50% by HPLC analysis. In evaluating the ratio "benefits: drawbacks" for this technique, the benefits of the method are few oxide by-products detectable. DMSO is then an oxidizing agent suitable for a peptide with residues sensitive to oxidation. However, DMSO is also a viscous organic solvent for HPLC system. For the protection of the HPLC system and peptide sample during purification, a high concentration of DMSO is not recommended to use. Additionally, DMSO oxidation could

not generate completely the disulfide bridge formation within AM. So, the method cannot be an appropriate technique which encounters with the ratio "benefits: drawbacks" (>1) in this study.

20.4.1.3. Disulfide bridge formation using oxygen

Air oxidation is the easiest way to yield disulfide bond of peptide. The drawbacks of the method are long reaction times, large volumes of solution and basic conditions, whereas benefits include an easy procedure and simplified purification. Although $K_3Fe(CN)_6$ oxidation can form a disulfide bond of peptide between two Cys in a very short time, by-products cannot be avoided during the procedure. While the by-products were reduced by DMSO oxidation, it is necessary to operate with a long reactive time and high concentration of DMSO to produce disulfide bridge formation and a higher yield of cyclic peptide. The large dilution volume and lower yield are the drawbacks of this method. However, all things considered, oxygen oxidation was found to have the best ratio of "benefits: drawbacks" in the present study. Accordingly, the proposed peptides were cyclized by oxygen. The oxygen oxidation established in the present study has high yield in a medium volume sample solution. The procedure is suitable to all peptides proposed in the study, and results, including peptide purity and yield, are all better than other.

20.4.2. The qualitative and quantitative detection of cyclization

Free –SH groups in peptides could be strong chelation groups for metal ions, whereas the disulfide bridge is crucial for the bioactivities of AM. It is necessary to determine precisely the amount of free –SH or –S-S- that exists in AM and its related fragments during the radiolabeling reaction and competitive binding assay in order to have comparable results. For example, in the study of ^{99m}Tc-labeling test, the DTPA-AM exhibited a poor capability as a chelator, and its labeling yield was lower than the linear AM with free –SH groups. In this case, if the linear form of DTPA-AM was cyclized partly to the disulfide bridge form (i.e. DTPA-AM mixed with DTPA-linear AM) the DTPA-linear AM would increase significantly the ^{99m}Tc-radiolabeling rate and give rise

to a false result. Correspondingly, in the competitive binding assay, the IC_{50} of AM and linear AM has a more than a 100-fold difference in concentration. If the sample of AM contained a high ratio of linear AM, the high differences between AM and linear AM could be reduced in the study of receptor-binding activity. Generally, the cyclization reaction is confirmed by the Ellman test. However, it is very difficult to determine a reaction totally completed only by colour indication. In the present study, analytical HPLC was used as the main method in monitoring disulfide bond formation, and quantitative and qualitative determination as well as isolation of linear and cyclic peptide. While the Ellman test was used as an accessory qualitative protocol in the present study, the analytical detection strongly ensured the degree of chemical cyclization of peptides and the quality and quantity of samples in biological assays.

20.4.3. The control on the side-reactions and by-products of peptide cyclization by oxygen

Disulfide bond formation undergoes a reversible oxidation between two –SH residues of Cys that are easier to be deprotonated. During an oxidation reaction, the disulfide bond can form in one peptide molecule, called intra-disulfide bridge, and between two peptide molecules, called inter-disulfide bridges, i.e. polymers. Three main factors are involved in the oxidation reaction: oxygen, pH, solvent and reactive volume. Firstly, the high pH can accelerate the oxidation on Cys, however, also increase the risk of oxidizing other oxygen-sensitive residues, such as Met. Secondly, the oxidation is also solvent-dependent, it is rapid and selective in the dipolar solvents (i.e. aq. MeOH, aq. ACN, aq. AcOH or aq. TFA) because the peptide molecules exhibit some secondary structures suitable for the disulfide bond formation in these solutions. Lastly, a large dilution can separate peptide molecules well so as to favor the formation of intra-disulfide bridge rather than polymers.

Fortunately, any oxidations of these residues as well as polymers in peptide synthesis have a different t_R than the native peptides. Generally, in the peptide preparation, the purification will always follow the cleavage and cyclization of peptide, and these by-

products are detectable by using MS spectrum. Thus, they can be eluted in different t_R, and then removed in the purification process.

20.5. Synthesis of AMY

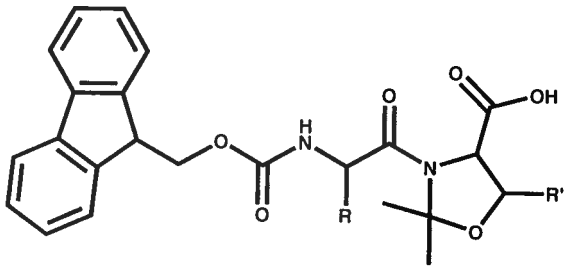

Figure 67: Molecular structure of Fmoc-pseudoproline (oxazolidine) dipeptide derivatives.

Fmoc-Thr(tBu)-Ser-$^{\Psi Me,Me}$pro: R'=H, R=$CH(OtBu)CH_3$

Fmoc-Lys(Boc)-Ser-$^{\Psi Me,Me}$pro: R'=H, R=$CH_2CH_2CH_2CH_2NH(Boc)$

Both Fmoc and Boc strategies were applied when AMY was synthesized by SPPS in the present study. The inherent aggregative propensity of AMY caused the poor purity of the crude product and very low yield. Additionally, the self-aggregated problem makes AMY too difficult to dissolve in ACN-TFA-H_2O during purification and disulfide bridge formation. Recently, pseudoproline dipeptides (Figure 67) have been proposed for the synthesis of difficult aggregation-prone sequences, such as AMY and its antagonist, AMY(8-37). The pseudoprolines are formed through a cyclocondensation reaction of Ser, Thr, or Cys residue side chains. This reaction links the side-chains of these amino acids to their respective N-terminal peptide nitrogen atoms, similar to that of the proline residue. As a result, the incorporation of pseudoproline (oxazolidine) dipeptides induces significant kinks in the backbone of the growing polymer-bound polypeptide chain and removes hydrogen bond donors, thus disrupting secondary structures such as β-sheets and preventing aggregation during chain assembly. It was reported that pseudoprolines can allow faster and more complete couplings (Abedini and Raleigh, 2005). The poor solubility of AMY in aq. ACN could be also improved by repeatedly treating and lyophilizing the crude peptide with acetic acid solution. Acetic acid was very helpful in

the present study during the purification and cyclization of AMY. However, in the present study no further investigation on AMY synthesis was made since AMY displayed no specific binding in dog lung homogenates by the receptor-binding activity study.

20.6. Peptide purity and yield data

Peptide purity in the present study was the amount of target peptide relative to all analytes that absorb at 230 nm, including smaller peptide fragments from synthesis and degradation by chemical reagents, as well as some incompletely deprotected peptides during cleavage. The purity did not take into account the amounts of salts that were usually present in samples because all peptides in the present study were purified from a solution with TFA, i.e. ACN in 0.06% TFA or 0.06% TFA only. The free TFA left in sample solution can be mostly removed by lyophilization. However, the salt of peptide with TFA is very difficult to be removed completely and the amounts of the salt cannot be evaluated and counted precisely. The yield of peptide was expressed by quotient in percentage that was calculated by the weights of crude and pure peptide powder after lyophilization for more than 48 h. The pure peptide was combined from the collected fractions that displayed a single peak with true t_R and MW by HPLC and MS analysis after purification. The mixture of the pure peptide and its side-peaks products was not purified further in the study.

20.7. Peptide lyophilization and storage

Lyophilization was always the routine method to obtain solid peptide from its solution. In the preparation of peptides, each peptide was at least lyophilized twice. The crude peptide after cleavage from the resin was concentrated and precipitated by ether (a. aq.). The solid crude peptide powder was dried in the air, and re-dissolved in water, 0.06% TFA/H_2O v/v, or acetic acid (for samples with low solubility). In the present study, the TFA and acetic acid are the best solvents for the peptide with Cys and some oxygen-sensitive residues because the acidic condition can protect and avoid the generation of unnecessary products. The first lyophilization of crude peptide can remove some impurities that have low

boiling points in peptide cleavage. The solution with pure peptide after purification by HPLC was evaporated by rotary evaporation to remove the organic solvent and excess water, and then lyophilized over a period of 48 h to remove residual volatile compounds and water.

After lyophilization, the pure solid products were sealed and kept at -20°C to prevent or minimize the degradation of the peptide. Since the repeated freezing and thawing could accelerate the peptide degradation, aliquots of peptide or labeled peptide prepared by distilled water or buffer (pH7.4) were separated in a small volume and frozen. All test sample solutions in the study were prepared freshly with chilled solvent from the aliquots. Furthermore, to ensure the accurate, repeatable and comparable data in various assays, a regular quantitative and qualitative analysis by RP-HPLC and MALDI-TOF MS was carried out for all sample solutions, especially the solutions applied in receptor-binding activity studies.

21. The development of ^{99m}Tc-labeled radiopharmaceuticals based on small peptides and their analogs

In the past decade, more efforts worked on the development of radiopharmaceuticals designed by using radiolabeled receptor-binding peptides. In fact, radiopharmaceuticals for tumor diagnosis and therapy attract more research towards the development of new radiolabeled receptor-binding peptides. To date, octreotide becomes the first clinical imaging agent, then Acutech, a thrombus imaging agent in blood clot detection, a GPIIb/IIIa rceptors antagonist labeled with technetium-99m (Polyakov *et al*, 2000). Also, more peptides, i.e. bombesin, CCK, neurotensin, GLP-1, RGD, and substance P, are in development or clinical trials (Dijkgraaf *et al*, 2007).

Octreotide is a synthetic analog with efficient and selective to neuroendocrine tumors by the rational design from natural somatostatin (Wynick and Bloom, 1991). So far, five human somatostatin receptor subtypes (HSRS 1, 2, 3, 4 and 5) have been cloned, and octreotide has no effects on HSRS1 and HSRS4 (Berk *et al*, 1999). Recently, it was

reported that a new 11-residue cyclic peptides, a somstostain analog, displayed very high receptor-binding affinity and selectivity for HSRS1 (Mansi *et al*, 2004).

Acutech is derived from RGD-containing small peptides because RGD, a tripeptide, has high selectivity and binding affinity to GPIIb/IIIa receptors that involve in platelets activation. The analogs of RGD tripeptide, such as P280, P748 and some cyclic antagonists, was modified by inserting linkers between RGD and technetium-99m, and in this case, to keep the radionuclide far from RGD and minimize the effect of the radiolabeling centre on the receptor-binding affinity of RGD (Liu, Edwards and Barrett, 1997).

In the field of peptide-based radiopharmaceuticals, small peptides play a key role in the development of peptide imaging agents. The studies of CCK imaging compounds in tumors mostly focus on the C-terminal cholecystokinin octapeptide amide, i.e. CCK26-33 or CCK8, because the short amino acid sequence can display high binding affinity for both CCK_A and CCK_B receptor. Furthermore, the modification of a sulphate moiety on the Tyr^{27} side chain of CCK8 can rise above 1000-fold receptor binding affinity to CCK_A receptor (Morelli et al, 2002). The C-terminal hexapeptide fragment, neurotensin(8-13), not only retains essential receptor-binding affinity similar to native neurotensin(1-13), but also exhibits a longer half-life in plasma than neurotensin. These analogs of the smaller peptide fragment are in the development of new radiopharmaceuticals for imaging oncogene neurotensin receptors in tumors (Zhang *et al*, 2006). Similarly, bomdesin-based imaging compounds in tumors are based on the 7-14 or 6-14 amino acid sequence of bomdesin(1-14) because these amino acid residues possess high receptor-binding affinity to their receptors by the study of bombesin structure-function relationship (Okarvi, 2008).

Collectively, smaller peptides and their analogs with rational chemical modifications can maintain or increase essential receptor-binding affinity and specificity for targeting receptors. Such radiolabled smaller peptides or analogs can then direct ligand-receptor imaging in clinical application to provide superior information on diseases and treatments process. Additionally, the development of ^{99m}Tc-labeled radiopharmaceuticals based on

small peptides is also required to satisfy clinical applications. Such new radiopharmaceuticals have to display a high selectivity for target organ or tissues, and easy to prepare in clinical routine operation with high radiochemical purity and stability.

In the development of peptide-based radiopharmaceuticals, besides the identification of new peptides with specific binding properties, the characterization of peptide structure-function relationship is the key in the rational design of new radiopharmaceuticals (Haberkorn *et al*, 2008). In the present study, ^{99m}Tc-linear AM has shown marvelous properties to satisfy clinical imaging requirements. Also, the lung imaging with ^{99m}Tc-linear AM *in vivo*, the characterization of AM receptor and the receptor-binding relationship in dog lungs provides large information to the rational design for smaller AM analogs. Moreover, those peptide-based imaging agents commercially available and less new radiolabeled receptor-binding peptide in development or clinical trials on pulmonary circulation imaging encourage us on the following studies for the development of new radiopharmaceuticals based on AM or its analogs that could display high binding affinity for the receptor subtypes in pulmonary system, and incorporation of technetium without loss of pharmacore specificity in the lungs.

Conclusions

I. The development of a peptide-based target-specific radiopharmaceutical, ^{99m}Tc-linear AM, for imaging human pulmonary circulation.

The investigation of new potential target-specific lung imaging agents was explored. In the study, peptide was applied as a molecule targeting the lungs, and 99m-technetium conjugated to AM gave visible images. ^{99m}Tc-linear AM was the most outstanding form to come from the screening of designed delivery system. The results showed that dog lung predominantly retained the radiopharmaceutical 60 min after the injected dose (<16 pmol labeled peptide), and gave a sharp lung image. The rapid and initially predominant extraction of radioactivity in the dog lung suggests that the radiotracer has high and receptor-specific lung uptake *in vivo*, and biodistribution characteristics favourable to lung imaging. At later time points (60-240 min after injection), the high kidney and bladder radioactivity observed in the dog were attributable to the main elimination route of the radiolabeled peptide, which suggests that a lung clearance pathway of the peptide exists. Additional data was also collected after surgeries made to mimic lung pathological conditions such as pulmonary embolism. Compared to MAA, which is presently used for the diagnosis of pulmonary circulation, the new potential pulmonary diagnostic agent in this thesis displays more advantages in clinical application.

II. Characterization of the receptor-specific binding sites found in dog lungs as AM_1 that appears to be acting as the receptor for AM clearance in the lungs.

With respect to the receptor-specific binding sites found in dog lungs, the investigation of the sites was followed in this thesis. By receptor-ligand binding technique, the receptor-specific binding sites in dog lungs were characterized using ^{125}I-AM as radioligand. The results have shown that human AM has a high binding affinity in dog lung homogenates with two binding sites. The agonist and antagonist of AM could bind the same sites with lower binding affinity, while the binding sites in dog lung exhibit low (>100 fold) binding affinity to AMY, AM2 and CGRPα. The receptor-binding sites were then characterized as an AM receptor. The AM binding site in dog lung homogenates has a higher potency ($P<0.01$) to antagonist AM(22-52) than CGRPα(8-37). It suggested that the AM receptor

with higher binding affinity found in the dog lungs is mainly the AM_1 receptor subtype, and it appears to be acting as the receptor for AM clearance in the lungs. In conclusion, the dog lungs express a specific AM receptor that exhibits AM_1 properties by receptor binding assay. The characterization of the receptor population found in dog lungs could be of benefit for the study of AM receptor subtypes in biological sciences.

III. Characterization of the C-terminal region in AM required by the receptor-binding activity, and N-terminal loop, disulfide bridge, α-helix secondary structures required by a high receptor binding affinity.

Furthermore, the optimal smaller peptide derived from AM segments was investigated in follow-up experiments. The goal being to simplify preparation, reduce the risk of side-bioactivity and lower the costs. By receptor-ligand binding assay, the information of AM's sequence and its secondary structures required by receptor binding sites was collected. The location of binding sites could be around the C-terminal amino acid sequence of human AM. AM fragments with N-terminal amino acid sequence and disulfide bridge formation but without C-termini cannot bind the AM receptors in the dog lung homogenates. The receptor binding affinity of AM was decreased when AM is truncated from the N-terminus. To maintain the AM receptor-binding affinity, the N-terminal loop, disulfide bridge and α-helix secondary structures are required by the receptor found in dog lungs. Among these sequences and secondary structures, the α-helix appears as an important structure required for the AM receptor-binding sites.

Additionally, a molecular tool was introduced, i.e. ^{125}I-Tyr^1-AM, for the biological and pharmacological research of AM. The present study elucidated the preparation, isolation and characterization of the radioligand, and evaluated its potential application in the receptor-ligand study of different species. The reagent shows high binding properties in the study over the commercial preparations. It will be a useful tool for AM study in the future. The saturation binding experiment comparing ^{125}I-AM and ^{125}I-Tyr^1-AM indicated and supported the notion that Tyr^{52} in the C-terminal region of AM is crucial to receptor binding sites, and iodination can affect the binding affinity of human AM in dog lungs.

Perspectives

Although AM binding sites have been found in the lung and heart of rats in various reports, ^{99m}Tc-linear AM has shown no selectivity for the dog heart in the current study. The low specificity of ^{99m}Tc-linear AM in the dog heart indicates a distribution of the different AM receptor subtypes. Interestingly, the high expression of RAMP1 and RAMP2 was detected in human heart and blood vessels by quantitative reverse-transcriptase polymerase chain reaction (RT-PCR) (Wunder *et al.*, 2008). Investigations of AM receptors in dog lungs and heart will help to uncover some of the issues of the AM receptor subtypes. Therefore, characterization of the AM receptor in other organs or tissues of dogs could be important to highlight the different distribution of AM receptor as well as its receptor subtypes, especially in the heart, kidneys and gallbladder. The synthetic peptides in Section 11 and methods in Section 8 of the thesis can be used in the following receptor characterization. The biodistribution research of AM receptor could help in interpreting some results in this thesis and guide the study on the new target molecules derived from AM. In these studies, the optimal screening system by organs or tissues exhibiting specific receptor-binding activities may furthermore contribute to the study of AM receptor subtypes.

All results reported in this thesis are about human AM in dogs and rats. In fact, some species differences were observed in the results. For future research, more attention should be paid to humans. Moreover, the study on human cells and tissues as well as humans by using radiolabeled AM or its derivatives synthesized in the thesis is expected. The study of the receptor-binding activity can be performed by using synthetic peptides and methods in the thesis on human cells in pulmonary system or lung tissues. Since the human antibodies for the receptor of CT peptide family are available now, it would be easy to confirm the receptor subtype, and devoid of the interspecies differences. The data in human cells will be helpful to guide the new radiotracer in clinical study, and the optimal screening system by human cells could be established, and applied in future screening of new drugs.

AM was studied as a target molecule for the human lung in the thesis. As a target molecule, AM is not the optimum molecule. Modification, truncation and non-peptide

antagonist study are essential for the development of a target molecule derived from AM. The study on new AM derivatives will focus on the bioactivities *in vitro* and *in vivo* because as a part of essential preclinical study, the bioactivities have to be determined by using excess dose of the radiotracer. The ligand binding and activation model of Class B GPCRs shows that the receptor binding affinity and full agonist activity in peptide ligand might not reside in the same segments or residues. The study on the amino acids that belong to essential or non-essential residues for the vasodilation activity of AM could benefit the modification of AM and its derivatives, as well as the design of new radiotracers in the future. The screening of essential amino acid residues can be carried out by using Ala scanning of AM. A series of Ala-substituted AM analogs that the amino acid in disulfide bridge and C-terminal region was changed to an Ala can be designed and synthesized by SPPS, and their vasodilation respond in the structure-activity relationship studies could be determined by rat aorta ring assay.

In this thesis, by using ^{99m}Tc-linear AM as radiotracer, a rapid elimination of radioactivity in plasma and a more than 1 h long retention in dog lungs were observed. In the study, both ^{99m}Tc and ^{99m}Tc-peptide are detectable and visible by using equipments but not linear AM alone. If the free 99m-Technetium released from ^{99m}Tc-linear AM and ^{99m}Tc-AM unbound to the receptor or AMBP-1 were responsible for the rapid elimination of radioactivity in plasma, the long retention of radioactivity in the lungs could be ^{99m}Tc-linear AM bound with AM receptors. It indicates that AM as a targeting molecule may involve in trapping ^{99m}Tc in the receptor binding. Since the internalization of AM with AM_1 was demonstrated in receptor-containing cells, and the receptor-mediated endocytosis of AM with ^{99}Tc is unknown, the study on the internalization kinetics of ^{99m}Tc-linear AM or ^{125}I-AM in AM_1-transfected cells could be useful to clarify AM pulmonary clearance from blood to kidneys and the long retention of radioactivity induced by AM in dog lungs.

In fact, a new AM derivative designed basis on AM(13-52), a partial agonist, is in the preclinical study as a lung imaging agent. Thus, all information gathered on AM SAR and receptor-binding activity in the thesis contributes to the development of new target

molecules. In the future, it is expected that the pharmacokinetics and biodistribution of the new lung-imaging agent derived from AM in humans, will be determined. In addition, dosimetric evaluation and the ability of lung perfusion imaging in humans will also be performed. The application of new target molecules derived from AM will not be limited to lung imaging. The field of the target molecule could be extended to target and treat AM-related pathologies when the molecule is conjugated with drugs treating some disorders in pulmonary circulation system.

References

ABEDINI, A., D. P. Raleigh. 2005. "Incorporation of pseudoproline derivatives allows the facile synthesis of human IAPP, a highly amyloidogenic and aggregation-prone polypeptide". Organic Letters, vol. 7, p. 693-696.

AIYAR, N., J. Disa, Z. Ao, D. Xu, A. Surya, K. Pillarisetti, N. Parameswaran, S. K. Gupta, S. A. Douglas, P. Nambi. 2002. "Molecular cloning and pharmacological characterization of bovine calcitonin receptor-like receptor from bovine aortic endothelial cells". Biochemical Pharmacology, vol.63, p.1949-1959.

AIYAR, N., J. Disa, M. Pullen, P. Nambi. 2001. "Receptor activity modifying proteins interaction with human and porcine calcitonin receptor-like receptor (CRLR) in HEK-293 cells". Molecular and Cellular Biochemistry, vol. 224, p. 123-133.

AL-SABAH, S., D. Donnelly. 2003. "A model for receptor-peptide binding at the glucagon-like peptide-1 (GLP-1) receptor through the analysis of truncated ligands and receptors". British Journal of Pharmacology, vol. 140, p. 339-346.

AMARA, S. G., J. L. Arriza, S. E. Leff, L. W. Swanson, R. M. Evans, M. G. Rosenfeld. 1985. "Expression in brain of a messenger RNA encoding a novel neuropeptide homologous to calcitonin gene-related peptide". Science, vol. 229, p. 1094–1097.

ANGELL, Y. M., J. Alsina, F. Albericio, G. Barany. 2002. "Practical protocols for stepwise solid-phase synthesis of cysteine-containing peptides". The Journal of Peptide Research, vol. 60, p. 292-299.

ANNIS, I., L. Chen, G. Barany. 1998. "Novel solid-phase reagents for facile formation of intramolecular disulfide bridges in peptides under mild conditions". Journal of the American Chemical Society, vol. 120, p. 7226-7238.

BEHR, T. M., M. Gotthardt, W. Becker, M. Béhé. 2002. "Radioiodination of monoclonal antibodies, proteins and peptides for diagnosis and the therapy. A review of standardized,

reliable and safe procedures for clinical grade levels kBq to GBq in the Göttingen/Marburg experience". Nuklearmedizin, vol. 41, p. 71-79.

BEINBORN, M. 2006. "Class B GPCRs: A hidden agonist within?". Molecular Pharmacology, vol. 70, p. 1-4.

BELTOWSKI, J., A. Jamroz. 2004. "Adrenomedullin – what do we know 10 years since its discovery?". Polish Journal of Pharmacology, vol. 56, p. 5-27.

BERK, S. C., S. P. Rohrer, S. J. Degrado, E. T. Birzin, R. T. Mosley, S. M. Hutchins, A. Pasternak, J. M. Schaeffer, D. J. Underwood, K. T. Chapman. 1999. "A combinatorial approach toward the discovery of non-peptide subtype-selective somatostatin receptor ligands". The Journal of Combinatorial Chemistry, vol. 1, p. 388-396.

BHOGAL, R., D. M. Smith, S. R. Bloom. 1992. "Investigation and characterization of binding sites for islet amyloid polypeptide in rat membrane". Endocrinology, vol. 130, p. 906-913.

BINET, V., B. Duthey, J. Lecaillon, C. Vol, J. Quoyer, G. Labesse, J.-P. Pin, L. Prézeau. 2007. "Common structural requirements for heptahelical domain function in class A and class C G protein-coupled receptors". The Journal of Biological Chemistry, vol. 282, p. 12154-12163.

BOMBERGER, J. M., N. Parameswaran, C. S. Hall, N. Aiyar, W. S. Spielman. 2005. "Novel function for receptor activity-modifying proteins (RAMPs) in post-endocytic receptor trafficking". The Journal of Biological Chemistry, vol. 280, p. 9297-9307.

BRAIN, S. D., A. D. Grant. 2004. "Vascular actions of calcitonin gene-related peptide and adrenomedullin". Physiological Reviews, vol. 84, p. 903-934.

CALVETE, J. J. 1995. "On the structure and function of platelet integrin alpha IIb beta 3, the fibrinogen receptor". Proceedings of the Society for Experimental Biology and Medicine, vol. 208, p. 346-360.

CASTRO, B., J. R. Dormoy, G. Evin, C. Selve. 1975. "Reactifs de couplage peptidique I (1)–l'hexafluorophosphate de benzotriazolyl N-oxytrisdimethylamino phosphonium (B.O.P.)". Tetrahedron Letter, vol. 16, p. 1219–1222.

CASTRO, M., V. O. Nikolaev, D. Palm, M. J. Lohse, J.-P. Vilardaga. 2005. "Turn-on switch in parathyroid hormone receptor by a two-step parathyroid hormone binding mechanism". Proceedings of the National Academy of Sciences of the United States of America, vol. 102, p. 16084-16089.

CHAKRAVARTY, P., T. P. Suthar, H. A. Coppock, C. G. Nicholl, S. R. Bloom, S. Legon, D. M. Smith. 2000. "CGRP and adrenomedullin binding correlates with transcript levels for calcitonin receptor-like receptor (CRLR) and receptor activity modifying proteins (RAMPs) in rat tissues". British Journal of Pharmacology, vol. 130, p. 189–195.

CHAMPION, H. C., J. A. Santiago, W. A. Murphy, D. H. Coy, P. J. Kadowitz. 1997. "Adrenomedullin-(22-52) antagonizes vasodilator responses to CGRP but not adrenomedullin in the cat". American Journal of Physiology-Regulatory, Integrative and Comparative Physiology, vol. 272, p. R234-R242.

CHAMPION, H. C., R. C. Fry, W. A. Murphy, D. H. Coy, P. J. Kadowitz. 1996. "Catecholamine release mediates pressor effects of adrenomedullin(15-22) in the rat". Hypertension, vol. 28, p. 1041-1046.

CHAMPION, H. C., D. E. Friedman, D. G. Lambert, W. A. Murphy, D. H. Coy, P. J. Kadowitz. 1997. "Adrenomedullin(16-31) has presser activity in the rat but not the cat". Peptides, vol. 18, p. 133-136.

CONNER, A. C., D. L. Hay, S. G. Howitt, K. Kilk, U. Langel, M. Wheatley, D. M. Smith, D. R. Poyner. 2002. "Interaction of calcitonin-gene-related peptide with its receptors". Biochemical Society Transactions, vol. 30, p. 451–455.

CONNER, A. C., J. Simms, J. Barwell, M. Wheatley, D. R. Poyner. 2007. "Ligand binding and activation of the CGRP receptor". Biochemical Society Transactions, vol. 35, p. 729–732.

COPP, D. H. 1969. "Endocrine control of calcium homeostasis". Journal of Endocrinology, vol. 43, p. 137–161.

COPPOCK, H. A., A. A. Owji, C. Austin, P. D. Upton, M. L. Jackson, J. V. Gardiner, M. A. Ghatei, S. R. Bloom, D. M. Smith. 1999. "Rat-2 fibroblasts express specific adrenomedullin receptors, but not calcitonin-gene-related-peptide receptors, which mediate increased intracellular cAMP and inhibit mitogen-activated protein kinase activity". Biochemical Journal, vol. 338, p. 15–22.

COPPOCK, H. A., A. A. Owji, S. R. Bloom, D. M. Smith. 1996. "A rat skeletal muscle cell line (L6) expresses specific adrenomedullin binding sties but activates adenylate cyclase via calcitonin gene-related peptide receptors". Biochemical Journal, vol 318, p. 241-245.

COTTRELL, G. S., D. Roosterman, J. C. Marvizon, B. Song, E. Wick, S. Pikios, H. Wong, C. Berthelier, Y. Tang, C. Sternini, N. W. Bunnett, E. F. Grady. 2005. "Localization of calcitonin receptor-like receptor and receptor activity modifying protein 1 in enteric neurons, dorsal root ganglia, and the spinal cord of the rat". The Journal of Conparative Neurology, vol. 490, p. 239-255.

DAGAR, S., A. Krishnadas, I. Rubinstein, M. J. Blend, H. Onyuksel. 2003. "VIP grafted sterically stabilized liposomes for targeted imaging of breast cancer: in vivo studies". Journal of Controlled Release, vol. 91, p. 123-133.

DANG, K., J. Disa, B. Gout, N. Aiyar. 1999. " Comparative affinities of adrenomedullin (AM) and calcitonin gene-related peptide (CGRP) for [^{125}I] AM and [^{125}I] CGRP specific binding sites in porcine tissues ". Journal of Receptor Signal Transduct Research, vol. 19, p. 803-817.

DEL ROSARIO, R. B., Y. W. Jung, K. E. Baidoo, S. Z. Lever, D. M. Wieland. 1994. "Synthesis and *in vivo* evaluation of a ^{99m}Tc-DADT-benzovesamicol: a potential marker for cholinergic neurons". Nuclear Medicine and Biology, vol. 21, p. 197-203.

DENNIS, T., A. Fournier, A. Cadieux, F. Pomerleau, F. B. Jolicoeur, S. St pierre, R. Quirion. 1990. "hCGRP$_{8-37}$, a calcitonin gene-related peptide antagonist revealing CGRP receptor heterogeneity in brain and periphery". The Journal of Pharmacology and Experimental Therapeutics, vol. 254, p. 123-128.

DIJKGRAAF, I., O. C. Boerman, W. J. Oyen, F. H. Corstens, M. Gotthardt. 2007. "Development and application of peptide-based radiopharmaceuticals". Anti-cancer Agents in Medicinal Chemistry, vol. 7, p. 543-551.

DILWORTH, J. R., S. J. Parrott. 1998. "The biomedical chemistry of technetium and rhenium". Chemical Society Reviews, vol. 27, p. 43-55.

DONG, M., Z. Li, M. Zang, D. I. Pinon, T. P. Lybrand, L. J. Miller. 2003. "Spatial approximation between two residues in the mid-region of secretin and the amino terminus of its receptor. Incorporation of seven sets of such constraints into a three-dimensional model of the agonist-bound secretin receptor". The Journal of Biological Chemistry, vol. 278, p. 48300-48312.

DONG, M., D. I. Pinon, R. F. Cox, L. J. Miller. 2004. "Molecular approximation between a residue in the amino-terminal region of calcitonin and the third extracellular loop of the

class B G protein-coupled calcitonin receptor". The Journal of Biological Chemistry, vol. 279, p. 31177-31182.

DONG, M., D. I. Pinon, L. J. Miller. 2005. "Insights into the structure and molecular basis of ligand docking to the G protein-coupled secretin receptor using charge-modified amino-terminal agonist probes". Molecular Endocrinology, vol. 19, p. 1821-1836.

DONG, M., D. I. Pinon, Y. W. Asmann, L. J. Miller. 2006. "Possible endogenous agonist mechanism for the activation of secretin family G protein-coupled receptors". Molecular Pharmacology, vol. 70, p. 206-213.

DOODS, H., G. Hallermayer, D. Wu, M. Entzeroth, K. Rudolf, W. Engel, W. Eberlein. 2000. "Pharmacological profile of BIBN4096BS, the first selective small molecule CGRP antagonist". British Journal of Pharmacology, vol. 129, p. 420–423.

DOODS, H. 2001. "Development of CGRP antagonists for the treatment of migraine". Current Opinion in Investigational Drugs, vol. 2, p. 1261–1268.

DSCHIETZIG, T., H. A. Azad, L. Asswad, C. Böhme, C. Bartsch, G. Baumann, K. Stangl. 2002. "The adrenomedullin receptor acts as clearance receptor in pulmonary circulation". Biochemical and Biophysical Research Communications, vol. 294, p. 315-318.

DUPUIS, J., A. Caron, N. Ruël. 2005. "Biodistribution, plasma kinetics and quantification of single-pass pulmonary clearance of adrenomedullin". Clinical Science, vol. 109, p. 97-102.

EDWARDS, D. S., S. Liu, J. A. Barrett, A. R. Harris, R. J. Looby, M. C. Ziegler, S. J. Heminway, T. R. Carroll. 1997. "New and versatile ternary ligand system for technetium radiopharmaceuticals: water soluble phosphines and tricine as coligands in labeling a

hydrazinonicotinamide-modified cyclic glycoprotein IIb/IIIa receptor antagonist with ^{99m}Tc". Bioconjugate Chemistry, vol. 8, p. 146-154.

EGUCHI, S., Y. Hirata, H. Iwasaki, K. Sato, T. X. Watanabe, T. Inui, K. Nakajima, S. Sakakibara, F. Marumo. 1994. "Structure-activity relationship of adrenomedullin, a novel vasodilatory peptide, in cultured rat vascular smooth muscle cells". Endocrinology, vol. 135, p. 2454-2458.

EGUCHI, S., Y. Hirata, H. Kano, K. Sato, Y. Watanabe, T. X. Watanabe, K. Nakajima, S. Sakakibara, F. Marumo. 1994. "Specific receptors for adrenomedullin in cultured rat vascular smooth muscle cells". FEBS Letters, vol. 340, p. 226-230.

ELLMAN, G. L. 1959. "Tissue sulfhydryl groups". Archives of Biochemistry and Biophysics, vol. 82, p. 70-77.

EVANS, B. N., M. I. Rosenblatt, L. O. Mnayer, K. R. Oliver, I. M. Dickerson. 2000. "CGRP-RCP, a novel protein required for signal transduction at calcitonin gene-related peptide and adrenomedullin receptors". The Journal of Biological Chemistry, vol. 275, p. 31438–31443.

FLÜHMANN, B., R. Muff, W. Hunziker, J. A. Fischer, W. Born. 1995. "A human orphan calcitonin receptor-like structure". Biochemical and Biophysical Research Communications, vol. 206, p. 341–347.

FONTENOT, J. D., J. M. Ball, M. A. Miller, C. M. David, R. C. Montelaro. 1991. "A survey of potential problems and quality control in peptide synthesis by the fluorenylmethoxycarbonyl procedure". Peptide Research, vol. 4, p. 19-25.

FOSTER, G. V., I. Macintyre, A. E. G. Pearse. 1964. "Calcitonin production and the mitochondrion-rich cells of the dog thyoid". Nature, vol. 203, p. 1029-1030.

FOURNIER, A., C. T. Wang, A. M. Felix. 1998. "Applications of BOP reagent in solid phase synthesis. Advantages of BOP reagent for difficult couplings exemplified by a synthesis of [Ala 15]-GRF(1-29)-NH_2". International Journal of Peptide Protein Research, vol. 31, p. 86–97.

FRITZBERG, A. R., R. W. Berninrer, S. W. Hadley, D. W. Wester. 1988. "Approaches to radiolabeling of antibodies for diagnosis and therapy of cancer". Pharmaceutical Research, vol. 5, p. 325-334.

GIBBONS, C., R. Dackor, W. Dunworth, K. Fritz-Six, K. D. Caron. 2007. "Receptor activity-modifying protein: RAMPing up adrenomedullin signaling". Molecular Endocrinology, vol. 21, p. 783-796.

HABERKORN, U., M. Eisenhut, A. Altmann, W. Mier. 2008. "Endoradiotherapy with peptides – status and future development". Current Medicinal Chemistry, vol. 15, p. 219-234.

HAGNER, S., R. V. Haberberger, D. Overkamp, R. Hoffmann, K. H. Voigt, G. P. McGregor. 2002. "Expression and distribution of calcitonin receptor-like receptor in human hairy skin". Peptides, vol. 23, p. 109-116.

HAGNER, S., U. Stahl, B. Knoblauch, G. P. McGregor, R. E. Lang. 2002. "Calcitonin receptor-like receptor: identification and distribution in human peripheral tissues". Cell Tissue Research, vol. 310, p. 41-50.

HAO, Q., J. K. Chang, H. Gharavi, Y. Fortenberry, A. Hyman, H Lippton. 1994. "An adrenomedullin (ADM) fragment retains the systemic vasodilator activity of human ADM". Life Sciences, vol. 54, p. 265-270.

HASHIMOTO, H., S. Hyodo, M. Kawasaki, M. Shibata, T. Saito, H. Suzuki, H. Otsubo, T. Yokoyama, H. Fujihara, T. Higuchi, Y. Takei, Y. Ueta. 2007. "Adrenomedullin 2 (AM2)/intermedin is a more potent activator of hypothalamic oxytocin-secreting neurons

than AM possibly through an unidentified receptor in rats". Peptides, vol. 28, p. 1104-1112.

HAYAKAWA, H., Y. Hirata, M. Kakoki, Y. Suzuki, H. Nishimatsu, D. Nagata, E. Suzuki, K. Kikuchi, T. Nagano, K. Kangawa, H. Matsuo, T. Sugimoto, M. Omata. 1999. "Role of nitric oxide-cGMP pathway in adrenomedullin-induced vasodilation in the rat". Hypertension, vol. 33, p. 689-693.

HAY, D. L., D. R. Poyner, P. M. Sexton. 2006. "GPCR modulation by RAMPs". Pharmacology and Therapeutics, vol. 109, p. 173-197.

HAY, D. L., S. G. Howitt, A. C. Conner, M. Schindler, D. M. Smith, D. R. Poyner. 2003. "CL/RAMP2 and CL/RAMP3 produce pharmacologically distinct adrenomedullin receptor: a comparison of effects of adrenomedullin$_{22-52}$, CGRP$_{8-37}$ and BIBN4096BS". British Journal of Pharmacology, vol. 140, p. 477-486.

HAY, D. L., D. R. Poyner, P. M. Sexton. 2008. "International union of pharmacology: Status of the calcitonin gene-related peptide subtype 2 receptor". Pharmacology Reviews, in press.

HINSON, J. P., S. Kapas, D. M. Smith. 2000. "Adrenomedullin, a multifunctional regulatory peptide". Endocrine Reviews, vol. 21, p. 138-167.

HIRAYAMA, N., K. Kitamura, T. Imamura, J. Kato, Y. Koiwaya, T. Eto. 1999. "Secretion and clearance of the mature form of adrenomedullin in humans". Life Sciences, vol. 64, p. 2505-2509.

HNATOWICH, D. J., W. W. Layne, R. L. Childs. 1982."The preparation and labeling of DTPA-coupled albumin". The International Journal of Applied Radiation and Isotopes, vol., 33, p. 327-332.

HOARE, S. R. 2005. "Mechanisms of peptide and nonpeptide ligand binding to Class B G-protein-coupled receptors". Drug Discovery Today, vol. 10, p. 417-427.

HOM, R.K., J. A. Katzenellenbogen. 1997. "Technetium-99m-labeled receptor-specific small-molecule radiopharmaceuticals: recent developments and encouraging results". Nuclear Medicine and Biology, vol. 24, p. 485-498.

HOWITT, S. G., D. R. Poyner. 1997. "The selectivity and structural determinants of peptide antagonists at the CGRP receptor of rat, L6 myocytes". British Journal of Pharmacology, vol. 121, p. 1000-1004.

ISHIMITSU, T., H. Ono, J. Minami, H. Matsuoka. 2006. "Pathophysiologic and therapeutic implications of adrenomedullin in cardiovascular disorders". Pharmacology & Therapeutics, vol. 111, p. 909-927.

ISHIZAKA, Y., Y. Ishizaka, M. Tanaka, K. Kitamura, K. Kangawa, N. Minamino, H. Matsuo, T. Eto. 1994. "Adrenomedullin stimulates cyclic AMP formation in rat vascular smooth muscle cells". Biochemical and Biophysical Research Communications, vol. 200, p. 642-646.

JIANG, W., H.-F. Jiang, D.-Y. Cai, C.-S. Pan, Y.-F. Qi, Y.-Z. Pang, C.-S. Tang. 2004. "Relationship between contents of adrenomedullin and distributions of neutral endopeptidase in blood and tissues of rats in septic shock". Regulatory Peptides, vol. 118, p. 199-208.

Joint international symposium on calcitonin gene-related peptide, amylin and calcitonin. 2004. "4th symposium on adrenomedullin and proadrenomedullin N-20 peptide". Neuropeptides, vol. 38, p. 110-131.

JUANEDA, C., Y. Dumont, J. G. Chabot, A. Fournier, R. Quirion. 2003. " Adrenomedullin receptor binding sites in rat brain and peripheral tissues ". European Journal of Pharmacology, vol. 474, p. 165-174.

JULIÁN, M., M. Cacho, M. A. García, S. Martín-Santamaría, B. de Pascual-Teresa, A. Ramos, A. Martínez, F. Cuttitta. 2005. "Adrenomedullin: a new target for the design of small molecule modulators with promising pharmacological activities". European Journal of Medicinal Chemistry, vol. 40, p. 737-750.

KAISER, E., R. L. Colescott, C. D. Bossinger, P. I. Cook. 1970. "Color test for detection of free terminal amino groups in the solid-phase synthesis of peptides". Analytical Biochemistry, vol. 34, p. 595-598.

KAMOHARA, M., A. Matsuo, J. Takasaki, M. Kohda, M. Matsumoto, S. Matsumoto, T. Soga, H. Hiyama, M. Kobori, M. Katou. 2005. "Identification of MrgX2 as a human G-protein-coupled receptor for proadrenomedullin N-terminal peptides". Biochemical and Biophysical Research Communications, vol. 330, p. 1146-1152.

KATAFUCHI, T., K. Hamano, K. Kikumoto, N. Minamino. 2003. "Identification of second and third calcitonin receptor-stimulating peptides in porcine brain". Biochemical and Biophysical Research Communications, vol. 308, p. 445–451.

KATAFUCHI, T., K. Kikumoto, K. Hamano, K. Kangawa, H. Matsuo, N. Minamino. 2003. "Calcitonin receptor-stimulating peptide, a new member of the calcitonin gene-related peptide family. Its isolation from porcine brain, structure, tissue distribution, and biological activity". The Journal of Biological Chemistry, vol. 278, p. 12046–12054.

KIM, W., S. O. Moon, M. J. Sung, S. H. Kim, S. Lee, H. J. Kim, G. Y. Koh, S. K. Park. 2002. "Protective effect of adrenomedullin in mannitol-induced apoptosis". Apoptosis, vol. 7, p. 527-536.

KITAMURA, K., E. Matsui, J. Kato, F. Katoh, T. Kita, T. Tsuji, K. Kangawa, T. Eto. 2001. "Adrenomedullin(11-26): a novel endogenous hypertensive peptide isolated from bovine adrenal medulla". Peptides, vol. 22, p. 1713-1718.

KITAMURA, K., J. Kato, M. Kawamoto, M. Tanaka, N. Chino, K. Kangawa, T. Eto. 1998. "The intermediate form of glycine-extended adrenomedullin is the major circulating molecular form in human plasma". Biochemical and Biophysical Research Communications, vol. 244, p. 551-555.

KITAMURA, K., J. Sakata, K. Kangawa, M. Kojima, H. Matsuo, T. Eto. 1993. "Cloning and characterization of cDNA encoding a precursor for human adrenomedullin". Biochemical and Biophysical Research Communications, vol. 194, p. 720–725.

KITAMURA K., K. Kangawa, M. Kawamoto, Y. Ichiki, S. Nakamura, H. Matsuo, T. Eto. 1993. "Adrenomedullin: a novel hypotensive peptide isolated from human pheochromocytoma". Biochemical and Biophysical Research Communications, vol. 192, p. 553–560.

KLEISNER, I., P. Komárek, I. Komárková, M. Konopková. 2000. "The use of redox polymers in labeling procedures of proteins and peptides with ^{99m}Tc. I. Properties of redox polymers and technique of labelling". Neclear Medicine Review, vol. 3, p. 65-68.

KLIBANOV, A. L., A. V. Martynov, M. A. Slinkin, I. Y. Sakharov, M. D. Smirnov, V. R. Muzykantov, S. M. Danilov, V. P. Torchilin. 1988. "Blood clearance of radiolabeled antibody: Enhancement by lactosamination and treatment with biotin-avidin or anti-mouse IgG antibodies". Journal of Nuclear medicine, vol. 29, p. 1951-1956.

KREJCAREK, G. E., K. L. Tucker. 1977. "Covalent attachment of chelating groups to macromolecules". Biochemical and Biophysical Research Communications, vol. 77, p. 581-585.

KUWASAKO, K., K. Kitamura, H. Onitsuka, T. Uemura, Y. Nagoshi, J. Kato, T. Eto. 2002. "Rat RAMP domains involved in adrenomedullin binding specificity". FEBS Letters, vol. 519, p. 113-116.

KWEKKEBOOM, D. J., E. P. Krenning, G. S. Kho, W. A. Breeman, P. M. Van Hagen. 1998. "Somatostatin receptor imaging in patients with sarcoidosis". European Journal of Nuclear Medicine, vol. 25, p. 1284-1292.

LAMAS, S., P. A. Marsden, G. K. Li, P. Tempst, T. Michel. 1992. "Endothelial nitric oxide synthase: molecular cloning and characterization of a distinct constitutive enzyme isoform". Proceedings of the National Academy of Sciences of the United States of American, vol. 89, p.6348-6352.

LEVER, S. Z., K. E. Baidoo, A. Mahmood, K. Matsumura, U. Scheffel, H. N. Jr. Wagner. 1994. "Novel technetium ligands with affinity for the muscarinic cholinergic receptor". Nuclear Medicine and Biology, vol. 21, p.157-164.

LEWIS, L. K., M. W. Smith, T. G. Yandle, A. M. Richards, M. G. Nicholls. 1998. "Adrenomedullin(1-52) measured in human plasma by radioimmunoassay: plasma concentration, adsorption, and storage". Clinical Chemistry, vol. 44, p. 571-577.

LIN, H.Y., T. L. Harris, M. S. Flannery, A. Aruffo, E. H. Kaji, A. Gorn, L. F. Jr. Kolakowski, H. F. Lodish, S. R. Goldring. 1991. "Expression cloning of an adenylate cyclase-coupled calcitonin receptor". Science, vol. 254, p. 1022–1024.

LISY, O., M. Jougasaki, J. A. Schirger, H. H. Chen, P. T. Barclay, J. C. JR. Burnett. 1998. "Neutral endopeptidase inhibition potentiates the natriuretic actions of adrenomedullin". American Journal of Physiology Renal Physiology, vol. 275, p. F410-414.

LIU, S., D. S. Edwards, J. A. Barrett. 1997. "^{99m}Tc labeling of high potent small peptides". Bioconjugate Chemistry, vol. 8, p. 621-636.

MANSI, R., D. Tesauro, A. De Capua, R. Fattorusso, C. Caracò, L. Aloj, E. Benedetti, G. Morelli. 2004. "Peptide-chelating agent conjugate for selective targeting of somatostatin receptor type 1: Synthesis and characterization". Biopolymers, vol. 76, p. 527-534.

MARTÍNEZ, A., M. J. Miller, K. J. Catt, F. Cuttitta. 1997. "Adrenomedullin receptor expression in human lung and in pulmonary tumors". The Journal of Histochemistry & Cytochemistry, vol. 45, p. 159-164.

MARUTSUKA, K., K. Hatakeyama, Y. Sato, A. Yamashita, A. Sumiyoshi, Y. Asada. 2003. "Immunohistological localization and possible functions of adrenomedullin". Hypertension Research, vol. 26, p. S33-S40.

MCCURDY, S. N. 1989. "The investigation of Fmoc-cysteine derivatives in solid phase peptide synthesis". Peptide Research, vol. 2, p. 147-152.

MCLATCHIE, L. M., N. J. Fraser, M. J. Main, A. Wise, J. Brown, N. Thompson, R. Solari, M. G. Lee, S. M. Foord. 1998. "RAMPs regulate the transport and ligand specificity of the calcitonin-receptor-like receptor". Nature, vol. 393, p. 333-339.

MILLER, M. J., A. Martínez, E. J. Unsworth, C. J. Thiele, T. W. Moody, T. Elsasser, F. Cuttitta. 1996. "Adrenomedullin expression in human tumor cell lines. Ite potential role as autocrine growth factor". The Journal of Biological Chemistry, vol. 271, p. 23345-23351.

MIMEAULT, M., A. Fournier, Y. Dumont, S. St-Pierre, R. Quirion. 1991. "Comparative affinities and antagonistic potencies of various human calcitonin gene-related peptide fragments on calcitonin gene-related peptide receptors in brain and periphery". The Journal of Pharmacology and Experimental Therapeutics, vol. 258, p. 1084-1090.

MIMEAULT, M., R. Quirion, Y. Dumont, S. St-Pierre, A. Fournier. 1992. "Structure-activity study of $hCGRP_{8-37}$, a calcitonin gene-related peptide receptor antagonist". Journal of Medicinal Chemistry, vol. 35, p. 2163-2168.

MORELLI, G., S. De Luca, D. Tesauro, M. Saviano, C. Pedone, A. Dolmella, R. Visentin, U. Mazzi. 2002. "CCK8 peptide derivatized with diphenylphosphine for rhenium labelling: Synthesis and molecular mechanics calculations". Journal of Peptide Science, vol. 8, p. 373-381.

MORIMOTO, R., F. Satoh, O. Murakami, K. Totsune, T. Suzuki, H. Sasano, S. Ito, K. Takahashi. 2007. "Expression of adrenomedullin2/intermedin in human brain, heart, and kidney". Peptides, vol. 28, p. 1095-1103.

MOTULSKY, H. 1995-2001. "The GraphPad guide to analyzing radioligand binding data". GraphPad Software, graphpad.com.

NAGAE, T., M. Mukoyama, A. Sugawara, K. Mori, K. Yahata, M. Kasahara, T. Suganami, H. Makina, Y. Fujinaga, T. Yoshioka, I. Tanaka, K. Nakao. 2000. "Rat receptor-activity-modifying protein (RAMPs) for adrenomedullin/CGRP receptor: cloning and upregulation in obstructive nephropathy". Biochemical and Biophysical Research Communications, vol. 270, p. 89-93.

NEHER, R., B. Riniker, R. Maier, P. G. H. Byfield, T. V. Gudmundsson, I. MacIntyre. 1968. "Human Calcitonin". Nature, vol. 220, p. 984-986.

NIKITENKO, L. L., N. Blucher, S. B. Fox, R. Blcknell, D. M. Smith, M. C. P. Rees. 2006. "Adrenomedullin and CGRP interact with endogenous calcitonin-receptor-like receptor in endothelial cells and induce its desensitization by different mechanisms". Journal of Cell Science, vol. 119, p. 910-922.

NISHIKIMI, T., H. Matsuoka, K. Shimada, H. Matsuo, K. Kangawa. 2000. "Production and clearance sites of two molecular forms of adrenomedullin in human plasma". American Journal of Hypertension, vol. 13, p. 1032-1034.

NISHIKIMI, T. 2007. "Adrenomedullin in the kidney-renal physiological and pathophysiological roles". Current Medicinal Chemistry, vol. 14, p. 1689-1699.

NOSSAMAN, B. D., C. J. Feng, D. Y. Cheng, B. J. Dewitt, D. H. Coy, W. A. Murphy, P. J. Kadowitz. 1995. "Comparative effects of adrenomedullin, an adrenomedullin analog, and CGRP in the pulmonary vascular bed of the cat and rat". Life Sciences, vol. 56, p. PL63-66.

NOTOYA, M., R. Arai, T. Katafuchi, N. Minamino, H. Hagiwara. 2007. "A novel member of the calcitonin gene-related peptide family, calcitonin receptor-stimulating peptide, inhibits the formation and activity of osteoclasts". European Journal of Pharmacology, vol. 560, p. 234-239.

OKARVI, S. M., I. al-Jammaz. 2003. "Synthesis, radiolabelling and biological characteristics of a bombesin peptide analog as a tumor imaging agent". Anticancer Research, vol. 23, p. 2745-2750.

OKARVI, S. M. 2008. "Peptide-based radiopharmaceuticals and cytotoxic conjugates: Potential tools against cancer". Cancer Treatment Reviews, vol. 34, p. 13-26.

OWJI, A. A., D. M. Smith, H. A. Coppock, D. G. A. Morgan, R. Bhogal, M. A. Ghatei, S. R. Bloom. 1995. "An abundant and specific binding site for the novel vasodilator adrenomedullin in the rat". Endocrinology, vol. 136, p. 2127-2134.

OWJI, A. A., J. V. Gardiner, P. D. Upton, M. Mahmoodi, M. A. Ghatei, S. R. Bloom, D. M. Smith. 1996. "Characterisation and molecular identification of adrenomedullin

binding sites in the rat spinal cord: A comparison with calcitonin gene-related peptide receptors". Journal of Neurochemistry, vol. 67, p. 2172-2179.

PARAMESWARAN, N., W. S. Spielman. 2006. "RAMPs: The past, present and future". Trends in Biochemical Sciences, vol. 31, p. 631-638.

PAXTON, R. J., J. G. Jakowatz, J. D. Beatty, B. G. Beatty, W. G. Vlahos, L. E. Williams, B. R. Clark, J. E. Shively. 1985. "High-specific-activity ^{111}In-labeled anticarcinoembryonic antigen monoclonal antibody: improved method for the synthesis of diethylenetriaminepentaacetic acid conjugates". Cancer Research, vol. 45, p. 5694-5699.

PETRIE, M. C., C. Hillier, F. Johnston, J. J. McMurray. 2001. "Effect of neutral endopeptidase inhibition on the actions of adrenomedullin and endothelin-1 in resistance arteries from patients with chronic heart failure". Hypertension, vol. 38, p. 412-416.

POLAKOV, V., V. Sharma, J. L. Dahlheimer, C. M. Pica, G. D. Luker, D. Piwnica-Worms. 2000. "Novel Tat-peptide chelates for direct transduction of technetium-99m and rhenium into human cells for imaging and radiotherapy". Bioconjugate Chemistry, vol. 11, p. 762-771.

POWELL, K. J., W. Ma, M. Sutak, H. Doods, R. Quirion, K. Jhamandas. 2000. "Blockade and reversal of spinal morphine tolerance by peptide and non-peptide calcitonin gene-related peptide receptor antagonists". British Journal of Pharmacology, vol. 131, p. 875–884.

POYNER, D. R., P. M. Sexton, I. Marshall, D. M. Smith, R. Quirion, W. Born, R. Muff, J. A. Fischer, S. M. Foord. 2002. "International Union of Pharmacology. XXXII. The mammalian calcitonin gene-related peptides, adrenomedullin, amylin, and calcitonin receptors". Pharmacological Reviews, vol. 54, p. 233–246.

RAMACHANDRAN, V., T. Arumugam, R. F. Hwang, J. K. Greenson, D. M. Simeone, C. D. Logsdon. 2007. "Adrenomedullin is expressed in pancreatic cancer and stimulates cell proliferation and invasion in an autocrine manner via the adrenomedullin receptor, ADMR". Cancer Research, vol. 67, p. 2666-2675.

RENNERT, R., I. Neundorf, A. G. Beck-Sickinger. 2008. "Calcitonin-derived peptide carriers: mechanism and application", Advanced Drug Delivery Reviews, vol. 60, p. 485-498.

RINK, T. J., K. Beaumont, J. Koda, A, Young. 1993. "Structure and biology of amylin". Trends in Pharmacological Sciences, vol. 14, p. 113-118.

ROH, J., C. L. Chang, A. Bhalla, C. Klein, S. Y. Hsu. 2004. "Intermedin is a calcitonin/calcitonin gene-related peptide family peptide acting through the calcitonin receptor-like receptor/receptor activity-modifying protein receptor complexes". The Journal of Biological Chemistry, vol. 279, p. 7264- 7274.

RORABAUGH, B. R., M. A. Scofield, D. D. Smith, W. B. Jeffries, P. W. Abel. 2001. "Functional calcitonin gene-related peptide subtype 2 receptors in porcine coronary arteries are identified as calcitonin gene-related peptide subtype 1 receptors by radioligand binding and reverse transcription-polymerase chain reaction". Journal of Pharmacology and Experimental Therapeutics, vol. 299, p. 1086–1094.

ROSENFELD, M. G., J. J. Mermod, S. G. Amara, L. W. Swanson, P. E. Sawchenko, J. Rivier, W.W. Vale, R. M. Evans. 1983. "Production of a novel neuropeptide encoded by the calcitonin gene via tissue-specific RNA processing". Nature, vol. 304, p. 129–135.

SABATES, B., T. Granger, E. Choe, J. Pigott, H. Lippton, A. Hyman, L. Flint, J. Ferrara. 1996. "Adrenomedullin is inactivated in the lungs of neonatal piglets". Journal of pharmacy and pharmacology, vol. 48, p. 578-580.

SAKATA, J., T. Shimokubo, K. Kitamura, S. Nakamura, K. Kangawa, H. Matsuo, T. Eto. 1993. "Molecular cloning and biological activities of rat adrenomedullin, a hypotensive peptide". Biochemical and Biophysical Research Communications, vol. 195, p. 921–927.

SANSOÈ, G., M. Aragno, R. Mastrocola, F. Restivo, G. Mengozzi, A. Smedile, F. Rosina, O. Danni, M. Parola, M, Rizzetto. 2005. "Neutral endopeptidase (EC 3.4.24.11) in cirrhotic liver: a new target to treat portal hypertension?". Journal of Hepatology, vol. 43, p. 791-798.

SANTIAGO, J. A., E. Garrison, W. L. Purnell, R. E. Smith, H. C. Champion, D. H. Coy, W. A. Murphy, P. J. Kadowitz. 1995. "Comparison of response to adrenomedullin and adrenomedullin analogs in the mesenteric vascular bed of the cat". European Journal of Pharmacology, vol. 272, p. 115-118.

SCHWARZ, N., D. Renshaw, S. Kapas, J. P. Hinson. 2006. "Adrenmedullin increases the expression of calcitonin-like receptor and receptor activity modifying protein 2 mRNA in human microvascular endothelial cells". Journal of Endocrinology, vol. 190, p. 505-514.

SHAPIRO, B. 1996. "Radiolabeled peptides as radiopharmaceuticals: the move of the future". Biomedicine and Pharmacotherapy, vol. 50, p. 410.

SHICHIRI, M., N. Fukai, N. Ozawa, H. Iwasaki, Y. Hirata. 2003. "Adrenomedullin is an autocrine/paracrine growth factor for rat vascular smooth muscle cells". Regulatory Peptides, vol. 112, p. 167-173.

SHIMEKAKE, Y., K. Nagata, S. Ohta, Y. Kambayashi, H. Teraoka, K. Kitamura, T. Eto, K. Kangawa, H. Matsuo. 1995. "Adrenomedullin stimulates two signal transduction pathways, cAMP accumulation and Ca^{2+} mobilization, in bovine aortic endothelial cells". The Journal of Biological Chemistry, vol. 270, p. 4412-4417.

SHIMOKUBO, T., J. Sakata, K. Kitamura, K. Kangawa, H. Matsuo, T. Eto. 1995. "Augmented adrenomedullin concentrations in right ventricle and plasma of experimental pulmonary hypertension". Life Sciences, vol. 57, p. 1771-1779.

SHIMOSAWA, T., Y. Shibagaki, K. Ishibashi, K. Kitamura, K. Kangawa, S Kato, K. Ando, T. Fujita. 2002. "Adrenomedullin, an endogenous peptide, counteracts cardiovascular damage". Circulation, vol.105, p. 106-111.

SHINDO, T., Y. Kurihara, H. Nishimatsu, N. Mcriyama, M. Kakoki, Y. Wang, Y. Imai, A. Ebihara, T. Kuwaki, K. H. Ju, N. Minamino, K. Kangawa, T. Ishikawa, M. Fukuda, Y. Akimoto, H. Kawakami, T. Imai, H. Morita, Y. Yazaki, R. Nagai, Y. Hirata, H. Kurihara. 2001. "Vascular abnormalities and elevated blood pressure in mice lacking adrenomedullin gene". Circulation, vol. 104, p. 1964-1971.

SILVESTRE, R. A., M. Salas, J. Rodríguez-Gallardo, O. García-Hermida, T. Fontela, J. Marco. 1996. "Effect of (8–32) salmon calcitonin, an amylin antagonist, on insulin, glucagon and somatostatin release: study in the perfused pancreas of the rat". British Journal of Pharmacology, vol. 117, p. 347–350.

STEINER, S., R. Muff, R. Gujer, J. A. Fischer, W. Born. 2002. "The transmembrane domain of receptor-activity-modifying protein 1 is essential for the functional expression of a calcitinin gene-related peptide receptor". Biochemistry, vol. 41, p. 11398-11404.

TAILLEFER, R., S. Edell, G. Innes, J. Lister-James. 2000. "Acute thromboscintigraphy with ^{99m}Tc-apcitide: results of the phase 3 multicenter clinical trial comparing ^{99m}Tc-apcitide scintigraphy with contrast venography for imaging acute DVT. Multicenter Trial Investigators". The Journal of Nuclear Medicine, vol. 41, p. 1214-1223.

TAKAHASHI, K., K. Kikuchi, Y. Maruyama, T. Urabe, K. Nakajima, H. Sasano, Y. Imai, O. Murakami, K. Totsune. 2006. "Immunocytochemical localization of

adrenomedullin 2/intermedin-like immunoreactivity in human hypothalamus, heart, and kidney". Peptides, vol. 27, p. 1383-1389.

TAKEI, Y., K. Inoue, M. Ogoshi, T. Kawahara, H. Bannai, S. Miyano. 2004. "Identification of novel adrenomedullin in mammals: a potent cardiovascular and renal regulator". FEBS Letter, vol. 556, p. 53-58.

TAM, C. W., K. Husmann, N. C. Clark, J. E. Clark, Z. Lazar, L. M. Ittner, J. Götz, G. Douglas, A. D. Grant, D. Sugden, L. Poston, R. Poston, I. McFadzean, M. S. Marber, J. A. Fischer, W. Born, S. D. Brain. 2006. "Enhanced vascular responses to adrenomedullin in mice overexpressing receptor-activity-modifying protein 2". Circulation Research, vol. 98, p. 262-270.

TAM, J. P., C.-R. Wu, W. Liu, J.-W. Zhang. 1991. "Disulfide bond formation in peptides by dimethyl sulfoxide. Scope and applications". Journal of the American Chemical Society, vol. 113, p. 6657-6662.

TAN, Y. V., A. Couvineau, S. Murail, E. Ceraudo, J. M. Neumann, J. J. Lacapère, M. Laburthe. 2006. "Peptide agonist docking in the N-terminal ectodomain of a class II G protein-coupled receptor, the VPAC1 receptor". The Journal of Biological Chemistry, vol. 281, p. 12792-12798.

The PIOPED Investigators. 1990. "Value of the ventilation/perfusion scan in acute pulmonary embolism. Results of the prospective investigation of pulmonary embolism diagnosis (PIOPED)". The Journal of the American Medical Association, vol. 263, p. 2753-2759.

UDAWELA, W., D. L. Hay, P. M. Sexton. 2004. "The receptor activity modifying protein family of G protein coupled receptor accessory proteins". Seminars in cell & developmental biology, vol. 15, p. 299-308.

VAN ROSSUM, D., U. K. Hanisch, R. Quirion. 1997. "Neuroanatomical localization, pharmacological characterization and functions of CGRP, related peptides and their receptors". Neuroscience & Biobehavioral Reviews, vol. 21, p. 649-678.

VÁZQUEZ, J., G. Qushair, F. Albericio. 2003. "Qualitative colorimetric tests for solid phase synthesis". Methods in Enzymology, vol. 369, p. 21-35.

WATANABE, T. X., Y. Itahara, T. Inui, K. Yoshizawa-Kumagaye, K. Nakajima, S. Sakakibara. 1996. "Vasopressor activities of N-terminal fragments of adrenomedullin in anesthetized rat". Biochemical and Biophysical Research Communications, vol. 219, p. 59-63.

WEINMAN, E. J., R. A. Hall, P. A. Friedman, L. Y. Liu-Chen, S. Shenolikar. 2006. "The association of NHERF adaptor proteins with G protein-coupled receptors and receptor tyrosine kinases". Annual Review of Physiology, vol. 68, p. 491-505.

WERLE, M., A. Bernkop-Schnürch. 2006. "Strategies to improve plasma half life of peptide and protein drugs". Amino Acids, vol. 30, p. 351-367.

WESTERMARK, P., C. Wernstedt, E. Wilander, K. Sletten. 1986. "A novel peptide in the calcitonin gene related peptide family as an amyloid fibril protein in the endocrine pancreas". Biochemical and Biophysical Research Communications, vol. 140, p. 827–831.

WHITE, M. M., W. K. Samson. 2007. "Intermedin 17-47 does not function as a full intermedin antagonist within the central nervous system or pituitary". Peptides, vol. 28, p. 2171-2178.

WILKINS, M. R., J. Redondo, L. A. Brown. 1997. "The natriuretic-peptide family". The Lancet, vol. 349, p. 1307-1310.

WILLIAMS, T. M., C. A. Stump, D. N. Nguyen, A. G. Quigley, I. M. Bell, S. N. Gallicchio, C. B. Zartman, B.-L. Wan, K. D. Penna, P. Kunapuli, S. A. Kane, K. S. Koblan, S. D. Mosser, R. Z. Rutledge, C. Salvatore, J. F. Fay, J. P. Vacca, S. L. Graham. 2006. "Non-peptide calcitonin gene-related peptide receptor antagonists from a benzodiazepinone lead". Bioorganic & Medicinal Chemistry Letters, vol. 16, p. 2595–2598.

WIMALAWANSA, S. J., H. R. Morris, A. Etienne, I. Blench, M. Panico, I. MacIntyre. 1990. "Isolation, purification and characterization of beta-hCGRP from human spinal cord". Biochemical and Biophysical Research Communications, vol. 167, p. 993-1000.

WISSKIRCHEN, F. M., D. W. Gray, I. Marshall. 1999. "Receptors mediating CGRP-induced relaxation in the rat isolated thoracic aorta and porcine isolated coronary artery differentiated by h(alpha) CGRP(8–37)". British Journal of Pharmacology, vol.128, p. 283–292.

WOOKEY, P. J., T. A. Lutz, S. Andrikopoulos. 2006. "Amylin in the periphery II: an updated mini-review". The Scientific World Journal, Vol. 6, p. 1642-1655.

WUNDER, F., A. Rebmann, A. Geerts, B. Kalthof. 2008. "Pharmacological and kinetic characterization of adrenomedullin 1 and calcitonin gene-related peptide 1 receptor reporter cell lines", Molecular Pharmacology, vol. 73, p. 1235-1243.

WYNICK, D., S. R. Bloom. 1991. "Clinical review 23: The use of the long-acting somatostatin analogue octreotide in the treatment of gut neuroendocrine tumors". The Journal of Clinical Endocrinology & Metabolism, vol. 73, p. 1-3.

YIN, H., L. Chao, J. Chao. 2004. "Adrenomedullin protects against myocardial apoptosis after ischemia/reperfusion through activation of Akt-GSK signaling". Hypertension, vol. 43, p. 109-116.

YU, S., T. Hsu. 2005. "Intermedin and its uses". United States Patent 6965013.

ZHANG, K., R. An, Z. Gao, Y. Zhang, M. R. Aruva. 2006. "Radionuclide imaging of small-cell lung cancer (SCLC) using ^{99m}Tc-labeled neurotensin peptide 8-13". Nuclear Medicine and Biology, vol. 33, p. 505-512.

ZIKOS, C., E. Papasarantos. 2006. "False results of the Kaiser (ninhydrin) test after the Fmoc-deprotection of certain amino acids coupled to proline during SPPS". The 29th European Peptide Symposium.

ZIMMERMANN, U., J. A. Fischer, K. Frei, A. H. Fischer, R. K. Reinscheid, R. Muff. 1996. "Identification of adrenomedullin receptors in cultured rat astrocytes and in neuroblastboma × glioma hybrid cells (NG108-15)". Brain Research, vol. 724, p. 238–245.

Résumé

Objectifs

Le diagnostic de certaines maladies requiert fréquemment l'imagerie moléculaire radiopharmaceutique. C'est un outil intéressant pour lequel, il existe deux générations de radiotraceurs, ou marqueurs biologiques : les radiotraceurs non-sépcifiques et les radiotraceurs sélectifs à une cible pharmaceutique. Les anticorps monoclonaux radiomarqués ont par exemple été initialement les molécules de choix dans le développement de radiotraceurs spécifiques à une cible pharmaceutique, étant donné leur grande affinité et spécificité. Ainsi, jusqu'à présent les anticorps monoclonaux ont permis l'étude et l'application de méthodes diagnostiques et thérapeutiques de médecine nucléaire pendant plus de deux décennies. Dans un effort de réduire ou éliminer les inconvénients inhérents à leur utilisation, comme l'élimination sanguine lente et leur concentration dans les tissus tumoraux, l'usage potentiel de fragments des anticorps à été exploré par de nombreux laboratoires. De plus, en parallèle, plusieurs chercheurs en médecine nucléaire ont développé un intérêt pour la découverte de nouveaux complexes moléculaires cibles à haute affinité dans les organes et les tissus.

Chez les humains, plusieurs fonctions biologiques sont régulées par des peptides par l'intermédiaire d'une interaction spécifique avec un récepteur. Ces molécules affichent une grande affinité et spécificité, combinées à une demi-vie plasmatique courte. Connus pour leurs fonctions stimulatrices, inhibitrices ou régulatrices, les peptides ont été considérés comme des agents potentiels pour des usages thérapeutiques. Par opposition aux anticorps, ils sont pratiquement non-immunogènes. C'est pour ces raisons qu'un nombre croissant de radiotraceurs pharmaceutiques, élaborés à partir de peptides, sont d'ailleurs utilisés pour le diagnostic de différentes pathologies ou à des fins curatives dans certains stades de la maladie. Ceci est particulièrement vrai pour les pathologies pulmonaires puisque des radiotraceurs pharmaceutiques sont utilisés pour le diagnostic du cancer du poumon, de l'embolie pulmonaire et de diverses conditions inflammatoires ou infectieuses. Par contre, il n'existe actuellement qu'un seul agent pour l'imagerie clinique de la circulation pulmonaire, soit les macroaggrégats d'albumine (MAA) marqués au

technétium 99 métastable (^{99m}Tc). Cet agent est utilisé exclusivement pour le diagnostic des anomalies physiques de la circulation pulmonaire observées lors d'une embolie. En fait, cet agent est assez volumineux pour se retrouver prisonnier des petits vaisseaux sanguins des poumons, ce qui permet la visualisation externe de la circulation. Toutefois l'utilisation des MAAs est limitée par l'impossibilité de visualiser les petits vaisseaux sanguins au-delà du point d'obstruction, ce qui limite la sensibilité de détection des défauts vasculaires et d'embolies à un stade précoce. De plus, cette technique présente un risque potentiel infectieux accru étant donné que l'agent est dérivé de l'albumine humaine.

La famille peptidique de la calcitonine est composée de la calcitonine (CT), de l'amyline (AMY), de deux CGRPs (*calcitonin gene-related peptide*), de l'adrénomédulline, de l'adrénomédulline-2/intermédine (AM2/IMD) et des CRSPs (*calcitonin receptor-stimulating peptide*). Ces peptides sont des hormones formées d'une seule chaîne d'acides aminés et ils partagent bien sûr une certaine homologie de séquence. Les peptides de la famille de la CT se retrouvent, chez les rats et les humains, dans plusieurs tissus périphériques ainsi qu'au niveau du système nerveux central et périphérique. La distribution tissulaire de ces peptides et de leurs sites de liaison reflète d'ailleurs les différences au niveau de leurs actions et de leurs propriétés biologiques. Tout particulièrement, les effets biologiques des peptides de cette famille sont médiés par une liaison à un complexe protéique couplé aux protéines G, soit le récepteur de la calcitonine (CTR) ou le CRLR (*calcitonin receptor-like receptor*), qui se trouve associé à des protéines chaperonnes, telles le RAMP (*receptor-activity-modifying-protein*) et le RCP (*receptor-component-protein*).

AM, un peptide de 52 acides aminés, est produit principalement dans les glandes surrénales, les poumons, les reins et dans les tissus cardiaques. Une puissante vasodilatation apparaît être la principale action physiologique de ce peptide. Des études de liaison dans différents tissus de rat ont révélé que la plus importante densité de sites de liaison spécifique se retrouvait dans le cœur et le poumon. En 1995, deux groupes de recherche ont démontré que les vaisseaux sanguins pulmonaires possédaient une

abondance de récepteurs pour l'AM et que ces derniers agissaient en tant que récepteurs de clairance dans la circulation pulmonaire. Donc, ce peptide possède des caractéristiques utiles pour le développement d'un radiotraceur permettant l'imagerie spécifique du poumon. Un tel composé pourrait remplacer les MAAs pour le diagnostic par exemple de l'embolie pulmonaire. Afin d'offrir un outil plus puissant à des fins diagnostiques et pour le suivi d'une réponse à un traitement du système pulmonaire, l'agent ^{99m}Tc-AM a été proposé en se basant sur une approche utilisant un ligand très affin au tissus pulmonaires.

Une longue chaîne peptidique, telle l'AM, représente un défi majeur lors de la synthèse en plus de constituer un investissement important en temps et en dérivés d'acides aminés. Le développement d'analogues peptidiques plus courts, beaucoup plus faciles à synthétiser et moins enclins à produire des réactions secondaires durant les conditions chimiques rencontrées lors de la synthèse ou lors des étapes menant au radiomarquage, serait donc bénéfique. De plus, les petits peptides ne sont pas immunogènes et ils sont rapidement éliminés de la circulation sanguine. Tous ces facteurs font que les peptides courts sont d'excellents candidats pour le développement de radiotraceurs ayant une cible spécifique. Étant donné que l'AM est un peptide bioactif, le meilleur candidat doit garder une affinité significative pour le récepteur ciblé tout en minimisant la liaison à des sites non-spécifiques et posséder une activité biologique réduite sur le système circulatoire. Toutefois, ce n'est pas simple puisque les propriétés agonistes ou antagonistes des peptides, de même que l'introduction d'un groupement chélateur dans la chaîne peptidique, sont des sources possibles de complications lors de l'utilisation de peptides comme agent pour l'imagerie. Il est donc crucial d'élaborer les nouveaux composés en accord avec les études de structure-activité effectuées sur des préparations bien caractérisées du récepteur peptidique.

Au sein de la famille de la CT, il est établi que les peptides agissent via un GPCR situé sur la membrane plasmatique. De ce fait, l'AM, un membre de cette famille, se lie et active au moins deux types de GPCR, nommés AM_1 et AM_2. De plus, l'AM possède une certaine affinité pour les récepteurs $CGRP_1$ et est capable de lier les récepteurs de la CT et de l'AMY à des concentrations de l'ordre du µM. Récemment, il a été rapporté que l'AM,

agissant en tant qu'hormone régulatrice, est également métabolisée dans la circulation pulmonaire via un récepteur de clearance de l'AM. Pourtant, aucune différence physiologique n'a été identifiée quant à l'activation des récepteurs AM_1 et AM_2; la signification fonctionnelle de cette apparente redondance de récepteurs reste donc à clarifier. Ainsi, une caractérisation des récepteurs de l'AM à l'aide d'agonistes et d'antagonistes spécifiques est essentielle afin d'établir clairement la fonction des sous-types de récepteurs de l'AM.

Méthodes

L'élaboration d'un radiotraceur ciblant un récepteur spécifique pour l'imagerie pulmonaire est décrite ci-après. Cet agent est composé d'un élément radioactif, le 99m-technétium, d'un transporteur pour le radioisotope, normalement un agent chélateur bifonctionnel (BCA), et d'une molécule-cible comme ligand du récepteur. Les techniques permettant la préparation de ce nouveau traceur incluent la modification chimique d'une molécule biologique, la conjugaison du transporteur à cette molécule et l'incorporation de l'isotope. Il est également possible d'insérer un espaceur moléculaire entre la molécule biologique et le transporteur afin de minimiser les effets de ces modifications sur l'affinité et la spécificité de liaison au récepteur, plus particulièrement si la molécule biologique est un petit peptide. Pour le système décrit ici, le ^{99m}Tc est utilisé comme source de radiation pour l'imagerie et l'AM agit comme molécule-cible pour le récepteur.

La synthèse peptidique en phase solide (SPPS) est particulièrement utile lorsqu'un grand nombre d'analogues est désiré et qu'un criblage rapide des peptides est planifié. Généralement, deux stratégies peuvent être utilisées pour la SPPS selon le schéma de protection de l'amine-α employé : l'utilisation du groupement protecteur Boc, qui est labile en milieu acide, ou du groupement 9-fluorènylméthyloxycarbonyle (Fmoc), qui est enlevé par un traitement avec une base. Lors d'une synthèse utilisant le groupement Fmoc, la chaîne peptidique est soumise à des traitements basiques à la pipéridine pour permettre la déprotection de l'amine-α et l'acide trifluoroacétique (TFA) est requis uniquement pour l'étape finale de déprotection du peptide et le clivage du support solide.

À l'opposé, les étapes de clivage et de déprotection pour une stratégie employant le groupement Boc nécessitent l'utilisation d'acides forts, comme le fluorure d'hydrogène (HF) et le TFA. Ces multiples traitements à l'acide sont plutôt robustes ce qui résulte souvent en un clivage prématuré de chaînes peptidiques et en diverses réactions secondaires. Étant donné que dans notre étude les peptides proposés comme agents potentiels pour l'imagerie possèdent une chaîne peptidique plutôt longue et qu'une stratégie de synthèse utilisant le groupement Fmoc engendre généralement un niveau relativement faible de réactions secondaires, les peptides, tels l'AM, et leurs analogues ont été conçus et synthétisés en accord avec une méthodologie standard Fmoc/hexafluorophosphate de benzotriazol-1-yl-oxy-tris(diméthylamino)-phosphonium (BOP). Le couplage direct d'un BCA, l'acide diéthylènetriamine-pentacétique (DTPA), sur la chaîne peptidique ancrée à la résine selon la méthodologie Fmoc/BOP n'a pas permis d'obtenir le produit désiré étant donné la faible solubilité du DTPA dans tous les solvants organiques couramment utilisés pour la Fmoc-SPPS. Pour cette étude, l'analogue DTPA-AM a été obtenu par le couplage de l'anhydride de DTPA à l'extrémité N-terminale du peptide-résine protégé obtenu par SPPS. La plus grande solubilité de l'anhydride de DTPA dans les solvants organiques a permis l'obtention du produit désiré, c'est-à-dire le DTPA-AM. Suite au clivage des peptides de leur support solide, la formation du pont disulfure a été effectuée par une oxydation à l'air et suivie par chromatographie liquide à haute performance (HPLC) analytique sur phase inverse. La cyclisation complète du peptide a aussi été confirmée au moyen du test d'Ellman. Finalement, tous les analogues peptidiques synthétiques ont été purifiés par HPLC et caractérisés par spectrométrie de masse de type MALDI-TOF (*matrix-assisted laser desorption ionization time-of-flight*).

Selon la structure moléculaire et chimique, deux types d'agents pour l'imagerie du poumon utilisant l'AM comme ligand-cible ont été développés pour cette étude : l'un composé du peptide et du radioisotope et l'autre formé de trois composantes, soit le peptide, l'isotope et le BCA. Leur élaboration a été effectuée en accord avec les études de type structure-activité de l'AM, plus précisément à partir d'analogues peptidiques affichant une bonne affinité pour le récepteur et sur lesquels la conjugaison du BCA a été

accompli en gardant cette portion éloignée de la région impliquée dans la liaison avec le récepteur. Cet agencement permet d'éviter ou du moins de minimiser les interférences possibles avec la structure secondaire du peptide et la liaison de haute affinité avec le récepteur. En tenant compte des méthodes de préparation et d'utilisation d'un radiotraceur, le conjugué DTPA-AM a d'abord été purifié et radiomarqué selon une approche de marquage en dernière étape (*postlabeling*). D'autre part, une approche de marquage direct a été privilégiée pour la préparation d'analogues linéaires de l'AM marqués au ^{99m}Tc. Une réaction utilisant des solutions de $SnCl_2$ et de sodium tétraoxyde de technétium a donné ces analogues qui ont été ensuite purifiés par HPLC analytique sur phase inverse ou par l'utilisation de cartouches C_{18} Sep-Pak. Les rendements des réactions de marquage et l'analyse de la formation de sous-produits ont été évalués par les techniques de HPLC, de ITLC (*instant thin layer chromatography*) et par la quantifiation des émissions de radiation au moyen d'un compteur gamma.

Toute nouvelle molécule potentiellement utile pour l'imagerie doit être évaluée *in vivo*. La disponibilité d'essais biologiques efficaces est donc un élément-clé dans la découverte de nouveaux produits en permettant d'orienter les chercheurs dans la sélection de composés prometteurs au dan diagnostique ou thérapeutique. Le rat est une espèce grandement utilisée pour le développement de méthodes d'imagerie étant donné sa petite taille et son faible coût. Par contre, le rat n'a pas semblé être le modèle de choix pour cette étude d'imagerie des poumons en raison de ses caractéristiques anatomiques. Or, la bonne capacité volumique et la similarité de grandeur du poumon de chien avec celui de l'humain ont favorisé ce modèle pour l'évaluation des agents potentiels pour l'imagerie à des fins de diagnostic et de traitements de pathologies chez l'être humain. Ainsi, des résultats plus précis d'imagerie du poumon et des informations structurales du tissu ont pu être obtenus en utilisant le chien comme modèle expérimental. Pour ce faire, une injection de 2 à 4 mCi d'AM, ou d'un analogue marqué au ^{99m}Tc (pureté ≥95%) a été effectuée dans la veine saphène droite de chiens (20-30kg) et l'évolution de la distribution de la radioactivité a été suivie grâce à une étude dynamique du thorax d'une durée de 30 min. Ensuite, une image totale du corps a été obtenue par un balayage avec une caméra gamma, à une vitesse de 10 cm/min, afin d'évaluer la biodistribution et la clearance dans

les différents organes et tissus. Également, des échantillons sanguins ont été prélevés de la veine saphène gauche afin de déterminer (l'évolution) la cinétique du traceur dans le plasma. Enfin, la pression artérielle et le rythme cardiaque ont été enregistrés tout au long de l'étude.

Pour des études biologiques ou pour le criblage de composés à caractère pharmaceutique, les radiotraceurs sont des outils très performants. Étant donné la courte demi-vie du ^{99m}Tc, de l'AM radiomarqué avec de l'iode-125 a donc été préparé afin de pouvoir effectuer la caractérisation des récepteurs spécifiques à l'AM retrouvés dans le poumon de chien. Quatre méthodes ont été utilisées pour le marquage à l'iode de l'AM ou de ses fragments : la méthode de Bolton et Hunter, la méthode utilisant les iodo-billes ou l'iodogène, la méthode à la lactoperoxydase et la méthode à la chloramine-T. Les réactifs d'iodation iodo-billes et iodogène, formés de molécules oxydantes ancrées à un support solide, sont à la fois pratiques, doux et efficaces pour accomplir l'iodation de protéines membranaires ou solubles; ainsi, le peptide ^{125}I-AM disponible commercialement est en général issu d'une réaction impliquant ces réactifs. Par contre, la méthode utilisant la lactoperoxydase permet une monoiodation plus sélective surtout en présence de multiples résidus tyrosine, comme c'est d'ailleurs le cas pour l'AM qui en possède trois. Dans cette étude les méthodes faisant appel à la chloramine-T et à la lactoperoxydase ont été évaluées. Il a été déterminé lors de l'iodation utilisant la chloramine-T qu'une monoiodotyrosine se trouvait à la position C-terminale du peptide et qu'un autre résidu avait également été marqué, possiblement la tyrosine située dans la région centrale de la chaîne peptidique. La tyrosine située en position N-terminale n'a pas semblé être iodée selon l'analyse par HPLC des produits de digestion de la carboxypeptidase sur le peptide suivant la réaction d'iodation. Enfin, les produits d'iodation de l'AM générés par la méthode faisant appel à la lactoperoxydase ont été étudiés après clivage enzymatique et au CNBr.

Les récepteurs sont souvent caractérisés par le biais de techniques pharmacologiques associées à une réponse physiologique. Dans les expériences qui ont suivi, l'étude a eu pour objectif de caractériser les sites de liaison responsables de la clearance de l'AM dans

le poumon de chien, étant donné qu'il n'existait pas de données précises pour définir la nature de ce récepteur. Les études de liaison par saturation permettent de quantifier la liaison spécifique à l'équilibre d'un radioligand à différentes concentrations. Les valeurs obtenues lors de ces études déterminent la densité de récepteurs et l'affinité de son ligand. Ainsi, des données recueillies sur un même récepteur en utilisant différents radioligands permettent d'évaluer leurs propriétés de liaison spécifique sur cette préparation. La constante de dissociation, notée K_d, est une indication de l'affinité du radioligand pour le récepteur; une faible valeur de K_d est associée à une forte affinité. La densité de récepteur pour un radioligand est évaluée par la valeur du Bmax; une valeur élevée indique une densité élevée de récepteurs dans le tissus ou les cellules. Les tests de liaison par compétition utilisent une quantité fixe de radioligand en présence de concentrations variées de ligand non-marqué. Ces études de liaison sont souvent utilisées afin d'identifier pharmacologiquement la nature d'un récepteur pour un peptide donné situé dans un tissu ou un type cellulaire particulier. Actuellement, dans la littérature, la liaison spécifique de l'AM à ses récepteurs a été étudiée chez le rat. Dans cette étude, des tests de liaison par compétition ont été effectués sur des tissus pulmonaires de rats et de chiens ainsi que sur des cellules endothéliales d'artère pulmonaire de vache (CPAE).

Résultats

Afin d'élaborer un système de transporteur de radioisotope avec une molécule-cible, l'AM humaine cyclisée et quatre analogues, soit l'AM linéaire, l'AM acétylée, l'AM linéaire et acétylée et le DTPA-AM, ont été préparés et marqués pour les expériences de criblage initiales. Il a été observé lors des expériences de marquage et de biodistribution *in vivo* que l'AM linéaire et acétylée pouvait agir en tant que chélateur du ^{99m}Tc et molécule-cible pour le poumon. De même, le ^{99m}Tc pouvait être chélaté par l'AM linéaire avec un bon rendement de marquage. D'ailleurs, il semble que la présence de fonctions sulfhydryles sur l'AM forme une molécule apte à transporter le ^{99m}Tc et présente de meilleures propriétés chélatrices que le DTPA-AM. En se basant sur les résultats de marquage au ^{99m}Tc et aux tests de liaison par compétition, le ^{99m}Tc-AM linéaire a été

identifié comme la molécule optimale de départ pour le développement d'un composé radiopharmaceutique.

Suite à une injection, les images ont montré que le ^{99m}Tc-AM linéaire était chez le chien principalement capté par les poumons. Une image stable, spécifique et de bonne qualité des poumons a été obtenue 30 min suivant l'injection. Suite à la captation intense et spécifique par les poumons, il semble que le radiotraceur se dissipe des tissus pulmonaires pour être éliminé par les reins, et le foie. Les études de biodistribution supportent une captation considérable par le tissu pulmonaire et donc l'importance des poumons comme organe cible pour ce radiotraceur. Proportionnellement, la captation par le cœur et le foie est mineure. Les enregistrements effectués tardivement suite à l'injection (60-240 min) montrent une concentration de la radioactivité dans les reins et la vessie probablement attribuable à la principale voie d'élimination du peptide radiomarqué. À l'examen des résultats de l'imagerie du poumon, de la biodistribution et de la cinétique du traceur dans le chien, il semble bien que la clearance de l'AM s'effectue spécifiquement par la voie pulmonaire. La perfusion pulmonaire par chirurgie a d'ailleurs confirmé l'applicabilité de ce nouveau radiotraceur en tant qu'agent diagnostique pulmonaire, aussi bien pour l'embolie pulmonaire que pour des infections.

La structure du complexe ^{99m}Tc-AM linéaire a été examinée par des essais de radiomarquage de fragments de l'AM, soit AM(13-52) linéaire, AM(16-52) linéaire, AM(17-52), AM(18-52), AM(19-52), AM(20-52), AM(21-52) et AM(22-52). Les résultats indiquent que le groupement sulfhydryle de la cystéine en position 21 capte l'oxyde de ^{99m}Tc libre, inhibant ainsi la transformation du pertechnetate libre en colloïdes lorsqu'en présence d'ions Sn^{2+}. Le groupement sulfhydryle de la cystéine en position 16 semble quant à lui contribuer à la stabilité du complexe intermédiaire et ainsi augmenter le rendement de marquage. De plus, certains groupements électrons-donneurs situés dans la portion N-terminale du peptide contribueraient également à la stabilisation du traceur ^{99m}Tc-AM-linéaire.

Étant donné qu'il n'existe actuellement aucune publication présentant une étude de liaison de l'AM chez le chien, des essais de liaison ont été effectués afin de caractériser les sites d'attachement du ^{99m}Tc-AM-linéaire dans le poumon de chien en utilisant les techniques d'analyse au moyen d'un ligand radiomarqué. Dans le cas présent, à cause du manque d'agonistes ou d'antagonistes sélectifs envers les sous-types de récepteurs de l'AM, la caractérisation de récepteurs spécifiques à l'AM a été basée sur une liaison de haute affinité pour l'AM et une affinité au moins 100 fois inférieure pour les autres membres de la famille de la calcitonine. Dans cette étude, les peptide humains et leurs analogues, soit hAM, hAM(13-52), hAM(22-52), hCGRPα, hCGRP(8-37), hAM2, hAM2(16-47) et AMY, ont été synthétisés en suivant un protocole standard de synthèse Fmoc/BOP et l'identité des peptides a été confirmée par HPLC et par spectrométrie de masse. Les essais de liaison ont été effectués en utilisant ^{125}I-AM comme ligand radiomarqué et l'AM et les autres peptides comme compétiteurs pour la liaison sur des homogénats de poumon de chien. L'agoniste non-sélectif AM a montré une liaison de haute affinité comportant deux sites de liaison. Le déplacement relatif observé pour les différents peptides est AM> AM(13-52)> CGRP≈ AM2≥ AM(22-52)≥ AM2(16-47)> CGRP(8-37)> AMY. Le récepteur de l'AM, AM_1, a donc été caractérisé biochimiquement par le biais d'agonistes et d'antagonistes connus de la famille peptidique de la CT. Ainsi, les résultats suggèrent fortement que les sites de liaison de l'AM retrouvés dans le poumon de chien sont principalement du sous-type AM_1.

L'AM est un long peptide de 52 acides aminés ne possédant pas de sélectivité envers les sous-types de récepteurs. L'étude de la structure primaire et secondaire nécessaire pour lier les sites de liaison trouvés dans les poumons de chien pourrait contribuer à approfondir les études de type structure-activité du peptide et au développement de plus petits peptides ou autres composés dérivés qui auraient une spécificité envers les poumons en tant que molécule-cible. Les substituts possibles de l'AM inclut l'AM linéaire, qui possède toute la séquence d'acides aminés de l'AM mais sans la structure du pont disulfure, AM(13-52), un agoniste n'ayant pas la structure en boucle de la portion N-terminale, AM(22-52), un antagoniste ne possédant ni la structure en boucle ni le pont disulfure, AM(1-25), un peptide correspondant à la portion N-terminale du peptide

incluant le pont disulfure, AM(26-52), un peptide formé du reste de la séquence peptidique, AM(1-40), un peptide comportant toute la séquence peptidique sauf la partie C-terminale et AM(40-52), composé uniquement de la portion C-terminale incluant l'extrémité amide de la Tyr. Donc afin de faire un criblage pour trouver un substitut plus facile à synthétiser et moins enclin à des réactions secondaires, la présente étude s'est penchée sur les acides aminés, le segment peptidique minimal et les structures secondaires de l'AM qui permettent de conserver une bonne affinité pour les récepteurs de l'AM dans le poumon de chien. Le déplacement relatif observé pour les différents analogues de l'AM est AM>> AM linéaire> AM(13-52)> AM(22-52)> AM(26-52)> AM(1-25), AM(40-52) et AM(1-40). Le déplacement de ^{125}I-AM lié aux homogénats de poumon de chien est moins efficace lorsque le peptide ne comporte pas de pont disulfure, de structure en boucle en N-terminal ou que la structure en hélice-α est compromise. Ceci suggère que ces structures sont essentielles et contribuent à la liaison de haute affinité de l'AM pour ses récepteurs dans le poumon de chien. Néanmoins, un fragment de l'AM ne possédant pas la portion C-terminale mais comportant toute la séquence et les propriétés des structures secondaires mentionnées ci-haut, tel AM(1-40), n'a montré aucun déplacement dans les tests de liaison.

La méthode faisant appel à la lactoperoxydase a résulté en une iodation sélective de Tyr^{I}-AM. À titre d'expérience comparative, la méthode faisant appel à la chloramine-T a donné lieu à plusieurs produits et à un rendement de réaction inférieur. L'évaluation des différentes méthodes a été effectuée en analysant les produits de clivage par le CNBr ou de séquençage enzymatique de AM(13-52), AM et AM iodé. Le mélange non-purifié de AM et de AM iodé obtenu après une iodation non radioactive à la lactoperoxydase a été digéré par la carboxypeptidase Y pour donner deux fragments mono-oxydés et leurs analogues monoiodés. Les résultats ont indiqué que l'atome d'iode se situait sur les fragments digérés d'AM et donc que l'iodation ne pouvait survenir sur la tyrosine en position C-terminale. L'atome d'iode peut donc se trouver en position N-terminale ou sur la tyrosine à l'intérieure de la chaîne peptidique en position 31. Par contre, la digestion enzymatique utilisant l'aminopeptidase M a échoué puisqu'aucun fragment plus court de l'AM n'a pu être trouvé par analyse de spectrométrie de masse. Étant donné qu'il n'y a

qu'une seule méthionine dans la séquence de l'AM et qu'elle est située dans la région N-terminale, le CNBr a été utilisé afin de déterminer quelle tyrosine était iodée. Suite au clivage chimique, un seul fragment d'AM monoiodé a été détecté. Ce résultat indique que l'iodation par la lactoperoxydase s'effectue sur la tyrosine située en N-terminal. Ces résultats ont été vérifiés par le clivage au CNBr de l'AM, et des AM mono et diiodé; le deuxième atome d'iode s'est avéré ne pas être introduit sur la tyrosine en N-terminal. Bref, le résultat de la réaction à la lactoperoxydase sur l'AM a bel et bien été le peptide monoiodé sur la tyrosine en position N-terminale, c'est-à-dire ^{125}I-Tyr^{1}-AM. Les essais de liaison de saturation utilisant ^{125}I-AM de source commerciale et ^{125}I-Tyr^{1}-AM ont montré une différence de l'ordre de trois fois pour les valeurs du K_d de même que pour le Bmax entre les deux radioligands. Ces résultats suggèrent qu'il existe une différence d'affinité pour les récepteurs situés dans le poumon de chien entre deux produits d'iodation de l'AM. Le profil pharmacologique des récepteurs de l'AM dans les poumons de chiens et de rats a été confirmé par les essais de liaison par compétition. Néanmoins, dans une étude subséquente aucun site de liaison spécifique n'a été trouvé dans les cellules endothéliales de l'artère pulmonaire de vache.

Conclusions

Jusqu'à présent, les produits radiopharmaceutiques ont joué un rôle important dans le diagnostic de pathologies humaines. Les outils d'imagerie contribuent également à faire le suivi clinique des traitements pour une condition particulière. Un diagnostic précoce est la clé de la lutte contre certaines maladies graves, par exemple le cancer. Les radiotraceurs spécifiques à une molécule-cible sont conçus en accord avec les propriétés des fonctions physiologiques et des pathologies et afin d'obtenir des cibles spécifiques pour un organe, un tissu, une tumeur ou une embolie. Il est aussi bénéfique de pouvoir détecter très tôt les changements pathologiques ou d'évaluer la progression par le biais de l'imagerie afin d'appliquer la méthode thérapeutique la plus appropriée pour un cas précis.

Cette thèse a été préparée avec comme objectif le développement d'un radiotraceur peptidique spécifique pour l'imagerie de la circulation pulmonaire humaine. Dans notre étude, un peptide a été utilisé comme molécule ciblant les poumons et la conjugaison du 99m-technétium à l'AM a donné des images claires et bien définies. Le ^{99m}Tc-AM-linéaire s'est avéré la forme la plus prometteuse après criblage. Les résultats ont montré que le radiotraceur était retenu majoritairement par le poumon de chien 30 min après l'injection initiale (<16 pmol de peptide marqué) pour donner une image nette des poumons. La captation initiale rapide de la radioactivité par le poumon de chien suggère que le radiotraceur est rapidement saisi in vivo par des récepteurs pulmonaires spécifiques et qu'il possède des caractéristiques de biodistribution favorables à l'imagerie du poumon. La forte concentration de radioactivité observée dans les reins et la vessie du chien lors des enregistrements tardifs (60-240 min après l'injection) serait attribuable à la principale route d'élimination du peptide radiomarqué, ce qui suggère l'existence d'une voie pulmonaire pour la clearance de ce peptide. De plus, l'imagerie a également été effectuée suite à une chirurgie mimant une condition pulmonaire pathologique, telle l'embolie pulmonaire. Comparativement aux MAAs qui sont présentement utilisés pour le diagnostic de la circulation pulmonaire, l'agent pour l'évaluation diagnostique pulmonaire présenté ici offre plusieurs avantages pour l'utilisation clinique.

En se basant sur les sites de liaison spécifiques des récepteurs trouvés dans le poumon de chien, la caractérisation de ces sites a été accomplie dans cette thèse. Cette caractérisation s'est effectuée par des essais de liaison récepteur-ligand utilisant ^{125}I-AM en tant que radioligand. Les résultats ont montrés que l'AM humaine possède une liaison de haute affinité avec deux sites de liaison dans les homogénats de poumon de chien. Les agonistes et les antagonistes de l'AM possédaient la capacité de se lier avec les mêmes sites de liaison mais avec une affinité moindre alors que l'affinité était faible (>100 fois moindre) pour les peptides AMY, AM2 et CGRPα. Ces sites de liaison ont donc été caractérisés comme étant des récepteurs de l'AM. Même si la fonction précise des sous-types de récepteurs de l'AM, soit AM_1 et AM_2, reste à clarifier, les sites de liaison de l'AM dans les homogénats de poumons de chien possèdent une affinité supérieure ($P<0.01$) pour l'antagoniste AM(22-52) que pour CGRPα(8-37). Ceci suggère que le site de liaison de

l'AM trouvé dans le poumon de chien ayant la plus grande affinité serait le sous-type de récepteur AM_1 et qu'il serait responsable de la clearance de l'AM par les poumons. En conclusion, les poumons de chien expriment un récepteur spécifique de l'AM possédant les caractéristiques de AM_1 selon les résultats des essais de liaison. Cette caractérisation de cette population de récepteurs trouvés dans le poumon de chien pourrait servir dans l'étude des sous-types de récepteurs de l'AM dans le cadre des sciences biologiques.

De plus, la suite des études à viser à déterminer quel serait le fragment optimal de l'AM qui pourrait être utilisé afin de simplifier la préparation, de diminuer la possibilité d'activité biologique non-associée à l'imagerie et de réduire les coûts de production. À travers des essais de liaison, des données ont été recueillies quant à la séquence et aux structures secondaires requises pour permettre la liaison au récepteur. La région de l'AM liant le récepteur pourrait se situer sur la séquence d'acides aminés en C-terminal de l'AM humaine. En effet, les fragments de l'AM possédant la portion N-terminale du peptide, y compris le pont disulfure, mais sans la portion C-terminale n'ont pu être en mesure de lier les récepteurs situés dans les homogénats de poumon de chien. Par contre, une perte d'affinité de liaison a été observée pour les analogues de l'AM tronqués à partir de l'extrémité N-terminale. Afin de maintenir une bonne affinité du peptide pour son récepteur, la boucle N-terminale, le pont disulfure et la structure en hélice α sont nécessaires à la liaison des sites situés dans les poumons de chien. Parmi ces éléments, la structure en hélice α semble être le pharmacophore le plus important pour la liaison de l'AM à ses récepteurs.

De plus, un nouvel outil moléculaire a été introduit ici, c'est-à-dire ^{125}I-Tyr^{1}-AM, pour les études biologiques de l'AM. D'ailleurs l'étude a permis d'élucider la préparation, l'isolation et la caractérisation de ce nouveau radioligand et d'évaluer son potentiel d'application à des études d'interaction ligand-récepteur chez différentes espèces. Ce radioligand a démontré avoir une grande affinité et spécificité de liaison dans les préparations utilisées dans cette étude comparativement à celui disponible commercialement. Il sera donc un outil appréciable pour les études futures de l'AM. Les essais de liaison par saturation comparant les deux radioligands, soit ^{125}I-AM et ^{125}I-Tyr^{1}-

AM, ont indiqué et supporté le fait que la tyrosine en position 52 dans la région C-terminale de l'AM est cruciale pour la liaison au récepteur. En fait, son iodation semble perturber l'affinité de liaison de l'AM humaine dans les poumons de chien.

Tous les résultats compilés dans cette thèse font référence à l'AM humaine utilisée chez le chien et le rat. De fait, des différences inter-espèces sont observables au sein des résultats. Plus particulièrement, trois aspects devraient faire l'objet d'études subséquentes. Premièrement, dans le cadre d'études précliniques, les activités biologiques in vitro et in vivo de ^{99m}Tc-AM-linéaire devront être évaluées surtout en présence de doses élevées du radiotraceur. De plus, des études de l'AM et de ses fragments sur des cellules ou des tissus humains et même sur de êtres humains est à envisager. Deuxièmement, la caractérisation des récepteurs de l'AM situés dans d'autres organes et tissus chez le chien devrait être poursuivie. En effet, malgré le fait que diverses études ont montré la présence de sites de liaison de l'AM dans le cœur et les poumons de rats, aucune sélectivité du ^{99m}Tc-AM-linéaire n'a été observée pour le cœur de chien dans cette étude. Cette caractérisation des récepteurs de l'AM dans d'autres organes et tissus de chien, et spécialement dans le cœur, contribuerait à une meilleure connaissance de la biodistribution des récepteurs de l'AM et de leurs sous-types. Finalement, la liaison du ligand à son récepteur et le modèle d'activation des GPCRs de la classe B pourraient varier d'un ligand à l'autre en termes d'élément-clés responsables de l'affinité de liaison et de l'activité agoniste complète. L'étude des pharmacophores serait essentielle pour apporter des modifications à ^{99m}Tc-AM-linéaire ou à ses fragments et pourrait donner un point de départ à l'élaboration de nouveaux radiotraceurs pour le futur.

Dans cette thèse, l'AM a été étudiée en tant que molécule-cible pour le poumon chez l'être humain. Par contre, l'AM dans sa forme native n'est pas une molécule-cible optimale. C'est pourquoi des études visant à modifier, à tronquer ou à construire des antagonistes non-peptidiques sont essentielles au développement d'une molécule-cible. De plus, l'application d'une telle molécule-cible ne serait pas limitée à l'imagerie pulmonaire. En effet, l'utilisation de cette molécule pourrait être étendue au traitement de pathologies reliées à l'AM par conjugaison avec des composés pharmaceutiques élaborés

pour le traitement de maladies cardiovasculaires, de problèmes rénaux, du cancer et de la septicémie. Bref, toutes les données recueillies au cours des études de type structure-activité sur l'AM vont contribuer au développement de nouvelles molécules d'intérêt. De même, la mise en place d'un système de criblage optimal utilisant soit des cellules, des tissus ou un modèle animal, permettrait une évaluation facilitée des nouveaux composés.